Cranfield
UNIVERSITY
Silsoe

Institute of Agritechnology

PostHarvest, Food and Marketing Group

EFFECT OF COSOLUTES ON POLYSACCHARIDES GELATION

Thesis presented by

Areti K. Tsoga

For the Degree of

Doctor of Philosophy

June 2001

Supervisors: Dr. S. Kasapis

Professor E. R. Morris

ACKNOWLEDGEMENTS

Time has finally passed and "the Silsoe adventure" has come to its end. For that I have to thank my supervisor, Prof. E. R. Morris, for all his support and interest throughout the years. It was a privilege to work with someone of his excellence. At the same time, Dr. R. K. Richardson for trusting me with his famous "Bobometer" and his support especially during the last and most difficult year. I could never forget Dr. Anwar Haque for his assistance and Mr. Allen Hilton, for his support and assistance.

From a more personal point of view I would like to acknowledge the support, companionship and patient of my colleague Alan Smith ("uncky" Alan) and thank him for the English lessons! Furthermore, I would like to thank Giouli Stylou, Pepi Paschaloudi, Vassia Souri, Natassa Minopoulou, Katerina Papamanoli, Vasso Papatzelou, Eleni Kiziridou, Vassilis Kalavros, Yiannis Antoniadis and Lampros Galanakis for not forgetting their "emigrant friend! A big thank you to Dr. Vasiliki Evageliou for her friendship and advice even after she went back to Greece. The Greek Community for the unforgettable moments at Silsoe and especially Yiannis Vouros for his songs and the endless evenings with Greek music; Kostas Vasileiou, my crazy housemate, for his support, understanding, friendship, cooking attempts and the lengthy games of backgammon; Elsa Giakoumaki, Stella Mokiou, Pericles Toukioglou, Nikos Lyrakos and Yiannis Ypsilos for the endless lunch and coffee breaks and for keeping me sane and showing me that Silsoe can actually be beautiful! I wish them all the best in their studies here and their personal lives. I could never forget Dr. Stefan Alevisopoulos for his camaraderie, encouragement and excursions with the "limo", as well as Kerensa Broensen for her friendship and support. A big thank you to Julia Kopeika, who, despite the short time of our acquaintance, she has been very supportive. Last but not least, a warm thank you to Dionyssios Melas for his valuable companionship, support and advice and especially for keeping me smiling when everything seemed to have come to a dead-end.

Finally, I would like to thank the people who mean the world to me; my family. My parents Konstantinos and Maria who supported me in every possible way all these years and tolerated my occasionally spontaneous behaviour and especially my brother Dr. George Tsogas, whose friendship was the most precious gift in Great Britain.

«Όσα βουνά κι αν ανεβείτε
απ'τις κορυφές τους θ'αγναντεύετε
άλλες κορφές, ψηλότερες,
μια άλλη πλάση ξελογιάστρα.

Κι στην κορυφή σα φτάσετε την κατάψηλη,
πάλι θα καταλάβετε πως βρίσκεστε
σαν πρώτα, κάτω απ'όλα τ'άστρα...»

Κωστής Παλαμάς

ABSTRACT

In the first stage of the investigation, the effect of high levels of sugars (mixture of 50% sucrose with 35% glucose syrup) on agarose (0.7 wt %) was characterized by low amplitude oscillatory measurements of storage modulus (G'), loss modulus (G'') and loss tangent (tan δ) as well as large deformation techniques. Samples were prepared at 90°C, and measured immediately, or after storage at 5°C. The combined Williams-Landel-Ferry (WLF)/free volume theory was used to derive the glass transition temperature, the fractional free volume, and the thermal expansion coefficient of the glass. Solution of high concentrations of sucrose crystallizes, but addition of the polymer encourages intermolecular interactions, which transform the mixture into a high viscosity glass. The mechanical properties of glucose syrup follow WLF behavior in the glass transition region and revert to an Arrhenius type prediction in the glassy state. Measurements on sugar samples and agarose-sugar mixtures were resolved into a basic function of temperature alone and a basic function of frequency (time) alone. The former traces the energetic cost of vitrification, which increases sharply with decreasing temperature. The latter, at long time scales, is governed by the infinite molecular weight of the agarose network. In the region of short times, the effect of free volume is active regardless of the sample composition.

In a continuation of investigating the significance of polymer-cosolute interactions, the effect of sucrose, glucose, fructose, sorbitol, xylitol, glycerol and ethan-1,2-diol on gelation of high methoxy pectin was studied under different experimental conditions. The main changes in procedure in comparison with the work on agarose were: (i) the polymer concentration was increased from 0.7 to 1.0 wt %, (ii) the mixtures prepared at pH 4 and subsequently acidified to pH 3, rather than being prepared at neutral pH, (iii) the cosolute concentration was varying from 50 to 65 wt % and (vi) the mixtures were studied through rheology, calorimetry and optical rotation. The samples were prepared at 95°C and changes in storage modulus (G') and loss modulus (G'') during cooling to 5°C, heating to 90° and re-cooling to 5°C, at 1°C/min, were measured at 1 rad s^{-1} and 0.5% strain. In all cases, the onset temperature for gelation during cooling and the moduli recorded at 5°C increased with increasing concentration of

cosolute. However, both values were substantially lower for the liquid cosolutes than for mixtures with solid cosolutes at the same concentrations. The difference is attributed to inhibition of pectin-pectin interactions by pectin-cosolute interactions, which in turn are inhibited by cosolute-cosolute interactions. On heating there was an initial reduction in modulus, with the same temperature-course as the increase on cooling; for the solids, this was followed by an increase attributable to hydrophobic association of methyl ester substituents. No such increase was seen with the liquid cosolutes, but DSC studies showed two reversible thermal transitions in all cases, one over the temperature-range of the initial gelation process on cooling and the other coincident with the increase in modulus on heating in the presence of solid cosolutes. The absence of any detectable increase in modulus on heating with the liquid cosolutes is attributed to accumulation of cosolute around the polymer chains promoting hydrophobic association between methyl ester groups on the same chain, or within clusters of chains, with, therefore no contribution to network structure. At high concentrations of the solid cosolutes, the increase in modulus on heating was followed by a decrease at higher temperature; this was attributed to excessive aggregation, and was reflected in lower moduli on subsequent re-cooling to 5°C, in contrast to the enhancement in gel strength after heating and cooling observed at lower concentration of the same cosolutes.

In the presence of fructose as cosolute, calorimetric studies showed an intense endotherm followed immediately by an intense exotherm on heating. These transitions occurred over approximately the same temperature-range as initial gelation on cooling and increased in magnitude with increasing concentration of the sugar. The displacement of both transitions to progressively higher temperature as the rate of heating was increased was much greater than anticipated from a simple thermal lag, indicating that the undelying structural changes are slow. The proposed interpretation is that fructose is capable of site-binding to pectin in both the ordered and disordered state

TABLE OF CONTENTS

CHAPTER 3

PHYSICAL TECHNIQUES AND PHASE TRANSITIONS

CHAPTER 4

THE RUBBER-TO-GLASS TRANSITION IN HIGH SUGAR AGAROSE SYSTEMS

CHAPTER 5

ROLE OF COSOLUTES IN GELATION OF HIGH-METHOXY PECTIN. PART 1. COMPARISON OF SUGARS AND POLYOLS

CHAPTER 6

ROLE OF COSOLUTES IN GELATION OF HIGH-METHOOXY PECTIN. PART 2. ANOMALOUS BEHAVIOR OF FRUCTOSE: CALORIMETRIC EVIDENCE OF SITE-BINDING

The purposes of this work were to establish the significance of polymer-cosolute interactions in the gelation mechanism of two biopolymers, namely agarose and high methoxy pectin.

For the reader to understand better this work, it is necessary to explain its structure. Chapter 1 deals with carbohydrates in order to give a general view of the nature of such an important group of natural polymers. Their structure, properties and mechanisms of solubilisation and gelation are thoroughly examined, thus allowing a better comprehension of the behaviour of the biopolymers investigated in the presented work. In a continuation of this, Chapter 2, refers in detail to agarose and pectin and Chapter 3, is about the techniques used to investigate these two biopolymers in the presence of cosolutes.

In Chapter 4 we examined highly concentrated systems of agarose (0.7 wt %) in the presence of high levels of cosolutes (50 wt % sucrose and 35 wt % glucose syrup). Cosolutes inhibit excessive intermolecular aggregation and allow the concentrated system to undergo vitrification at subzero temperatures. Its characteristics were examined through the combined WLF/free volume theory, which was initially applied to synthetic polymers.

In a continuation of the work, high methoxy pectin (1.0 wt %) was investigated in the presence of various cosolutes at concentrations varying from 50 to 65 wt %. Both the sugars and the sugars alcohols used, promote gelation by binding to water, thus decreasing the amount of available solvent for pectin to remain in the disordered state. However, their interactions with the polymer determine the character of the resulting system. Cosolutes that condense non-specifically or accumulate around pectin helices are examined in Chapter 5, whereas Chapter 6 refers to those, which specifically bound to both the disordered and ordered state of pectin and alter the character of the produced gel.

CHAPTER 1

BIOPOLYMERS

1.1. INTRODUCTION

Carbohydrates and proteins are the principal groups of natural polymers. These biopolymers share certain properties such as water binding and hydration, viscosity, gelation, emulsification and foaming ability, all of which are exploited in food product applications.

1.2. PROTEINS

Proteins are essential to life; they are involved in body structure, the immunological defence system and part of the hormones. They are composed of different amino acids, which are linked together with peptide bonds. The structure of an amino acid is shown in Figure 1.1 where the central carbon atom is called the α carbon and the R group represents the side chain. With the exception of glycine, where R is a hydrogen atom, the α-carbon atom in amino acids is asymmetric. R may be a simple alkyl group; however it can also be a more complex structure containing a second carboxyl or amino group or even an aromatic ring structure (Regenstein & Regenstein, 1984).

The first categorisation of proteins distinguishes them between simple and combined ones. The formers are composed solely of amino acids, whereas the latter include proteins which have other chemical compounds attached, such as carbohydrates and lipids. Examples of this category are the glycoproteins, which contain carbohydrates, the lipoproteins (which essentially behave like proteins) and the proteolipids (which generally act as lipids), the chromoproteins, which contain chromophores that absorb in the visible light region and are

coloured, and the metalloproteins, where a metal group is attached (Regenstein & Regenstein, 1984).

Another classification of proteins divides them into two major categories: globular proteins, which have a compact molecular structure, and fibrous proteins, which exist in nature as extended filaments (Van Holde, 1977; Regenstein & Regenstein, 1984).

According to the structural organisation of proteins we distinguish four levels, with only the first two applying to fibrous proteins:

1. primary structure (the sequence of amino acid along the protein chain)
2. secondary structure (the local configuration of chain sequences into helixes, sheets, bends, or stretches with irregular geometry)
3. tertiary structure (the overall three dimensional arrangement of the polypeptide chain within the globule) and
4. quaternary (association of individual globules into larger structures).

1.3. CARBOHYDRATES

Carbohydrates, or "hydrates of carbon", usually have the formula $C_n(H_2O)_n$ which explains the origin of their name, where n is 3 or more. They are polyhydroxy aldehydes or ketones or compounds that can be hydrolysed to them. According to the number of individual saccharide units they contain, carbohydrates (Rees, 1977; Alexander, 1998; Sutton et al., 2000) are classified into three main categories:

- monosaccharides
- oligosaccharides and
- polysaccharides

1.3.1. Monosaccharides

Monosaccharides are the simplest group of carbohydrates and most of them are referred to as "sugars" or " sweeteners" due to their sweet taste, which varies from sugar to sugar

(Alexander, 1998). They have three to eight carbon atoms, but the common ones are these with five or six. The suffix "-ose" is included in the names of monosaccharides that have a carbonyl group and are sugars (Coultate, 1993; Alexander, 1998), and the number of carbon atoms is indicated by terms such as triose, tetrose and pentose. Furthermore, the prefixes "aldo-" and "keto-" show whether the carbonyl group is at the first or a subsequent carbon atom (Coultate, 1993). "Aldo" sugars are called aldoses and if they contain six carbons are called aldohexose, while "keto" sugars are called ketoses and a ketose with five carbon atoms is called ketopentose (Sutton et al., 2000). A common pentose is xylose and common hexoses are glucose and fructose (in the "aldo" and "keto" forms, respectively).

Figure 1.2 shows glucose and fructose in a two-dimensional view known as the Fischer projection, which does not give any information about the conformation of the molecules in three dimensions (Alexander, 1998). To obtain information about the three-dimensional conformation of the molecules, we must look at their stereochemistry. Stereoisomers are compounds that have the same molecular formula but which can exist in two different, non-superimposable, mirror image forms, identified as D and L. In aqueous solution, both isomers rotate the plane of polarised light by the same amount, but in opposite directions. If the rotation is to the right, the isomer is called "dextrorotary", whereas if the rotation is to the left the isomer is known as "laevorotary" (Rees, 1977; Coultate, 1993; Alexander, 1998; Sutton et al., 2000). Sugars are classified as D or L according to the configuration of the penultimate carbon atom (e.g. at C(5) for hexoses). Sugars in the D series are usually, but not invariably, dextrorotatory and conversely L sugars are usually, but not always, laevorotatory. Almost all naturally occurring monosaccharides belong to the D-series (Coultate, 1993), apart from L-rhamnose and L-fucose (Rees, 1977), but other L-sugars occur in polysaccharides (e.g. L-guluronate in alginate and 3,6-anhydro-L-galactose in agar).

Apart from the symbols D- or L-, (+) and (-) are used to denote rotation to the right or the left, respectively. The unfashionable names of dextrose and laevulose stem from the dextrorotatory and laevorotatory properties of D-(+)-glucose and D-(-)-fructose, respectively (Coultate, 1993).

Over the years, chemists have synthesised innumerable derivatives of monosaccharides. Reduction of the carbonyl group to a hydroxyl gives sugar alcohols such as xylitol and sorbitol. Oxidation of the hydroxymethyl (CH_2OH) group to COOH gives uronic acids, which frequently occur in natural polysaccharides.

When a carbohydrate is composed of five or six carbon atoms it exists in nature as a ring form. The aldehyde or ketone group interacts with one of the hydroxyl groups of the carbon chain and the result is a cyclic hemiacetal or a cyclic hemiketal, respectively (Alexander, 1998; Sutton et al., 2000). The reacting groups may be only four carbons apart, where a five-membered ring with one oxygen, known as a furanose ring, is produced. Alternatively, the reacting groups may be five carbons apart, in which case a six-membered pyranose ring is formed. The terms "pyranose" and " furanose" come from the compounds pyran and furan, whose structures are shown in Figure 1.3.a and Figure 1.3.b, respectively (Coultate, 1993). The hemiacetal or hemiketal bond produced is easily broken and is in equilibrium with the open chain form (Sutton et al., 2000). The carbon atom that was previously in the ketone or aldehyde form and has interacted to form the ring structure, is known as the "anomeric" carbon, and becomes a stereocenter or chiral centre (its bonding groups can have different spatial orientations). In this case, the hydroxyl groups can have two different orientations. The form in which the hydroxyl group is in the "up" position in the flat-ring (Haworth) projection shown in Figures 1.4 and 1.5 is known as the β anomer; in the α anomer the hydroxyl group is in the "down" position (Coultate, 1993; Alexander, 1998; Sutton et al., 2000).

Due to the stereochemistry of carbon and oxygen, sugar rings cannot be planar. In the case of a furanose ring, there are two most probable shapes, which respectively have four of the ring atoms coplanar and the fifth atom out of the plane, and three of the ring atoms coplanar with two out of the plane: the envelope and the twist forms (Figures 1.6a,b). It appears that furanoses in solution are an equilibrium of rapidly interconverting forms such as these that do not differ greatly from each other (Rees, 1977; Coultate, 1993).

There are two possible configurations of the pyranose ring that retain unstrained tetrahendral bonding. These are the so-called "boat" and "chair" forms illustrated in Figure 1.7. In the $^{1,4}B$ boat form, carbons 1 and 4 are pitched upwards from the central plane of

the ring (when viewed in the conventional projection shown in the figure). An inverse form ($B_{1,4}$) is also possible, where the so-called bow and stern carbons are turned downwards. Both, however, are highly unstable, because of the eclipsing of the bonds across the C(2)-C(3) and C(5)-O(5) linkages and steric compressions between the inward-pointing "masthead" substituents on C(1) and C(4). Neither problem arises in the chair conformations, where the bonds are fully staggered and C(1) and C(4) point away from one another. The chair form in which C(1) lies above the plane of the ring and C(4) points downwards is denoted as $^{1}C_{4}$, and the converse arrangement is designated $^{4}C_{1}$.

In both chair conformations, the hydrogen atoms and OH groups at each of the ring carbons are present either in well-separated *equatorial* positions, pointing away from the ring, or in more crowded *axial* positions above or below the ring (Figure 1.8). Changing from one chair form to the other converts all axial groups to equatorial and all equatorial groups to axial. The relative stability of the two chair conformations is dominated by the energetic advantage of having the bulky C(6) group oriented equatorially, free of steric compressions. For sugars in the D series, this requirement is satisfied by adoption of $^{4}C_{1}$ geometry; in the mirror-image L series, where the absolute stereochemistry at the position of the ring-closure, C(5), is reversed, the corresponding stable arrangement is $^{1}C_{4}$.

In the stable chair conformation ($^{4}C_{1}$ (D) or $^{1}C_{4}$ (L)) (Figure 1.9) the hydroxyl group at C(1) is axial for the α configuration and equatorial for β. The identity of the sugar depends on the configuration at C(2), C(3) and C(4) (with eight possible combinations, only, five of which occur in nature). In glucose (and its derivatives) O(2), O(3) and O(4) are all equatorial; O(2) is axial in mannose; O(4) is axial in galactose; O(3) and O(4) are both axial in gulose (which occurs as L-guluronic acid in alginate); all three are axial in idose (found as L-iduronate in heparin and related animal polysaccharides, but not in plant or bacterial polysaccharides available commercially).

1.3.2. Sugar alcohols (Polyols)

As mentioned above, sugar alcohols, or polyols, are produced via the reduction of the carbonyl group to a hydroxyl. They are synthesised industrially by reduction of the

corresponding aldose sugar with hydrogen (Coultate, 1993; Sutton et al., 2000). Polyhydric alcohols (or polyols), as they are also known, are carbohydrate derivatives that contain only hydroxyls as functional groups. Therefore, they are generally water-soluble, hygroscopic materials that exhibit moderate viscosities at high concentrations in water. Their use in food is constantly growing, because of demand for their reduced-calorie sweetener properties (Lindsay, 1996). Their polyhydroxy structure provides them with water-binding properties. Other specific properties include control of viscosity and texture, retention of moisture, reduction of water activity, control of crystallisation, improvement or retention of softness, improvement of rehydration properties of dehydrated foods, addition of bulk and use as a solvent for flavour compounds. Sugar alcohols are generally sweet, but less so than sucrose, and short-chain members, such as glycerol, are slightly bitter at high concentrations. As they are characterised by a negative heat of solution when they are consumed in the dry form, they contribute a pleasant cooling sensation (Lindsay, 1996).

Among the most well known and widely used polyols there are xylitol, sorbitol and mannitol. The polyols used in the work reported in this thesis were sorbitol, xylitol, glycerol, and ethan-1,2-diol. Mannitol and erythritol were excluded because of crystallisation problems.

Sorbitol

Sorbitol, also known as D-glucitol, is a sugar alcohol with 6 carbon atoms, originating from D-glucose. It is a sugar replacer or sweetener with 60% more sweetness and 50% fewer calories than sucrose. It maintains moisture in candies and provides taste and body in sugar-free sweets and chewing gums (IFT, 2000). The conversion of glucose to sorbitol is shown in Figure 1.10, and is accomplished by reaction with gaseous hydrogen using a metal catalyst such as nickel or palladium (Alexander, 1998).

Xylitol

Xylitol, a 5 carbon atom natural sweetener (Figure 1.11), is derived from xylose by reduction. It is equivalent to sucrose in sweetness, but does not cause tooth decay and is

safe for diabetics. Apart from the conventional way of production by hydrogenation of xylose from wood fibre, xylitol can be obtained through biocatalysis. The microorganism used is a yeast-like fungus *Pichia guilliermondii (Candida guilliermondii,* asexual state), which has the benefit of high yields with almost no production of ethanol (Leathers &Dien, 2000).

Glycerol and Ethan-1,2-diol

Glycerol, or propan-1,2,3-triol, is a liquid polyol with 3 carbon atoms and 3 hydroxyl groups (Figure 1.12), which can be esterified. As any other short-chain member of the polyols, it exhibits a slightly bitter taste when used at high concentrations (Lindsay, 1996). Ethan-1,2-diol is also a liquid polyol, but with 2 carbon atoms and 2 hydroxyl groups.

1.3.3. Oligosaccharides

Oligosaccharides contain up to approximately 10 monosaccharide units. The prefix "oligo" comes from the Greek word "ολιγο-" which means "few". The constituent monosaccharides are joined together by condensation of the hydroxyl group on the anomeric carbon atom of one sugar with any hydroxyl group on the next, with formal elimination of a molecule of water. Chemically, the hemiacetal or hemiketal of the first monosaccharide is converted to, respectively, an acetal or ketal. The linkages formed in this way between consecutive sugars are known as glycosidic bonds.

When a disaccharide is composed of two identical monosaccharides, there are numerous possible structures. The most abundant disaccharide is sucrose: α-D-glucopyranosyl-(1→2)-β-D-fructofuranose (Figure 1.13). As the glucose and fructose units are joined through, respectively, their hemiacetal and hemiketal groups, conversion to the open chain form, with a free carbonyl group, cannot occur, and sucrose is not, therefore, a reducing sugar. Under mildly acid conditions or the action of the enzyme invertase, sucrose is readily hydrolysed to its component monosaccharides (Figure 1.14). This phenomenon is termed inversion and the resulting mixture invert sugar, due to the effect of the hydrolysis on the optical rotation properties of the solution. Another well-known disaccharide is

lactose, the sugar of milk, which is β-D-galactopyranosyl-(1→4)-α-D-glucopyranose (Figure 1.15). Because the glucose ring is still in the hemiacetal form (i.e. with an OH group on the anomeric carbon atom), capable of converting to a carbonyl group in the open chain form, lactose is a reducing disaccharide (Coultate, 1993).

When a glycosidic link connects the reducing group of one monosaccharide to one of the hydroxyl groups of another, the resulting compound is a disaccharide. Further such linkages will produce trisaccharides, tetrasaccharides and ultimately polysaccharides (Coultate, 1993).

1.3.4. Polysaccharide types

Polysaccharides occur widely in nature. Those used in commerce and industry are isolates from terrestrial and marine plants or produced by chemical modification of natural polysaccharides, and a few are the product of total biochemical synthesis (Table 1). In the food industry, polysaccharides have numerous applications as thickeners, stabilisers and gelling agents.

Polysaccharides can be classified in many different ways. Obvious possibilities includes division into charged and uncharged; branched and unbranched; homopolymeric (i.e. containing only one type of monosaccharide) or heteropolymeric (with two or more different types of monosaccharide). They can also be classified by source: land plants; marine algae (seaweeds); animals; bacteria and fungi, or by biological function: structural rigidity (e.g. cellulose and chitin); energy storage (e.g. starch; glycogen; seed galactomannans); wound repair (e.g. gum arabic and related exudates); crosslinking and hydration of soft tissue (e.g. alginate; pectin; carrageenan; agar) and environmental control (xanthan and perhaps gellan)

Another method of classification is by the monosaccharides present and the way in which they are linked together. Major categories of polysaccharides, grouped by this method of chemical classification, include the following.

α-D-Glucans

This group contains the non-reducing glucose polysaccharides formed by α-D-glucopyranosyl residues (Coultate, 1993). The most prominent representatives are starch and its derivatives, dextran (a structurally heterogeneous glucan containing linear and branched sequences with a dominance of 1→6 and a smaller percentage of 1→2, 1→3 and 1→4 linkages) and pullulan, a linear, water-soluble polysaccharide containing repeating trimers of 1,4-α-D-glucopyranose and 1,6-α-D-glucopyranose in a 2:1 ratio (Aspinall, 1983).

β-(1→4)-Glucans

This category contains cellulose and its derivatives, and the galactomannans and glucomannans. The latter are represented by locust bean gum and guar gum (1,4-β-D-mannan with 1,6-α-D-galactose substituents) and konjac gum, a 1,4-β-D-glucomannan, with glucose and mannose residues both occurring in the polymer backbone. These gums are notable for showing synergistic interactions with other polysaccharides (xanthan; carrageenan; agar) and for their tendency to self-associate (Walter, 1998).

Fructans

In this class, fructose is the repeating monomer. The main fructans are inulin, which is found significantly in dahlia tubers, onions, garlic and Jerusalem artichoke and levan, a branched isomer of inulin (Aspinall, 1983).

Glycuronans

These are polymers of uronic acids (which at neutral pH, exist in the charged, uronate form); they are also known as polyuronates. The polyuronates of importance in the food industry are alginate and pectin. Alginate is (1→4)-linked linear co-polymer of β-D-mannuronate and α-L-guluronate, with residues arranged in long homopolymeric blocks of each type (poly-D-mannuronate and poly-L-guluronate), and in heteropolymeric blocks

with the two sugars arranged in an approximately (but not exactly) alternating sequence. It forms gels by chelation of Ca^{2+} ions between poly-L-guluronate chains (Painter, 1983).

The primary structure of pectin is based on homopolymeric sequences of (1→4)-linked α-D-galacturonate (almost the mirror image of the poly-L-guluronate sequences in alginate), but with some of the carboxyl groups occurring as methyl esters (Christensen, 1986). The percentage of carboxyls that are substituted in this way in known as the "degree of esterification" (DE). The structure and properties of pectin are discussed in greater detail in the following chapter.

(1→3), (1→4)-linked galactans

These include two families of algal polysaccharides used widely as food hydrocolloids: carrageenans and agars. The carrageenans have a primary structure based on a linear alternating sequence of α-D-galactose linked at positions 1 and 4 and β-D-galactose linked at positions 1 and 3, with different degrees and patterns of sulphation (Painter, 1983). In the gelling carrageenans available commercially (iota and kappa), the (1→4)-linked residues occur predominantly as the 3,6-anhydride; closure of the anhydride bridge requires conversion of ring geometry from $^4C_1$ to $^1C_4$, with consequent conversion of the bonds at C(1) and C(4) from diaxial to diequatorial. This allows the chains to form coaxial double helices, which is a necessary requirement for gelation (Rees et al., 1982). In lambda carrageenan, which is also available commercially, the anhydride bridge is absent, preventing helix formation and gelation; it is therefore used as thickener, but not as a gelling agent (Towle, 1973).

In the gelling polysaccharides of the agar series, the (1→4)-linked residue also exists predominantly at the 3.6-anhydride, but is in the L-configuration rather than D. As a consequence, the double helices in agar gels have left-handed geometry, in contrast to the right-handed helix structure adopted by carrageenans (Arnott et al., 1974; Millane et al., 1988). The parent member of the agar series is agarose, which is an unsubstituted neutral galactan. Agarose helices, being uncharged, associate readily into large aggregates, which cause thermal hysteresis between gelation and melting and reverse gel strength (Dea, 1989). Natural agars occur with different degrees of sulphation (lower than in

carrageenans), and may also have other substituents such as *O*-methyl and pyruvic acid ketal. These inhibit aggregation, with consequent reduction in gel strength and in extent of hysteresis (Guiseley, 1970).

Complex repeating sequences

Some polysaccharides of plant origin, notably gum arabic, have complex primary structures, but these arise from enzymic modification after initial biosynthesis (Aspinall, 1983), and are normally irregular and non-repeating. Bacteria, however, are capable of synthesising structurally regular polysaccharides with large oligomeric repeating units. Succinoglycan, which is produced commercially but is not allowed for food use, has an octasaccharide repeating sequence. The two food-allowed materials of this type are xanthan and gellan.

Xanthan has a (1→4)-linked β-D-glucan backbone (as in cellulose), but this is solubilised by charged trisaccharide sidechains of:

β-D-Man*p*-(1→4)- β-D-Glc*p*A-(1→2)-α-D-Man*p*-(1→

attached at O(3) of alternate glucose residues. The inner and outer mannose residues of the sidechains are substituted, non-stoichiometrically, with, respectively, acetyl at O(6) and 4,6-linked pyruvic acid ketal. Xanthan forms pourable "weak gel" networks by packing of the sidechains along the polymer backbone, to give ordered helices which associate weakly in solution (Morris, 1984).

Gellan has a linear tetrasaccharide repeating sequence (Jansson et al., 1983) of:

→3)-β-D-Glc*p*-(1→4)-β-D-Glc*p*A-(1→4)-β-D-Glc*p*-(1→4)-α-L-Rha*p*-(1→

The polymer is biosynthesised with an L-glyceryl substituent on O(2) of the 3-linked glucose and, in at least a proportion of the repeat units, an acetyl group on O(6) of the same residue (Kuo et al., 1986). In normal production of commercial gellan gum, however, both substituents are removed almost completely by exposure to alkali. Gelation of gellan gum

(Baird et al., 1992) occurs by formation of 3-fold double helices (Chandrasekaran et al., 1988) similar to those of carrageenan, which associate further in the presence of appropriate metal cations (Mg^{2+}; Ca^{2+}; Na^{+}; K^{+}).

From a broader viewpoint, Rees (1977) classified polysaccharide primary structures into the following categories:

- Periodic sequence: the sugar units are arranged in a repeating pattern along the chain, e.g. amylose and cellulose.
- Interrupted sequence: the sugars also have a repeating sequence, although separated or interrupted by departures from regularity, e.g. alginates and carrageenans.
- Aperiodic sequence: these are characterised by irregular sequences, linkage positions, or occasionally configurations. Sometimes the structure is composed of a number of short sugars chains; thus the overall molecule is branched, e.g. the carbohydrate sequences in immunoglobulin IgG.

1.3.5. Polysaccharides conformations

The shape (conformation) of polysaccharide chains is determined by rotation about the bonds in the glycosidic linkage between adjacent residues. The angles of rotation about the bonds are denoted by the Greek letters φ and ψ, as shown in Figure 1.16 for cellobiose; however, an extra angle, symbolized as ω, is used when the linkage is through the –OH group at C(6), as in the case of dextran. Polysaccharides in solution normally exist as disordered coils with φ and ψ (or φ, ψ and ω) fluctuating continually. In the ordered state of polysaccharides, both φ and ψ angles are constant, which results in a regular repeating chain shape. The values of φ and ψ for such ordered structures can be determined by X-ray fibre diffraction (Rees, 1977).

The nature of the ordered state is mainly controlled by the orientation of the bonds to and from the constituent monosaccharide rings. Linkage patterns can be classified as follows:

- **Equatorial bonds at C(1) and C(4)**: in this case the linkages are parallel and slightly offset from each other, giving extended ribbons in the ordered state and expanded coils in solution (e.g. galactomannans).

- **Axial bonds at C(1) and C(4)**: the linkages are parallel but offset from each other by the full width of the sugar ring. The resulting ordered geometry has the shape of a buckled ribbon, characteristic of the poly-D-galacturonate sequences of pectin and poly-L-guluronate sequences of alginate.
- **One axial and one equatorial bond between C(1) and C(4) or equatorial linkages between C(1) and C(3)**: both types of linkages lead to hollow helix ordered structures as for example in the case of amylose (first pattern) and curdlan (second pattern).
- **Bonds between C(1) and C(6)**: ordering of these chains is extremely difficult due to the linkage flexibility.
- **Bonds between C(1) and C(2)**: as these positions are neighboring to each other, severe steric obstructions are developed, giving contorted chain geometry.

Consequently, according to the above classification (Rees, 1977), polysaccharides are divided into four different chain families:

- Ribbon family with equatorial bonds at C(1) and C(4) or axial bonds at C(1) and C(4),
- Hollow helix family with one axial and one equatorial bond at C(1) and C(4) or equatorial linkages at C(1) and C(3),
- Loosely joined family with bonds at C(1) and C(6), and
- Crumpled family with bonds at C(1) and C(2).

1.3.6. Polysaccharide solubility

The majority of polysaccharides contain glycosyl units with three hydroxyl groups available for hydrogen-bonding to water. Furthermore, both the ring oxygen atom and the glycosidic oxygen atom that connects one sugar ring to another can also form hydrogen bonds with water molecules. Consequently, glycans exhibit a strong affinity for water and often hydrate readily (BeMiller & Whistler, 1996). However, the degree of solubility in water depends on the structure and conformation of the polysaccharide. Charged molecules are more water-soluble because of the electrostatic repulsions between the chains. Moreover, the presence of branches on the chain backbone increases the solubility as they increase the entropy for the disordered conformation in solution. Flexible polymer chains are also more water-soluble (Rees et al., 1982).

Once hydrated, polysaccharides control and modify the mobility of water in food products and, simultaneously, water influences significantly the physical of the polymer. Together they determine the functional properties of most food systems, including their texture (BeMiller & Whistler, 1996).

The hydration water, which makes up only a small part of the total water in gels and fresh tissue in foods, is naturally hydrogen bonded to polysaccharide molecules. Moreover, its structure is sufficiently modified by the presence of the molecule that it will not freeze; it is also referred as plasticizing water. These water molecules, however, are not permenantly bound to the polymer. It appears that, although their motions are retarded, they are able to exchange freely and rapidly with other water molecules (BeMiller &Whistler, 1996).

1.4. GELATION OF BIOPOLYMERS

Biopolymer gels consist of a continuous network of macromolecules interspersed by a liquid, usually water. The liquid prevents the polymer network from collapsing into a compact mass and the network assures that the liquid will not flow away. The network is built up by crosslinking of the biopolymer chains. Polymer gels can be divided into two main categories:

- **Chemical gels**: macromolecules crosslinked by covalent bonds between certain atoms of the chain, which are permanent and cannot be broken by heat. Therefore, chemical gels are thermally irreversible (Braudo & Plaschina, 1995)

- **Physical gels**: characteristic of thermo-reversible gels formed from both synthetic and biological macromolecules. Their formation is attributed to the development of non-covalent crosslinking involving intermolecular junction zones (Ross-Murphy, 1991).

The non-covalent interactions include hydrogen bonding, dipolar interactions, van der Waals forces, anion-cation interactions and hydrophobic interactions. Each one of the above-mentioned bonds is weak, but when they act together they co-operate, and the result s a strong junction zone. Nevertheless, the junction zones are weaker than the covalent ond in chemical gels; thus the gels are often thermally reversible. In addition, both the

number of junction zones and their position may fluctuate with time and temperature (Ross-Murphy, 1991).

Formation of physical gels can be induced by changes in temperature, pH, ionic strength, and type of ions present in the solution, and by introduction of co-solutes, as studied in the work reported in this thesis. The state and properties of the resulting gels are also affected by changes in the above-mentioned conditions. Since the formation and dissociation of the junction zones are chemical processes, they are governed by the second law of thermodynamics:

$$\Delta G = \Delta H - T\Delta S \qquad (1.1)$$

where ΔH is the enthalpy change of the system, ΔS is the entropy change of the system, T is absolute temperature and ΔG is the free energy of the reaction (Sutton et al., 2000). The second law of thermodynamics provides information regarding the probability of spontaneous changes in the physical state (Roos, 1995). For a reaction to proceed, ΔG must be negative (i.e. the overall free energy of the system must decrease).

In normal polysaccharide gelation, by conversion of disordered chain sequences into ordered junctions, there is a loss of conformational freedom, giving a reduction in entropy (i.e. ΔS is negative, and the contribution to ΔG from $-T\Delta S$ is therefore positive). For junction formation to occur, this positive contribution must be outweighed by a larger, negative value of ΔH (corresponding to the heat released on formation of non-covalent bonds between the chains). Raising the temperature increases the relative importance of entropy (i.e. increases $-T\Delta S$), and thus promotes melting; conversely, decreasing temperature increases the relative importance of enthalpic interactions (bonding) and therefore promotes formation of intermolecular junctions. The mid-point temperature of the transition (T_m) comes when these two opposing factors are in exact balance (i.e. when $\Delta H = T\Delta S$). Thus T_m is related to ΔG and ΔH by:

$$T_m = \Delta H / \Delta S \qquad (1.2)$$

For hydrophobic gelation, the effect of temperature is reversed. The dominant entropic factor is not loss of conformational freedom by the polymer chains, but the reduction in potential partners for hydrogen-bonding, and consequent loss of combinatorial entropy,

when an apolar group is inserted into an aqueous environment. The reduction in entropy becomes progressively more significant as temperature is increased, and can result in apolar groups ("hydrophobic substituents") clumping together to minimize contacts with water.

Often, the way in which biopolymers gel can be related (Morris, 1986) to their biological function:

- **Storage materials**: these have compact, ordered structures. To gel they must be heated and subsequently cooled. The resulting gels are thermally irreversible (e.g. starch, egg proteins);

- **Structural materials**: these are biopolymers whose role is to generate structure in plant and animal tissues. They gel during cooling through a reversible process, or may be "persuaded" to gel by changes in ionic environment (e.g. pectins; gelatin).

Gel formation requires a balance between sufficient polymer-polymer interactions to develop a cohesive long-range network, and sufficient polymer-solvent interaction to prevent the network collapsing to an insoluble precipitate (Morris, 1986; Morris, 1987). A schematic representation of how this balance is achieved for many naturally-occurring polysaccharides is shown in Figure 1.17.

Co-existence of "soluble" (disordered) and "insoluble " (ordered) regions within the same chain can occur in a variety of ways. The simplest is when the primary sequence is of the block co-polymer type, incorporating regions which, in isolation, would be insoluble, together with others that are soluble under the same conditions. This is the case for calcium alginate gels, where poly-α-L-guluronate associates with calcium ions to form junction zones, while the poly-β-D-mannuronate and mixed mannuronate and guluronate chain sequences remain soluble in the presence of calcium. Equally, an irregular or block-wise distribution of short sidechains along the polysaccharide backbone can provide the appropriate balance between interchain association in unsubstituted or sparingly substituted regions of the molecule, and solubilisation from more heavily substituted regions where side chains present a physical and entropic barrier to ordered packing. An example of this is the effect of number and distribution of galactose residues on the interaction properties of galactomannans (Morris, 1987).

According to Flory-Stockmayer theory, for a polymer having *f* potential binding sites per hain, there is a critical proportion of them, α_c that must react before a continuous network an be formed:

$$\frac{1}{f-1} = a_c \qquad (1.3)$$

For values of α less than α_c, only aggregates of limited size can exist. However, as soon as x reaches α_c, the largest aggregate (i.e. with most sites for further binding) becomes the 'gel fraction". At this point, which is called the gel point, the viscosity and weight-average molecular weight depart to infinity, although various sizes of clusters can be found. As gelation progresses beyond α_c, the number of aggregates of finite size decreases and eventually goes to zero. As the degree of crosslinking increases, the rigidity of the gel rises sharply up to a point where equilibrium between bond making and breaking has been achieved. However, complete association can lead to a solid precipitate rather than a hydrated network, and therefore maximum gel strength is attained at lower degrees of crosslinking (Morris, 1995).

REFERENCES

Alexander, R. J. (1998). *Sweeteners: Nutritive*. Eagan Press. USA:

Arnott, D., Fulmer, A., Scott, W. E., Dea, I. C. M., Moorhouse, R. & Rees D. A. (1974). The agarose double helix and its function in agarose gel structure. *Journal of Molecular Biology*, **90**, 269-284.

Aspinall, G. O. (1983). *The Polysaccharides vol.2*. Academic Press. USA.

Baird, J. K., Talashek, T. A. & Chang, H. (1992). Gellan gum: effect of composition on gel properties. In G. O. Phillips, P. A. Williams & D. J Wedlock, *Gums and stabilisers for the Food Industry 6*, IRL Press, Oxford, pp.479-487..

BeMiller, J. N. & Whistler, R. L. (1996). Carbohydrates. In O. R. Fennema, *Food Chemistry*, Marcel Dekker, New York, pp. 157-223.

Braudo, E. E. & Plashchina, I. G. (1995). Mechanical properties of thermo-reversible gels in relation to their structure and the conformations of their macromolecules. In E. Dickinson & E Lorient *Food Macromolecules and Colloids*, The Royal Academy of Chemistry, UK, pp. 480-487.

Chandrasekaran, R., Millane, R. P., Arnott, S. & Atkins, E. D. T. (1988). The crystal structure of gellan. *Carbohydrate Research*, **175**, 19881-15.

Christensen S. H. (1986). Pectins. In M. Glicksman, *Food Hydrocolloids, vol. III*, CRC Press, USA, pp. 205-230..

Coultate, T. P. (1993). *Food: The Chemistry of its Components*. Cambridge, UK: Royal Society of Chemistry.

Dea, I. C. M. (1989). Industrial Polysaccharides, *Pure and Applied Chemistry*, **61**, 1315-1322.

Guiseley, K.B. (1970). The relationship between methoxyl content and gelling temperature of agarose. *Carbohydrate Research*, **13**, 247-256.

Institute of Food technologists, News Release, August 2000 http://ift.micronexx.com/INDEX.SEARC.../990107.shtml?L+mystore (01-08-2000)

Jansson, P. E., Lindberg, B. & Sandford, P. A. (1983). Structural studies of gellan gum, an extracellular polysaccharide elaborated by *Pseudomonas elodea*. *Carbohydrate Research*, **124**, 135-139.

Kuo, M. S., Mort, A. J. & Dell, A. (1986). Identification and location of L-glycerate, an unusual acyl substituent in gellan gum. *Carbohydrate Research*, **156**, 173-187.

Leathers, T. D. & Dien, B. S. (2000). Xylitol production from corn fibre hydrolysates, by a two-stage fermentation process. *Process Biochemistry*, **35**, 765-769.

Lindsay, R. C. (1996). Food additives. In O. R Fennema, *Food Chemistry*, Marcel Dekker, New York, pp. 767-823.

Millane, R. P., Chandrasekaran, R., Arnott, S. & Dea, I. C. M. (1988). The molecular structure of kappa-carrageenan and comparison with iota-carrageenan. *Carbohydrate Research*, **182**, 1-17.

Morris, E. R. (1984). Rheology of hydrocolloids. In G. O. Phillips, D. J. Wedlock & P. A. Williams, *Gums and Stabilizers for the Food Industry 2*, Pergamon Press, UK, pp. 57-77.

Morris, E.R. (1987). Rheology and processing of polysaccharide systems. In S. S Stivala, V. Crescenzi & I. C. M. Dea, *Industrial polysaccharides: The impact of biotechnology and advanced methodologies*, Gordon & Breach Science, Amsterdam, pp. 431-457.

Morris, E. R. (1995). Polysaccharide rheology and in-mouth perception. In A. M. Stephen, *Food Polysaccharides and their Applications*, Marcel Dekker, USA, pp. 517-545.

Morris, V. J. (1986). Gelation of polysaccharides. In J. R. Mitchell & D. A. Ledward, *Functional Properties of Food Macromolecules*, Elsevier Applied Science, UK, pp. 121-170.

Painter, T. J. (1983). Algal Polysaccharides. In G. O. Aspinall, *The Polysaccharides vol. 2*, Academic Press, USA, pp. 196-285.

Rees, D. A. (1977). *Polysaccharide Shapes*, Chapman and Hall, London.

Rees, D. A., Morris, E. R., Thom, D. & Madden, J. K. (1982). Shapes and interactions of carbohydrate chains. In G. O. Aspinall, *The Polysaccharides vol.1*, Academic Press, New York, pp. 195-290.

Regenstein, J. M. & Regenstein, C. E. (1984). *Food Protein Chemistry*, Academic Press, New York.

Roos, Y. H. (1995). *Phase Transitions in Foods*, Academic Press, USA.

Ross-Murphy, S. B. (1991). Concentration dependence of gelation time. In E. Dickinson, *Food Polymers, Gels and Colloids*, The Royal Society of Chemistry, UK, pp. 357-368.

Sutton, R., Rockett, B. & Swindells, P. (2000). *Chemistry for the life sciences*, Lifelines, London.

Towle, G. (1973). Carrageenan. In R. L. Whistler & J. N. BeMiller, *Industrial Gums: Polysaccharides and their derivatives*, Academic Press, New York, pp. 84-121.

Van Holde, K. E. (1977). Effect of amino acid composition and microenvironment on protein structure. In J. R. Whitaker & S. R Tannenbaum, *Food Proteins*, AVI Publishing Company, USA, pp. 1-13.

Walter, R. H. (1998). *Polysaccharide Dispersions: Chemistry and Technology in Food*, Academic Press, USA.

'able 1: Origin of polysaccharides (from Walter, 1998).

Source	Polysaccharides
Terrestrial plants	Starch, cellulose, inulin guar, karaya, pectin
Marine plants	Agar, algin, carrageenan, furcellaran
Bacteria	Xanthan, gellan, curdlan, dextran, cellulose
Fungi	Pullulan
Derivatisation	Carboxymethylcellulose (CMC), methylcellulose
Synthesis	Cyclodextrins, polydextrose
Animals	Glycogen, hyaluronic acid, chitin

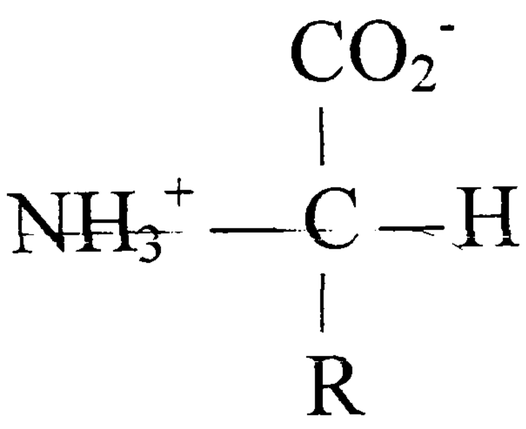

Figure 1.1. Structure of an amino acid (from Regenstein & Regenstein, 1984)

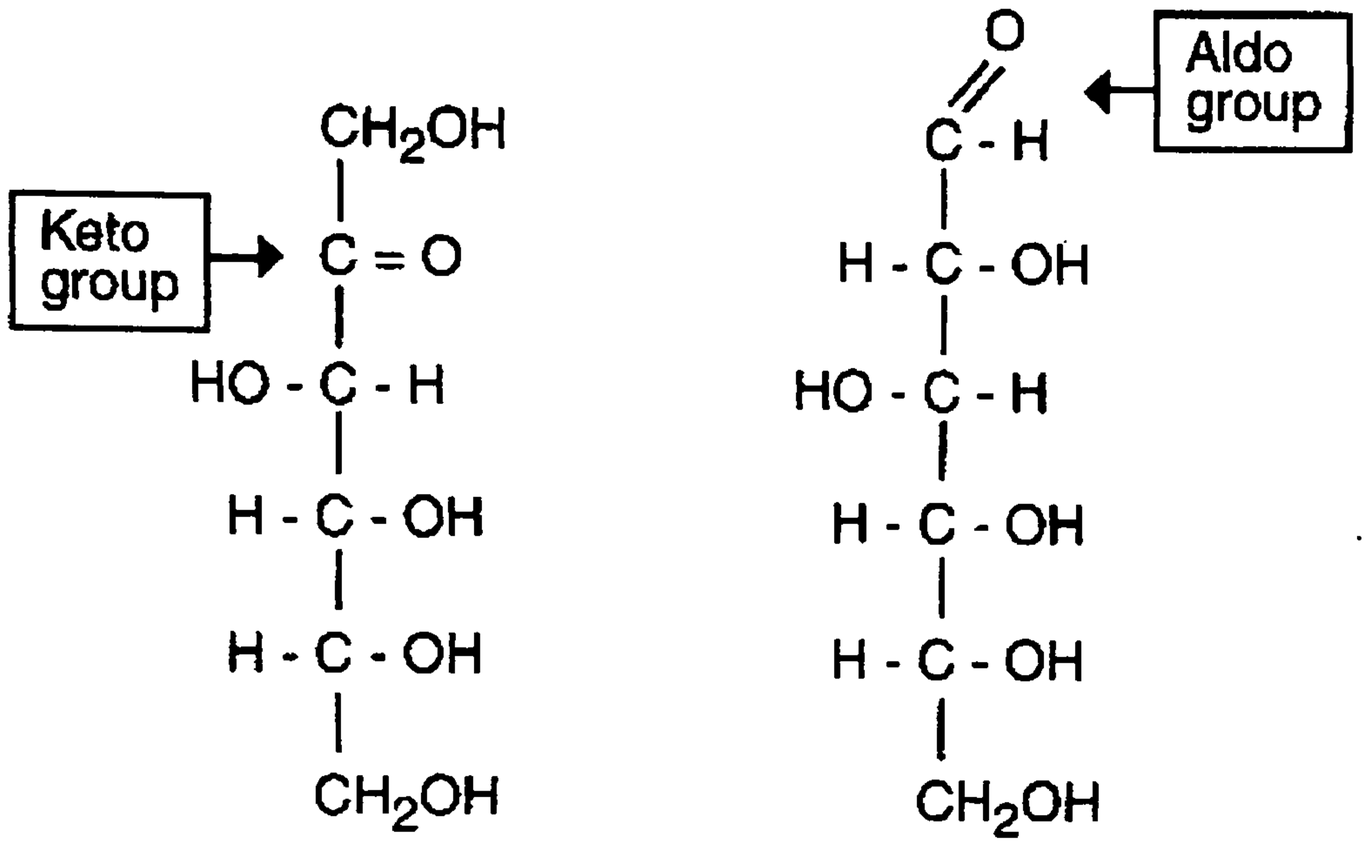

Figure 1.2. Structures of a ketohexose (fructose) and an aldohexose (glucose) (from Alexander, 1998)

a **b**

Figure 1.3 Structures of pyran (a) and furan (b) (from Coultate, 1993)

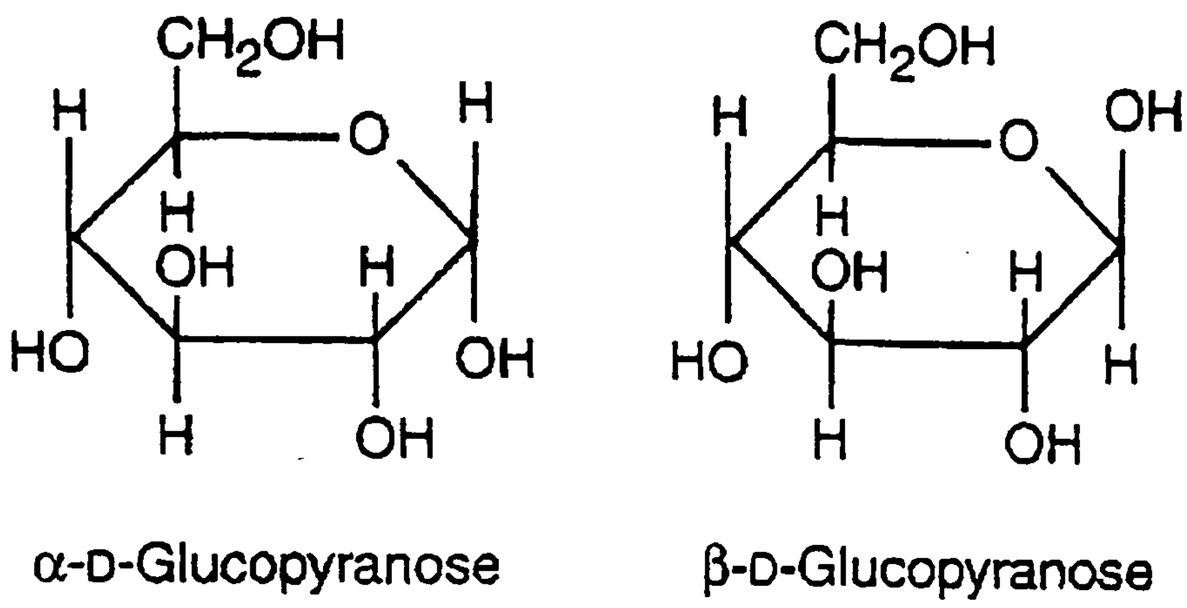

Figure 1.4. Haworth projections of D-glucose in the pyranose configuration (from Alexander, 1998).

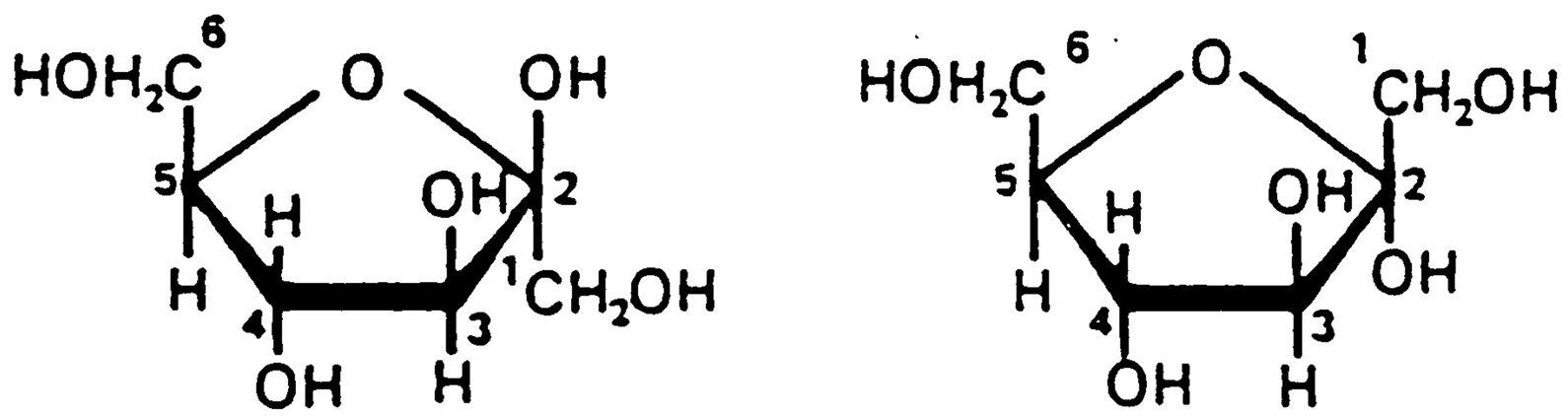

Figure 1.5. Haworth projections of D-fructose in the furanose configuration (from Coultate, 1993).

a b

Figure 1.6. The envelope and twist forms for a furanose ring (from Coultate, 1993).

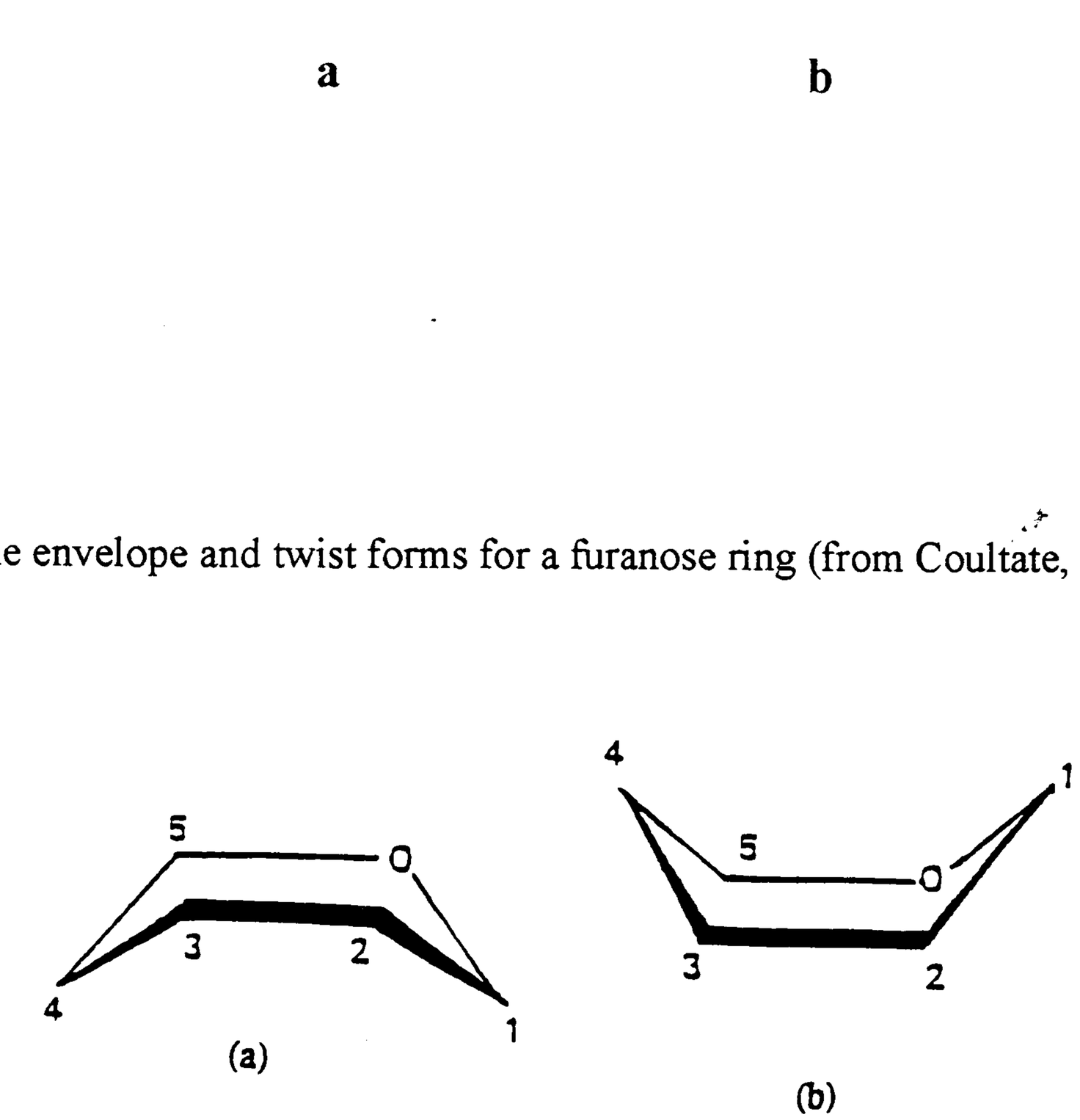

Figure 1.7. The boat and chair conformation of pyranose sugar ring. Rings (a) and (b) exhibit the B_1 and ^1B conformations of the boat form, and ring (c) and (d) the C_1 and ^1C forms of the chair (from Rees, 1977).

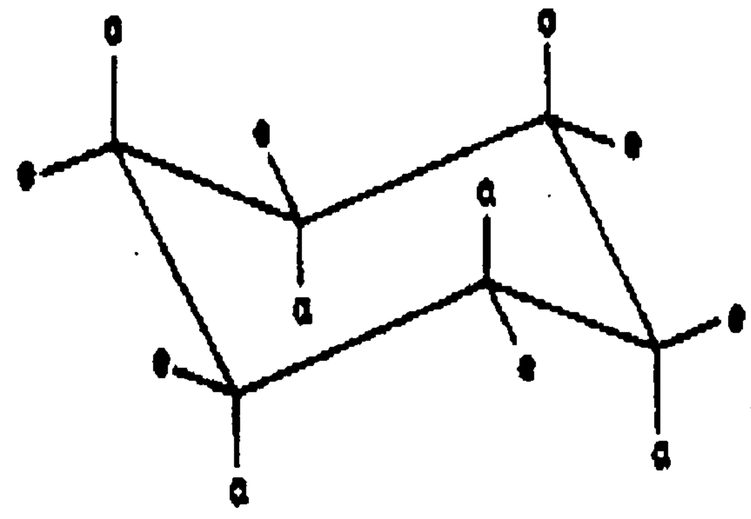

Figure 1.8. The "chair-type" structure for most of the six-membered ring sugars (from Coultate, 1993).

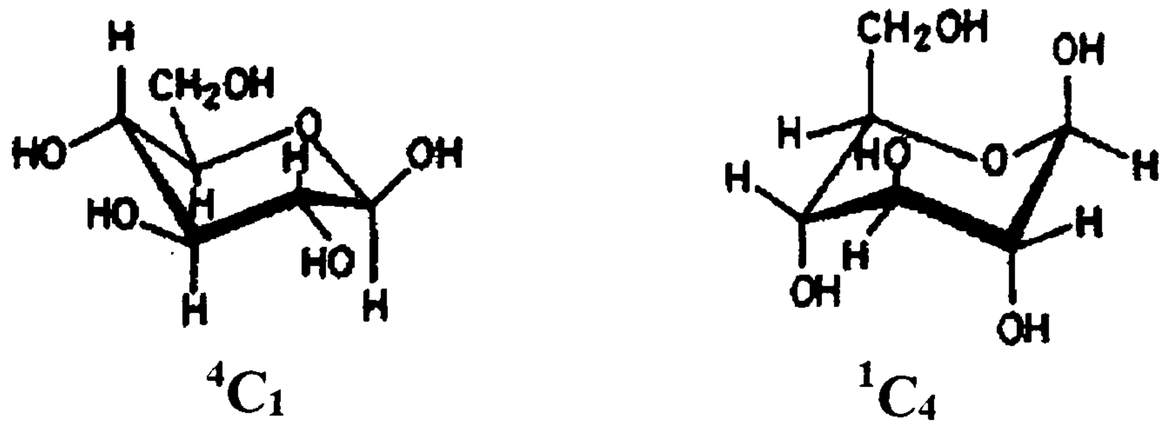

Figure 1.9. $^4C_1$ (C1) and $^1C_4$ (1C) conformations for a six-membered ring structure (from Coultate, 1993).

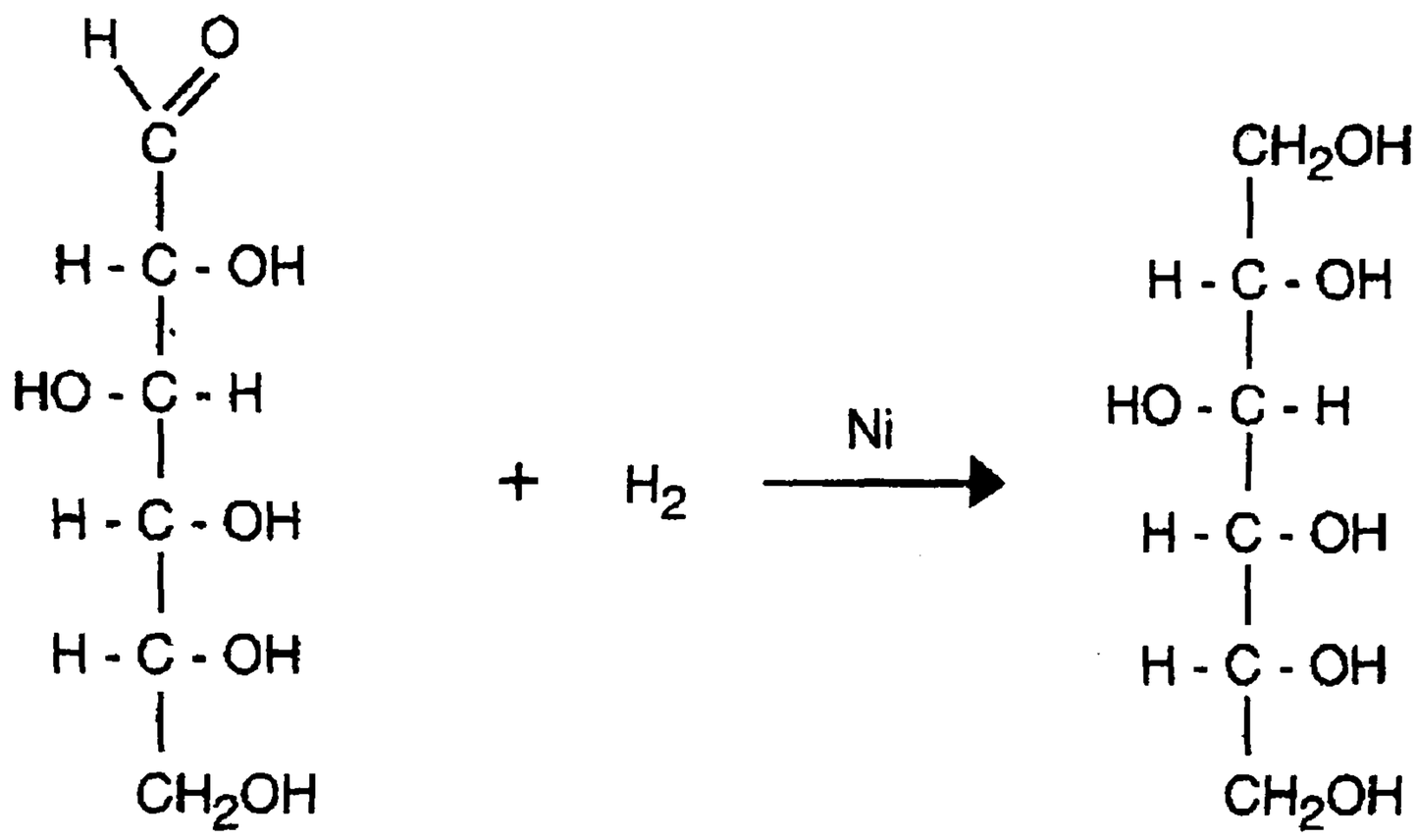

Figure 1.10. Production of D-sorbitol from reduction of D-glucose (from Alexander, 1998).

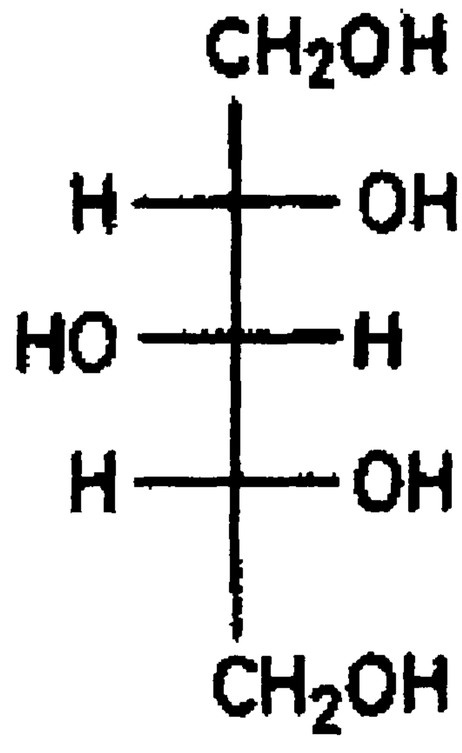

Figure 1.11. Structure of xylitol (from Coultate, 1993).

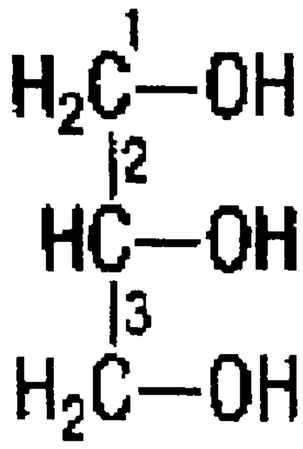

Figure 1.12. Chemical structure of propan-1,2,3-triol (from Sutton et al., 2000).

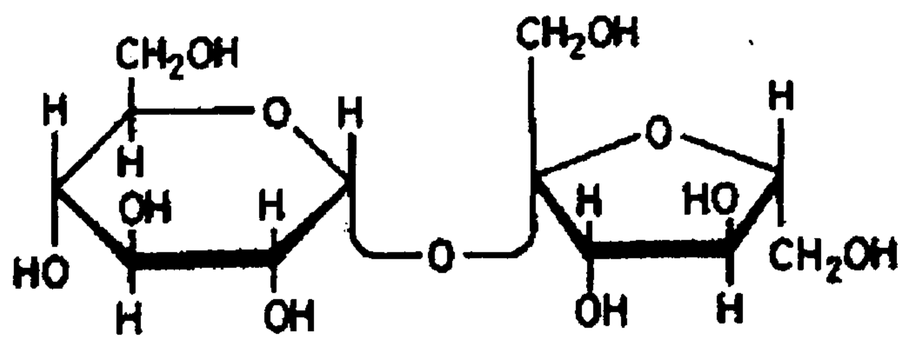

Figure 1.13. Structure of sucrose as a composite of α-D-glucose and β-D-fructose (from Coultate, 1993).

$$C_6H_{11}O_5 - O - C_6H_{11}O_5 + H_2O = C_6H_{12}O_6 + C_6H_{12}O_6 + \text{heat}$$

Sucrose: Mol. Wt. = 342.3 Water = 18.02 Glucose - 180.16 Fructose = 180.16

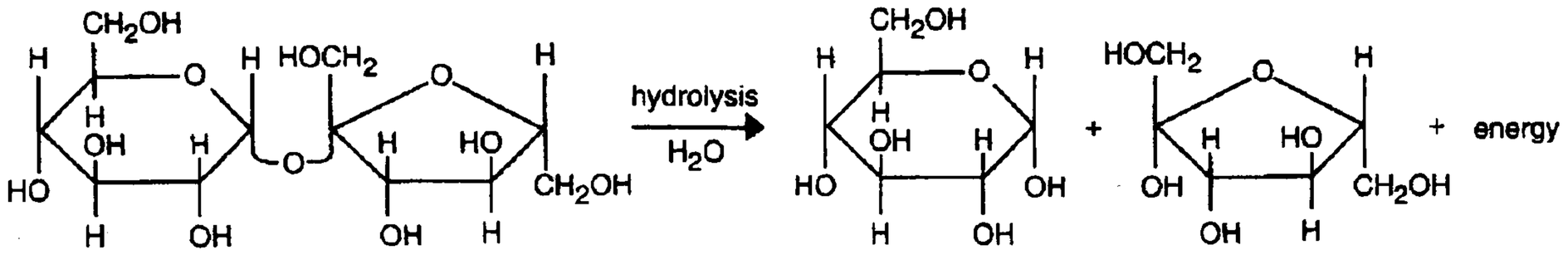

Figure 1.14. The hydrolysis of sucrose to glucose with Haworth projections for all sugars (Alexander, 1998).

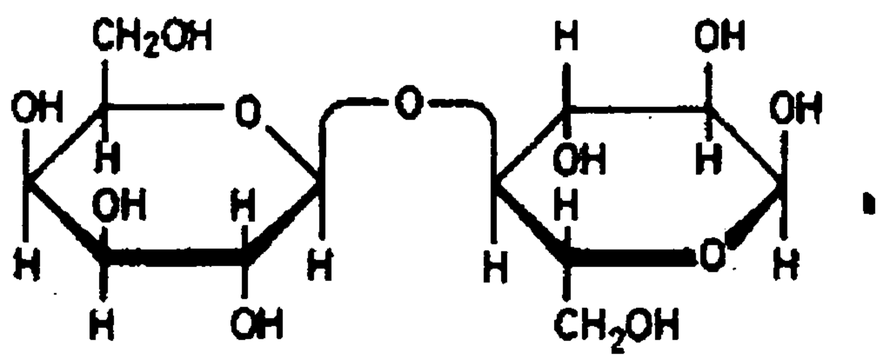

Figure 1.15. Structure of lactose as a composite of β-galactose and α-D-glucose (from Coultate, 1993)

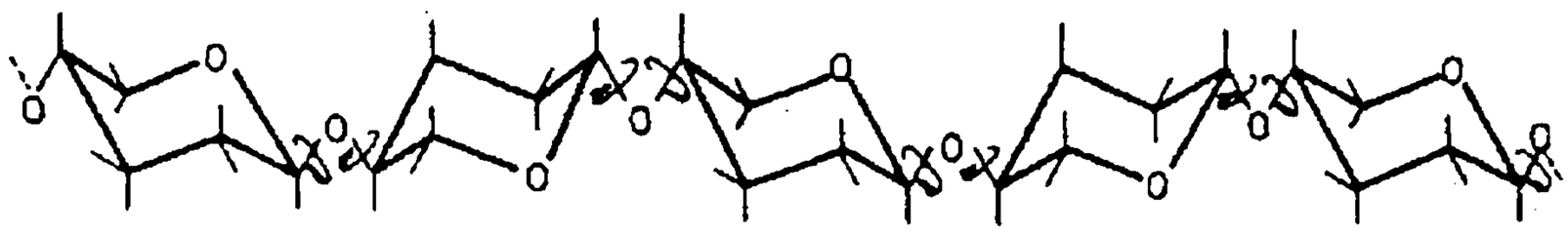

Figure 1.16. Bonds oscillations on a chain of 1,4 linked D-glucose units, exhibiting in solution (from Rees, 1977).

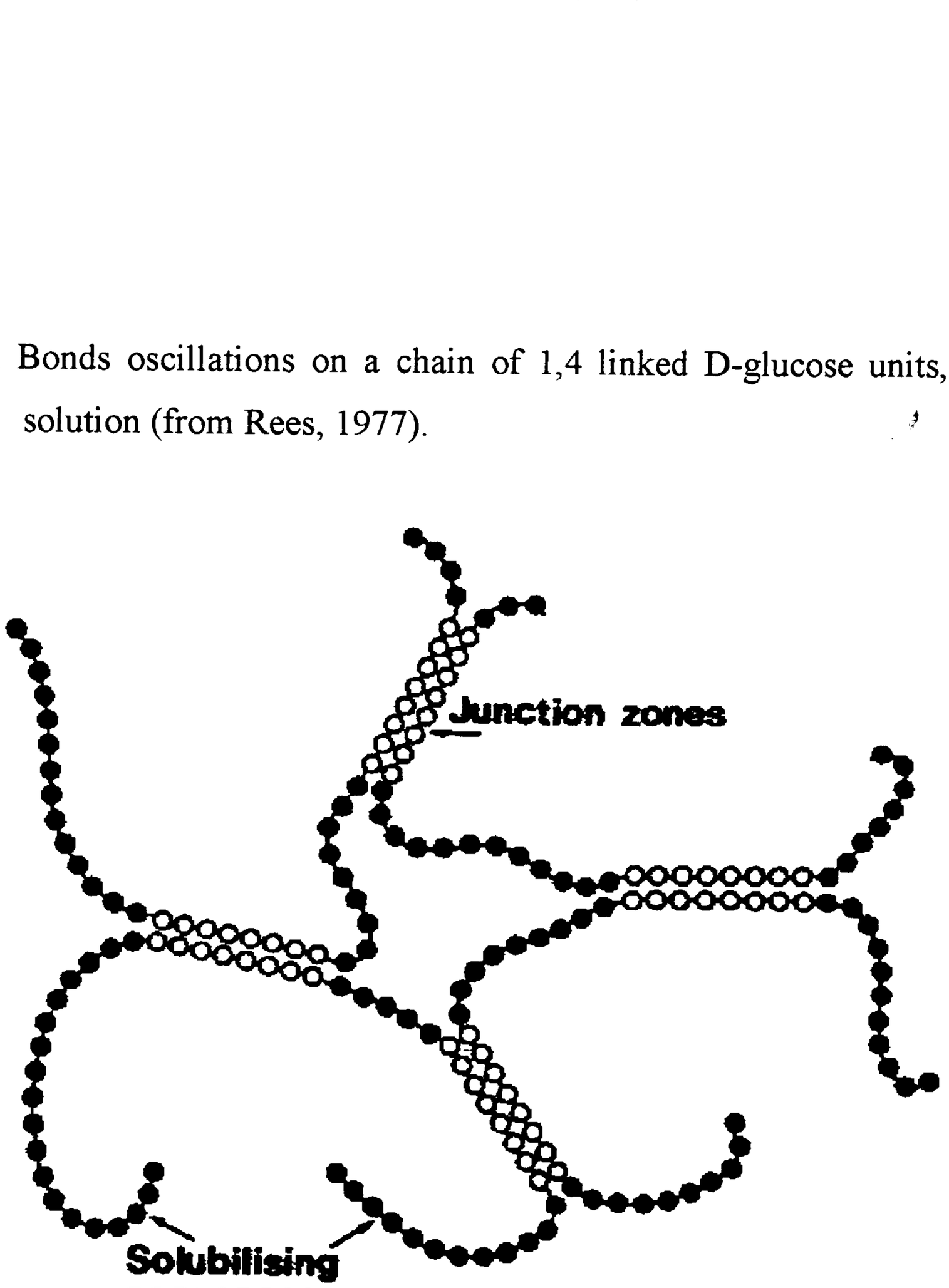

Figure 1.17. Schematic representation of a polysaccharide gel network (from Morris E. R., 1987).

CHAPTER 2

AGAROSE AND PECTIN POLYSACCHARIDES

2.1. INTRODUCTION

This chapter gives an overview of the sources, structures and properties of the materials studied in the present work, namely agarose and pectin.

2.2. AGAROSE

2.2.1. Sources

Agarose is a structural polysaccharide occur in different species of red seaweed (*Rhodophyceae*) (Painter, 1983). It is actually a low-sulfate, pyruvic acid-free component of agar; the other is agaropectin (Selby & Wynne, 1973). Due to its low sulphate content it is widely used as a model for gelling materials, as a texture modifier in the food industry and as a bacterial medium in the biomedical field (Watase et al., 1989; Watase et al., 1990).

2.2.2 Structure

Agarose is a linear polysaccharide with an alternating repeating sequence of 1,3-linked β-D-galactopyranose (the A units) and 1,4-linked (3→6)-anhydrogalactopyranose (the B units) (Araki & Arai, 1967) as Figure 2.1 and Figure 2.2 show. The AB, or agarobiose, unit may

be isolated as a disaccharide in high yield because the 3,6-anhydro ring on nearly every B unit causes it to be labile to hydrolysis (Selby & Wynne, 1973).

→3)-β-D-Galp-(1→4)-3,6-anhydro-α-L-Galp-(1→

The 3,6-anhydro units are in the L form, which is reflected in left-handed helix geometry (Arnott et al., 1974) in contrast to the carrrageenan double helix as discussed in section 1.3.4. The neutral repeating sequence of agarose also occurs with varying degrees of sulfation in natural agars, and may also carry *O*-methyl and/or pyruvate ketal groups (Guiseley, 1970). Furthermore, the anhydride bridge may be absent in a proportion of the 4-linked residues, which changes the geometry of the sugar ring to a form that is sterically incompatible with incorporation in the ordered double helix structure. The presence of this "kinking" residue is essential for the development gel networks (Rees et al., 1982), as it terminates the ordered interchain association and allows each chain to participate in more than one intermolecular junction zone.

2.2.3. Mechanism of gelation

At high temperature agarose exist in solution as disordered, random coils, but upon cooling it undergoes a co-operative conformational transition to a rigid, ordered form (Rees et al., 1982). It is generally accepted that agarose gels are cross-linked by ordered aggregates of double helices (Morris & Norton, 1982; Watase et al., 1988; Watase et al., 1989; Watase et al., 1990). Moreover, "kinking" residues promotes the formation of a three-dimensional network by limiting the length of the individual helices and thus allowing chains to participate in several different "junction zones" (Figure 2.3). According to San Biagio and his co-workers (1986), the gelation of agarose is a three-step process: first the interstrands of agarose appear, then the coil-to-helix transition takes place and finally, the double

helices aggregate and form bundles. Both ends of each chain are bound to two of the junction zones by weak secondary interactions such as hydrogen bonds, entanglement and van der Waals interactions.

The agarose double helices appear to have an interior cavity (Figure 2.4) with a diameter of 0.45 nm (measured at the narrowest points between atomic centres. The double helix interior is lined with different types of atoms. These atoms include oxygen atoms that are frequently engaged in hydrogen bonds, namely O(2) of galactose and O(5) of 3,6-anhydrogalactose (Arnott, et al., 1974). According to this, Arnott and his co-workers (1974) suggested that the agarose cavity is occupied by water molecules, which participate in a hydrogen bond that contributes to the stability of the double helix. They also indicated that it is possible to place a water molecule in the cavity in a distance of 0.27 nm from four of the oxygen atoms lining the cavity: two (namely O(2) of galactose and O(5) of 3,6-anhydrogalactose) from each strand of the double helix. The water molecule has no unfavourable steric interactions with the interior of the double helix and the arrangement of the oxygen atoms about the water oxygen is very nearly tetrahedral. This comes in agreement with the work of Watase et al., (1988) who proposed that water is the single solvent in which agarose forms gels and that it is a necessary part in the aggregation of the helices and the formation of the junction zones. They also pointed out that the higher the molecular weight of the agarose used the stronger the interactions with the water are. A schematic demonstration of the water phase in agarose gels is shown in Figure 2.5. Freezable disordered water and non-freezing water exists in junction zones, which consist of aggregated double helices of agarose molecules. Long flexible chains connect junction zones, which are somewhat crystalline, and the other regions are somewhat amorphous. The amorphous regions of agarose gels consist of long flexible molecular chains and free water. A part of the freezable disordered water, which exists in junction zones in agarose gels, will convert to hexagonal crystals just after the thawing (Watase et al., 1988).

Aggregation stabilises the individual helices, with melting of aggregates and associated loss of gel structure on heating occurring at higher temperature than helix formation and gelation on cooling. Across the carrageenan/agar series, both the extent of aggregation and thermal hysteresis increase as the charge density and the extent of substitution of the polysaccharide decreases, with a corresponding reduction in the polymer concentration required for gel formation (Dea, 1989). The resulting gels are brittle and have an increasing tendency to spontaneous contraction and loss of fluid ("syneresis") (Arnott et al., 1974).

2.2.4. Gel properties

Agarose is insoluble in cold water but soluble in hot. Its sols are heat-stable with essentially constant viscosity in neutral pH and it gives gels even at concentrations of 0.1 wt % or lower (Dea, 1989). Agarose gels exhibit thermal hysteresis (San Biagio et al., 1986; Dea & Rees, 1987; Dea, 1989) and the melting temperature is dependent on the concentration used. The corporation of sugar increases gel firmness and enhances gel transparency (Watase et al., 1990).

Sucrose and glucose are believed to promote the formation of the helices and their aggregation. After the aggregation takes place the structure of the junction zones will be stabilised and their number will be increased. However, the excessive addition of these sugars weakens the gel-forming ability of agarose. The mechanism by which, after a certain concentration of sucrose or glucose the gel-forming ability of agarose is decreased, is related to the available free water in the system. The latter is necessary to form junction zones and any excessive addition of the sugars makes it insufficient. Therefore, the agarose molecules are forced to change conformation and to change the structure of the junction zones, in addition to immobilising free water. Both of these phenomena are happening simultaneously, but it is not yet clear, which is the predominant one (Watase et al., 1990).

chains, which reduce the galacturonic acid content below the legally permitted limit and (iii) the relatively low molecular weight, which decreases the pectins quality. The alternative production of pectin from onion is questionable regarding whether such a source would be commercially attractive from either the availability of sufficient raw material or the image of onion pectin (May, 1990).

Both the quality and the yield of the pectin extracted from the above mentioned raw materials depend on, mainly, the source and the type of the fruit used. Other important factors are the ripeness of the fruit on harvesting and any diseases occurred to the plant. Apart from that, both the weather and the growing location have a significant effect. At the same time the procedures the peel went through are of major importance, such as, for example, the time the peel was held after juice processing, which should be as short as possible due to the enzymes present in some loss that degrade pectin, the washing of the peel, which could result to the partial wash away of pectin, and the drying, which should not be done at temperatures above 50°C to avoid burning the pectin (May, 1990).

2.3.2. Manufacturing processes

Commercially, pectin is extracted (Figure 2.6) by treating the raw material with hot dilute mineral acid at ~ pH 2. The precise length of time depends on the raw material, the type of pectin desired and the manufacturer. The hot pectin is separated from the solid residue as efficiently as possible. However, this is not easy since the solids are by now soft and the liquid phase is viscous, with the viscosity increasing with pectin concentration and molecular weight. The pectin extract may be further clarified by filtration through a filter aid such as kieselguhr. Apple pectin is then treated with carbon to remove colour and with α-amylase to degrade starch, which could otherwise precipitate from the liquid product. The clarified extract is then concentrated under vacuum in order to achieve efficient

concentration at low temperature and to prevent degradation of the pectin. Powered pectin can be produced by mixing the concentrated liquid from either apple or citrus with an alcohol (isopropanol, methanol or ethanol). The pectin separates as a stringy gelatinous mass, which is pressed, washed, dried and ground. An alternative precipitation process, introduced by Joseph and Havighorst in 1952, utilises the fact that pectin can be co-precipitated in the presence of colloidal aluminium hydroxide. Among the advantages of this method is that the pectin extract does not have to be concentrated and certain impurities are more readily eliminated. The extract is then cooled and mixed with a solution of an aluminium salt and sufficient ammonia or sodium carbonate to give a pH of about 4. The pectin (a greenish-yellow floc, which tends to float on the liquor), is separated by a screen or by flotation and pressed to remove a sufficient quantity of aqueous liquor. The yellow mass is further suspended in alcohol, treated with acid and partially neutralised before drying. The disadvantages of this process are firstly, that highly esterified pectin does not precipitate well with aluminium and secondly, that the overall recovery is normally poorer than with the alcohol process. Since pectin is extracted from a variety of raw materials, production of a consistent product is normally achieved by blending of a number of production batches and diluting them with sugar or dextrose to a standard performance (May, 1990).

These processes yield a pectin with a degree of esterification (DE) of approximately 70%, which is called "rapid set" pectin. To produce other types, some of the ester groups must be hydrolysed. This is mainly carried out by the action of acid, either before or during a prolonged extraction, in the concentrated liquid, or in alcoholic slurry before separation and drying. This procedure results in a range of slower setting high methoxyl and calcium reactive low methoxyl pectins. Alternatively, alkaline can be used, but since pectin readily degrades at neutral or alkaline pH by a β-elimination reaction, this must be carried out at low temperature. The use of ammonia for alkaline hydrolysis leads to conversion of some

of the ester groups into amide groups, producing "amidated pectins", which are usually low methoxyl (Christensen, 1986; May, 1990).

2.3.3. Structure

According to De Vries and his co-workers (1982), pectins are complex structures whose canonical primary sequence can be described as follows: (1) "Smooth" regions made up of a backbone of linear (1→4)–linked α-D-galacturonic acid (pectic acid) that may be partially methyl esterified (pectinic acid). (2) "Hairy" regions in which the galacturonic acid residues are interspersed with (1→2) linked α-L-rhamnopyranosyl residues (the rhamnogalacturonan moiety); attached to which are oligosaccharide side chains, containing mainly D-galactopyranose and L-arabinofuranose residues (Cros et al., 1996) (Figure 2.7). The presence of rhamnose affects the flexibility of the polymer (the higher the rhamnose content the higher the flexibility) (Oakenfull & Scott, 1984; Oakenfull & Scott, 1985; Oakenfull, 1991). The side braches may also consist of D-xylose, less frequently of D-mannose, L-fucose, D-glucose and ever more rare of sugars 2-*O*-methyl-D-xylose, 2-*O*-methyl-L-fucose and D-apiose, linked primarily through C(4) of the rhamnosyl residues. However, it is possible to find substitution of the galacturonyl residues at either C(2) or C(3) (Hwang & Kokini, 1992). Among the three main sources of pectin, the sugar beet has the highest content of rhamnose (5.5%), galactose and arabinose, but has negligible amounts of xylose. Apple pectin contains 2.5% rhamnose and relatively low amount of xylose, whereas citrus pectin contains only 1.5% rhamnose, minor amounts of galactose and negligible amounts of xylose (Axelos & Thibault, 1991).

Sidechains degrade during extraction with acid and, therefore, pectin molecule, for practical purposes, may be considered as an unbranched chain containing 200-1000 galacturonic acid units linked together by α-1,4-glucosidic bonds (Christensen, 1986). Some of the

galacturonic acid units are esterified and present as galacturonic acid methyl esters (Figure 2.8). Remaining acid groups can be partly or fully neutralised to form ammonium, potassium or sodium salts (Christensen, 1986).

According to the degree of esterification (DE), which is the fraction of methyl esterified residues, expressed as a percentage of the total content of galacturonic acid, pectin is classified into the following categories:

- High methoxy pectin (HM) for DE > 50% (Figure 2.9). These can be further classified as a rapid set (DE = 70-75%), medium set (DE = 65-69%) and slow set (DE = 60-64%).
- Low methoxy (LM) has DE < 50%.
- Amidated low methoxy pectin, produced if ammonia is used for alkaline de-esterification. This type of pectin contains galacturonic acids, galacturonic acid methyl esters and galacturonamide units in the molecular chain (Figure 2.10).
- "Pectic acid" for DE < 10%. (Christensen, 1986).

2.3.4. Stability and solution properties

The molecular weight of commercial pectins varies according to the raw material, the extraction procedure and the isolation method. However, the average normally falls within the range 50,000 to 150,000 Dalton (Christensen, 1986; Oakenfull, 1991).

Pectins are relative stable under acid conditions, but degrade in neutral or slightly alkaline environment (May, 1990). At pH lower than 3.0 and elevated temperatures glycosidic bonds are hydrolysed and pectin is degraded. Simultaneously, de-esterification takes place and long holding times may cause high-ester pectin to adopt gradually slower setting characteristics (Christensen, 1986). At pH values above 4.5, high methoxyl pectin is stable only at room temperature. At higher temperatures both the viscosity and the gelling properties are lost due to chain cleavage by β-elimination. In this reaction only glycosidic

bonds next to an esterified carboxyl group are broken, and therefore, low methoxy pectins are more stable than high methoxy. Any application procedures involving holding of pectin solutions at elevated temperature leads to depolymerisation and de-esterification of the pectin. Both processes are strongly depending on the solution pH (Christensen, 1986; May, 1990).

Pectin's rheological properties are highly affected by the content of neutral sugar sidechains, but DE is also a significant factor in determining both the conformational and the rheological properties of the polymer (Hwang & Kokini, 1992). Viscosity of high methoxy pectin solutions generally increases with increasing the degree of esterification. This may be explained by an increase in the structuring water molecules around the methyl ester groups. In the case of low methoxy pectin, low degrees of esterification or a block-wise occurrence of carbonyl groups will lead to high viscosities reflecting an inferior solubility of these pectins (Christensen, 1986, Oakenfull, 1991).

2.3.5. Pectin gelation

In contrast with high methoxyl pectins, the gelation in low methoxyl takes place by ionic linkages via calcium bridges between two carboxyl groups belonging to two different chains in close contact (Morris et al., 1982; Powell et al., 1982). The mechanism of gelation is known as the "egg-box" mechanism, which was first suggested for alginates by Grant and co-workers in 1973 (Figure 2.11). According to this, a section of two pectin chains, free of ester groups, is held together by a number of calcium ions. The latter form chelate bonds with oxygen atoms from both galacturonan chains, thus fitting into "cavities" in the structure. The extension of the crystallites is restricted by the presence of methyl ester groups, rhamnose insertions or any other irregularity in the chains (Morris et al., 1982; Powel et al., 1982). Provided that calcium concentration is in excess, further calcium-induced association can occur by aggregation of dimers.

According to Christensen (1986), low methoxyl pectin's reactivity with calcium to form a gel is controlled by both the degree of esterification and the degree of amidation. Non-

amidated low methoxyl pectins with a DE of 25 to 35% and amidated low ester pectins with a DE of 20 to 30% and degree of amidation of 18% to 25% are characterised as highly calcium reactive or rapid setting and form gels in systems with low calcium concentration or low soluble solids. On the other hand, non-amidated low ester pectins with a DE of 35% to 45% and amidated low methoxyl pectins with DE of 30% to 40% and degree of amidation of 10% to 18% are less calcium reactive or slow setting and are used in systems with high calcium content or relatively high soluble solids.

The calcium concentration in the system affects significantly the gelation of low methoxyl pectins. The texture of these gels can be controlled by adjusting the ion to pectin ratio (May, 1990). A high pectin concentration with relatively little calcium will give an elastic gel, whereas the use of more calcium with a minimum of pectin will produce a much more brittle gel, which may show some syneresis. However, apart from the calcium content in the system, gelation of low methoxyl pectin is affected by the presence of sequestrants, such as citrate, other fruit anions, sugars (e.g. fructose) or sugar alcohols (e.g. sorbitol), and the molecular weight of the pectin (the shorter the galacturonan chain the weaker the gel).

The content of unesterified carboxylate groups in high methoxy pectin is insufficient to allow intermolecular junctions to be formed by site-binding of Ca^{2+}. Instead, gelation is induced by reduction in pH and incorporation of high concentrations of a low molecular weight cosolute (typically ~ 65 wt % sucrose at ~ pH 3.0). On the basis of X-ray fibre diffraction studies, Walkinshaw and Arnott (1981a,b) suggested that the junction zones of the resulting gels are made up of aggregated 3-fold helices (Figure 2.12).

As indicated previously (Section 2.3.3), the rate of gelation of high methoxy pectin on cooling from the pre-gel solution increases with increasing DE. There is an accompanying increase in the temperature at which gelation occurs (Christensen, 1986; May, 1990). Both effects can be explained by the progressive reduction in intermolecular electrostatic repulsion as the ester content is increased (and hence the content of COO^- groups is decreased). The purpose of reducing pH in preparation of high methoxy pectin gels is to suppress electrostatic repulsion further, by partial conversion of COO^- to COOH. The

role of the cosolute is discussed in detail in Chapters 5 and 6, in the light of investigations carried out as part of the present work.

REFERENCES

Araki, C. & Arai, K. (1967). Studies of the chemical constitution of Agar-agar XXIV. Isolation of a new disaccharide as conversion product from acidic hydrolysate. *Bulletin of the Chemical Society of Japan*, **40**, 1452-1456.

Arnott, S., Fulmer, A., Scott, W. E., Dea, I. C. M., Moorhouse, R. & Rees D. A. (1974). The agarose double helix and its function in agarose gel structure. *Journal of Molecular Biology*, **90**, 269-284.

Axelos, M. A. V. & Thibault, J. F. (1991). Influence of substituents of the carboxyl groups and of the rhamnose content on the solution properties and flexibility of pectins. *International Journal of Biology of Macromolecules*, **13**, 77-82.

Christensen, S. H. (1986). Pectins, In M.Glicksman, *Food Hydrocolloids, vol. III*, CRC Press, USA, pp. 205-230.

Cros, S., Garnier, C., Axelos, M. A. V., Imberty, A. & Pérez, S. (1996). Solution conformations of pectin polysaccharides: determination of chain characteristics by small angle neutron scattering, viscometry, and molecular modelling. *Biopolymers*, **15**, 339-352.

De Vries, J. A., Rombouts, F. M., Voragen, A. G. J. & Pilnik, W. C. (1982). Enzymic degradation of apple pectins. *Carbohydrate Polymers*, **2**, 25-33.

Dea, I. C. M. (1987). Affinity interactions between agarose and beta-1,4-glycans-A model for polysaccharide associations in algal cell-walls. *Carbohydrate Polymers*, **7**, 183-224.

Dea, I. C. M. (1989). Industrial Polysaccharides. *Pure and Applied Chemistry*, **61**, 1315-1322.

Grant, G. T., Morris, E. R., Rees, D. A., Thom, D. & Smith, P. J. C. (1973). Biological interactions between polysaccharides and divalent cations: the egg-box model. *FEBS Letters*, **32**, 195-198.

Guiseley, K.B. (1970). The relationship between methoxyl content and gelling temperature of agarose. *Carbohydrate Research*, **13,** 247-256.

Hwang, J. & Kokini, J. L. (1992). Contribution of the side branches to rheological properties of pectins. *Carbohydrate Polymers*, **19**, 41-50.

Iijima, M., Nakamura, K., Hatakeyama, T. & Hatakeyama, H. (2000). Phase transition of pectin with sorbed water. *Carbohydrate Polymers*, **41**, 101-106

Morris, E. R. & Norton, I. T. (1982). Polysaccharide aggregation in solutions and gels. In E. Wyn-Jones & J. Gormally, *Aggregation Processes in Solution*, Elsevier, Amsterdam, pp. 549-593.

Morris, E. R., Powell, D. A., Gidley, M. J. & Rees, D. A. (1982). Conformations and interactions of pectins I. Polymorphism between gel and solid states of calcium polygalacturonate. *Journal of Molecular Biology*, **155**, 507-516.

Oakenfull, D. G. & Scott, A. G. (1984). Hydrophobic interactions in gelation of high methoxy pectins. *Journal of Food Science*, **49**, 1093-1098.

Oakenfull, D. G. & Scott, A. G. (1985). Gelation of high methoxyl pectins. *Food Technology in Australia*, **37**, 156-158.

Oakenfull, D. G. (1991). The Chemistry of High Methoxyl Pectin. In R. H. Walter, *The Chemistry and Technology of Pectin*, Academic Press, London, pp. 87-118.

Painter, T. J. (1983). Algal polysaccharides. In G. O. Aspinall, *The Polysaccharides vol.2*, Academic Press, USA, pp. 196-285.

Powell, D. A., Morris, E. R., Gidley, M. J. & Rees, D. A. (1982). Conformations and interactions of pectins II. Influence of residue sequence of chain association in calcium pectate gels. *Journal of Molecular Biology*, **155**, 517-531.

Rees, D. A., Morris, E. R., Thom, D. & Madden, J. K. (1982). Shapes and interactions of carbohydrate chains. In G. O. Aspinall, *The Polysaccharides vol. 1*, Academic Press, New York, pp. 195-290.

San Biagio P. L., Madonia, F., Newman, J. & Palma, M. U. (1986). Sol-sol structural transition of aqueous agarose systems. *Biopolymers*, **25**, 2255-2269.

Selby, H. H. & Wynne W. H. (1973). Agar. In R. L. Whistler & J. N. BeMiller, *Industrial Gums*, Academic Press, UK, pp. 29-48.

Walkinshaw, M. D. & Arnott, S. (1981a). Conformations and interactions of pectins I. X-ray diffraction analyses of sodium pectate in neutral and acidified forms. *Journal of Molecular Biology*, **153**, 1055-1073.

Walkinshaw, M. D. & Arnott, S. (1981b). Conformations and interactions of pectins II. Models for junction zones in pectinic acid and calcium pectate gels. *Journal of Molecular Biology*, **153**, 1075-1085.

Watase, M., Nishinari, K. & Hatakeyama, T. (1988). DSC study on properties of water in concentrated agarose gels. *Food Hydrocolloids*, **2**, 427-438.

Watase, M., Nishinari, K., Clark, A. H. & Ross-Murphy, S. B. (1989). Differential scanning calorimetry, x-ray, and NMR of very concentrated agarose gels. *Macromolecules*, **22**, 1196-1201.

Watase, M., Nishinari, K., Williams, P.A. & Phillips, G. O. (1990). Agarose gels: effect of sucrose, glucose, urea and guanidine hydrochloride on the rheological and thermal properties. *Journal of Agricultural and Food Chemistry*, **38**, 1181-1187.

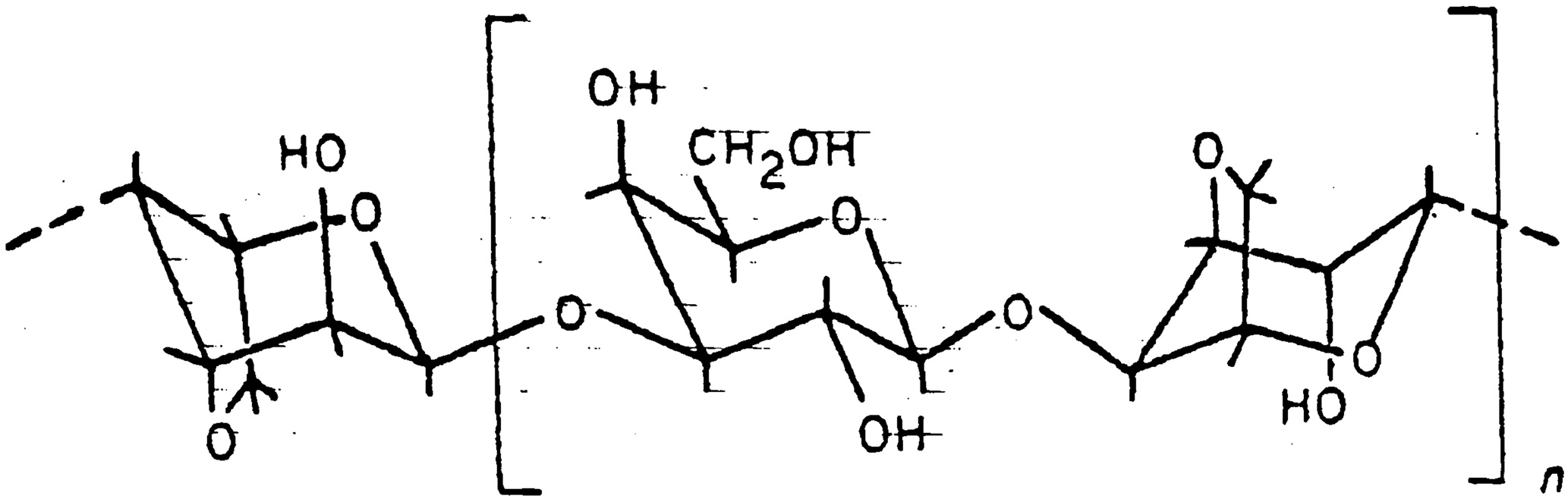

Formula I

Figure 2.1. Chemical formula of agarose (from Arnott et al., 1974).

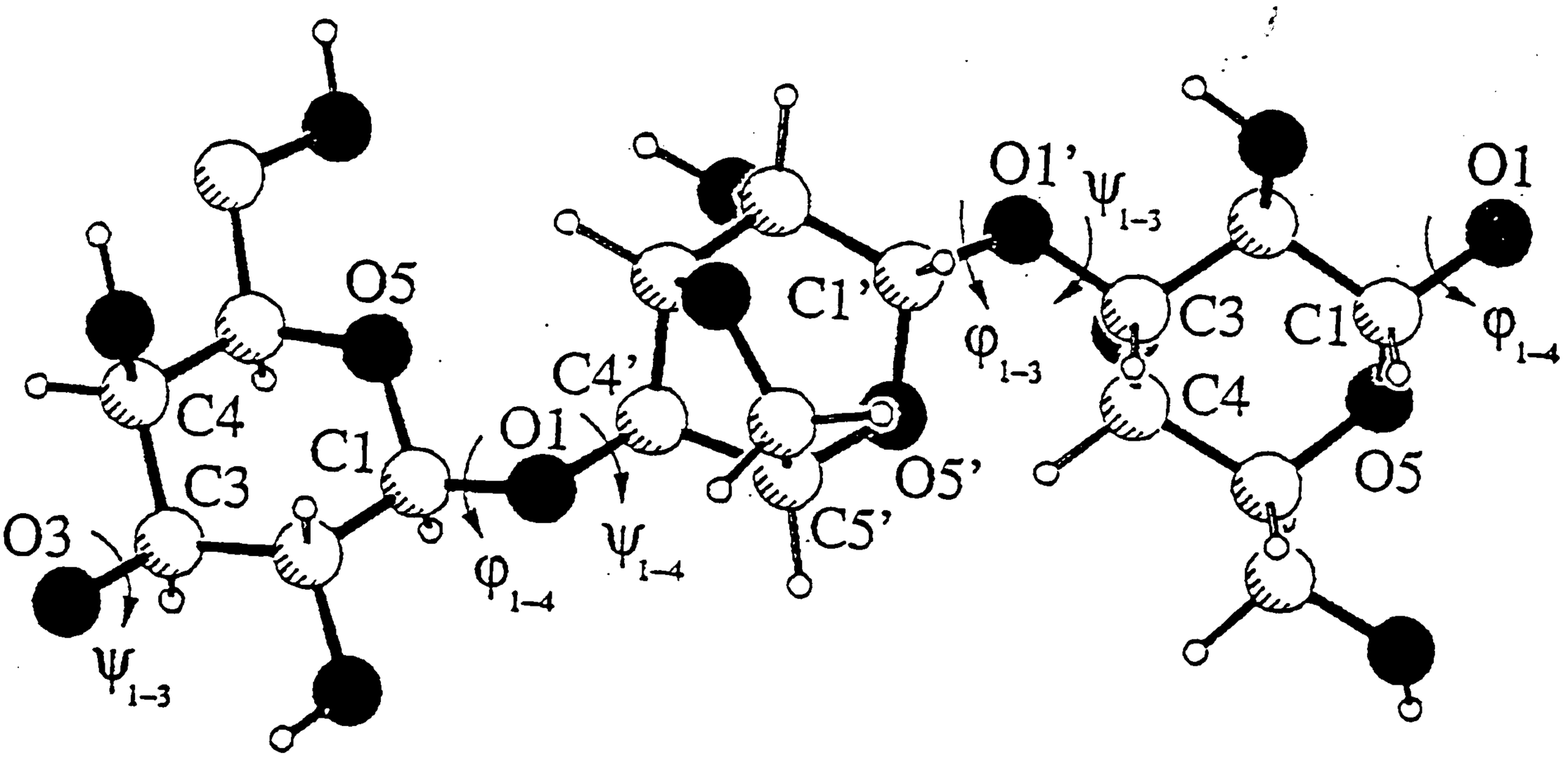

Figure 2.2. Idealised repeating unit of agarose (from Kouwijzer et al., 1998).

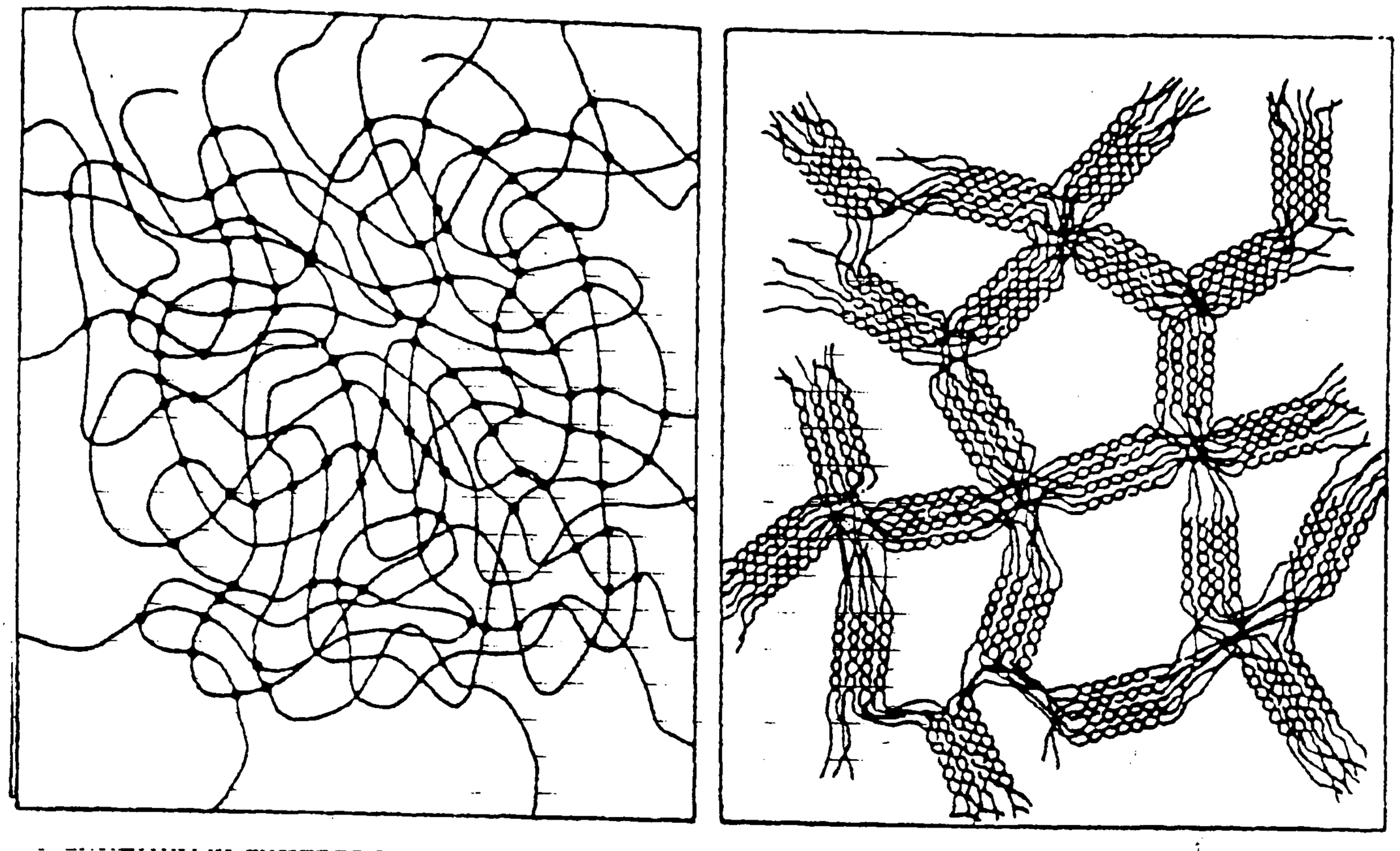

Figure 2.3. A schematic representation of the agarose gel network (right), in comparison with a network which is formed from random chains at similar polymer concentration. The aggregates in agarose gels may actually contain 10 to 10^4 helixes (from Arnott et al., 1974).

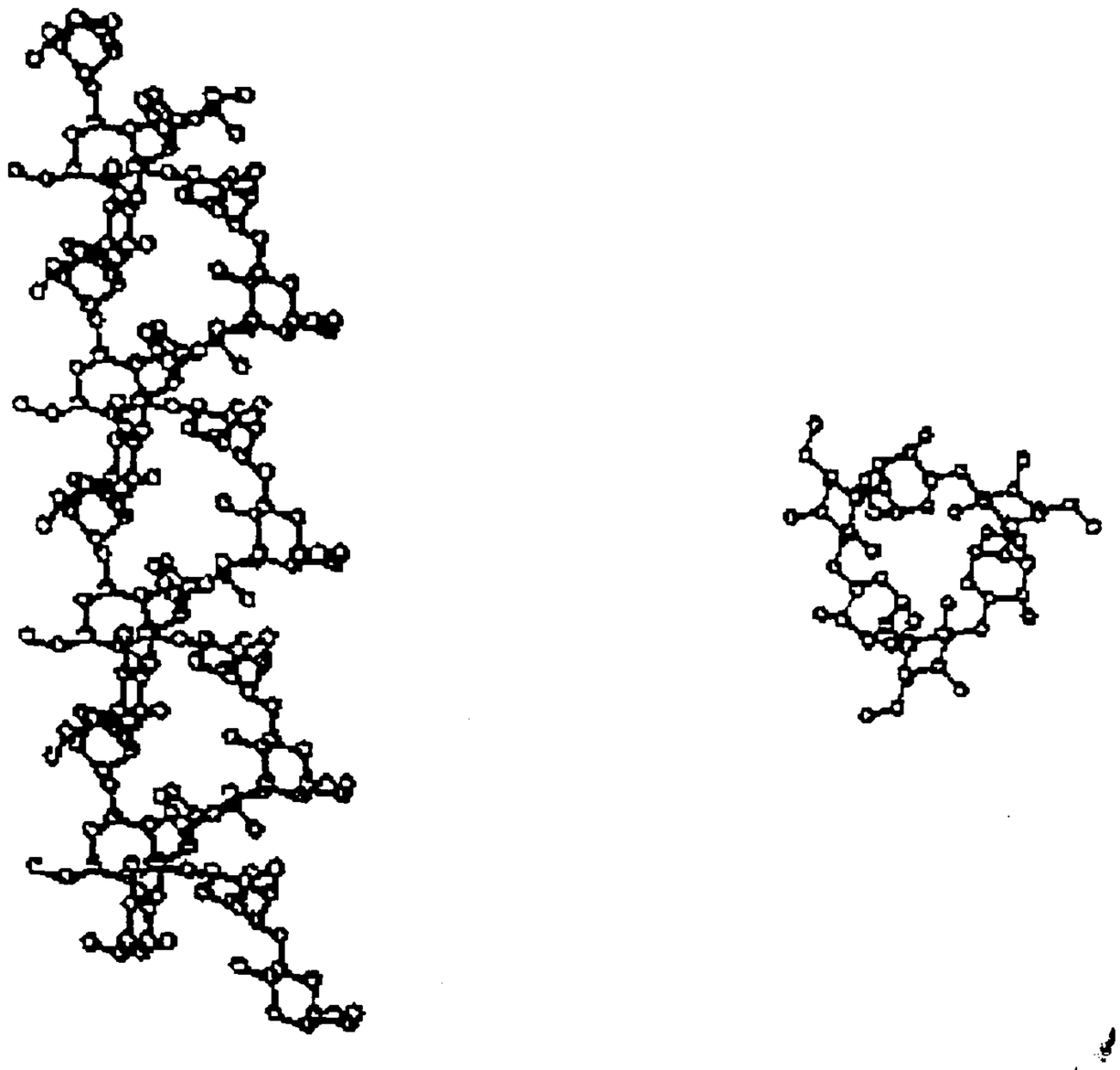

Figure 2.4. A view of the agarose double helix (a) perpendicular to the helix axis and (b) down the helix axis. The location of the hydroxymethyl groups on the perimeter of the double helix permits sulphate substitution on O(6) without the introduction of unfavourable steric interactions (from Arnott et al., 1974).

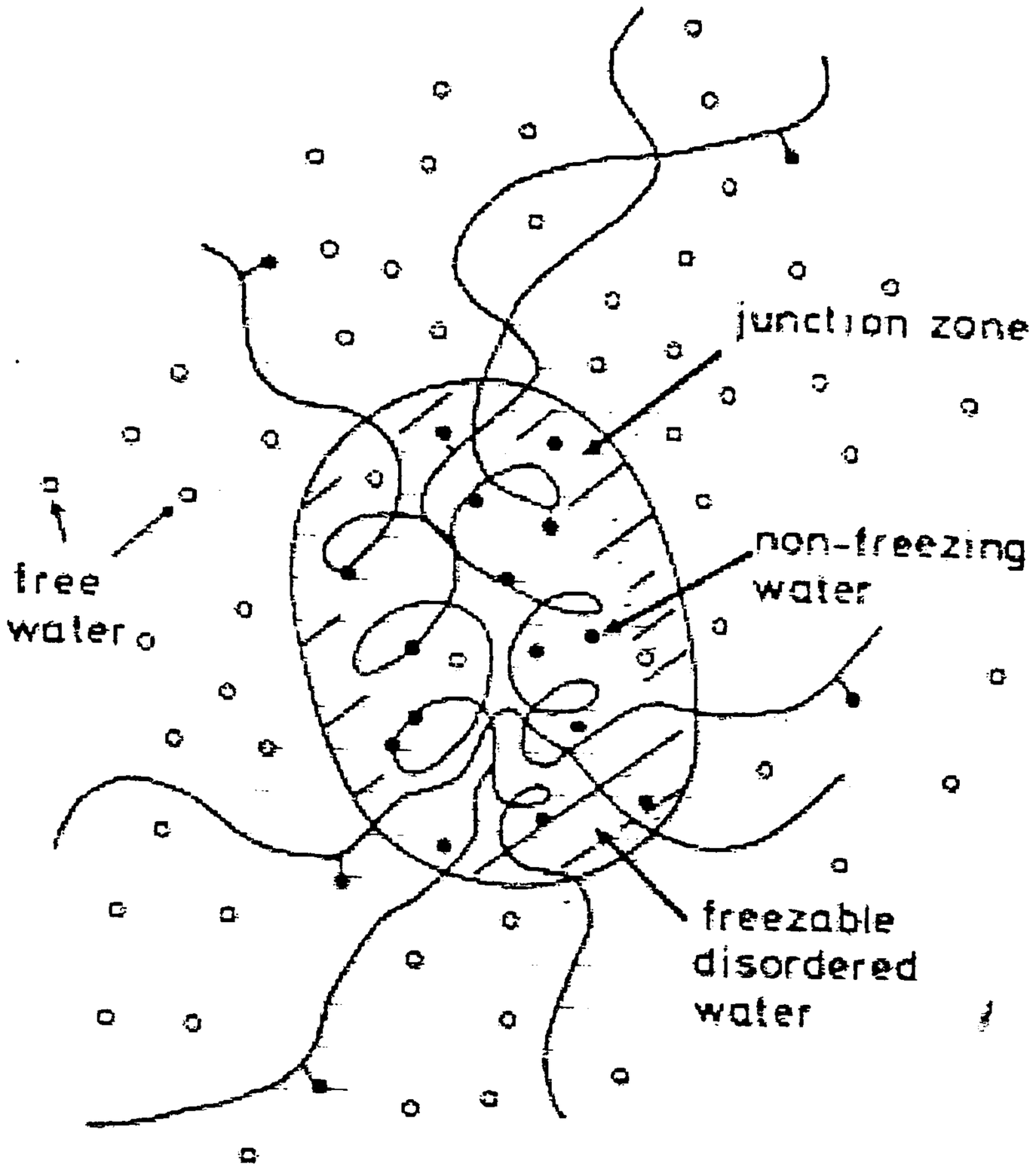

Figure 2.5. Schematic representation of water phases in polymer gels. Assembly of spirals, junction zones; shaded part, freezable disordered water; the other part, amorphous region consisting of flexible chain molecules and free water; black circles, non-freezing water; open circle, free water (from Watase et al., 1988).

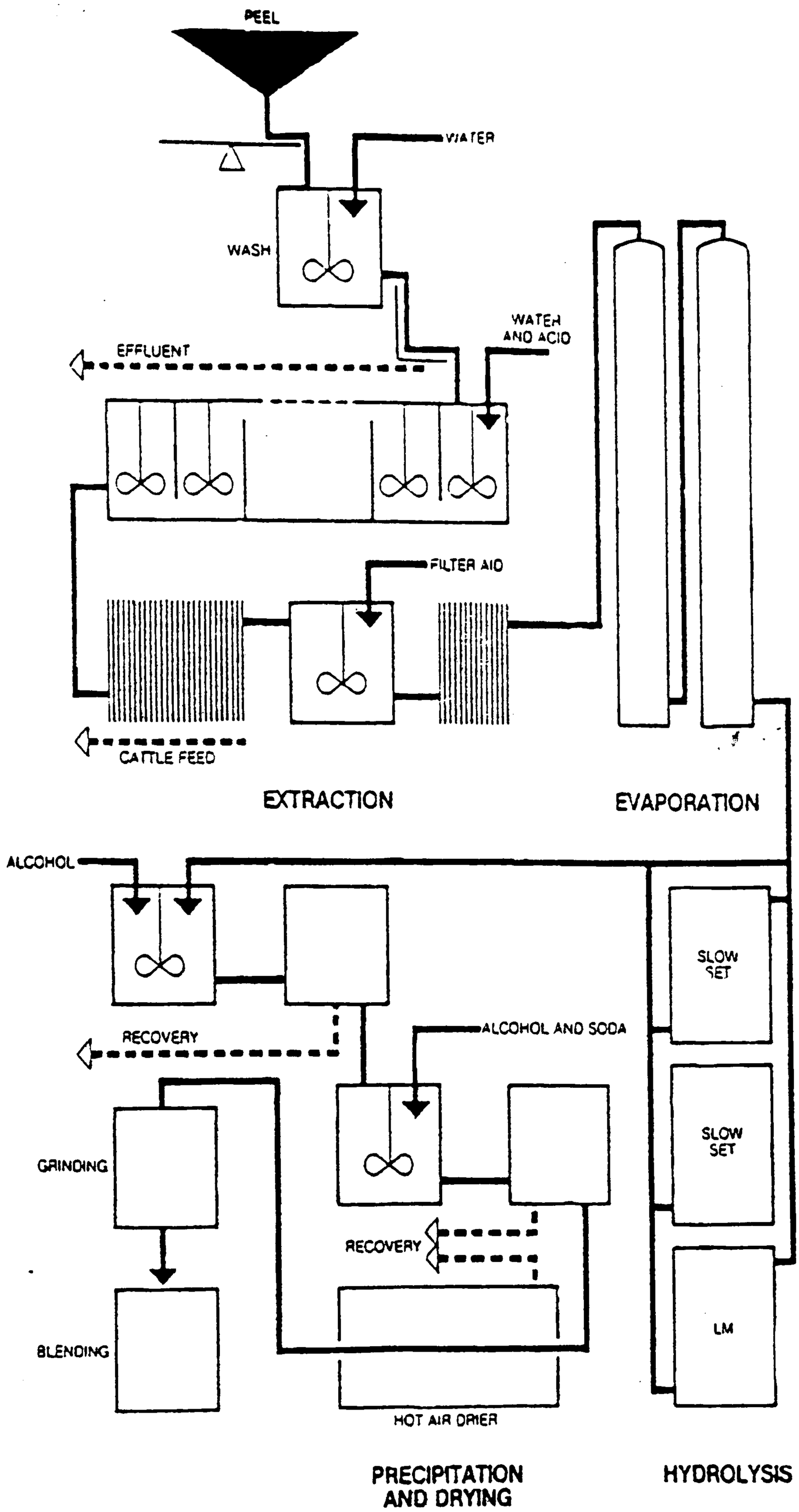

Figure 2.6. Manufacture of pectin (from May, 1990)

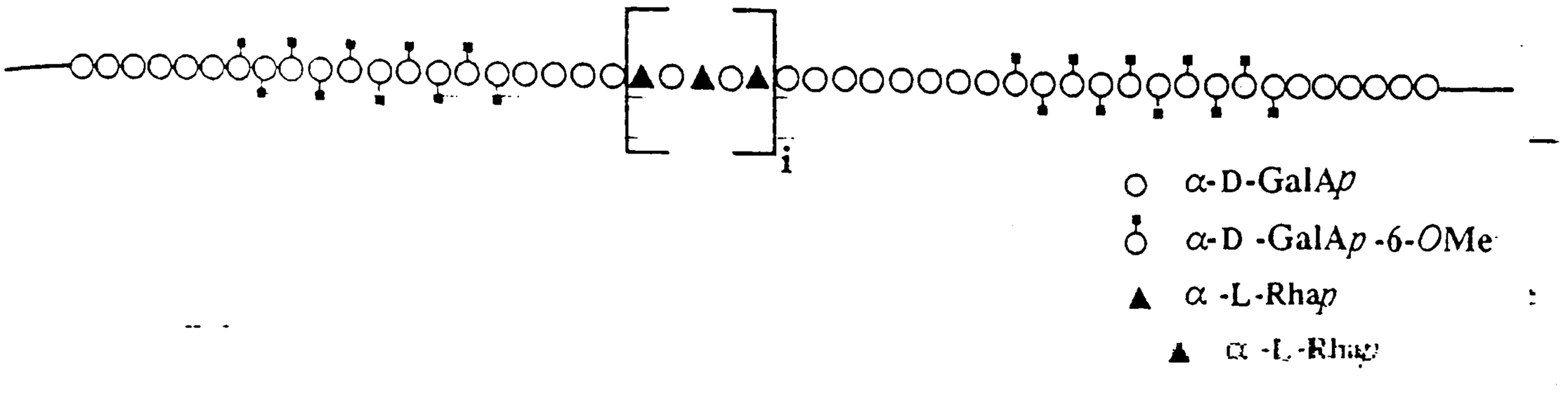

Figure 2.7. Schematic representation of a canonical primary structure of pectins, showing the distribution of homogalacturonan blocks (with and without the methoxyl group) and the insertion of rhamnogalacturonan blocks of unknown degree of polymerisation *i*. In these blocks, the rhamnose units are sites for attachments of various neutral sugar chains (from Cros et al., 1996).

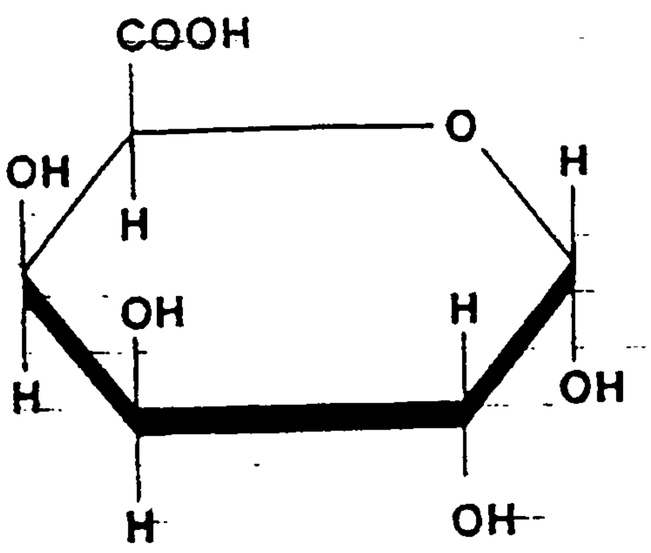

D-Galacturonic acid

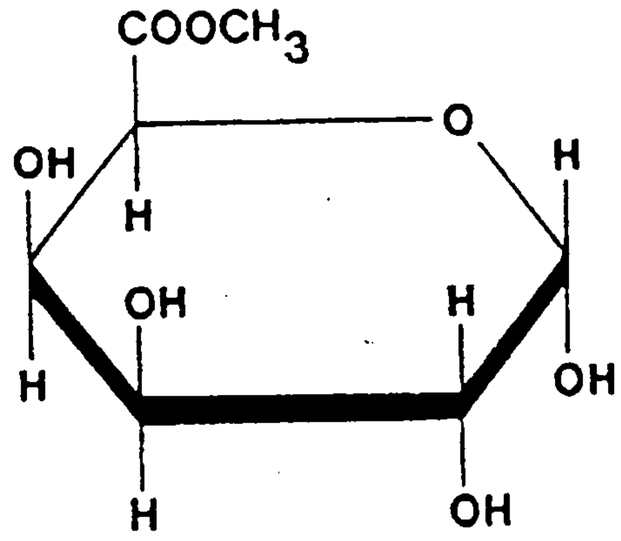

D-Galacturonic acid methyl ester

Figure 2.8. Principal units of pectin's molecule (from Christensen, 1986).

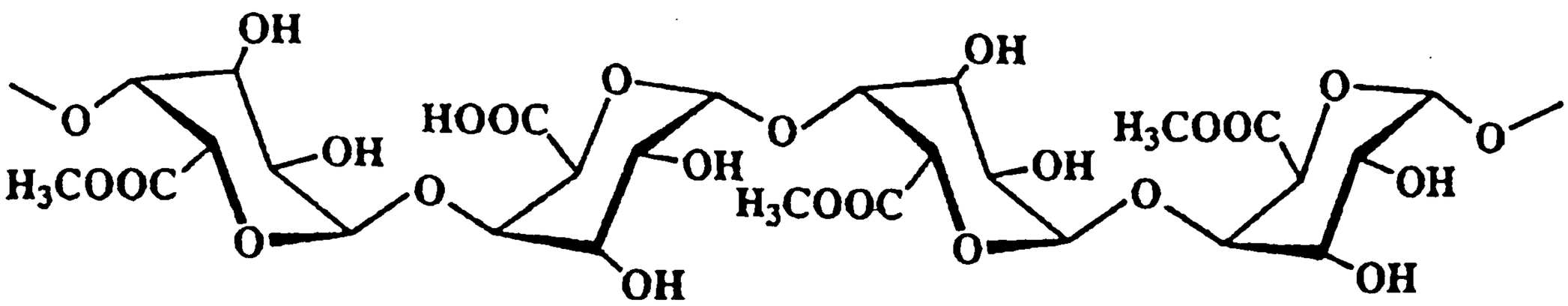

Figure 2.9. Chemical structure of pectin. Segment of high methoxyl pectin with a degree of esterification of 75% (from Iijima et al., 2000).

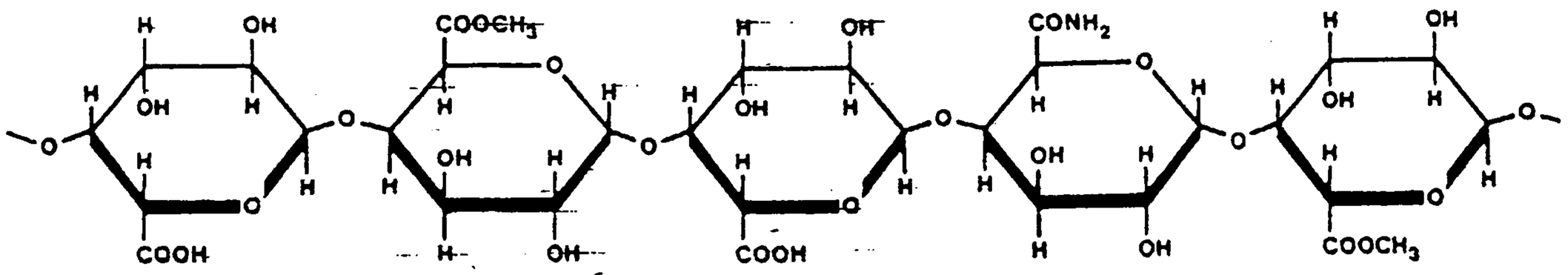

Figure 2.10. Section of a low methoxyl pectin molecule with a degree of esterification of ~40% and a degree of amidation of ~ 20% (from Christensen, 1986).

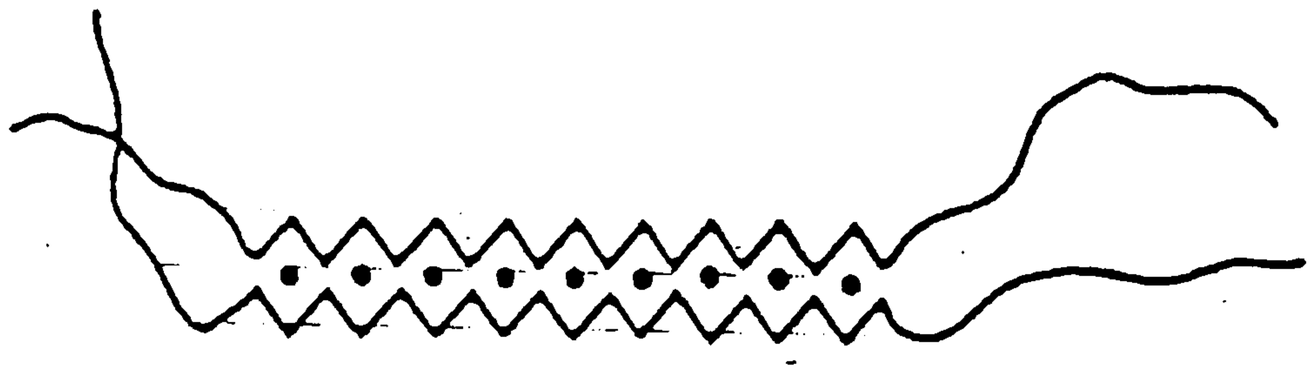

a

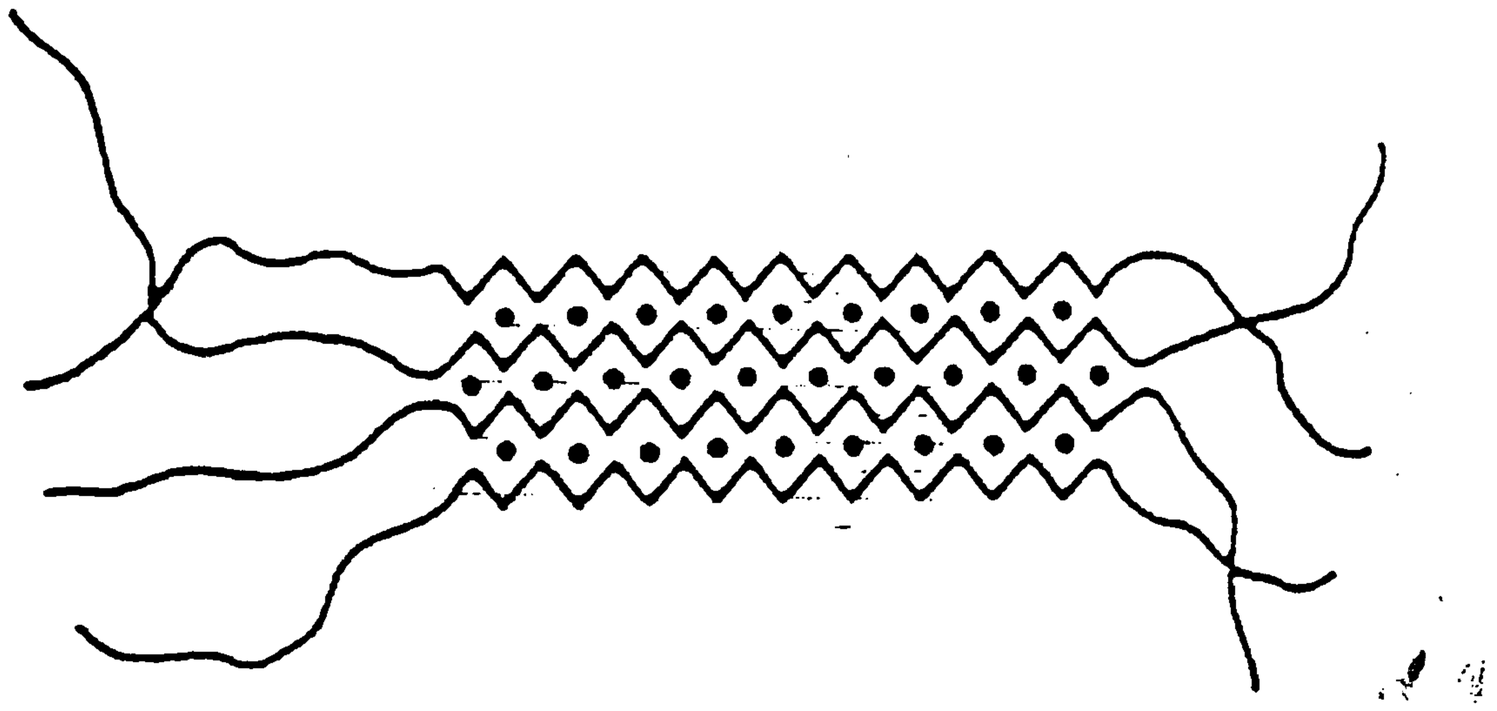

b

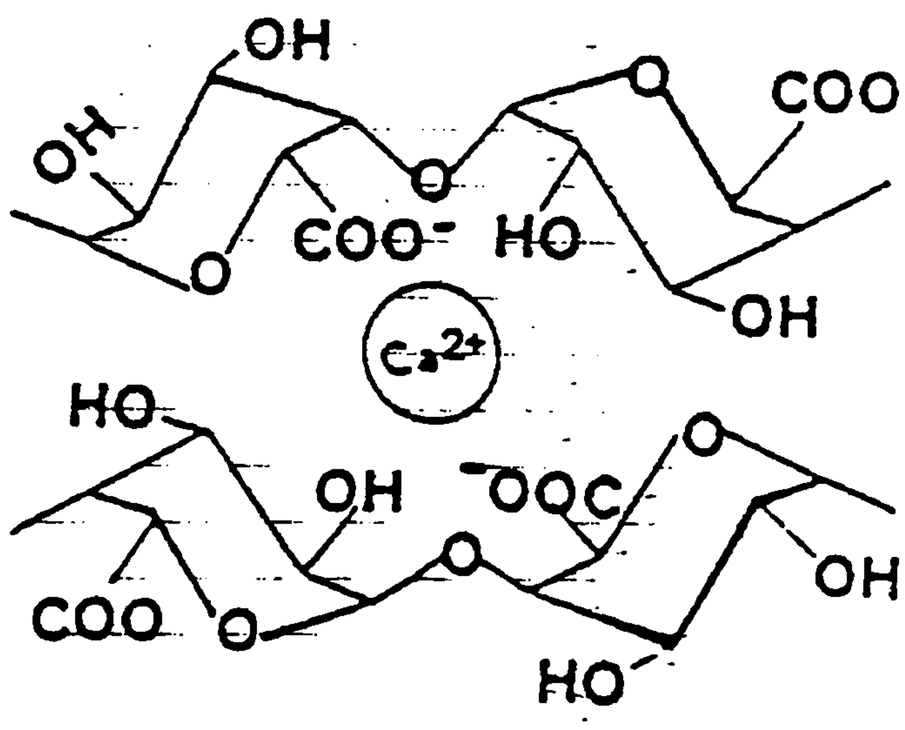

C

Figure 2.11. Schematic representation of calcium binding to polygalacturonate sequences: (a) "egg-box" dimer, (b) aggregation of dimers and (c) "egg-box" cavity (from Grant et al., 1973).

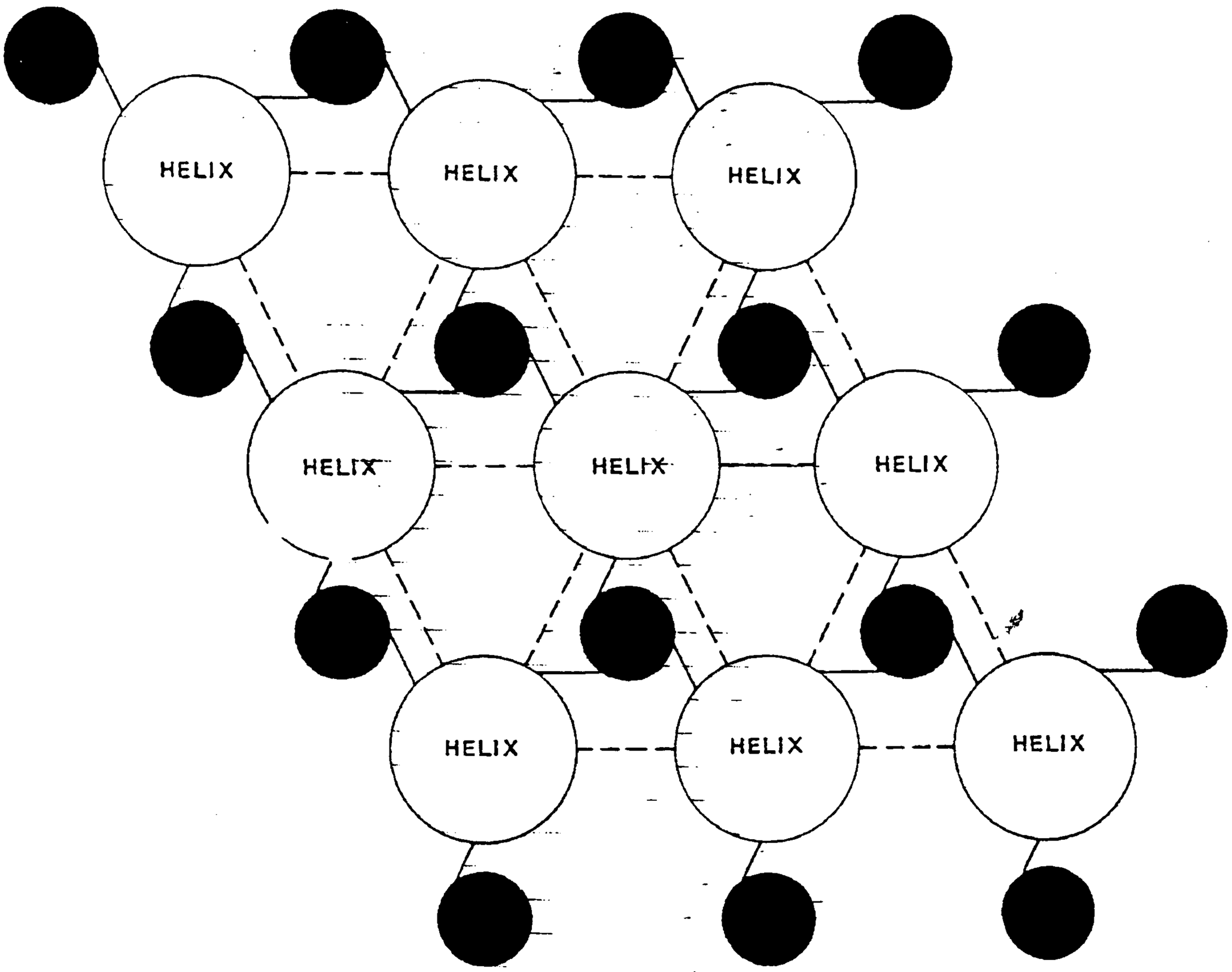

Figure 2.12. Model of junction zone in high methoxyl pectin gel as suggested by Walkinshaw et al. Parallel polygalacturonan chains, viewed along the helix axis, are packed in a hexagonal lattice. The structure is sustained by intermolecular hydrogen bonds (dotted lines) and reinforced by columns of methyl groups (filled circles) (from Christensen, 1986).

CHAPTER 3

PHYSICAL TECHNIQUES AND PHASE TRANSITIONS

3.1. DEFINITIONS OF TERMS

Rheology, which comes from the Greek word "ρεω" and means to flow, is the study of the relationship between stress and strain within a material as a function of time, frequency, temperature etc.

Stress is the force per unit area acting on a sample and has the units of pressure (Pa or Nm^{-2}). A body under stress experiences deformation and the change in dimension per unit dimension (fractional deformation) is called "strain" and is a dimensionless ratio.

An ideal solid is called a "Hookean solid" after the English inventor Robert Hooke. For a perfect Hookean solid the stress (σ) is directly proportional to the strain (γ) (Hooke's law):

$$\sigma = G \cdot \gamma \qquad (3.1)$$

The energy necessary for the deformation of a perfect solid is stored in the form of a recoverable potential energy. The proportionality constant G is called modulus.

A perfect liquid represents the opposite extreme of behaviour. We use the term Newtonian liquid, after Sir Isaac Newton. According to Newton's law for an ideal liquid, the stress is directly proportional to the rate of strain ($d\gamma/dt$) and the proportionality constant is the viscosity (η), which characterizes the resistance to flow.

$$\sigma = \eta \, d\gamma/dt \qquad (3.2)$$

The necessary energy for the flow of liquid is dissipated in the form of heat. However, most materials combine both elastic and viscous characteristics and they are called viscoelastic. Their properties are measured using various types of experimental procedures, the most commonly adopted being mechanical spectroscopy .

3.2. MECHANICAL SPECTROSCOPY

3.2.1. Introduction

If a sample is subjected to a time-dependent strain-wave of the form

$$\gamma = \gamma_o \sin\omega t \qquad (3.3)$$

where γ is the time-dependent strain, γ_o is the maximum strain amplitude and ω is the angular frequency, then the resulting shear-stress wave will also be a sine-wave but differing in amplitude and phase, i.e.

$$\sigma = \sigma_o \sin(\omega t+\delta) \qquad (3.4)$$

where σ is the time dependent stress, σ_o is the maximum stress amplitude and δ is the phase angle difference between the two waves.

For an ideal elastic (solid) system, the stress will be proportional to the corresponding strain and the strain and stress waves will therefore be in phase with each other (Figure 3.1a and 3.1b). For a viscous (perfect liquid) system, the stress will be proportional to the strain-rate at any given time and thus the maximum stress will occur when the slope of the strain wave is maximum (this gives a phase shift of $\pi/2$ radians) (Figure 3.1c). Finally, for a viscoelastic system the amplitude of the stress-wave is proportional to the strain amplitude, but with contributions from both in-phase and out-phase components giving a phase angle $0< \delta < \pi/2$ (Figure 3.1d) (Richardson & Kasapis, 1998).

The ratio of the stress component in phase with the strain to that strain, G', is known as storage or elastic modulus because the necessary energy to deform an elastic material is recovered (eq.3.5). On the other hand, the ratio of the stress component 90° out of phase with the strain to that strain, G'', is called loss or viscous modulus, since, for a liquid, the energy is dissipated as heat (eq. 3.6). In simple terms, therefore, the elastic modulus shows the solid character and the viscous modulus the degree of liquid-like behaviour. Another useful parameter is tanδ, the loss tangent, (eq.3.7), which is a measure of the liqud vs solid characteristic. This is sometimes useful in detecting underlying processes during sample changes such as the gelation process, (Pomeranz & Meloan, 1994).

$$G' = \frac{\sigma_o}{\gamma_o}\cos\delta \qquad (3.5)$$

$$G'' = \frac{\sigma_o}{\gamma_o}\sin\delta \qquad (3.6)$$

$$\frac{G''}{G'} = \tan\delta \qquad (3.7)$$

(When this ratio is above 1, the viscous character dominates, whereas below 1, the elastic character is dominant).

As for the dynamic moduli, two components of dynamic viscosity can be defined (Ferry, 1980). The real dynamic viscosity η' is the ratio of stress in-phase with strain rate to the strain rate, whereas the imaginary dynamic viscosity η'' is the ratio of stress out-phase with strain rate to the strain rate. This means that G' and G'' can be related to η' and η'' in the following manner (eq. 3.8 and eq. 3.9).

$$\frac{G''}{\omega} = \eta' \qquad (3.8)$$

$$\frac{G'}{\omega} = \eta'' \qquad (3.9)$$

Two other useful parameters are the complex modulus and the complex dynamic viscosity. The former is defined as:

$$|G^*| = \left|G'^2 + G''^2\right|^{1/2} = \sigma_o / \gamma_o \qquad (3.10)$$

and the latter as:

$$\frac{G^*}{\omega} = \eta^* \qquad (3.11)$$

To characterize the viscoelastic behaviour of various food systems, it is often necessary to perform the experiments during structural changes e.g. gelation. In this case, the measurements should be taken in a relatively short period without influencing the natural mechanisms of the process and small deformation oscillatory experiments can provide this information.

3.2.2. Oscillatory measurements on biopolymer systems

Examination of the sample by measuring the above parameters over a range of frequency provides us with an accurate indication of the structural type. A plot of, for instance, G', G'' and η^* is called the mechanical spectrum. Four general types of behaviour are observed depending underlying structure as shown in Figure 3.2.

- **Dilute solution**: only few molecules are present and they can be considered to be in isolation and hence without any kind of interaction with each other. Their main effect is to disturb the solvent flow resulting in a predominantly viscous system, η^* being constant with frequency and G'' increasing with a slope of 1 (Figure 3.2a). However, at higher frequencies, the storage modulus also increases with a slope of 2 (Ferry, 1980; Morris, 1984; Ross-Murphy, 1984).

- **Concentrated solution**: with increasing the concentration of the polymer, the molecules begin to interact until eventually they start to interpenetrate giving an

entanglement-coupled system (Figure 3.2b). At low frequencies, the spectrum is similar to that of a dilute solution. However, at higher frequencies disentanglement of the chains within the oscillation period is extremely difficult and therefore, an elastic character dominates. Under these circumstances, the spectrum appears similar to that of a permanent gel network with G'>G'' and η^* decreasing sharply with ω (Ferry, 1980; Morris, 1984; Ross-Murphy, 1984).

- **Gels**: in true gels (Figure 3.2c) G' is well above G'' and both are frequency independent. At the same time, η^* is continuously decreasing with a slope of –1 (Ferry, 1980; Morris, 1984; Ross-Murphy, 1984).

- **Weak gels**: as shown in Figure 3.2d, G' is still above G'', but both moduli reveal small frequency dependence. Tanδ has higher values than in true gels, about 0.1 to 1. This unusual behaviour originates from the rigid, ordered conformation adopted by the polymer chains in solution, which is further stabilised by weak bonding (Ross-Murphy, 1984), and under sufficient stress, the solution can flow freely.

3.2.3. Concentration dependence of gel modulus

From the Flory-Stockmayer theory of gelation it becomes obvious that the modulus depends strongly on the concentration of the biopolymer. In 1987, Clark modified the existing theoretical equation by Hermans, involving an equilibrium constant (K) between bond making and breaking, to give the following equation:

$$K = \frac{\alpha}{Nf(1-\alpha)^2} \qquad (3.12)$$

or

$$K = \frac{M\alpha}{cf(1-\alpha)^2} \qquad (3.13)$$

since, N = c/M, where N is the number of moles per unit volume, M is the molecular weight, c is the polymer concentration, *f* is the functionality of the biopolymer and α is the fraction of sites that have reacted (as discussed in Section 1.4, eq.1.3).

For $\alpha = \alpha_c$ the corresponding concentration is the critical one, c_o, meaning the minimum concentration required for the formation of the gel. A possible explanation of c_o is that below this critical concentration the intramolecular associations are more favoured therefore, no network formation is possible. Combination of equations 3.12 and 3.13 gives:

$$c_o = \frac{M(f-1)}{Kf(f-2)^2} \qquad (3.14)$$

It is obvious that the higher the molecular weight the higher the functionality of the polymer would be. By this technique we can produce general curves relating G with c/c_o, which are found to accurately emulate the properties of real systems. Fitting of these equations to real data has been used to obtain estimates of, for instance, c_o and functionality. Furthermore, this technique is useful as obvious deviation from predicted behaviour is a good indication of a different gelling mechanism. The generally observed relationship between G and c at concentrations well above c_o is also correctly predicted.

3.2.4. Rheometer types

The instruments used to perform rheological measurements, (rheometers), can be separated into two main groups depending on their method of operation.

- **Controlled strain machines**: the sample experiences a pre-determined strain or strain-rate imposed by a powerful motor *via* one side of the measuring geometry. The resulted stress is detected at the opposing sample fixture by a low-compliance transducer (Ross-Murphy, 1994; Richardson & Kasapis, 1998).

- **Controlled stress machines**: here, a given stress is applied and the resulting strain is measured using a displacement transducer (Ross-Murphy, 1994; Richardson &

Kasapis, 1998). These rheometers consist of a "drag-cup" rotor, optical strain detector and upper sample geometry all on a common shaft supported in an air-bearing, the housing of which also contains the motor windings. The sample is confined between the upper geometry and the lower stationary fixture and the required stress can be imposed with negligible losses in the air-bearing. The resulting strain is measured as an angular displacement of the single moving part. Due to the their simple construction and the fact that the stress is easily adjusted by controlling the current passing through the motor coils, these are less expensive than the strain-controlled rheometers.

In both these rheometer types, measurements are usually carried out in the linear viscoelastic region where the strain is sufficiently small such that the sample structure is unaffected. The most significant qualities required in rheometers are sensitivity and dynamic range, as they are often used to measure gelling systems where the structure transforms from a weak solution to a strong gel during a single experimental procedure (Richardson & Kasapis, 1998).

Regardless the type of the rheometer used, there are three main geometries employed for shear measurements. In the cone-and-plate geometry (Figure 3.3a), the strain or rate of strain is constant over the whole working area (Ross-Murphy, 1994). However, since a full cone would touch the plate, it is truncated slightly to avoid this problem whilst minimizing any strain error. In spite of this, any small dimensional changes in the rheometer could still cause contact with the plate, so cone-and-plate geometries are not appropriate for temperature sweep experiments, but are ideal for isothermal measurements on both linear and non-linear systems (Richardson & Kasapis, 1998).

The second geometry is the parallel plate (Figure 3.3b); the most generally useful, as suggested by Ross-Murphy (1994). Here, although the strain varies from a maximum at the periphery down to zero at the centre of the plate, it is suitable for measurements on strain-independent systems over a wide range of temperature.

Finally, the third type is the concentric cylinder geometry (Figure 3.3c), which is often used in simple viscometers and for dilute solutions because the sample is contained and the torque to sample-volume ratio may be high. Once more, the rate of strain is not uniform across the sample with the maximum at the inner surface. Any errors are minimized by the fact that the gap is small (≤ 0.1 of the outer cylinder radius). Since measurements are made

in the body of the examined system with a wide gap at the upper surface, any "skin" effects are small. A thick layer of silicone oil can be flooded over the surface to prevent any water evaporation and therefore, this geometry is ideal for dynamic and creep experiments over long periods of time, especially at elevated temperatures (Richardson & Kasapis, 1998).

3.3. TEXTURE PROFILE ANALYSIS

The rheological techniques described previously involved small deformations to monitor mechanical properties non-destructively. However, to determine and mimic desirable qualities for end-use, it is often the large deformation, breakdown properties occurring during processes such as chewing and swallowing that are more important.

The first attempt to model mastication was the MIT denture tenderometer, where a set of dentures was monitored and a force-time curve was obtained during the imitated chewing. The disadvantage of this technique was that little information other than peak force could be obtained from the analysis of the curve (Bourne, 1978).

The method generally adopted in the food industry for the study of such properties involves the compression of cylindrical samples plugs between two parallel plates moving together at a pre-determined constant rate. Using a load cell, the force developed during this procedure is monitored at fixed time intervals to produce a force-deformation curve characteristic of the sample material. At one extreme, a brittle gel generates a sharp, early peak corresponding to high breaking stress at low breaking strain. On the other hand, a smooth increase in stress to a fixed value with no yield point is indicative of a viscous liquid response. Between these extremes, plastic materials give a smooth, shallow yield shoulder followed by a plateau (Richardson & Kasapis, 1998). Due to the difficulty in producing identical sample cylinders in soft solid samples, and the inherently random nature of crack propogation, reproducibility is significantly less for the other rheological methods described earlier and averaging of the results from several samples is usually necessary to generate accurate estimates of, for instance, yield parameters.

In order to relate such measurements to sensory analysis in a more direct way, the "two-bite" test procedure was developed. Analysis of the force-time curve leads to the extraction of seven textural parameters, five of which are measured and two calculated from the measured ones. These are:

- **Fracturability** or brittleness, which is the force at the first significant break in the curve,
- **Hardness**, which is defined as the peak force during the first compression cycle (first bite),
- **Cohesiveness**, which is the ratio of the positive force area during the second compression to that during the first (A_2/A_1),
- **Adhesiveness**, which is defined as the negative force area for the first bite, representing the necessary work to pull the compressing plunger away from the sample,
- **Springiness** or elasticity, which is the height that the food recovers during the time that elapses between the end of the first bite and the start of the second,
- **Gumminess**, which is defined as the product of hardness x cohesiveness. It is characteristic of semisolid systems with low degree of hardness and a high degree of cohesiveness, and
- **Chewiness**, which is the product of gumminess x springiness (Bourne, 1978; Pomeranz et al., 1994).

A typical force-time curve obtained from a texture profile analyser is shown is Figure 3.4.

3.4. OPTICAL ROTATION

As we have already discussed, sugars with an asymmetric carbon atom in their molecule exist in two stereoisomeric forms, which rotate polarised light in opposite directions to equal extents. Any compound that rotates the polarized light is optically active. The active atom in the molecule is specified by a star and is called the asymmetric centre.

In the old system for optical rotation, if by looking towards the light source the rotation was clockwise, the compound was dextro- (+). In contrast, if the rotation was anticlockwise the compound was levo- (-). However, this method was not accurate enough, since not all (+) showed right rotations and not all (-) compounds had left rotations. Therefore, a new system was introduced, the Cahn-Ingold-Prelog one, which is based on the atoms' configuration around a specific center. This system is often called the RS system, where R stands for the rightr (R=restus) and S for the left (S=sinister).

The machine that measures the optical rotation is called a polarimeter and it operates at various wavelengths. Its principle of operation is as follows. A ray of light passes through a polariser that lines it up in one direction only. This polarised light passes through the sample to an analyzer that is rotated to the new plane of polarisation, thus determining the rotation due to sample. A polarimeter, therefore, consists of a monochromatic source, a polariser, which polarises the radiation, the sample, which rotates the radiation and an analyser that measures how mush the rotation is (Figure 3.5).

The equation used in polarimetry is

$$[\alpha]_{\lambda}^{\tau} = \frac{\alpha}{lc} \qquad (3.15)$$

where, [a] is the specific rotation in degrees, τ is the temperature in °C, λ is the wavelength of radiation used, α is the observed rotation angle in degrees, l is the length of the experimental tube in dm and c is the concentration in g/mL (for pure liquids c is replaced by density d). (Pomeranz & Meloan, 1994).

Optical rotation is employed to investigate the changes in a polysaccharide system undergoing, for instance an order-disorder transition since the technique is a direct probe of molecular conformation.

3.5. DIFFERENTIAL SCANNING CALORIMETRY

The energy changes involved in any chemical reaction can be investigated through the method of calorimetry (Sutton et al., 2000). In simple calorimetry, the heat produced by a reaction is transferred to a known mass of where in the insulated calorimeter and the subsequent temperature rise of the water is observed. Provided that the mass of water is known, as well as its heat capacity, the amount of heat given out by the reaction can be calculated as shown below:

Heat gained by water and calorimeter = Heat released by the reaction = Change in temperature (ΔT) x Mass of water in grams (m) x Heat capacity of water in Joules per Kelvin per gram (Sutton et al., 2000).

A differential scanning calorimeter is commonly used to investigate phase transitions in foods such as crystallization and melting of water, lipids, and other food components, protein denaturation, gelatinisation and retrogradation of starch (Roos, 1995). In a DSC experiment two cells are used; one filled with the sample and the other with the pure solvent as the reference material. Both cells contain the same mass in order to compensate for the heat required to heat the solvent, thus allowing measurement of, for instance, transition energy alone with increased sensitivity. The cells are contained in a hermetically sealed block, which is subjected to a programmed rate increasing, or decreasing, temperature. The difference in amount of heat supplied to sample and reference during this process is measured either directly (heat flux DSC) or by measuring the energy supplied to the individual cells so as to maintain them at the same temperature as in the compensation DSC (Wright, 1984).

The output of a DSC is, therefore, in the form of a thermograph depicting differential heat flow (dq/dt) against temperature. Absorption or emission of heat is detected as a deviation from balance, the area of which represents the total heat exchanged during the transition and hence the transition enthalpy ΔH. The other important parameters obtained using DSC are the transition mid-point temperature (T_m) and the temperature at maximum heat flow $T_{(max)}$. To correct for thermal lag, these are measured at a number of scan-rates and true values estimated by extrapolation to zero-scan-rate.

3.6. PHASE TRANSITIONS

Phase transitions in food are usually connected to compositional or temperature changes during processing or storage. Since foods are complex systems consisting of water and at least one more component whose physical states determine the physical state of the food itself, it is important to determine possible states of various ingredients as a function of time with phase diagrams (Roos, 1995).

A phase is defined as "the physically and chemically homogenous state of a material that is clearly separated from other matter". A phase transition, as result of changes in temperature, pressure, etc., can be observed from changes in the internal energy of the system, its volume, the number of moles or its mass. An equilibrium between two phases requires that both of them have the same pressure and temperature. The three basic physical states of pure substances are solid, liquid and gas. All three of them are equilibrium states and any change from one to another takes place in conditions specific to an individual material (Roos, 1995).

3.6.1. Physical states and molecular mobility of food systems

Food solids may be separated into lipids and water-soluble components, chiefly carbohydrates and proteins. In the first category, the physical state is related to the transitions between various polymorphic forms and the liquid state of lipids. Water-soluble components, however, may exist in either noncrystalline amorphous, in the crystalline, or in solution states Their water content significantly affects both their physical state and phase transitions. The higher the water, the higher the molecular mobility of both carbohydrates and proteins and trerefore, the lower the viscosity and likely stability of the system.

3.6.2. Glass transition

The glass transition is a characteristic of amorphous materials, either synthetic or natural. Melting of crystalline polymers leads to the formation of an amorphous melt, which upon supercooling exhibits either a viscoelastic, "rubbery" state or a solid, glassy state. The transition between the rubbery and the glassy state is called the glass transition (Roos, 1995; Champion et al., 2000).

Superficially, glassy materials exhibit similar mechanical properties to solids although their molecules have no defined order. The most common method of supercooling materials to produce a glass in synthetic polymers is quenching, although rapid evaporation of solvent molecules, as may occur in food processing is also used. At low temperatures the system is vitreous, i.e. glassy, hard and brittle, but with increasing temperature it shows less viscous, rubbery, behaviour. The temperature at which the system is transformed from a brittle and hard state to that of a rubber is called the glass transition temperature T_g. In the case of polymers, the glass transition temperature is defined as the temperature at which the material softens because of the onset of long-range coordinated molecular motion (Sperling, 1986; Roos, 1995).

3.6.2.1. Characterisation of the physical states

In the case of amorphous materials their physical properties depend on composition, temperature and time. Five distinct, different states from the lowest to the highest temperature can be recognised as follow:

1. **The glassy state**: the viscosity is extremely high (>10^{12} Pa.s) and the storage modulus is typically about 10^9-10^{11} Pa, with the loss modulus significantly smaller than G'. The system behaves like a brittle, transparent solid (Roos, 1995, Champion et al., 2000). Moreover, any kind of molecular motions are restricted to vibrations and short-range rotational motions (Sperling, 1986).

2. **Glass transition temperature range**: in this temperature range the mechanical properties transform to those of a viscoelastic rubber, if the system is a polymeric one, or of a viscous liquid, for low molecular weight schemes (Champion et al.,

2000). The modulus increases with frequency and drops considerably to 10^6 Pa, which results in a less rigid material, and the molecular mobility is also affected (Roos, 1995).

3. **Rubbery plateau region**: this is the region where the modulus stays constant over a temperature range and the system exhibits a long-range rubber elasticity. The temperature range is specific to a particular system and is affected by the molecular weight and the linearity of the molecules i.e. the higher the molecular weight the broader the plateau with increased crosslinking enhancing rubber elasticity (Roos, 1995).

4. **Rubbery flow region**: over this temperature range, the system may show both rubber elasticity and flow depending on the experimental time scale. However, flow is characteristic of linear polymers as strongly crosslinked systems remain in the rubbery plateau region until they decompose at high temperatures.

5. **Liquid flow region**: it follows the rubbery plateau region or rubbery flow region with increasing temperature or longer experimental times (Roos, 1995).

3.6.2.2. Glass transition theories

The basic theories of the glass transition are the free volume theory, the kinetic theory and the thermodynamic theory, although other have also been developed to explain the molecular basis of the glass transition ((Roos, 1995, Champion et al., 2000).

1. **Free volume theory**: this assumes that molecular motion is dependent on the presence of holes, vacancies or voids, which provide the necessary free volume for molecular rearrangement. The theory is based on the change in volume expansion coefficient, which takes place at the glass transition, and assumes that the fractional free volume *f*, is constant in the glassy state but increases above T_g, according to equation 3.16.

$$f = f_g + a_f(T - T_g) \qquad (3.16)$$

where, f_g is the fractional free volume at T_g and α_f is the thermal expansion coefficient of the free volume (Ferry, 1980).

The fractional free volume is defined by equation 3.17 and the specific free volume by the equation 3.18.

$$f = \frac{v_f}{v} \tag{3.17}$$

$$v_f = v - v_o \tag{3.18}$$

where, v is the macroscopic volume, v_f is the specific free volume and v_o is the volume occupied by the molecules (Tant & Wilkes, 1981).

2. **Kinetic theory**: this theory considers the time-dependent characteristics of the glass transition and the time-dependent molecular relaxations that occur over the glass transition temperature range. It assumes that matter may exist with or without holes and assigns a molar excess energy ε_h for the no-hole situation and an activation energy ε_j for the disappearance of a hole. In the glassy state, the number of holes are assumed to be frozen and not accessible to molecules.

3. **Thermodynamic theory**: it uses the concept that glass transition achieves equilibrium at infinitely long experimental times and requires that the entropy of the glassy phase is negligibly higher than the crystalline phase (Roos, 1995).

3.6.3. Reaction kinetics

The rate of chemical reactions, enzymatic changes and microbial growth in food systems is affected by the phase transitions. The main significance of reaction kinetics is to estimate the overall rate at which various changes may take place under a range of conditions.

The majority of the physicochemical changes in food systems are temperature-dependent and to a great extent they follow the Arrhenius equation (eq.3.19 and 3.20), particularly if the water content is high.

$$k = k_o e^{-\frac{E_a}{RT}} \tag{3.19}$$

$$\ln k = \ln k_o - \frac{E_a}{RT} \tag{3.20}$$

where, k is the rate constant, k_o is the frequency factor, E_a is the activation energy, R is the gas constant and T is the absolute temperature.

The Arrhenius equation is one of the most significant and is used to model the temperature dependence of various physicochemical properties of food. However, deviations form the Arrhenius kinetics are possible and the activation energy can easily be changed with a alteration in the physical state of the examined system. Some reasons for potential variations are listed below:

- Crystallization of amorphous sugars may release water and change the proportion of reactants in the solute-water phase,
- Freeze-concentration of solutes increases the concentration of reactants in the unfrozen solute matrix,
- Increase in the water activity with increasing temperature may cause an additional increase in the reaction rate,
- Reactions with different activation energies is possible to predominate at different temperatures,
- Partition of reactants between oil and water phases may vary with temperature due to phase transitions and solubility,
- Reaction rates often depend on the pH, which is also temperature dependent,
- Solubility of gases, especially oxygen, in water decreases with increasing temperature,
- Evaporation may alter the reaction rates, and
- Proteins at high temperatures become more or less susceptible to chemical reactions because of denaturation (Labuza & Riboh, 1982; Roos, 1995).

Another major temperature-dependent factor is the molecular mobility of the system, which affects, for instance, rates of deteriorative changes in the food systems and is examined by the Williams-Landel-Ferry equation (eq.3.21).

$$\log a_T = \frac{-C_1(T - T_s)}{C_2 + (T - T_s)} \qquad (3.21)$$

where, C_1 and C_2 are constants, T_s is the reference temperature and a_T is the ratio of relaxation times τ and τ_s, as shown in equation 3.22.

$$a_T = \frac{\tau}{\tau_s} \qquad (3.22)$$

where τ and τ_s are the relaxation times of configurational rearrangements at a temperature, T, to that at a reference temperature, T_s, respectively.

It should be noticed that WLF equation is applicable at temperatures from T_g to T_g+100^{O}C, whereas the Arrhenius equation is applied at temperature below T_g (Williams et al., 1955).

The molecular mobility of a polymer, therefore, is related to the relaxation time of the system, the latter being a measure of the time required by the molecules to respond to an external stress at a constant temperature. The temperature dependence of relaxation time arises from the fact that a temperature increase leads to a rise in the molecular mobility. Relaxation processes are observed both in the glass transition region and the glassy state, although in the latter the molecular motions are with a lower amplitude and co-operativity than in the glass transition region (Ferry, 1980).

The relationship between relaxation times and temperature is used in the time-temperature superposition principle, which is used to evaluate the mechanical properties of systems at different temperatures or frequencies. In principle the TTS assumes that relaxation data obtained at one temperature can be shifted along the time axis to another temperature, allowing the characterization of the viscoelastic behaviour of amorphous food materials.

A master curve obtained for a particular system using a shift factor that assumes WLF temperature dependence of relaxation times above T_g. The modulus measured at frequency f at temperature T is equivalent to the modulus measured at frequency fa_T at a reference

temperature T_o, where a_T refers to the ratio of relaxation times at T and T_o. as we have already mentioned above (Ferry, 1980).

REFERENCES

Bourne M. C. (1978). Texture profile analysis. *Food Technology*, **32**, 62-72.

Champion, D., Le Meste, M. & Simatos, D. (2000). Towards an improved understanding of glass transition and relaxations in foods: molecular mobility in the glass transition range. *Trends in Food Science and Technology*, **11**, 41-55.

Clark, A. H. (1987). The application of network theory to food systems. In J. M. V. Blanshard & P. Lilford, *Food structure and behaviour*, Academic Press, London, pp. 13-34.

Ferry, J. D. (1980). *Viscoelastic Properties of Polymers*, Willey & Sons, New York.

Labuza, T. P. & Riboh, D. (1982). Theory and application of Arrhenius kinetics to the prediction of nutrient losses in foods. *Journal of Food Technology*, **36**, 66,68,70,72,74.

Morris, E. R. (1984). Rheology of hydrocolloids. In G. O. Phillips, D. J. Wedlock & P. A. Williams, *Gums and Stabilizers for the Food Industry 2*, Pergamon Press, pp. 57-77.

Morris, E. R. (1995). Polysaccharide rheology and in-mouth perception. In A. M. Stephen, *Food Polysaccharides and their Applications*, Marcel Dekker, USA,pp. 517-545.

Pomeranz, Y. & Meloan, C. E. (1994). *Food Analysis: Theory and Practice*, Chapman & Hall, USA.

Richardson, R. K. & Kasapis, S. (1998). Rheological methods in the characterisation of food biopolymers. In D. L Wetzel, *Instrumental methods of food and beverages analysis*, Elsevier, Amsterdam, pp.

Roos, Y. H. (1995). *Phase Transitions in Foods*, Academic Press, USA.

Ross-Murphy, S. B. (1984). Rheological methods. In H. W. S. Chan, *Biophysical methods in food research*, Blackwell Scientific Publications, Oxford, 138-198.

Ross-Murphy S. B. (1994). *Physical Techniques for the Study of Food Biopolymers*, Blackie Academic & Professional, UK.

Sperling, L. H. (1986). *Introduction to Physical Polymer Science*, John Wiley & Sons, New York.

Sutton, R., Rockett, B. & Swindells, P.(2000). *Chemistry for the life sciences*, Lifelines, London.

Tant, M. R. & Wilkes, G. L. (1981). An overview of the nonequilibrium behaviour of polymer glasses. *Journal of Polymers Engineering and Science*, **21**, 874-895.

Williams, M. L., Landel, R. F. & Ferry. J. D. (1955). The temperature dependence of relaxation mechanisms in amorphous polymers and other glass-forming liquids. *Journal of the American Chemical Society*, 77, 3701-3707.

Wright, D. J. (1984). Thermodynamical methods in food research. In In H. W. S. Chan, *Biophysical methods in food research*, Blackwell Scientific Publications, Oxford, pp. 1-36.

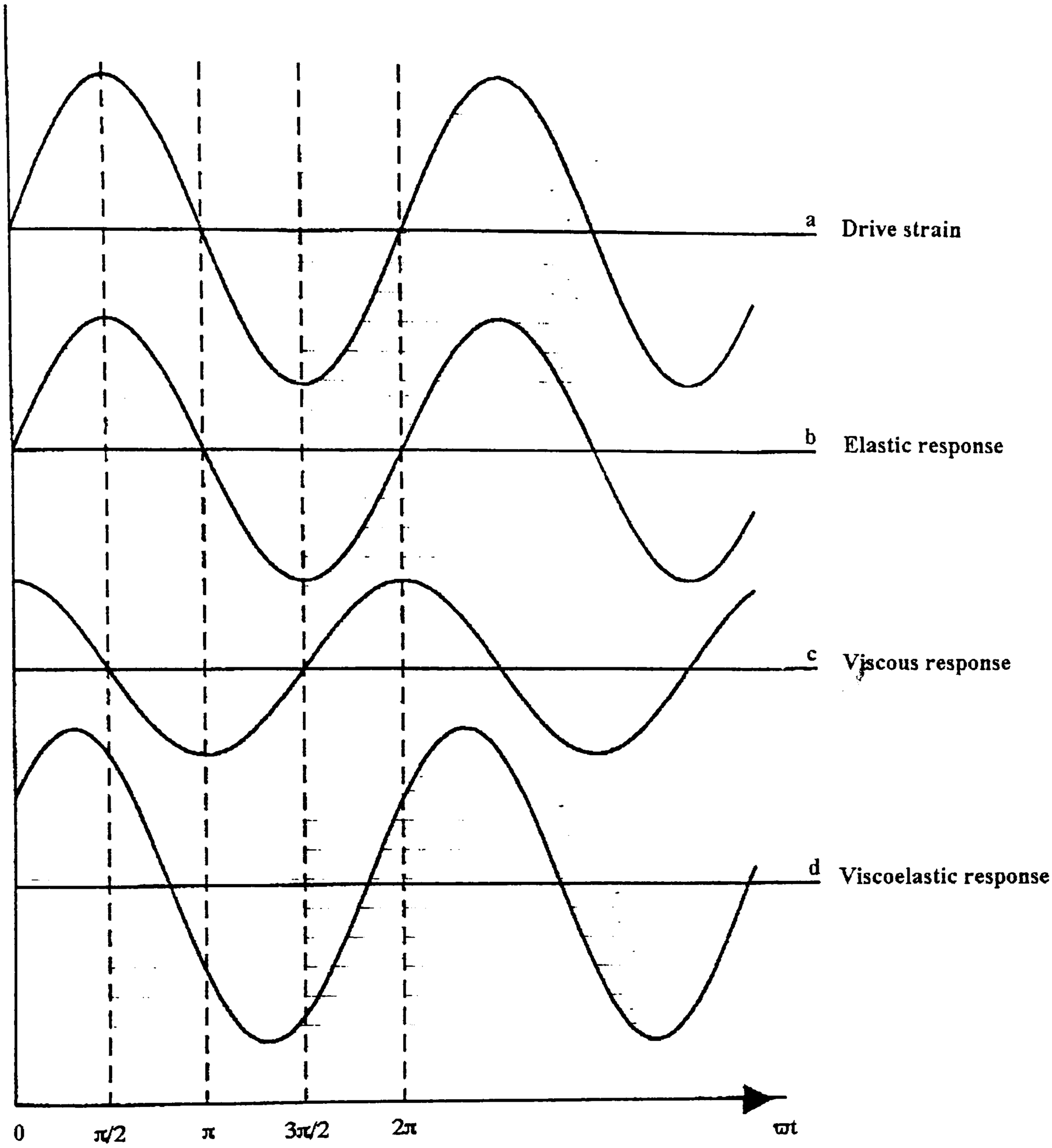

Figure 3.1. Resultant stresses due to a sinusoidal drive strin (a) for elastic (b), viscous (c), and viscoelastic (d) materials (from Richardson & Kasapis, 1998).

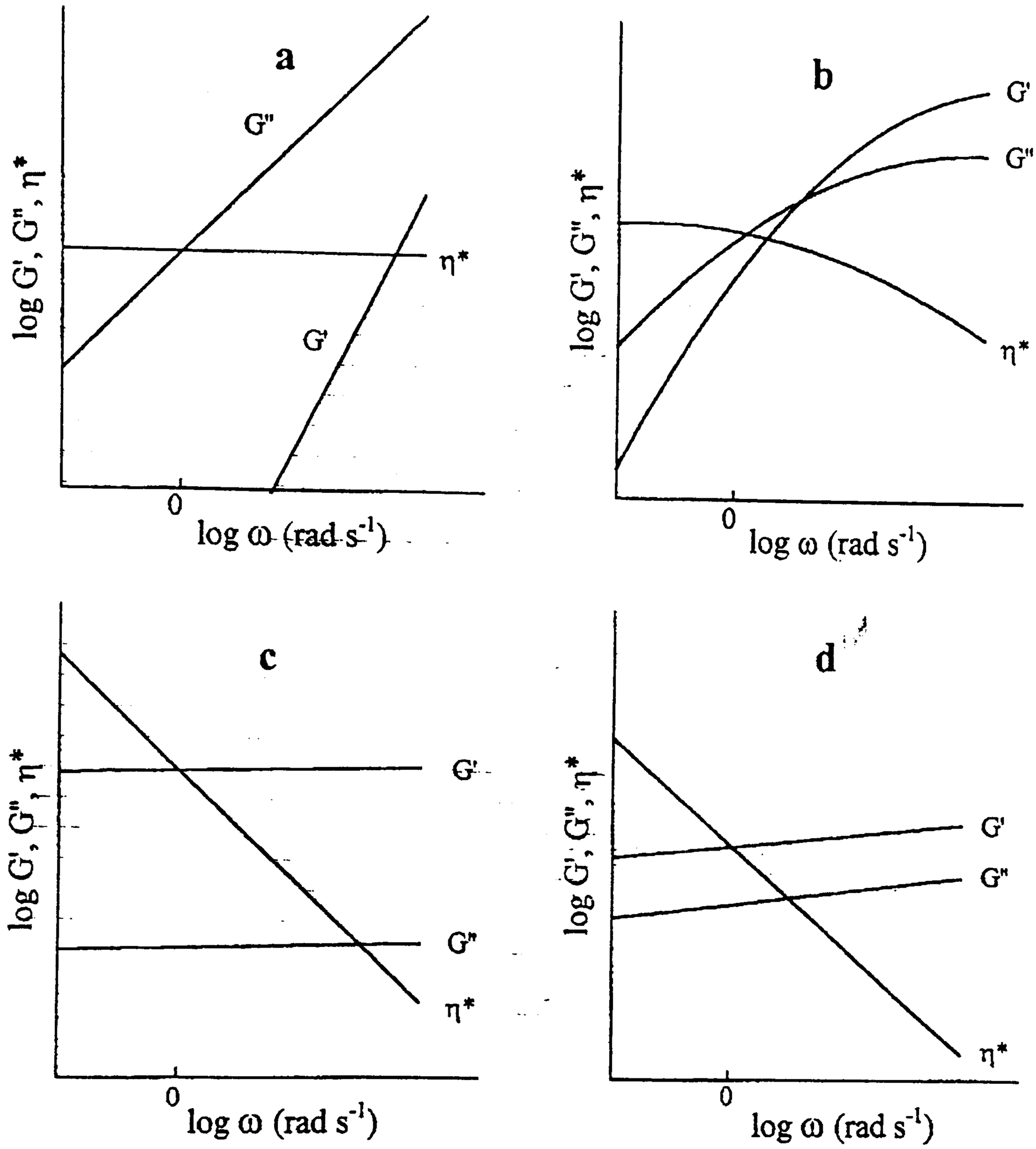

Figure 3.2. The four principal categories of mechanical spectra: (a) Dilute solution, (b) entangled solution, (c) strong gel, and (d) "weak gel" (from Richardson & Kasapis, 1998).

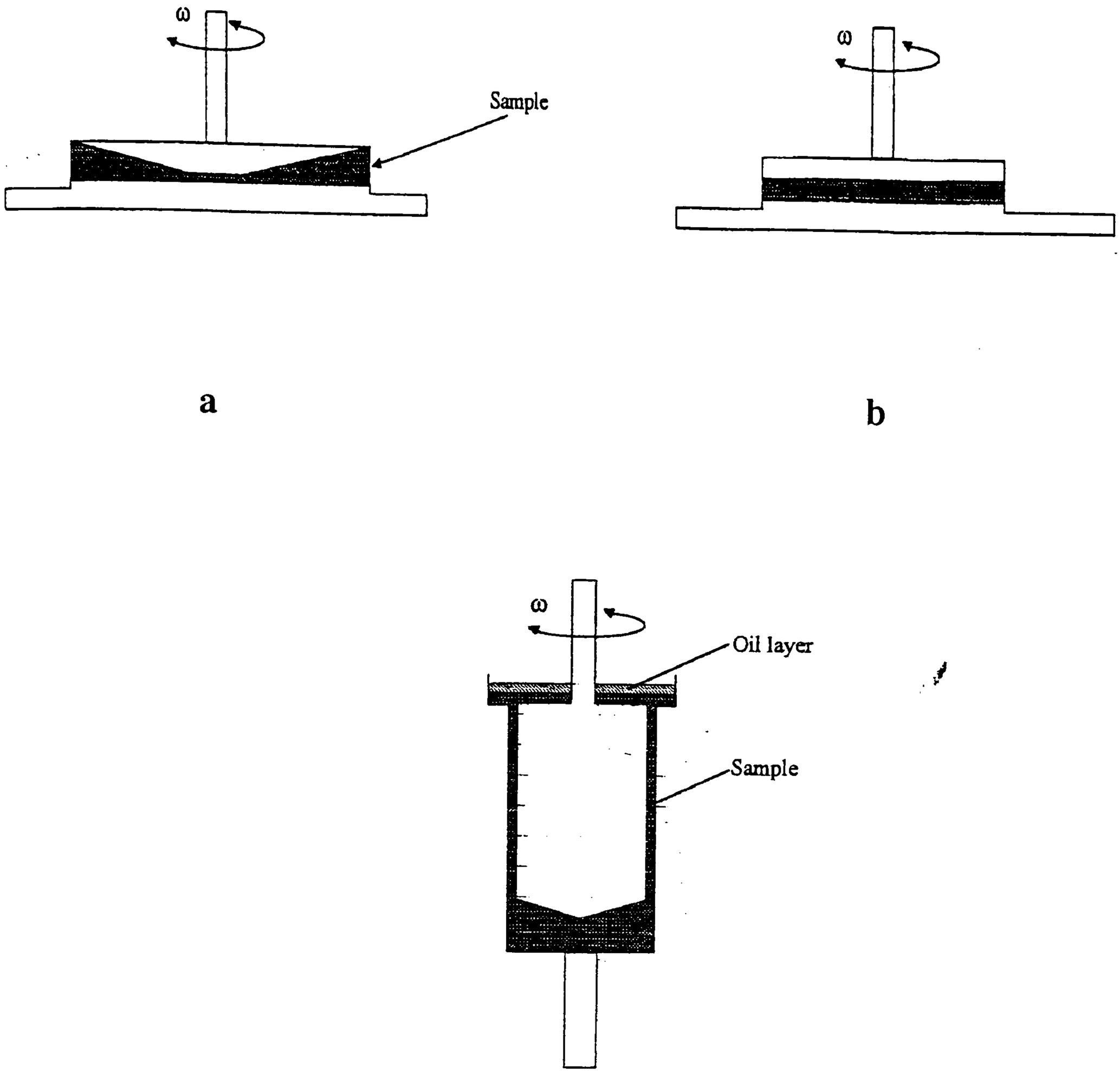

Figure 3.3. The three standard geometries used in rheometers: (a) cone-and-plate, (b) parallel, and (c) concentric cylunder (from Richardson & Kasapis, 1998).

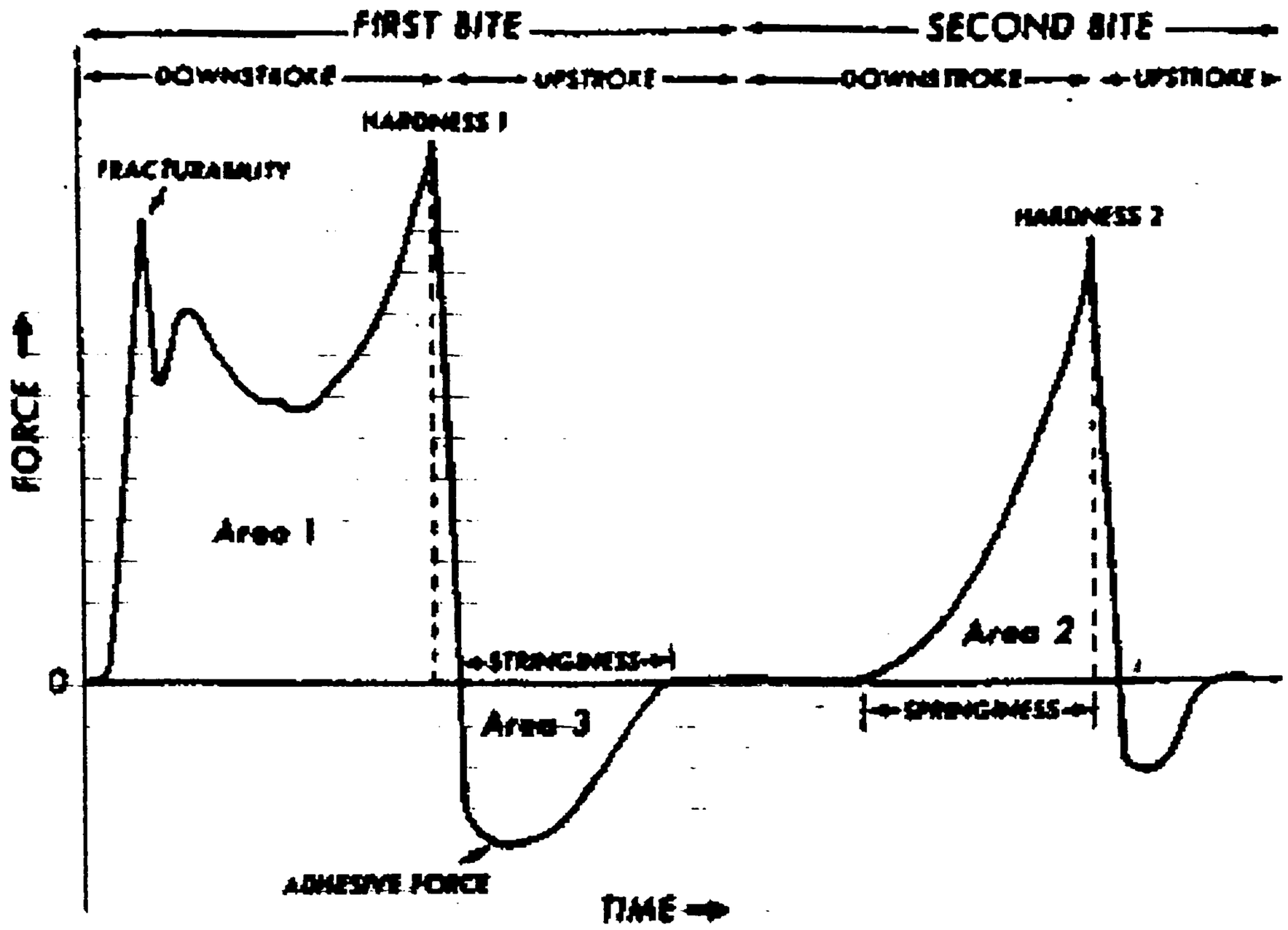

Figure 3.4. A typical TPA curve from the Instron Universal Testing Machine, (from Bourne, 1978).

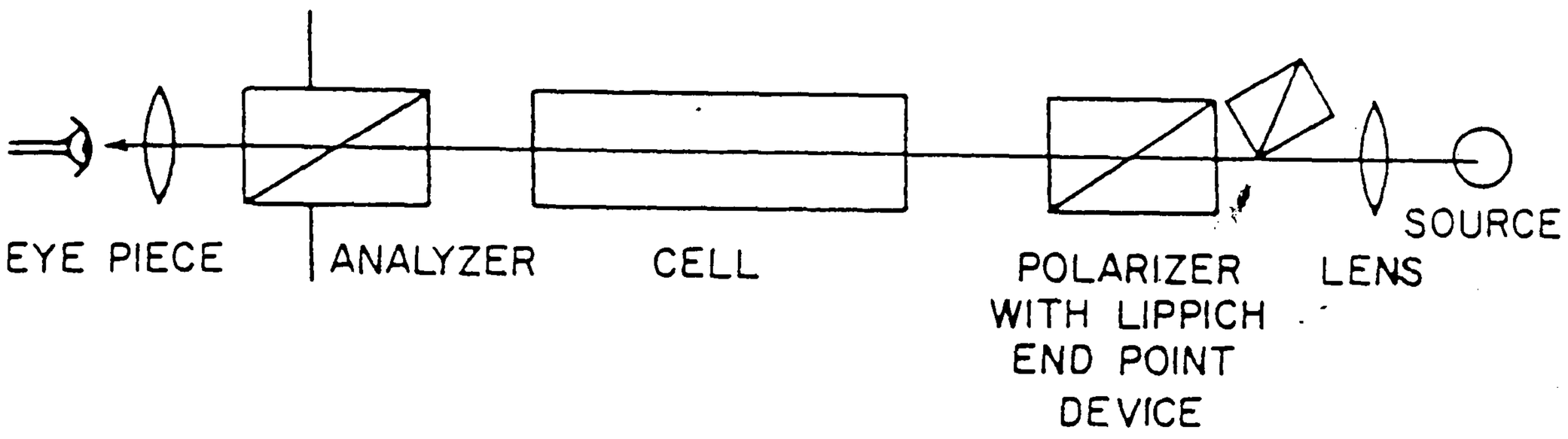

Figure 3.5. Components of a polarimeter (from Pomeranz & Meloan, 1994).

By: Tsoga, A., Kasapis, S. and Richardson, R. K.

Published in: Biopolymers

CHAPTER 4

THE RUBBER-TO-GLASS TRANSITION IN HIGH SUGAR AGAROSE SYSTEMS

4.1. ABSTRACT

The small and large deformation properties of agarose in the presence of high levels of sugar were investigated. Mixtures can he described as lightly cross-linked rubbers, which undergo vitrification upon cooling. The combined Williams-Landel-Ferry (WLF)/free volume framework was used to derive the glass transition temperature, the fractional free volume, and the thermal expansion coefficient of the glass. Sucrose-rich cosolute crystallizes, but addition of the polymer encourages intermolecular interactions, which transform the mixture into a high viscosity glass. The mechanical properties of glucose syrup, a noncrystalline sugar, follow WLF behavior in the glass transition region and revert to an Arrhenius-type prediction in rite glassy state. Measurements on sugar samples and agarose-sugar mixtures were resolved into a basic function of temperature alone and a basic function of frequency (time} alone. The former traces the energetic cost of' vitrification, which increases sharply with decreasing temperature. The latter, at long time scales, is governed by the infinite molecular weight of the agarose network. In the region of short times, the effect of free volume is active regardless of the sample composition.

4.2. INTRODUCTION

For about 50 years data have been available on the linear viscoelasticity of synthetic amorphous polymers and diluted systems (Marvin, 1954). To start with, the methodology

comprises temperature sweeps at a single frequency and frequency sweeps at a fixed temperature that yield the solid and the liquid-like components of the complex shear modulus, G' and G", respectively. A thorough analysis, however, requires disentanglement of the real temperature and time (1/frequency) effects on the mechanical properties of materials. To achieve this, a series of frequency sweeps are attempted covering as wide a temperature range as possible followed by horizontal superposition of the data. Thus the rubber-to-glass transition of synthetic macromolecules generates a smooth master curve, a result that argues for the uniform temperature dependence of all relaxation processes (Williams et al., 1955). The superposition yields a shift factor vs temperature graph that indicates how much the temperature shifts the frequency scale and a G', G" vs frequency graph that illustrates how much the viscoelasticity is affected by that shift. The approach is of great interest since it unveils the molecular innerworkings of a macromolecule in response to changing external stimuli.

The spectacular change in viscoelasticity of a polymer undergoing vitrification was followed by the relation of Williams, Landel and Ferry (the WLF equation), which allowed prediction of the glass transition temperature (T_g) (Williams et al., 1955). The utility of the equation was consolidated by marrying it with the theory' of free volume, which stipulates that at T_g the thermal expansion coefficient undergoes a discontinuity following completion of the conformational rearrangements of the polymeric backbone (Kovacs, 1964). It was found that for a plethora of distinct polymer systems the free volume at T_g is only a fraction of the total volume (ranging from 1 to 7%). Master curves were also recast as the distribution function of relaxation times, which unveils the time dependence of structural properties. In doing so, Ferry and co-workers used mainly data of dynamic oscillation since comparison of the distribution function from the real and imaginary parts of the complex shear modulus affords an extra check of the validity of the approach (Ferry & Williams, 1952). Finally, the WLF equation can be used to calculate the temperature dependence of the energy of activation for viscoelastic relaxations, which should contrast with the predictions of the reaction-rate theory typically yielding an Arrhenius form (Williams, 1955).

Clearly, the combined dynamic oscillation/WLF framework is of consequence and successful application to biological glasses can serve as a basis for the understanding of molecular processes in these systems. The present investigation observes the glass transition of the high sugar/agarose system and considers its nature in an effort to document the universal utility of the approach in biological macromolecules.

4.3. EXPERIMENTAL

4.3.1. Materials

The agarose sample was supplied by Sigma (product number: A 0576). It is a material of high gel strength (verified in Figure 1) with water and sulphate contents of less than 7 and 0.12%, respectively. Sucrose was of commercial grade. The glucose syrup used was a Cerestar product (Batch NX4). The dextrose equivalent of the sample is ≈ 42. The total level of solids is 81% and glucose syrup compositions in this work refer to dry solids. GPC analysis provides the following relationship between degree of polymerization and surface area (%) of the glucose syrup spectrum:

DPI	17.54
DP2	12.99
DP3	10.55
DP4	8.79
DPS	7.29
DP6	5.28
DP7	4.78
DP8	4.21
DP9	3.19
DP10	1.96
>DPl0	23.40

4.3.2. Methods

High sugar agarose samples were prepared as follows: The polymer was dispersed in distilled water at ambient temperature and then heated to 97° C to dissolve using vigorous stirring for 30 min. Once fully hydrated, the temperature was lowered to 80°C and first sucrose followed by glucose syrup was added. The final formulation contained 0.7 wt % agarose, 50 wt % sucrose, and 35 wt % glucose syrup. We also run aqueous agarose systems (0.7 wt %) to illustrate the dramatic change in viscoelasticity in the presence of cosolute.

Samples were loaded on the preheated platen (70°C) of a controlled stress Carri-Med CSL5OO rheometer and cooled, in the case of aqueous agarose gels to 5 or to-34°C for the high solids systems. Cooling runs were followed by heating to 95°C and in both cases the scan rate was 1°C/min. The frequency of oscillation was set at the experimentally convenient frequency of 1 Hz and the mechanical response was monitored at 0.1% strain. i.e., well within the linear viscoelastic region. Parallel plates ranging in diameter from 4 to 0.4 cm. were alternated, thus recording accurately the viscoelasticity of melts at the upper range of temperature and eliminating any inherent machine compliance in the high modulus glassy state. This allowed measurements to be taken within the range of 10^1 to $\approx 10^{10}$ Pa.

For the implementation of time-temperature superpositions, fresh samples were made, cooled to –34°C and then heated, taking frequency sweeps at constant temperature intervals of three degrees centigrade (cooling and heating scans at 1°C/min). The experimentally available frequency window was between 0.001 and 10 Hz, but horizontal superposition of data allowed construction of master curves over eight orders of magnitude. The measuring gap between the two parallel plates was 1mm and the exposed edges of the sample were covered with silicone fluid (Dow Corning 200/10cs) to minimize the loss of moisture. Particular care was taken during sample preparation and loading, which ensured that duplicate runs of selected samples reproduced the rubber-to-glass transformation within a 3 % margin.

The changing nature of viscoelasticity was also captured in compression testing using the

Texture Profile Analyser of Stable Microsystems. Aqueous and high sugar (85 wt %) preparations of agarose (0.7 wt %) were poured into ring molds of 28 mm diameter and 13 mm height, and left to set overnight at refrigerator temperature. Gels were removed from the ring molds and compressed at 0.85 mm/s (2"/min) to 10% of their original height using a plunger of 60 mm diameter. Experiments were repeated and averages of five runs are reported.

4.4. RESULTS AND DISCUSSION

4.4.1. Sugar-induced transformation of the agarose network

Before we present the case of sugar-agarose viscoelasticity, a digression is necessary to report on the nature of the polysaccharide network in an aqueous environment. Agarose is a linear copolymer of alternating (1→3)-β-D-galactopyranose and (1→4)-3,6anhydro-α-L galactopyranose repeat units with a variable attachment of sulphate, pyruvate and/or *O*-methyl groups (Stanley, 1995). Clearly, the degree and site of substitution will modify the physical properties of an aqueous preparation. As seen for other polysaccharides, hydration of the powder following, for example, the routine of the preceding section unleashes fluctuating, disordered coils. Cooling of the solution sees a steep rise in the values of shear modulus, which signifies the transformation to a three-dimensional, ordered structure. In Figure 4.la the conformational transition commences at 35°C and results in the development of a rigid gel (G' is ≈12 kPa at 5°C). Mechanical spectra at the end of cooling runs generate a flat frequency response for both G' and G" with a low tan δ value (G"/G' = 0.025) typical of hydrogels (Ross-Murphy, 1984). Subsequent heating unveils substantial thermal hysteresis with the network melting at a temperature just below the boiling point (Figure 4.1b). The rheological evidence is congruent with the formation of an enthalpic network where the structural knots are highly aggregated intermolecular associations (Morris & Norton, 1983). On the basis of x-ray fiber diffraction and optical rotation evidence, it has further been postulated that an aggregate is composed of a plethora of coaxial double helices (Arnott et al., 1974).

Having verified the small deformation properties of the aqueous agarose network, we induced a "shock" by changing dramatically its surroundings to a high solids system (85 wt % sugar). As shown in Figure 4.la, addition of sugar creates a viscous solution, which upon cooling follows a distinct structural progression from the agarose-water system. Thus, the solid-like component dominates at moderately low temperatures (below 18°C), leading to a gradual build up of a network with a high "sol fraction" (tan δ = 0.538 at 5°C). Dropping the temperature below zero degrees centigrade would freeze the aqueous agarose matrix resulting in an increase in storage modulus of several decades, thus effectively terminating the experiment. In contrast, the agarose-sugar system undergoes a gradual "reliquification" and transforms into a high viscosity solution (G" ≈ 0.5 MPa at -3O°C). This part of the mechanical response is perfectly reversible, showing overlapping cooling and heating modulus traces, which converge at –10°C (lower temperature end in Figures 4.la and 4.1b). Qualitatively, the effect of temperature on the agarose-sugar system follows the changes that characterize high molecular weight polymers in their passage from the melt to the rubbery and the glass transition zone.

Thus in the absence of crystallinity or substantial order in the polymer/solvent domains, the phenomenon of thermally reversible glass transitions is particularly marked (Arridge, 1975; Favier et al., 1995). The large degree of hysteresis observed between the cooling and heating profiles of the aqueous agarose gel (sixty degrees) contrasts strongly with that in the presence of sugar (seventeen degrees) and argues for reduced conformational order in the latter. Clearly, a morphology where substantial parts of the network remain in the disordered form should possess elastic properties, which can be readily identified on a compression experiment.

In Figure 4.2 we compressed agarose disks with and without sugar and plotted results in the form of stress vs "true' units of strain, i.e., $\varepsilon = \ln(L_o)/L)$, where L_o is the original height and L is the height of the sample during deformation. As anticipated, the aggregated agarose chains form a brittle gel, which fractures early at about 29 % deformation. In contrast, the presence of sugar only allows limited intermolecular associations, thus leaving the bulk of the polymeric

material as flexible entities capable of extensive stretching before relaxing, The yield point of the elastic sugar-agarose structure in Figure 4.2 is just above 100% deformation. Similar modification from a brittle to an elastic polysaccharide network with increasing sugar concentration has been observed for deacylated gellan (Sworn & Kasapis, 1998) a result that suggests a common pattern of behavior in the high solids environment. The implications of this transformation to the dynamic mechanical properties of our sample will now be examined.

4.4.2. Separation of variables of frequency and temperature

The preponderance of flexible chains, adjoining light cross-links in the agarose network, makes the entropic component of viscoelasticity dominant, which manifests itself in the vitrification of our sample at subzero temperatures (Figure 4.1). A "true" glass transition relates to the conformational rearrangements of the polymeric backbone and should be followed equally by changing the temperature or frequency (time) of measurement. Thus one is able to perform a time-temperature superposition (TTS) on the basis that the effect of a change in temperature is primarily to shift the frequency scale (Tobolsky, 1956). To explore the applicability of TTS to the sugar-agarose system, we recorded a series of mechanical spectra around the experimentally accessible rubber-to-glass transformation and the outcome is reproduced logarithmically in Figure 4.3.

The data for G' and G" covering the long time-scales of the upper range of temperature remain relatively flat within the rubbery region, whereas further cooling sees a rapid reinforcement of viscoelasticity that unveils part of the glass transition. Horizontal superposition of the modulus traces along the abscissa creates the master curve of Figure 4.4a, which includes the viscoelastic ratio, tanδ (G"/G'). The initial drop in tanδ signifies the build up of the rubbery region followed by the onset of vitrification and the concomitant rise of the viscoelastic ratio above one. Our measurements extend well within the glass transition since the tanδ trace reaches a maximum and descends toward the value of one that denotes the beginning of the glassy state.

Superposition of the mechanical spectra of the glass transition generates a series of shift factors (α_T) that, following the synthetic polymer approach, we fitted using the WL F equation (eq.4.1):

$$\log a_T = -C_1^o(T - T_o) \Big/ \left(C_2^o + T - T_o\right) \tag{4.1}$$

For dynamic mechanical data, $\alpha_T = G'(T)/G'(T_o)$ with T_o being the arbitrary-chosen reference temperature, C_1^o (eq.4.2) and C_2^o (eq. 4.3) are the WLF constants, which acquire physical significance when examined in the light of the free volume theory (Ferry & Williams, 1952):

$$C_1^o = B \Big/ 2.303 f_o \tag{4.2}$$

$$C_2^o = f_o \Big/ a_f \tag{4.3}$$

The fractional free volume f_o, is the ratio of free to total volume of the molecule, a_f is the thermal expansion coefficient, and B is usually set to one.

A straightforward calculation recasts the WLF equation as a linear dependence of the experimental temperature steps on the derived shift factors. This is reproduced for the sugar-agarose system in Figure 4.4b. The intercept and gradient of the linear fit allow estimation of the C_1^o and C_2^o values (eq. 4.4 and eq. 4.5, respectively), which for the reference temperature of -22°C (T^o = 251 K) are 10.62 and 68.63 deg, respectively. Based on the observation that the glass transition temperature appears to be fifty degrees above the Vogel temperature (Ferry, 1980; Vogel, 1921) it was found that the T_g of our sample was ≈ - 41°C (in this context the Vogel temperature, T_∞, is equal to $T_o - C_2^o$). Relaxation processes within the glass transition are governed by free volume effects, an assumption that allows application of the WLF equation to any reference temperature, T_g included. Thus using the following relations,

$$C_1^o = C_1^g C_2^g \Big/ \left(C_2^g + T_o - T_g\right) \tag{4.4}$$

$$C_2^o = C_2^g + T_o - T_g \tag{4.5}$$

the C_1^g and C_2^g values were found to be 14.6 and 50 deg, respectively. Finally, from equations 4.2 and 4.3 the fractional free volume at the glass transition temperature, f_g, is 0.03 and the thermal expansion coefficient is 6 $\times 10^{-4}$ deg^{-1}, both values being in agreement with the literature on synthetic polymers.

The working protocol of this section follows the efforts of Ferry and co-workers to disentangle the complicated dependence of mechanical behavior on temperature at constant frequency (or time) for synthetic polymers. In the sugar-agarose case, the test of Figure 4.1 was reproduced more informatively using two separate functions, that of frequency alone and another of temperature alone (Figures 4.4a and 4.4b, respectively). We are going to pursue further the theme of separation of the above variables once we have dealt with the structural properties of single sugar preparations.

4.4.3. The vitrification of a sugar solution

Information on the viscoelastic behavior of a sugar solution is interesting in its own right and as a baseline for a better understanding of the contribution of the polymer in the mixture. In Figure 4.5 we focus on the variation of G' and G" during controlled cooling (1°C/min) at subzero temperatures. For the case of 50 wt % sucrose plus 35wt % glucose syrup (i.e. the agarose cosolute), clear solutions turn cloudy solids seen by eye and verified on the rheometer by the convergent moduli reaching a rigidity of 3.8 MPa at -34°C. Parallel work using differential scanning calorimetry (DSC) shows the presence of an endothermic peak during heating, a result that argues for the crystallization of sucrose and water in the mixture (Ong et al., 1998). As in the case of the rheological profile, the event unfolded gradually and extended

from -17 to –6°C with the temperature at maximum heat flow being -9°C. The higher melting temperatures observed in the DSC experiment should be attributed to the rapid heating rate (10°C/min). Strikingly, the presence of agarose transforms the viscoelasticity by introducing a rubbery network capable of binding to sucrose, thus preventing its crystallization, with the mixture undergoing vitrification as a whole (Figure 4.1).

To induce vitrification phenomena in a sugar solution, we substituted glucose syrup for sucrose in the sample keeping the level of solids constant (85 wt %). Glucose syrup forms a clear solution of reinforced viscosity due to the presence of higher molecular weight fractions than sucrose (see Materials). The polydisperse nature of the material prevents crystallization, with the outcome of controlled cooling being the slow process of vitrification that is completed at -27°C (observed T_g: Figure 4.5). In contrast with the sucrose-rich mixture, a clear glass is obtained that achieves values of storage modulus of 1.1GPa at -34°C. As for the sugar-agarose mixture, mechanical spectra were recorded every three degrees covering the glass transition and the glassy state of glucose syrup. Horizontal superposition of the data produces the master curve of Figure 4.6, which unveils a frequency window of seven decades. The extensive shift of frequencies sees an analogous development in modulus values ranging over six orders of magnitude. As far as we are aware, this is the first glassy state recorded with rotational dynamic oscillation for a biological material.

Shift factors obtained from the superposition of the mechanical spectra were fitted with the WLF expression (eq. 4.6) that incorporates the Vogel temperature:

$$\log \alpha_T = \frac{C_1^o (T - T_o)}{(T_\infty - T)} \qquad (4.6)$$

Using a least-squares routine the value of T_∞ was optimized to yield a linear fit of log a_T vs (T – T_o)/ (T - T_∞) that intercepts the origin. If preferred, an identical determination of the WLF parameters can be made using equation 4.1, but the graphical display of equation 4.6 serves better the ensuing argument. In Figure 4.7a the reference and Vogel temperatures are 260 and

193 K, respectively. Thus we can derive a glass transition temperature of –30°C (calculated T_g), which is in good agreement with the experimental cross-over of moduli in Figure 4.5 (observed T_g = -27° C). Using equation 4.3 the WLF constants at T_g were found to be C_1^g=10.2 and C_2^g= 50 deg. Further, the free volume at T_g is 4% of the total volume (f_g = 0.04), with the thermal expansion coefficient being 8 x 10^{-4} deg^{-1}.

The minimization routine fails to resolve the differences between the calculated and the observed values of shift factors at the lower end of the temperature range in Figure 4.7a. This is the realm of the glassy state where it is hypothesized that the WLF framework becomes inappropriate. Recently, dynamic mechanical data were used to show that the transition from the flow to the rubbery region in a high sugar polysaccharide system is followed by the Arrhenius equation in the following form (Sworn & Kasapis, 1998):

$$\log a_T = \frac{E_a}{2.303R}\left(\frac{1}{T} - \frac{1}{T_o}\right) \tag{4.7}$$

Equation 4.7 implies that the dependence of log relaxation times on temperature is linear, thus yielding a constant energy of activation. Application of the Arrhenius relation to our data can be seen in Figure 4.7b. Clearly, the W'LF curvature of the glassy state in Figure 4.7a is transformed into a linear relationship of a_T vs 1/T in Figure 4.7b, whereas the linear WLF fit of the glass transition deviates increasingly from the Arrhenius prediction. It appears, therefore, that the glass transition temperature is a true turning point where large configurational vibrations requiring free volume cease to be of overriding importance. Instead, the emerging constant energy of activation reflects the need to overcome an energetic barrier for the occurrence of local rearrangements from one state to the other.

4.4.4. Two basic functions of temperature and frequency in the sugar-agarose system

The shift in the frequency scale with temperature and thus the magnitude of shift factors is governed by the choice of reference temperature and is followed by equation 4.1. Direct comparison of the temperature function between polymer/cosolute and sugar, however, is afforded with the concept of activation energy, which is independent of the arbitrary, choice of reference temperature. From the WLF equation, a function yielding a temperature dependent form of apparent activation energy for viscoelastic relaxation can be obtained. At the glass-transition temperature this reduces to (Ferry & Fitzgerald, 1954):

$$E_a = {Rd\ln a_T}\Big/{d\left(1/T\right)} = {2.303RC_1^g T_g^2}\Big/{C_2^g} \qquad (4.8)$$

which for the sugar-agarose and the glucose syrup preparations gives 72.9 and 50.3 kcal, respectively. This is depicted in Figure 4.8a, where the E_a trace of the latter rises faster as its glass transition temperature is approached (observed T_g = -27°C). If the samples are heated, the E_a curves drop sharply and there is relatively little change in energy of activation at the upper range of temperature. Further, they cross over, with the trace of the sugar-agarose rubber becoming dominant, thus reflecting the additional energetic content of the cross-links of the agarose network.

Regarding the frequency variable, an alternative to the dynamic oscillation presentation in Figures 4.4a and 4.6 is the distribution function of relaxation times. It may be derived from the following (Ferry et al., 1950):

$$\Phi(-\ln\omega) = G'\left({d\log G'}\Big/{d\log\omega}\right) = G''\left(1 - {d\log G''}\Big/{d\log\omega}\right) \qquad (4.9)$$

Thus equation 4.9 interrelates the storage and loss moduli, although they follow independent

paths as a function of frequency. Φ also appeals to synthetic polymer scientists because it can combine stress relaxation and dynamic data into one calculation (Ferry et al., 1951). Figure 4.8b illustrates the logarithmic plots of Φ vs τ (1/frequency) of our samples reduced to -34°C. They have been drawn using G' data but are identical to the curves obtained from the loss modulus. At long time scales, the functional chains of agarose form a three-dimensional structure of infinite molecular weight, which appears to be permanent within the experimental constraints. In the case of glucose syrup, the architecture of a soft rubber is supplanted by a viscous mass of flexible molecules that flows incessantly. In the region of short times the function Φ shows a steep rise for both systems, a result that reflects the free volume effect on a material regardless of its pole position. At extremely short relaxation times the values of Φ should plummet since the change in modulus (or in the rheological terminology "the contribution to instantaneous rigidity") between lnτ and Inτ + dlnτ is negligible. The onset of the drop in Φ values is noted in the glassy state of glucose syrup at time-scales below one second.

4.5. CONCLUSIONS

Agarose is an alternating heteropolysaccharide capable of forming linkages that give rise to overall helix geometry. These are stabilized by hydrogen bonding with water molecules leading to highly enthalpic aggregated systems incapable of showing glass transition phenomena. It appears, however, that in the presence of high levels of sugar extensive intermolecular order is not thermodynamically stable with the polysaccharide chains maintaining flexibility. In addition, sucrose interacts sufficiently with the agarose chains to prevent its crystallization in the system. As a result, the high sugar/polysaccharide mixture undergoes vitrification as a whole, which can be followed by the combined framework of the WLF/free volume theory. Parallel work on deacylated gellan has now been completed (Sworn & Kasapis, 1998) and augers well for the universal utility of the approach in sugar/polysaccharide mixtures, as accomplished to great effect in synthetic polymer science.

REFERENCES

Arnott, S., Fulmer, A., Scott, W. E., Dea, I. C. M., Moorhouse, R. & Rees D. A. (1974). The agarose double helix and its function in agarose gel structure. *Journal of Molecular Biology*, **90**, 269-284.

Arridge, R. G. C. (1975). *Mechanics of polymers*, Oxford University Press, UK.

Favier, V., Chanzy, H. & Cavaille', J. Y. (1995). Polymer nanocomposites reinforced by cellulose whiskers, *Macromolecules*, **28**, 6365-6367.

Ferry, J. D., Sawyer, W. M., Browning, G. V. & Groth A. H. (1950). Mechanical properties of substances of high molecular weight. VIII. Dispersion of dynamic rigidity and viscosity in concentrated polyvinyl acetate solutions. *Journal of Applied Physics*, **21**, 513-517.

Ferry, J. D., Fitzgerald, E. R., Johnson, M. F. & Grandine, L. D. (1951). Mechanical properties of substances of high molecular weight. X. The relaxation distribution function in polyisobutylene and its solutions. *Journal of Applied Physics*, **22**, 717-722.

Ferry, J. D. & Williams, M. L. (1952). Second approximation methods for determining the relaxation time spectrum of a viscoelastic material. *Journal of Colloid Science*, **7**, 347-353.

Ferry, J. D. & Fitzgerald, E. R. (1954). Dynamic rheological properties of linear polymers. In V. G. Harrison, *Proceedings of the second international congress of rheology*, Butterworths Scientific: London, pp.140-149.

Ferry, J. D. (1980). *Viscoelastic Properties of Polymers*, John Wiley & Sons, New York.

Kovacs, A. J. (1964). Transition vitreuse dans les polyméres amorphes. Etude

phénoménologique. *Journal of Advanced Polymer Science*, **3**, 394-507.

Marvin, R. S. (1954). The dynamic mechanical properties of polyisobutylene. In V. G. Harrison, *Proceedings of the 2nd International Congress Rheology*, Butterworths Scientific: London, pp.156-163.

Morris, E. R. and Norton, I. T. (1982). Polysaccharide aggregation in solutions and gels. In E.Wyn-Jones & J. Gormally, *Aggregation Processes in Solution*, Elsevier, Amsterdam, pp.549-593.

Ong, M. H., Whitehouse, A. S., Abeysekera, R., Ai-Ruqaie, I. M. & Kasapis, S. (1998). Glass transition-related or crystalline forms in the structural properties of gelatin oxidised starch glucose syrup mixtures, *Food Hydrocolloids*, **12**, 273-281.

Ross-Murphy, S. B. (1984). Rheological methods. In H. W.-S. Chan, *Biophysical Methods in Food Research*, Blackwell Scientific Publications, Oxford, pp.138-198.

Stanley, N. F. (1995). Agars. In A. M. Stephen, *Food Polysaccharides and their Applications*, Marcel Dekker, New York, pp.187-204.

Sworn, G. & Kasapis, S. (1998). Effect of conformation and molecular weight of co-solute on the mechanical properties of gellan gum gels. *Food Hydrocolloids*, **12**, 283-290.

Sworn, G. & Kasapis, S. (1998). The use of Arrhenius and WLF kinetics to rationalise the mechanical spectrum in high sugar gellan systems, *Carbohydrate Research*, **309**, 353-361.

Tobolsky, A. V. (1956). Stress relaxation studies of the viscoelastic properties of polymers. *Journal of Applied Physics*, **27**, 673-685.

Vogel, H. (1921), Das temperaturabhängigkeitsgesetz der viskosität von flüssigkeiten. Phys Z., **22**, 645-646.

Williams M. L., (1955), Journal of Physics Chemistry, 59, 95-96.

Williams, M. L., Landel, R. F. & Ferry, J. D. (1955). The temperature dependence of relaxation mechanisms in amorphous polymers and other glass-forming liquids. *Journal of the American Chemical Society*, 77, 3701-3707.

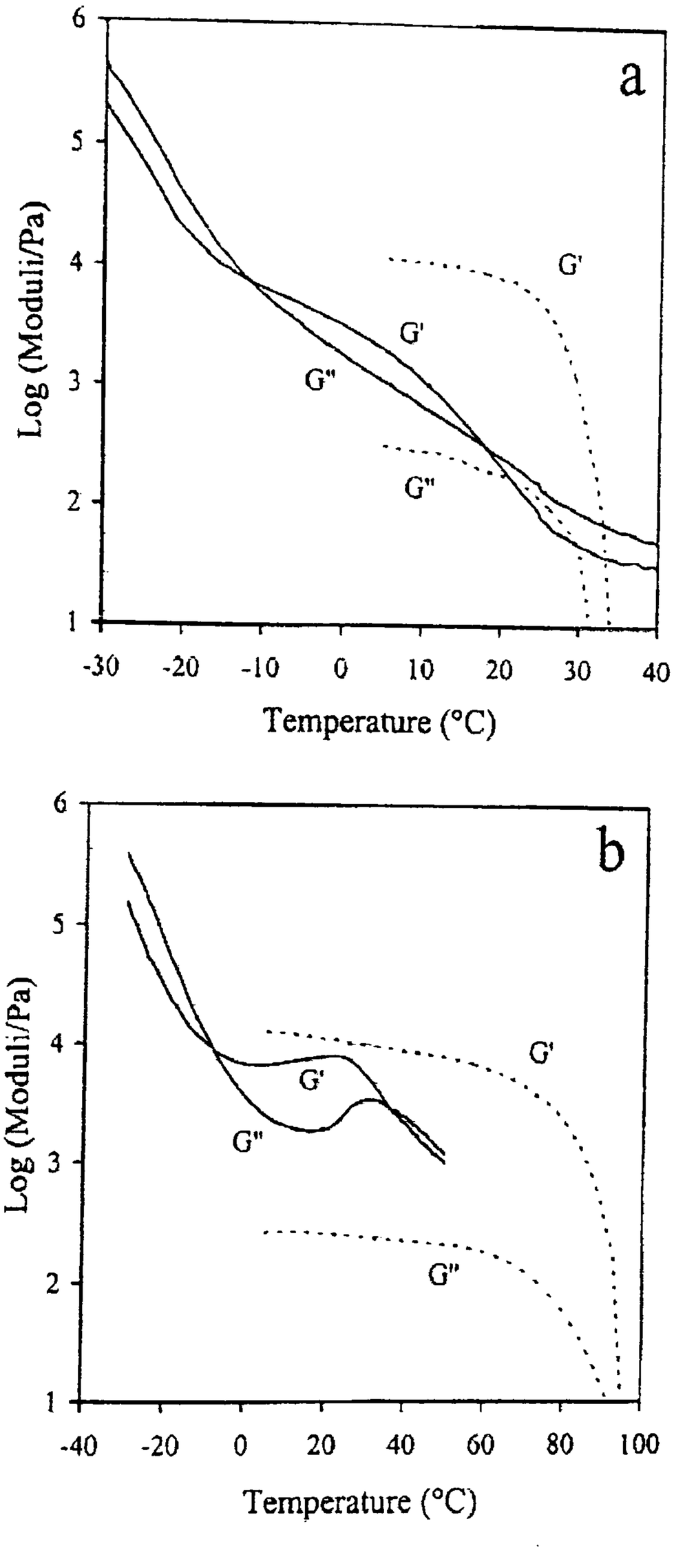

Figure 4.1. (a) Cooling and (b) heating traces of G' and G" for 0.7 wt % agarose with 50 wt % sucrose + 35 wt % glucose syrup (solid lines) and an aqueous preparation of 0.7 wt % agarose (dashed lines). Scan rate: 1°C/min; frequency : 1 Hz; strain 0.1%.

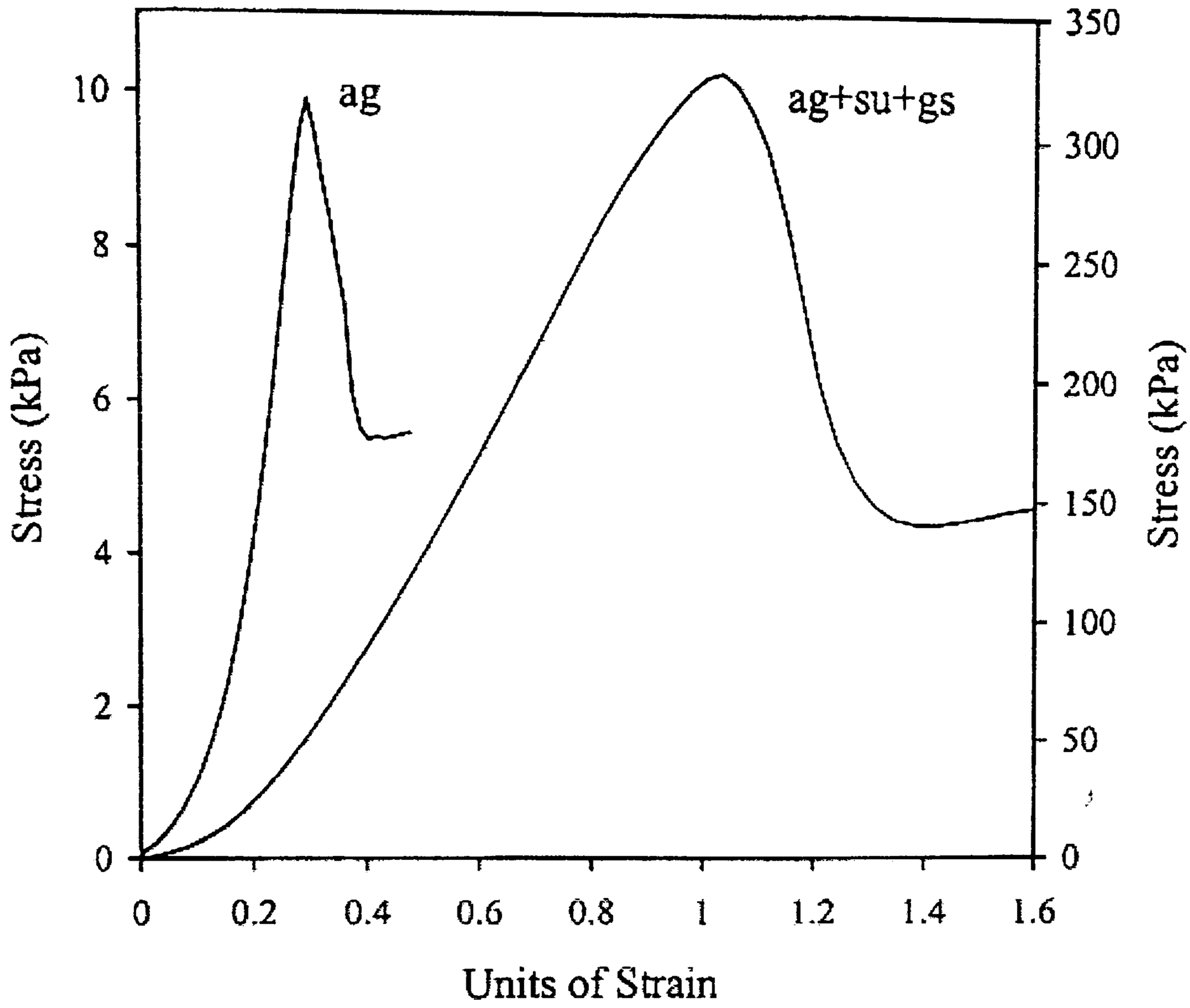

Figure 4.2. Stress-strain profiles of 0.7% agarose gels (left, y axis) and 0.7 wt % agarose with 50 wt % sucrose + 35 wt % glucose syrup (right, y axis). Compression rate: 0.85 mm/s; temperature: 5°C.

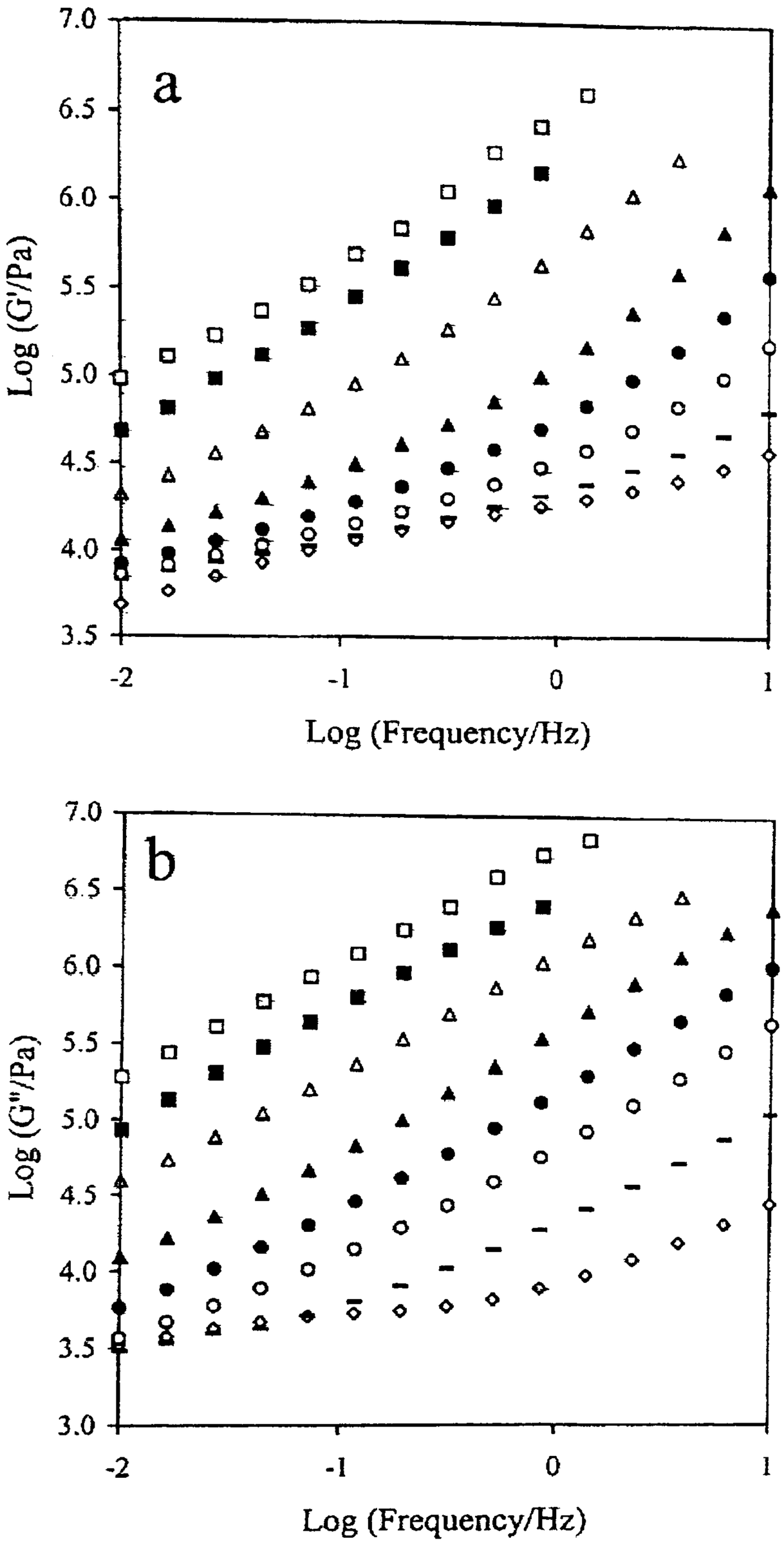

Figure 4.3. Frequency sweeps of (a) G' and (G") for 0.7 wt % agarose with 50 wt % sucrose + 35 wt % glucose syrup at -4 (◊), -13 (-), -19 (○), -22 (●), -25 (Δ), -28 (Δ), -31 (■), and -34°C (□). Traces at -7, -10, and -16°C have not been plotted to avoid confusion.

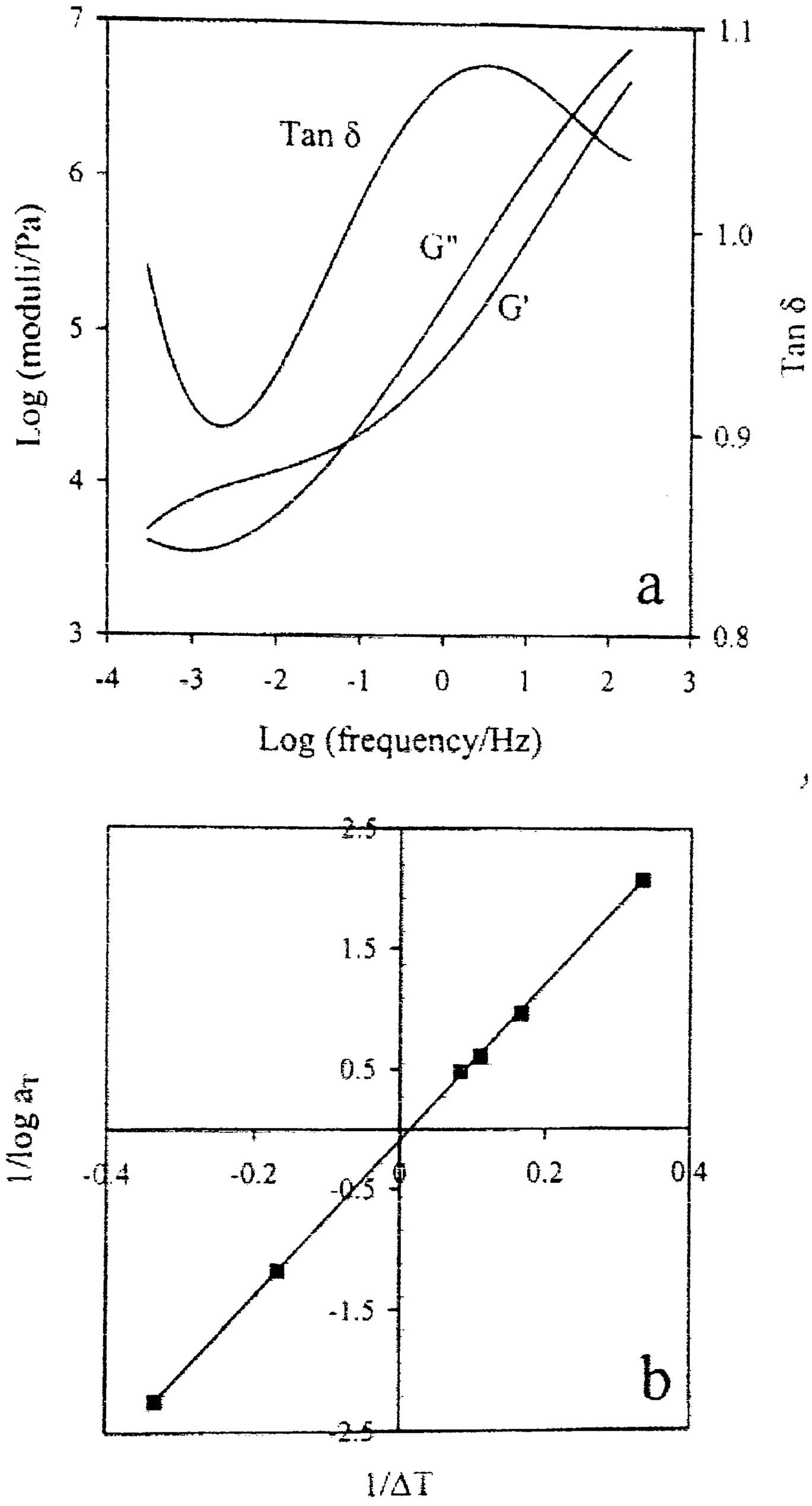

Figure 4.4. (a) Master curve for 0.7 wt % agarose with 50 wt % sucrose + 35 wt % glucose syrup and (b) the experimentally derived shift factors with the straight line denoting the WLF fit.

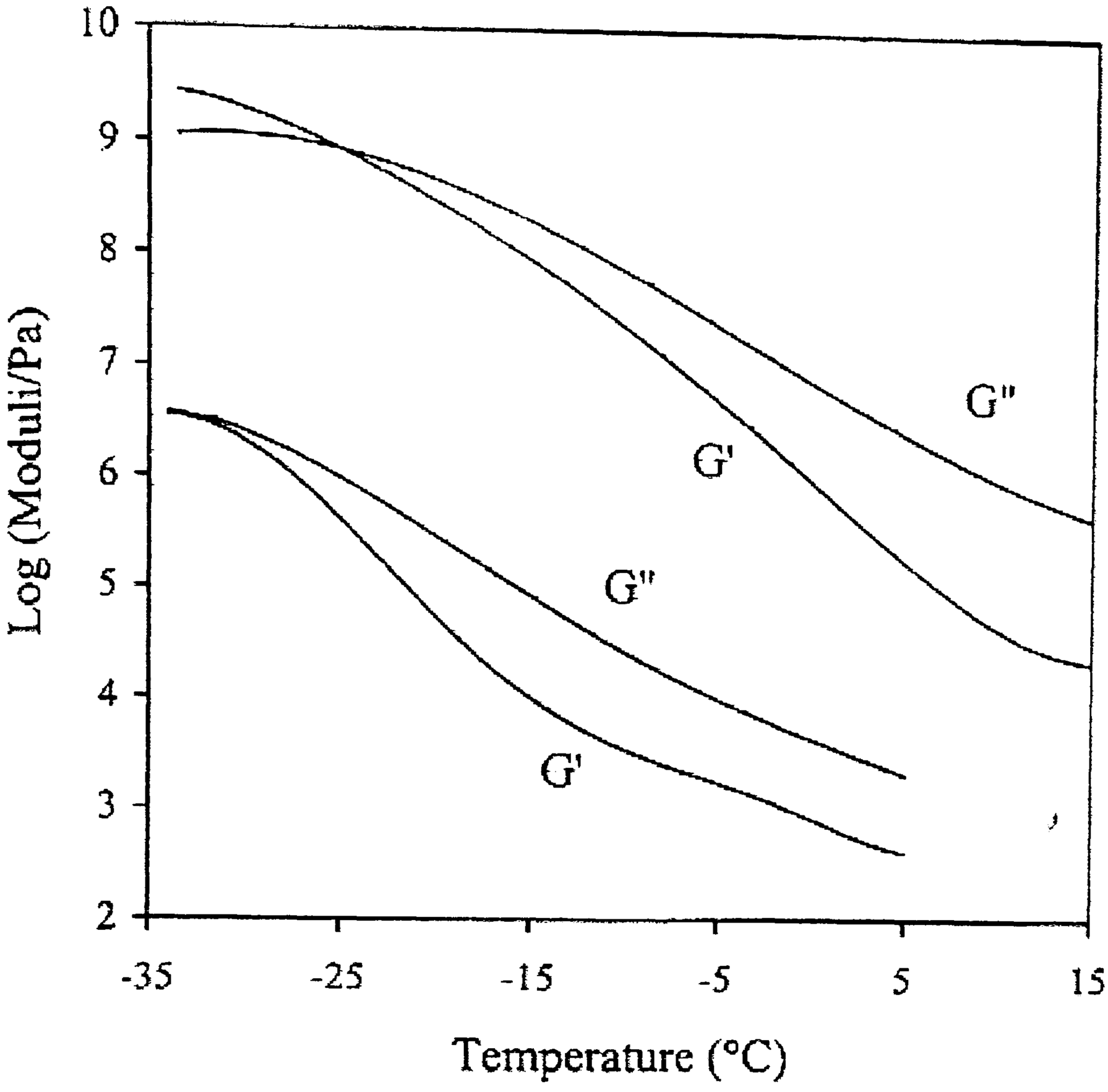

Figure 4.5. Cooling profiles of G' and G" for 50 wt % sucrose + 35 wt % glucose syrup (bottom trace) and 85 wt % glucose syrup (top trace). Conditions as in Figure 4.1.

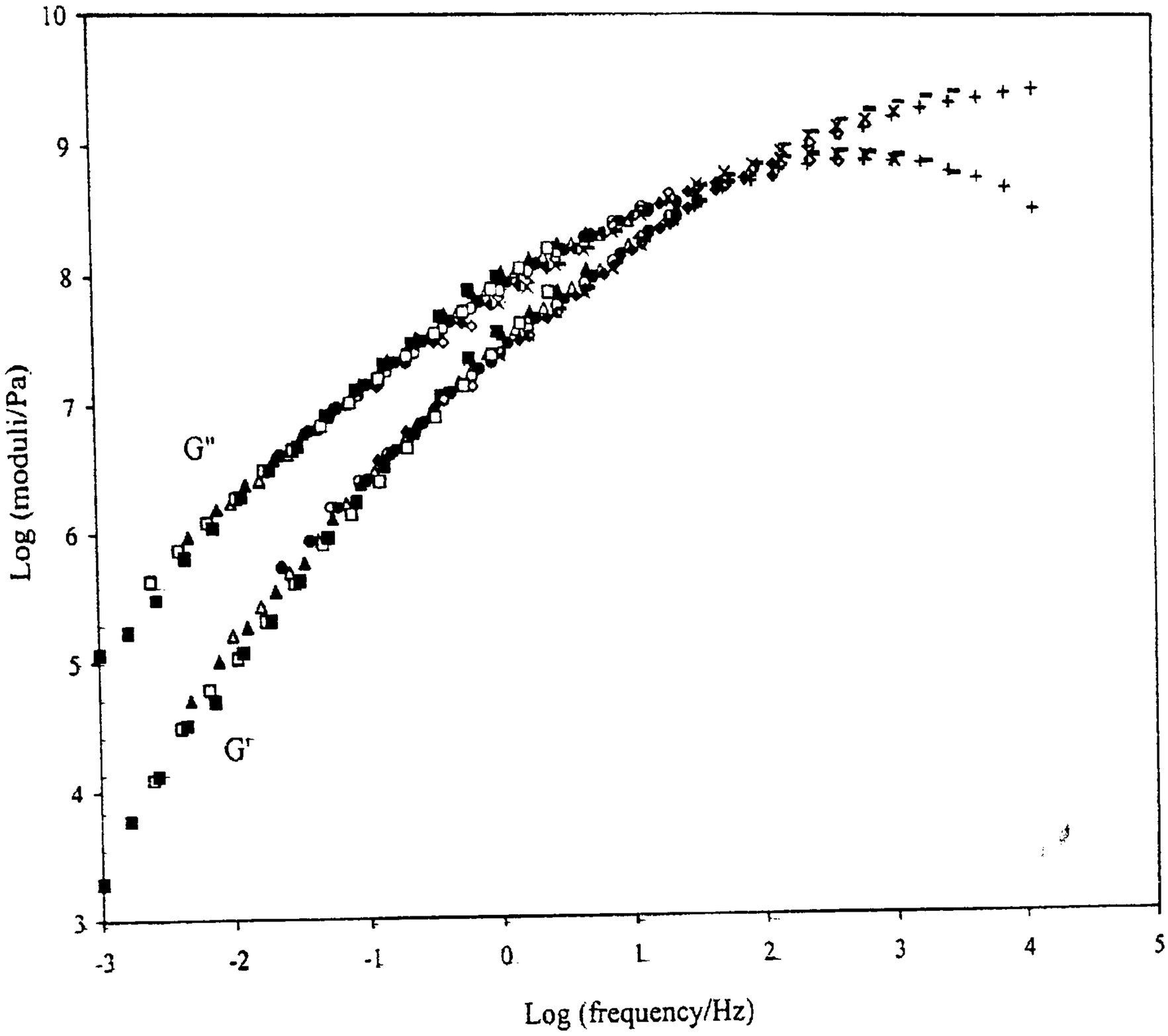

Figure 4.6. Master curve of G' and G" for 85 wt % glucose syrup combining frequency sweeps recorded at the following temperatures: -4 (■). -7 (□), -10 (Δ), -13 (Δ), -16 (●), -19 (○), -22 (◆), -25 (◊), -28 (×), -31 (–), and -34 (+).

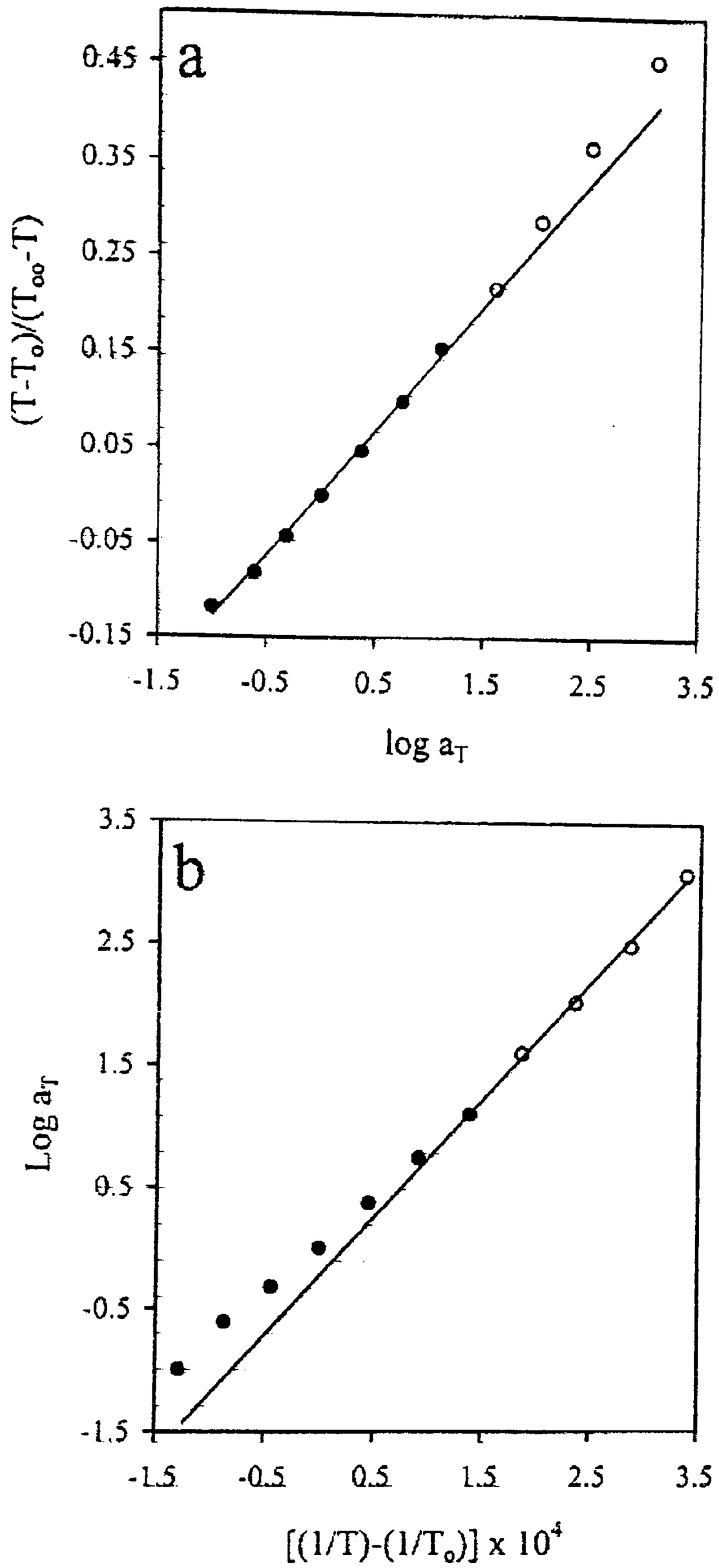

Figure 4.7. (a) Experimentally derived shift factors for 85 wt % glucose syrup plotted in relation to T_∞ with the straight line reflecting the WLF fir and (b) the same shift factors plotted against 1/T with the straight line reflecting the Arrhenius fit.

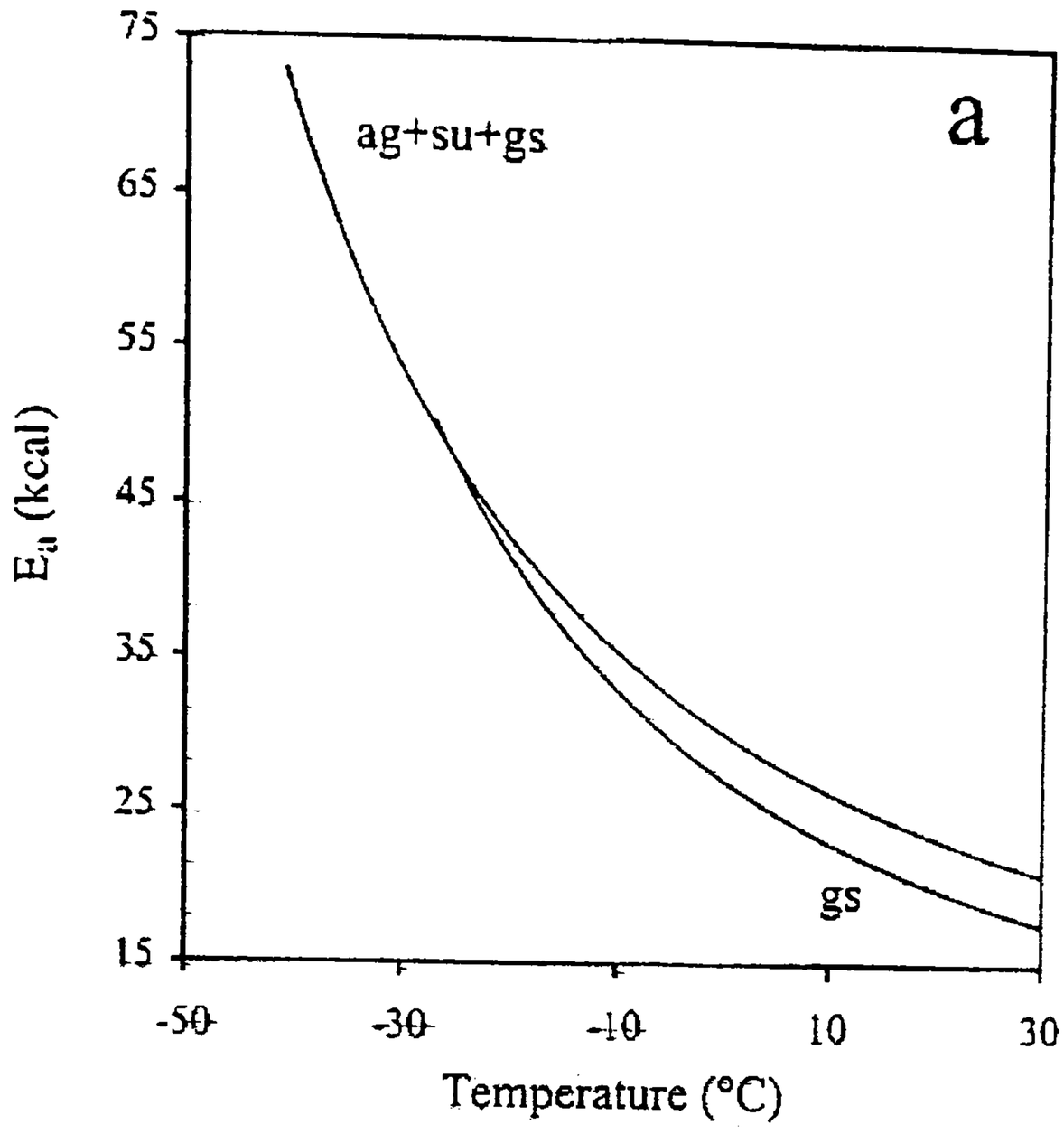

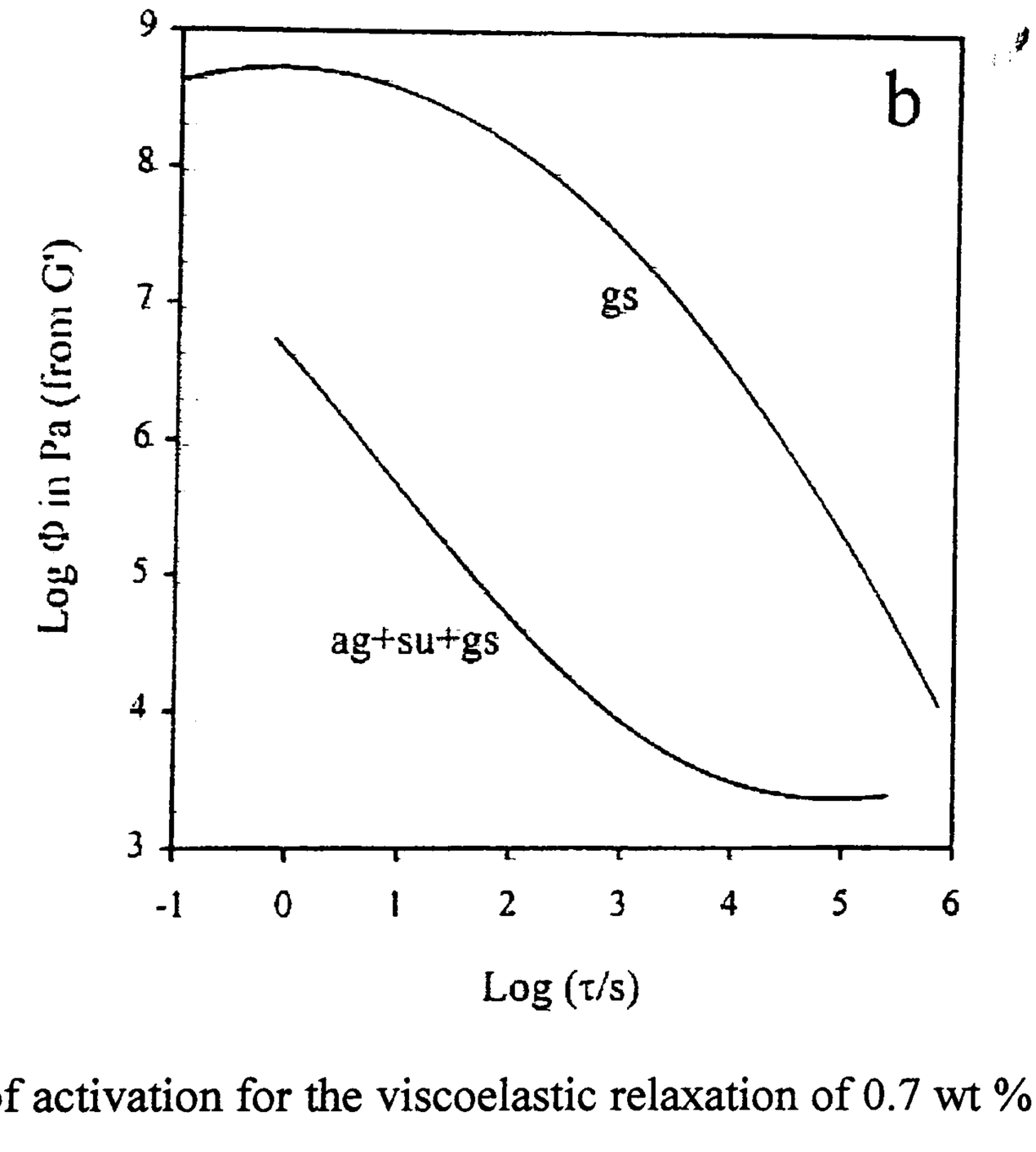

Figure 4.8. (a) Energy of activation for the viscoelastic relaxation of 0.7 wt % agarose with 50 wt % sucrose + 35 wt % glucose syrup and 85 wt % glucose syrup and (b) the distribution function of relaxation times for the two samples normalized at -34°C.

By: Tsoga, A., Richardson, R. K. and Morris, E. R.

For submission to: Food Hydrocolloids

CHAPTER 5

ROLE OF COSOLUTES IN GELATION OF HIGH-METHOXY PECTIN. PART 1. COMPARISON OF SUGARS AND POLYOLS

5.1. ABSTRACT

Mixtures of high-methoxy pectin (DE 70; 1.0 wt %; pH 3.0) with ethan-1,2-diol, glycerol, xylitol, sorbitol, glucose, fructose or sucrose at concentrations of 50, 55, 60 and 65 wt % were prepared at 95°C and changes in storage modulus (G') and loss modulus (G'') during cooling to 5°C, heating to 90°C and re-cooling to 5°C (at 1°C/min) were measured at 1 rad s^{-1} and 0.5 % strain. In all cases, the onset temperature for gelation during cooling and the moduli recorded at 5°C increased with increasing concentration of cosolute. Both values, however, were substantially lower for the liquid cosolutes (ethan-1,2-diol and glycerol) than for mixtures incorporating the same concentrations of the solid cosolutes. The difference is attributed to inhibition of pectin–pectin interactions by pectin–cosolute interactions, which in turn are inhibited by cosolute–cosolute interactions, these being weaker for the liquid cosolutes than for the solids (as indicated by lower melting points). On heating, there was an initial reduction in modulus, with the same temperature-course as the increase on cooling; for the solid cosolutes, this was followed by an increase attributable to hydrophobic association of methyl ester substituents. No such increase was seen with the liquid cosolutes, but differential scanning calorimetry (DSC) studies showed two (reversible) thermal transitions in all cases, are over the temperature-range of the initial gelation process on cooling and the other coincident with the increase in modulus on heating in the presence of the solid cosolutes. The absence of any detectable increase in modulus on

heating with the liquid cosolutes is attributed to accumulation of cosolute around the polymer chains (i.e. pectin–cosolute interactions) promoting hydrophobic association between methyl ester groups on the same chain, with therefore no contribution to network structure. At high concentrations of the solid cosolutes, the increase in modulus on heating was followed by a decrease at higher temperature; this is attributed to excessive aggregation, and was reflected in lower moduli on subsequent re-cooling to 5°C, in contrast to the enhancement in gel strength after heating and cooling that was observed at lower concentrations of the same cosolutes.

5.2. INTRODUCTION

The primary structure of pectin is based on linear sequences of (1→4)-linked α-D-galacturonate, which are interspersed by shorter rhamnogalacturonan regions with alternating sequences of galacturonate and rhamnosyl residues (de Vries, Rombouts, Voragen & Pilnik, 1982). In native pectin the rhamnogalacturonan regions of the polymer backbone are linked covalently to long, neutral-sugar sidechains, but these are extensively degraded during commercial extraction, having only trace amounts of neutral sugars other than rhamnose. A proportion of the galacturonate residues occur as the methyl ester; the ester content can be decreased by mild hydrolysis, and is characterised by the "degree of esterification" (DE), the percentage of galacturonate residues in the ester form. Pectins can be classified as "high-methoxy" or "low-methoxy", depending on whether the DE is above or below 50%.

Commercial low-methoxy pectins typically have DE values in the range 30-35 %, and form gels with Ca^{2+} cations. According to the "egg-box" model of Grant, Morris, Rees, Smith and Thom (1973), the intermolecular junctions in these gels consist of poly-D-galacturonate sequences in an ordered, 2-fold conformation, stabilised by chelation of divalent cations between the polysaccharide chains. Dimeric junctions with a single array of site-bound

cations are particularly stable, but larger assemblies can be formed at higher concentrations of Ca^{2+} (Morris, Powell, Gidley & Rees, 1982).

High-methoxy pectins normally have DE values in the approximate range 58-76 %, and are gelled by reduction in pH (typically to ~ pH 3.0) in the presence of high concentrations of cosolute (typically 60-65 wt % sucrose); this is the procedure used in production of conventional jams and jellies. It is well known in the Industry that comparatively minor changes in cosolute (such as partial replacement of sucrose by corn syrup) can have a large effect on gel strength the rate of gel formation on cooling (Christensen, 1986; May, 1990). Also, as a practical expedient in laboratory studies, particularly those using chiraptical techniques to monitor changes in conformation (e.g. Morris et al., 1980), pectin gelation has been induced using an achiral cosolute such as ethan-1,2-diol (ethylene glycol). To our knowledge, however, no systematic comparison has been made of the effectiveness of different cosolutes in inducing gelation of high-methoxy pectin under acidic conditions. That was the purpose of the present investigation. For reasons that are explained more fully in the following paper (Tsoga, Richardson & Morris, 2001), the cosolutes used were sucrose, glucose, fructose, sorbitol, xylitol, glycerol and ethan-1,2-diol.

5.3. MATERIALS AND METHODS

High-methoxy pectin (DE 70) in the free-acid form was kindly supplied by the Copenhagen Pectin Division of Hercules. A stock solution was prepared at ~ 5 wt % and adjusted to pH 4.0 by addition of trisodium citrate. Mixtures were prepared at 95°C, by adding the required volume of the stock solution to a solution of the cosolute, and brought to the required weight by addition of water or continued evaporation, as appropriate. Pilot experiments were carried out to determine the volume of a concentrated solution of citric acid required to give a pH of 3.0 in the gels formed on cooling. As the final stage in sample preparation, this volume was added to the pectin–cosolute mixture, which was then

immediately loaded onto an oscillatory rheometer pre-heated to 95°C and/or filled into a DSC pan, also at ~ 95°C. Mixtures were prepared at cosolute concentrations of 50, 55, 60 and 65 wt %; pectin concentration was held fixed at 1.0 wt %. All cosolutes and reagents were Analar grade from BDH. Distilled deionised water was used throughout.

Small-deformation oscillatory measurements (0.5 % strain) were made using highly truncated cone-and-plate geometry (diameter 50 mm; cone angle 0.05 rad; minimum gap 1 mm) on a sensitive prototype rheometer designed and constructed by one of us (R.K.R.). Temperature was varied at a fixed rate of 1°C/min, controlled by a Haake circulating water bath and measured using a thermocouple in contact with the stationary element. Measurements of G' and G" during cooling and heating were made at a fixed frequency of 1 rad s^{-1}. After loading at 95°C, the samples were coated around their periphery with light silicone oil, to minimise evaporation, cooled to 5°C, heated to 90°C, and re-cooled to 5°C. At the end of each cooling or heating stage (i.e. at 5°C, 90°C and 5°C) a mechanical spectrum was recorded to show the variation of G' and G" with frequency.

Differential scanning calorimetry (DSC) measurements were made on a Setaram microcalorimeter, using a typical sample mass of ~ 0.88 g, and with cosolute concentration held fixed at 55 wt %. After filling at 95°C, the sample pan was allowed to cool to ambient temperature and weighed. A reference pan was brought to within ± 1 mg of the same mass by filling with a solution of the appropriate cosolute at the same concentration (55 wt %) as in the mixture with pectin. Sample and reference pans were then loaded into the calorimeter at ambient temperature, cooled to 5°C, and held at 5°C for 1 h. The pans were then heated to 95°C and immediately cooled again to 5°C. A second heating and cooling cycle was performed after a further equilibration period of 1 h at 5°C. All heating and cooling scans were made at a fixed scan rate of 0.5°C/min.

5.4. RESULTS

5.4.1. Rheological changes on cooling and heating

Figures 5.1-5.4 show the changes in G' and G" (1 rad s^{-1}; 0.5 % strain) observed during initial cooling from 90 to 5°C, reheating to 90°C, and cooling again to 5°C (at 1°C/min) for 1.0 wt % high-methoxy pectin (pH 3.0) in the presence of, respectively, 50, 55, 60 and 65 wt % xylitol. A broadly similar pattern of response was observed for the other solid cosolutes studied (sorbitol, glucose, fructose and sucrose).

At the lowest concentration of cosolute (50 wt %; Figure 5.1), gelation occurs as a single smooth process, with a steep increase in both moduli below the onset temperature for network formation. On subsequent heating, there is an initial reduction in moduli, following the same temperature course as the increase observed on cooling, but at higher temperatures both moduli increase again. Similar behaviour was observed by Evageliou, Richardson and Morris (2000) with sucrose as cosolute and was attributed to the formation of a thermally-reversible pectinic acid network at low temperature, with hydrophobic association between methyl ester substituents giving rise to the subsequent increase in modulus on heating. On cooling again to 5°C (Figure 5.1), there is a further increase in both moduli. This effect was again observed (Evageliou et al., 2000) with sucrose as cosolute, and was tentatively ascribed to progressive segregation, during thermal cycling, of sequences with an ester content lower than the overall average for the pectin sample, giving rise to more stable pectinic acid junctions, and sequences of higher than average ester content, giving enhanced hydrophobic association.

The mechanical spectra recorded at the end of the cooling, heating and cooling cycles with 50 wt % xylitol as cosolute are shown in Figures 5.5, 5.6 and 5.7, respectively. After initial cooling to 5°C (Figure 5.5), the response is typical of a very weakly cross-linked network, with G' exceeding G" by only about a factor of 3, and with a substantial frequency-dependence of both moduli. On heating to 90°C (Figure 5.6) the overall values of G' are

somewhat lower than after initial cooling to 5°C (Figure 5.5), but the separation between G' and G" is increased to well over an order of magnitude and the frequency-dependence is greatly decreased. These indicators of enhancement in network quality persist on re-cooling to 5°C, but with a large (~ 30-fold) increase in both moduli.

The temperature-dependant changes in moduli observed (Figure 5.2) with 55 wt % xylitol as cosolute were essentially the same as at 50 wt % (Figure 5.1), but with an overall increase in moduli and displacement of the onset of gelation on initial cooling to somewhat higher temperature. On further increase in xylitol concentration to 60 wt %, however, substantial differences were observed. As shown in Figure 5.3, there were two discernable 'waves' of increase in modulus on cooling, and on re-heating to 90°C the initial reduction and subsequent increase in moduli were followed by a significant reduction at higher temperature. When the temperature was lowered again to 5°C, the increase in modulus was far less pronounced than at lower concentrations of cosolute (Figure 5.1 and 5.2), and the final value of G' at 5°C was slightly lower than after initial cooling. Depletion in gel strength on heating and re-cooling became even more pronounced when the concentration of cosolute was raised further, to 65 wt % (Figure 5.4).

The mechanical spectra obtained at the end of the cooling, heating and cooling cycles with 65 wt % xylitol as cosolute are shown in, respectively, Figures 5.8, 5.9 and 5.10. In contrast to the enhancement in network character seen on heating from 5°C (Figure 5.5) to 90°C (Figure 5.6) for pectin in the presence of 50 wt % xylitol, the spectrum recorded at 90°C with 65 wt % xylitol as cosolute (Figure 5.9) is less gel-like (greater frequency-dependence; smaller separation between G' and G") than after initial cooling to 5°C (Figure 5.8), and the gel-like character is further decreased on re-cooling to 5°C (Figure 5.10).

As indicated earlier, the rheological changes observed during thermal cycling for pectin in the presence of the other solid cosolutes studied were quantitatively similar to those described above for mixtures with xylitol. There were, however, substantial quantitative differences, which are summarized in Figures 5.11 and 5.12.

Figure 5.11 shows the values of G' after re-heating to 90°C, expressed as a fraction of the corresponding values after initial cooling to 5°C. For all of the solid cosolutes studied, the ratio increases as the concentration of cosolute is raised from 50 to 55 wt %, indicating an increase n the degree of crosslinking from hydrophobic association during heating. With xylitol as cosolute, the ratio decreases abruptly as the cosolute concentration is raised from 55 to 60 wt %; this can be traced to the decrease in modulus at high temperature during heating (Figure 5.3), which does not occur at lower concentrations of xylitol (Figures 5.1 and 5.2). A similar reduction, originating in the same way, can be seen (Figure 5.11) for sorbitol, glucose and sucrose. With sorbitol as cosolute, the reduction is closely similar in magnitude to that observed for xylitol, and occurs over the same interval of cosolute concentration. For sucrose, the reduction is also closely similar in magnitude, but occurs at higher concentration (between 60 and 65 wt % cosolute). With glucose as cosolute, the reduction is less pronounced. As shown in Figures 5.13 -5.15, however, it again originates from a decrease in modulus at high temperature during heating at concentrations of 60 wt % (Figures 5.14) and 65 wt % (Figure 5.15) which does not occur at lower concentration (55 wt %; Figure 5.13). For mixtures prepared with fructose as cosolute, the initial increase in ratio observed for the other cosolutes persists (Figure 5.11) up to the highest concentration studied (65 wt %). This anomalous behaviour, and its possible origin, are discussed and described in greater detail in the following paper (Tsoga et al., 2001).

Figure 5.12 also shows the values of G' at 5°C after heating to 90°C divided by the corresponding values before heating. The overall pattern is similar to that shown in Figure 5.11 for the moduli at 90°C scaled in the same way to the initial values at 5°C, although the individual ratios are much higher (reflecting the increase in moduli during the second reduction in temperature from 90 to 5°C). The greatest enhancement in gel strength by heating to 90°C and re-cooling is with 55 wt % sucrose as cosolute, where G' is increased by a factor of ~ 500. For the same concentration of xylitol, sorbitol or glucose the enhancement is smaller, but still appreciable (~ 10-fold increase in G'). For all the solid cosolutes studied, with the exception of fructose, the ratio of G' values after and before

heating to 90°C in the presence of 65 wt % cosolute is less than 1.0 i.e. heating and re-cooling pectin gels with this high content of cosolute causes a reduction in gel strength, rather than the enhancement observed at lower concentrations of the same cosolutes. Fructose is again anomalous, showing a progressive increase in the degree of enhancement in gel strength after heating and re-cooling as the fructose concentration is increased from 50 to 65 wt %.

As an illustrative sample of the effect of the liquid cosolutes studied (glycerol and ethan-1,2-diol), Figure 5.16 shows the changes in G' and G" (1 rad s^{-1}, 0.5% strain) observed during initial cooling from 90 to 5°C, re-heating to 90°C, and cooling again to 5°C (at 1°C/min) for high-methoxy pectin (1.0 wt %; pH 3.0) in the presence of 60 wt % glycerol. Reduction in moduli on heating follows the same temperature-course as the increase observed on initial cooling. The subsequent increase in moduli on re-cooling, however, occurs at appreciably higher temperature than on initial cooling (immediately after preparation of the sample), but, in contrast to the large differences seen (Figure 5.12) for the solid cosolutes, there is little separation between the observed moduli at 5°C before and after heating to 90°C. As shown in Figure 5.17, the mechanical spectra recorded at the end of the first and second cooling processes are also closely similar. The same pattern of behaviour was observed at the other concentrations of glycerol used (50, 55 and 65 wt %), and with ethan-1,2-diol as cosolute. In all cases the moduli recorded at 5°C before and after heating to 90°C remained closely similar, with no indication of any significant additional crosslinking from hydrophobic associations formed during heating. The changes in gelation temperature between the first and subsequent cooling processes are discussed in greater detail in the following paper (Tsoga et al., 2001), where they are compared with the changes observed with fructose as cosolute.

5.4.2 Differential scanning calorimetry (DSC)

As shown in Figures 5.11 and 5.12, and illustrated in Figures 5.1-5.4, the increases in moduli attributable to hydrophobic association during heating for most of the solid cosolutes studied are most pronounced at a cosolute concentration of 55 wt %, which was therefore the concentration chosen for systematic comparison of thermal processes by DSC.

Figure 5.18 shows the DSC traces recorded during two consecutive cycles of heating and cooling between 5 and 95°C (at a scan rate of 0.5°C/min) for 1.0 wt % pectin (pH 3.0) in the presence of 55 wt % xylitol, which is again used as an illustrative example. Two thermal transitions are clearly evident in all scans, endothermic on heating and exothermic on cooling. For clarity of presentation, the heating traces are plotted (Figure 5.18) with the heat-flow axis reversed (i.e. running from top to bottom), so that the endothermic troughs appear as peaks which can be compared directly with the exothermic peaks observed on cooling. The sharp spikes at low temperature in the heating traces and at high temperature on cooling come from transient thermal imbalance at the beginning of each scan (the "start-up kick" of the calorimeter). The illustrative traces in Figure 5.18 are centred around + 450 μw on heating and -450 μw on cooling. These values reflect the difference in heat capacity between the sample and reference pan (because of the replacement of pectin by water in the reference, and possibly also because of slight differences in the concentration of xylitol in the sample and reference), and are of no fundamental significance.

The main conclusions to be drawn from Figure 5.18 are that there are two detectable thermal processes, and that their positions and intensities are roughly the same on cooling as on heating. The maxima, however, occur at slightly higher temperature in the heating scans; this can be explained by finite rate of heat transfer from the wall of the DSC pan to the interior of the sample ("thermal lag"), which has the effect of making the true temperature of the sample slightly lower than the nominal temperature (as plotted on the horizontal axis of Figure 5.18) in the heating direction and slightly higher on cooling. The

same general features were apparent in the DSC traces obtained for the other cosolutes. Another general finding illustrated in Figure 5.18 is that there were no significant or systematic differences between the results recorded during the first and second cycles of heating and cooling. Average values from the two heating scans and two cooling scans were therefore used for comparison of the different cosolutes (at 55 wt % of each). The average traces (with arbitrary vertical displacements to facilitate comparison) are shown in Figure 5.19.

The DSC traces for pectin in combination with 55 wt % sucrose were entirely different from those obtained using the other cosolutes, and are shown in Figure 5.20. It should be noted first that the thermal changes are massive; the vertical axis in each frame of Figure 5.20 spans 3000 μw, in comparison with 300 μw for the illustrative scans shown in Figure 5.18 for pectin–xylitol. The dominant feature in each of the traces in Figure 5.20 is an intense exothermic process at high temperature, irrespective of whether measurements were made in the heating or cooling direction; the magnitude of this process is greater in the first cycle of heating and cooling than in the second. Our interpretation is that it arises from hydrolysis of sucrose at high temperature under the acidic conditions used in the experimental sample (pH 3.0). Acidic hydrolysis of sucrose was also encountered as a complicating factor in the studies reported by Evageliou et al. (2000). The DSC traces for pectin in the presence of 55 wt % sucrose are therefore omitted from the comparisons shown in Figure 5.19. The other trace that is omitted from Figure 5.19 is the heating curve for pectin with 55 wt % fructose. The DSC heating scans with fructose as cosolute were very different from those obtained for the other cosolutes studied, and seemed sufficiently interesting and informative to merit a separate, detailed study, which is reported in the following paper (Tsoga et al., 2001).

The averaged traces for the remaining samples (Figure 5.19) show an obvious family relationship between the various cosolutes. Two thermal processes can be seen in each of them, the first spanning the temperature-range of gel formation on initial cooling and the

second corresponding to the increases in moduli observed during heating for pectin in the presence of moderate concentrations of the solid cosolutes (e.g. 50 and 55 wt % xylitol; Figures 5.1 and 5.2). It seems reasonable, therefore, to assign these two DSC transitions to formation and dissociation of, respectively, pectinic acid junctions and hydrophobic associations. The second transition, however, is at least equally evident for mixtures of pectin with the liquid cosolutes where, as illustrated in Figure 5.16, there was no indication of network formation during heating, indicating that the same molecular changes occur in each sample, but that their rheological consequences depend on the type (and concentration) of cosolute used.

To explore further the underlying thermal processes, the averaged traces were each fitted to two Gaussian bands, defined by the temperature (T_0) and height (H_0) at the peak maximum and with the half-width (w) at 1/e of H_0. The height (H) at any temperature (T) and the peak area (A) are then given by:

$$H = H_o \exp\left\{-(T - T_o)^2 / W^2\right\} \qquad (5.1)$$

$$A = H_o W \pi^{1/2} \qquad (5.2)$$

Before implementing the curve-fitting procedure, the heat-flow values were first scaled to a constant sample mass of 1 g and converted from μw to mJ/°C, as follows. Denoting the scan rate as R deg/min (i.e. 60/R s/°C) and the sample mass as M mg, then the heat flow = F μw = F μJ/s = 60 F/R μJ/°C = (60 F/R)(1000/M) μJ/°C/g of sample = 60 F/RM mJ/°C/g of sample. The peak area then gives a direct measure of ΔH in units of mJ/g of sample. For the 1.0 wt % samples used in the present work ΔH in J/g of polymer is then obtained by multiplying by 100.

In the fitting procedure, the baselines were assumed to be linear, but not necessarily horizontal. Each fitted DSC trace was therefore defined by 8 parameters: the position,

height and width of the two constituent transitions, the slope of the baseline, and its intercept with the vertical (heat flow) axis at T = 0°C. These parameters were varied, using the "Solver" fraction in Microsoft Excel, to minimise the root-mean-square deviation between the observed and fitted traces.

Figure 5.21 shows the fits obtained for pectin in combination with 55 wt % xylitol, which is again used as an illustrative example. The standard of agreement between the experimental values and the fitted curves is excellent, except at the start of each trace (i.e. at low temperature on heating and at high temperature on cooling), where it would be reasonable to expect the peak shape to be distorted by the start-up kick of the calorimeter. The first transition is centred at ~ 22°C, and extends up to ~ 50°C, which agrees well with the onset temperature for gelation of the same sample in the rheological studies (Figure 5.2). The second peak is centred at ~ 65°C, and is much broader, extending down to the temperature at which the moduli recorded during heating rose above those observed on initial cooling (Figure 5.2). The ΔH values (from the area of the fitted peaks) are ~ 24 J/g for the second peak at higher temperature. Broadly similar fits were obtained for the other cosolutes, but with the first transition being more intense (ΔH ≈ 44 J/g) and occurring at higher temperature (~ 29°C) with the liquid cosolutes than with xylitol and the other solid cosolutes for which avert comparison could be made (glucose and sorbitol). In view of the large number of adjustable parameters, however, these fits must be treated with caution, but the general conclusion of a comparatively sharp transition at around 25°C and a broader, more intense, transition at higher temperature emerged from all of them and, as discussed above, agrees well with the rheological changes observed during cooling and heating of pectin in the presence of the solid cosolutes.

a. Relative effectiveness of different cosolutes

Two criteria were used to compare the effectiveness of the various cosolutes studied in inducing gelation of high methoxy pectin (1.0 wt %) on initial cooling under acidic conditions: the values of G' recorded on completion of cooling to 5°C and the temperature at which gelation occurred. As a rough index of gelation temperature, the temperature (T_1) at which G' reached a value of 1 Pa s during initial cooling was taken. In cases where the modulus at high temperature was already greater (or very close to) 1 Pa s, the steep increase in log G' with decreasing temperature (Figures 5.1-5.4) was extrapolated downwards and the temperature at the point of intersection with a horizontal line at G' = 1 Pa s was taken. The resulting values are shown in Figure 5.22. Within the experimental scatter of the results, the cosolutes studied can be grouped into two categories: (i) fructose and the liquid cosolutes (glycerol and ethan-1,2-diol) and (ii) the other solid cosolutes (sucrose, glucose, sorbitol and xylose). The same division is more clearly evident (Figure 5.23) in the values of G' attained on completion of cooling to 5°C. At low concentrations of cosolute, the values of onset temperature and modulus for the two categories converge, but as the concentration is raised there is progressive divergence, with the values of both T_1 (Figure 5.22) and G' (Figure 5.23) for samples incorporating sucrose, glucose, sorbitol or xylose rising above the corresponding values for glycerol, ethan-1,2-diol and fructose.

The final values of G' recorded at 5°C after heating to 90°C and re-cooling are shown in Figure 5.24. The separation between values obtained with fructose, glycerol and ethan-1,2-diol as cosolute and those for glucose, sorbitol and xylitol is still apparent, but sucrose now stands out on its own, giving moduli almost two orders of magnitude greater, in the centre of the concentration-range studied, than those obtained with any of the other cosolutes.

5.5. DISCUSSION

As outlined in Section 5.1, there are two requirements for inducing gelation of high methoxy pectin: (i) reduction in pH (typically to ~ 3.0) and (ii) incorporation of a high concentration of cosolute. The reduction in pH has the effect of suppressing electrostatic repulsion between the polymer chains by converting unesterified carboxyl groups from the charged (COO^-) form to the uncharged (COOH) form, thus facilitating association of the chains into intermolecular junctions. One obvious function of the cosolute is to replace a large proportion of the water, making less water available to maintain the polymer chains in the unassociated, hydrated state in solution. Another factor that is often cited in discussion of the role of cosolutes in promoting polysaccharide gelation is their ability to reduce the solvent-quality of the remaining water by binding to it. For sugars, correlations have been made (e.g. Watase, Kohyama & Nishinari, 1992) with the content of equatorial hydroxy groups, whose spacing is particularly compatible with the lattice structure of water (Tart, Suggett, Franks, Ablett and Quickender, 1972). This concept cannot, however, be applied to sorbitol and xylitol, which are incapable of adopting ring structures, but, as shown in Figures 5.22 and 5.23, these cosolutes are at least as effective as glucose and sucrose in promoting gelation of high methoxy pectin.

More generally, however, it has been argued convincingly by Nilsson, Picullel and Malmsten (1990) that, to understand the behaviour of solvent–polymer–cosolute systems, all possible parimise interactions must be considered explicitly. These authors carried out a detailed theoretical and experimental study of the gelation of agarose in mixtures with a wide range of different cosolutes. Experimentally, a strong correlation was shown between the coil–helix transition temperature of agarose in the presence of these cosolutes and their order of elution from a column of cross-linked agarose beads, with the cosolutes that were retained longest on the column giving the lowest transition temperatures. The clear inference is that associative interactions between polymer and cosolute act in competition with the polymer–polymer interactions required for formation of intermolecular junctions

(agarose double helices). One system (water–agarose–urea) was analysed in detail by a theoretical lattice model, with the conclusion that polymer–cosolute interactions are the primary factor in modification of polymer–polymer association, and that cosolute–water interactions have only an indirect influence, by altering the concentration of cosolute available for interaction with the polymer chains.

By extension of the same line argument, cosolute–cosolute interactions would also be expected to act in competition with interactions between the polymer and cosolute. The strength of association between molecules of the same substance is obviously reflected in the melting point. Ethan-1,2-diol and glycerol have low melting points (-13°C and 18.2°C, respectively). The melting point of sucrose is much higher (185.5°C). The other solid cosolutes studied have intermediate values: xylitol, 93.5°C; fructose, 103°C; sorbitol, 111°C; glucose, 150°C. Leaving aside the anomalous behaviour of fructose, which is discussed separately in the following paper (Tsoga et al., 2001), these different bands of melting point correlate well with the differences in the effectiveness of the various cosolutes in inducing gelation of high methoxy pectin, and in particular with the final moduli recorded at 5°C after thermal annealing (Figure 5.24). Sucrose, which has the highest melting point, gives the highest final gel strength; this can be explained by strong associative interactions between the cosolute molecules acting in competition with the polymer–cosolute interactions which inhibit association of the polymer chains. Conversely, the cosolutes with the lowest tendency to self-association (ethan-1,2-diol and glycerol) would be more available for association with the polymer, and therefore cause greater inhibition of network formation, with those of intermediate melting point having an intermediate effect, as observed.

The above argument would apply with equal validity to the effect of different cosolutes on any gelling biopolymer. High methoxy pectin, however, has the additional feature of two different mechanisms of intermolecular association over different ranges of temperature. As discussed in greater detail elsewhere (Gilsenan et al., 2000; Evageliou et al., 2000), gelation

of pectin on initial cooling under acidic conditions can be attributed to formation of 3-fold helices, which associate to give a crosslinked network. This process, and its complete or partial reversal on heating, occurred (Figures 5.1-5.4 and 5.16) for all the pectin–cosolute mixtures studied.

As discussed in Section 5.3.1, the increases in moduli during heating, which were most clearly detectable at low or intermediate concentrations of the solid cosolutes (Figures 5.1 and 5.2), can be attributed to hydrophobic association of methyl ester groups. The DSC endotherm observed on heating over the same temperature range as the increase in gel moduli was matched (Figure 5.19) by a corresponding exotherm on cooling, indicating that the hydrophobic associations are thermally reversible, but the curve-fitting analysis shown in Figure 5.21 suggests that full dissociation does occur not until temperatures well below the onset of interchain association through 3-fold helices. It seems likely, therefore, that during thermal cycling (Figures 5.1-5.4) there is a progressive interchange between the two types of intermolecular junction, with crosslinking at low temperature occurring predominantly by association of 3-fold helices and hydrophobic association becoming dominant at high temperature but with both acting together over a substantial range of intermediate temperatures.

The reductions in moduli observed at high temperature during heating of pectin gels formed with high concentrations of solid cosolutes (Figures 5.3 and 5.4) indicate the hydrophobic association can cause depletion of gel strength as well as enhancement. A likely interpretation is that the reductions came from excessive association, leading to formation of large aggregates which do not contribute significantly to network crosslinking. Aggregated bundles of pectin chains held together by hydrophobic association at high temperature are also likely to be present in the pre-gel solutions prior to cooling. This may explain the two 'waves' of structure formation observed during initial cooling of some of the pectin–cosolute preparations (e.g. Figure 5.3), with the first wave coming acid-induced association of solvated chain sequences (possibly those of lowest ester content, with least

tendency to hydrophobic association) and the second wave arising from chains released by dissociation of hydrophobic aggregates as the temperature is decreased.

None of the samples prepared using soluble cosolutes (ethan-1,2-diol or glycerol) showed an increase in modulus on heating. An obvious interpretation, on the basis of rheological studies alone, would be that these cosolutes inhibit hydrophobic association, possibly by providing a more compatible solvent environment for the methyl ester groups of the pectin chains. However, as shown in Figure 5.19, the DSC endotherm accompanying hydrophobic association of pectin on heating in the presence of solid cosolutes, and the corresponding exotherm on cooling, were also observed, and indeed were more pronounced, with ethan-1,2-diol or glycerol as cosolute. It seems reasonable to conclude, therefore, that hydrophobic association does occur with these cosolutes, but that it makes no detectable contribution to network crosslinking. A possible explanation is that accumulation of cosolute around the polymer (which, for the reasons discussed above, would be greatest for the liquid cosolutes) acts as a barrier to intermolecular contacts between the chains, with hydrophobic association therefore occurring preferentially between methyl ester substituents within the same pectin molecule.

The rheological changes that occur during thermal cycling of pectin in the presence of ethan-1,2-diol or glycerol are discussed in greater detail in the following paper (Tsoga et al., 2001), where they are compared with those observed with fructose as cosolute.

5.6. CONCLUSIONS

The principal conclusions from this investigation are as follows:

1. Cosolutes promote gelation of high methoxy pectin by replacement of water, making less water available to maintain the polymer chains in solution.

2. Their effectiveness is decreased by associative interactions between the polymer and cosolute, which act in competition with the polymer–polymer interactions required for network formation.

3. Polymer–cosolute interactions are decreased by cosolute–cosolute interactions, which are weaker for liquid cosolutes than for solids (as is evident from lower melting points).

4. The inhibitory effect of polymer–cosolute interactions is therefore greatest for liquid cosolutes, and decreases as the tendency to self-association of the cosolute (as reflected in the melting point) increases.

5. Network crosslinking occurs predominantly by association of 3-fold helices at low temperature and by hydrophobic association of methyl ester substituents at high temperature. At intermediate temperatures, both mechanisms act together.

6. Hydrophobic associations formed on heating in the presence of low concentrations (50 or 55 wt %) of solid cosolutes causes an increase in gel strength; at high concentrations, gel strength decreases at high temperature, due to excessive aggregation.

7. Accumulation of liquid cosolute around the polymer chains promotes hydrophobic association between methyl ester substituents on the same molecule, rather than leading to intermolecular association, with consequent loss of network structure on heating.

REFERENCES

Christensen, S. H. (1986). Pectins. In M. Glicksman, *Food Hydrocolloids*, Vol III, Boca Raton, Florida, USA: CRC Press, pp. 205-230.

De Vries, J. A., Rombouts, F. M., Voragen, A. G. J., & Pilnik, W. (1982). Enzymatic degradation of apple pectins. *Carbohydrate Polymers*, **2**, 25-33.

Evageliou, V., Richardson, R. K. & Morris, E. R. (2000). Effect of pH, sugar type and thermal annealing on high-methoxy pectin gels. *Carbohydrate Polymers*, **42**, 245-259.

Gilsenan, P. M., Richardson, R. K. & Morris, E. R. (2000). Thermally-reversible acid-induced gelation of low-methoxy pectin. *Carbohydrate polymers*, **41**, 339-349.

Grant, G. T., Morris, E. R., Rees, D. A., Smith, P. J. C. & Thom, D. (1973). Biological interactions between polysaccharides and divalent cations: the egg-box model. *FEBS Letters*, **32**, 195-198.

May, C. D. (1990). Industrial pectins: sources, production and applications. *Carbohydrate Polymers*, **12**, 79-99.

Morris, E. R., Gidley, M. J., Murray, E. J., Powell, D. A. & Rees, D. A. (1980). Characterisation of pectin gelation under conditions of low water activity, by circular dichroism, competitive inhibition and mechanical properties. *International Journal of Biological Macromolecules*, **2**, 327-330.

Morris, E. R., Powell, D. A., Gidley, M. J. & Rees, D. A. (1982). Conformations and interactions of pectins. I. Polymorphism between gel and solid states of calcium polygalacturonate. *Journal of Molecular Biology*, **155**, 507-516.

Nilsson, S., Piculell, L. & Malmsten, M. (1990). Nature of macromolecular denaturation by urea and other cosolutes: experiments on agarose interpreted within a lattice model of adsorption from a mixed solvent. *Journal of physical Chemistry*, **94**, 5149-5154.

Tait, M. J., Suggett, A., Franks, F., Ablett, S. & Quickenden, P. A. (1972). Hydration of monosaccharides: a study by dielectric and nuclear magnetic relaxation. *Journal of Solution Chemistry*, **1**, 131-151.

Tsoga, A., Richardson, R. K. & Morris, E. R. (2001). Role of cosolutes in gelation of high-methoxy pectin. Part 2. Anomalous behaviour of fructose: calorimetric evidence of site-binding. *Food Hydrocolloids*, submitted (accompanying typescript).

Watase, M. Kohyama, K. & Nishinari, K. (1992). Effects of sugars and polyols on the gel-sol transition of agarose by differential scanning calorimetry. *Thermochimica Acta*, **206**, 163-173.

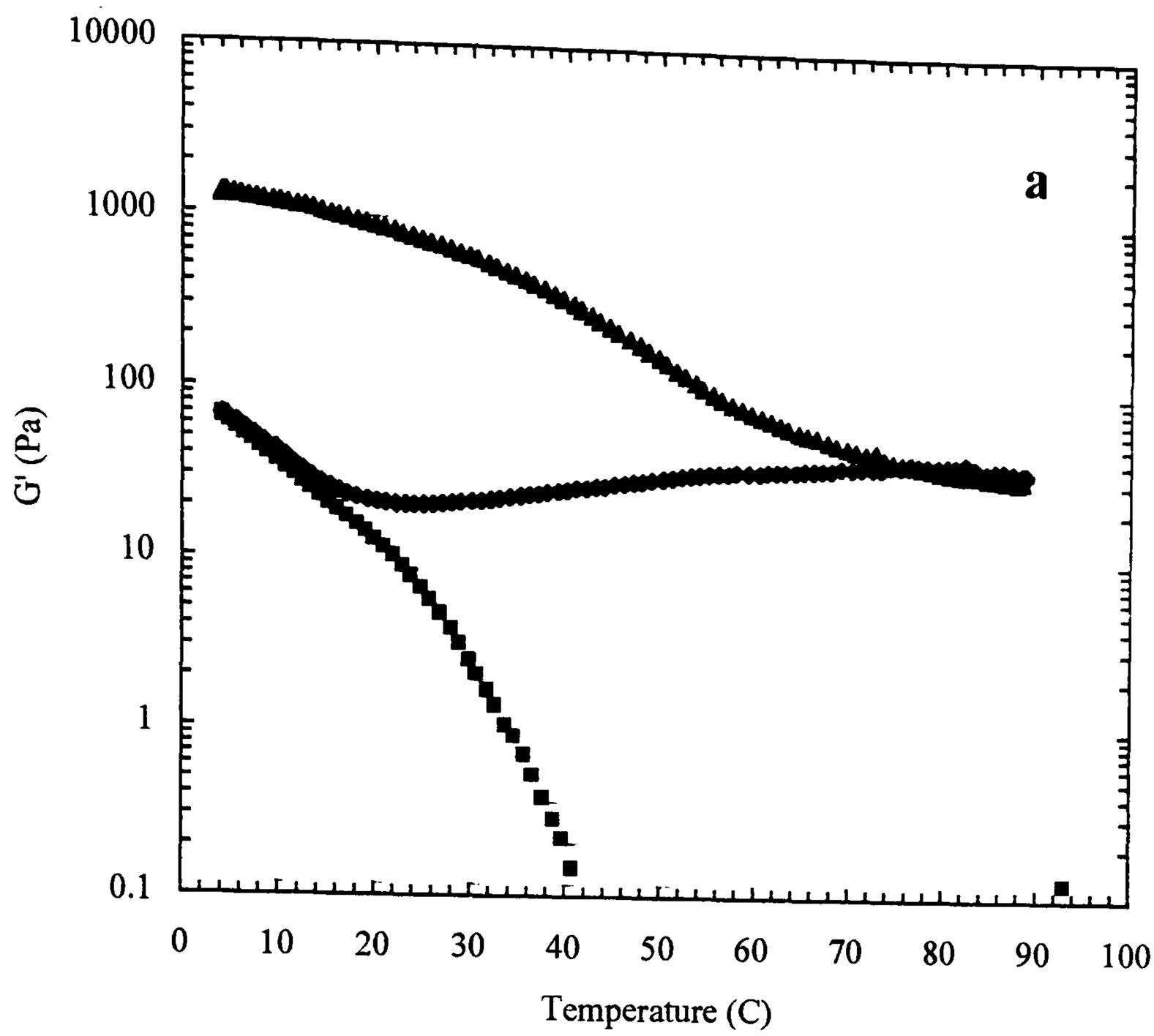

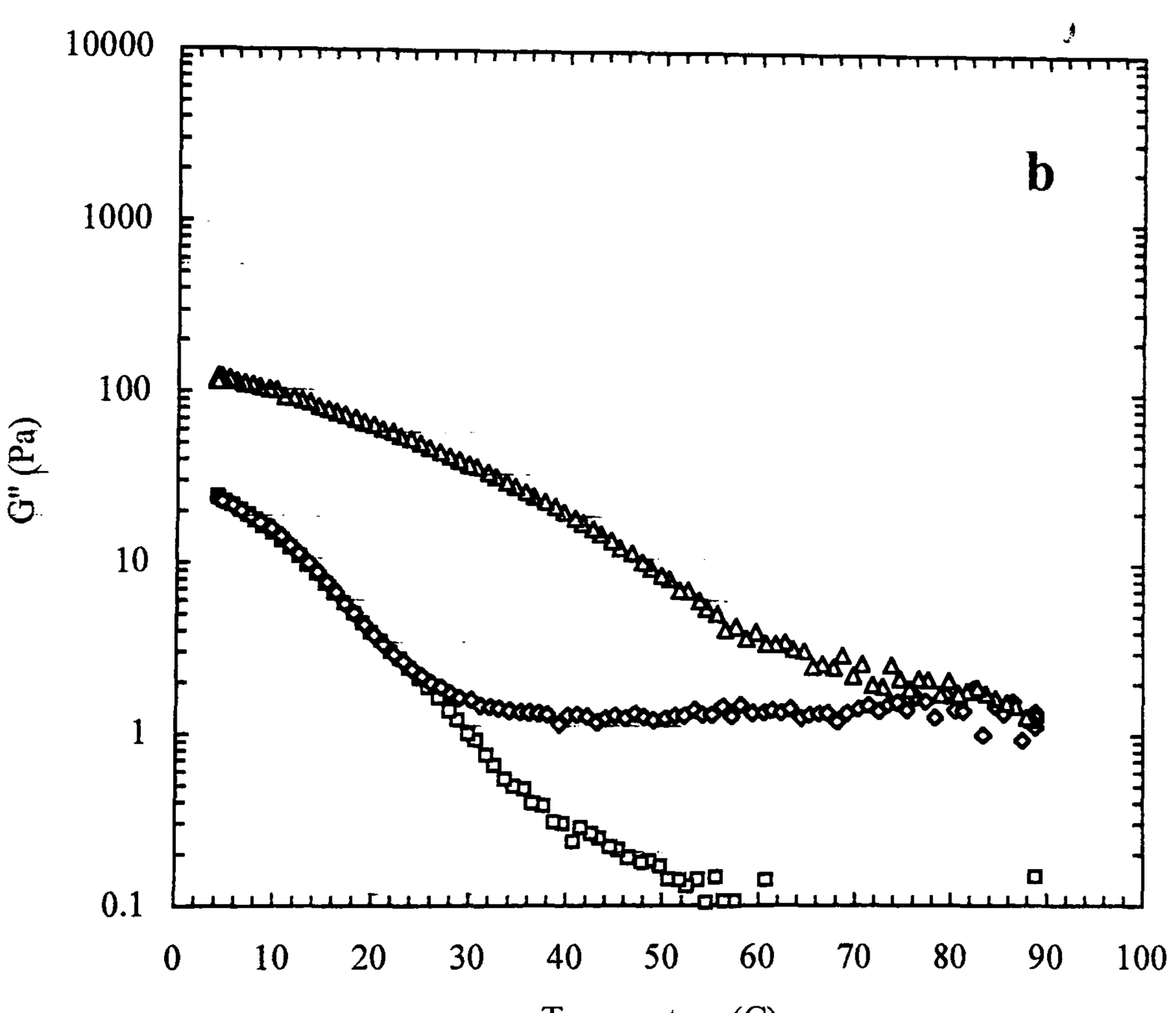

Figure 5.1. Changes in G' (filled symbols) and G" (open symbols), measured at 1 rad s^{-1} and 0.5 % strain, for 1.0 wt % high methoxy pectin (DE 70; pH 3.0) on initial cooling (squares), heating (diamonds) and re-cooling (triangles) at 1.0 °C/min in the presence of 50 wt % xylitol.

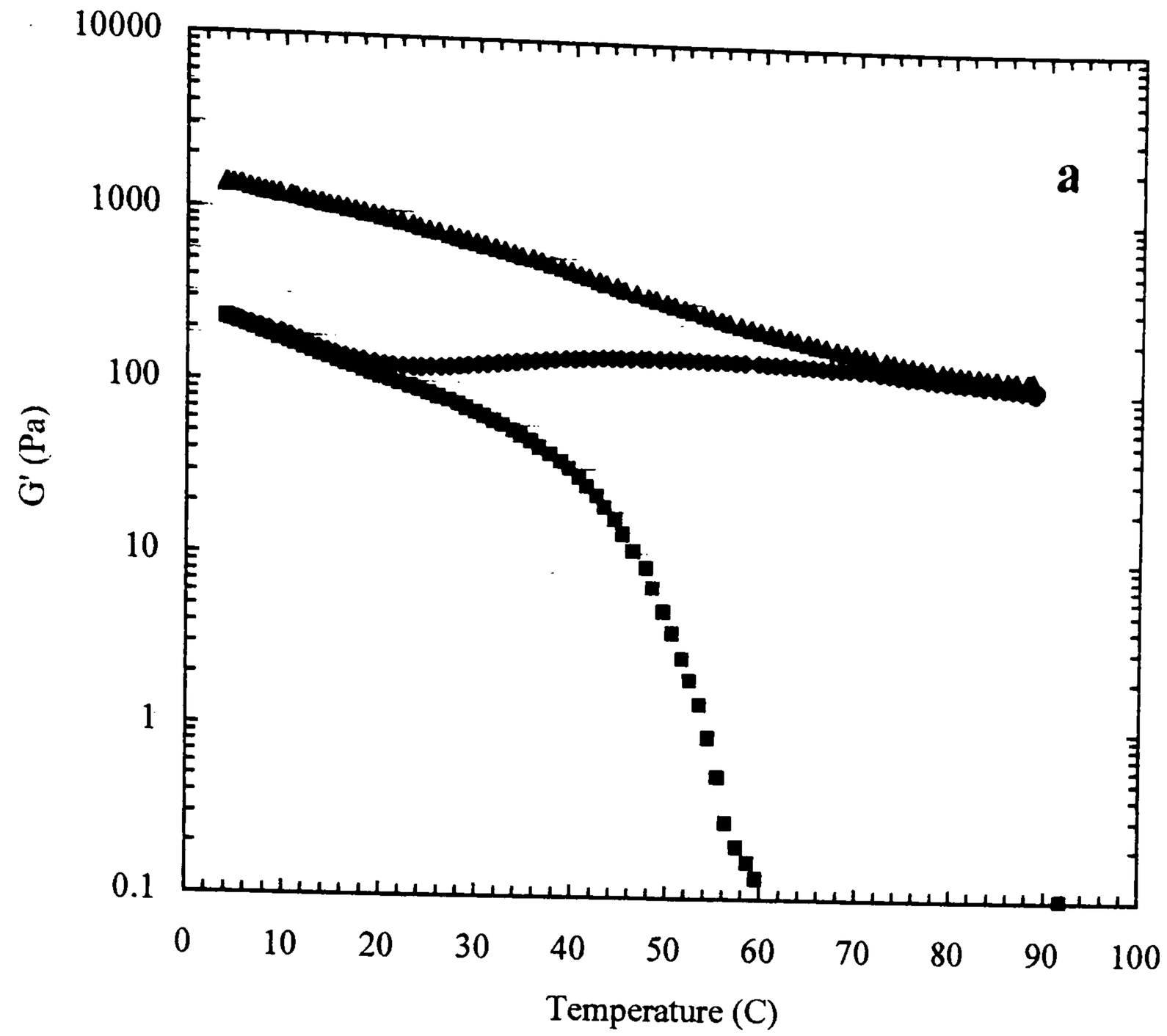

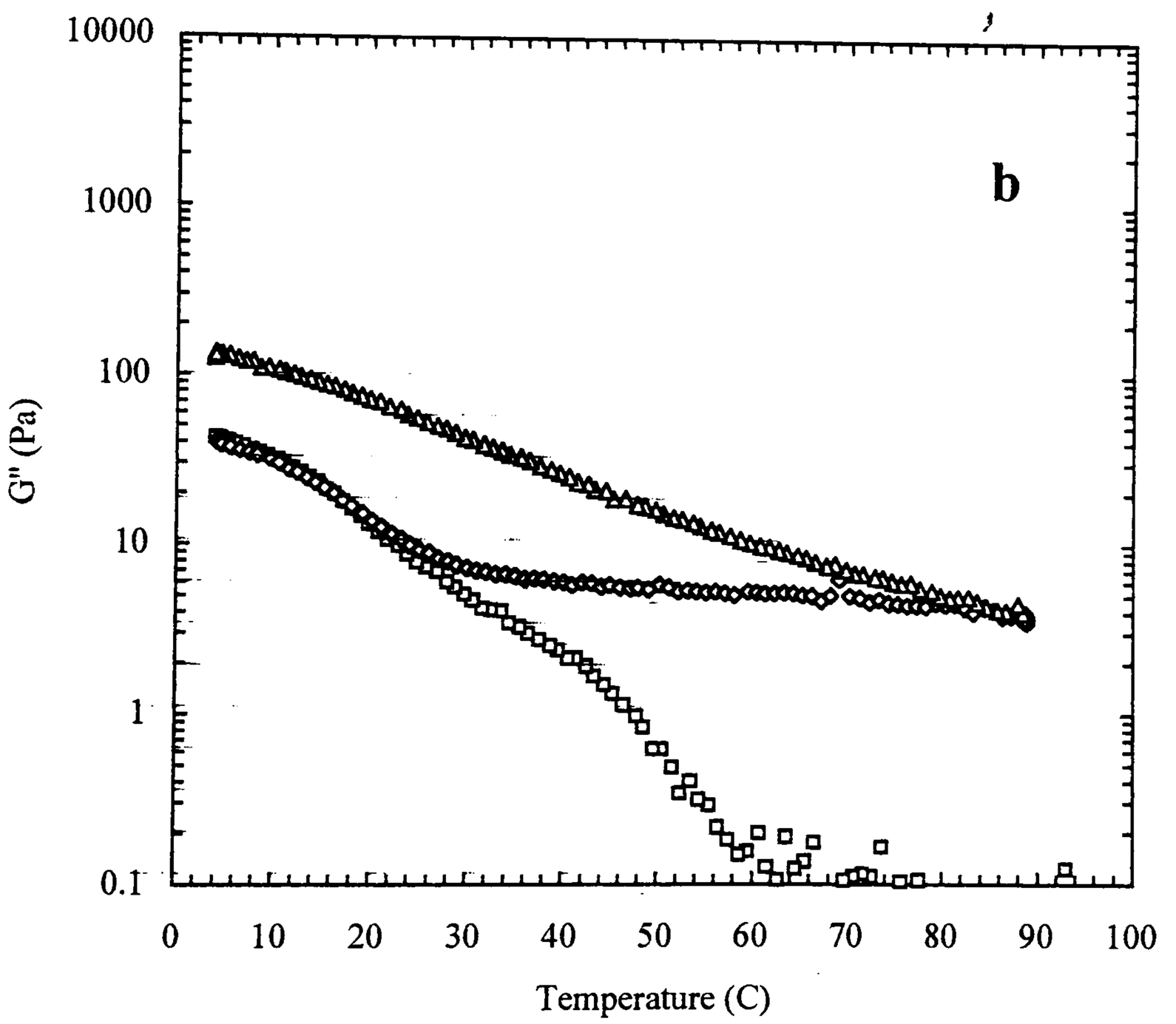

Figure 5.2. Changes in G' (filled symbols) and G" (open symbols), measured at 1 rad s^{-1} and 0.5 % strain, for 1.0 wt % high methoxy pectin (DE 70; pH 3.0) on initial cooling (squares), heating (diamonds) and re-cooling (triangles) at 1.0 °C/min in the presence of 55 wt % xylitol.

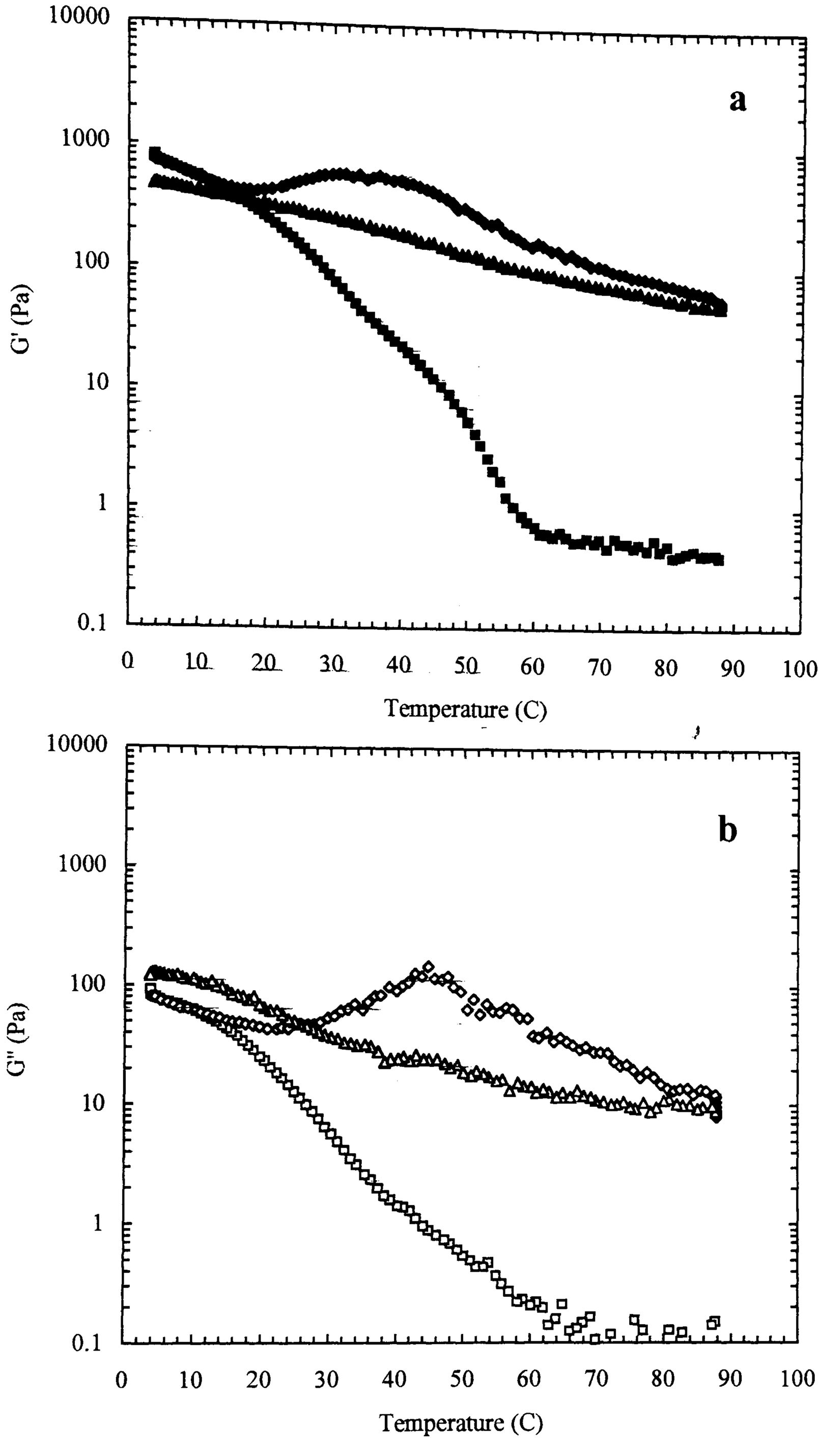

Figure 5. 3. Changes in G' (filled symbols) and G" (open symbols), measured at 1 rad s^{-1} and 0.5 % strain, for 1.0 wt % high methoxy pectin (DE 70; pH 3.0) on initial cooling (squares), heating (diamonds) and re-cooling (triangles) at 1.0 °C/min in the presence of 60 wt % xylitol.

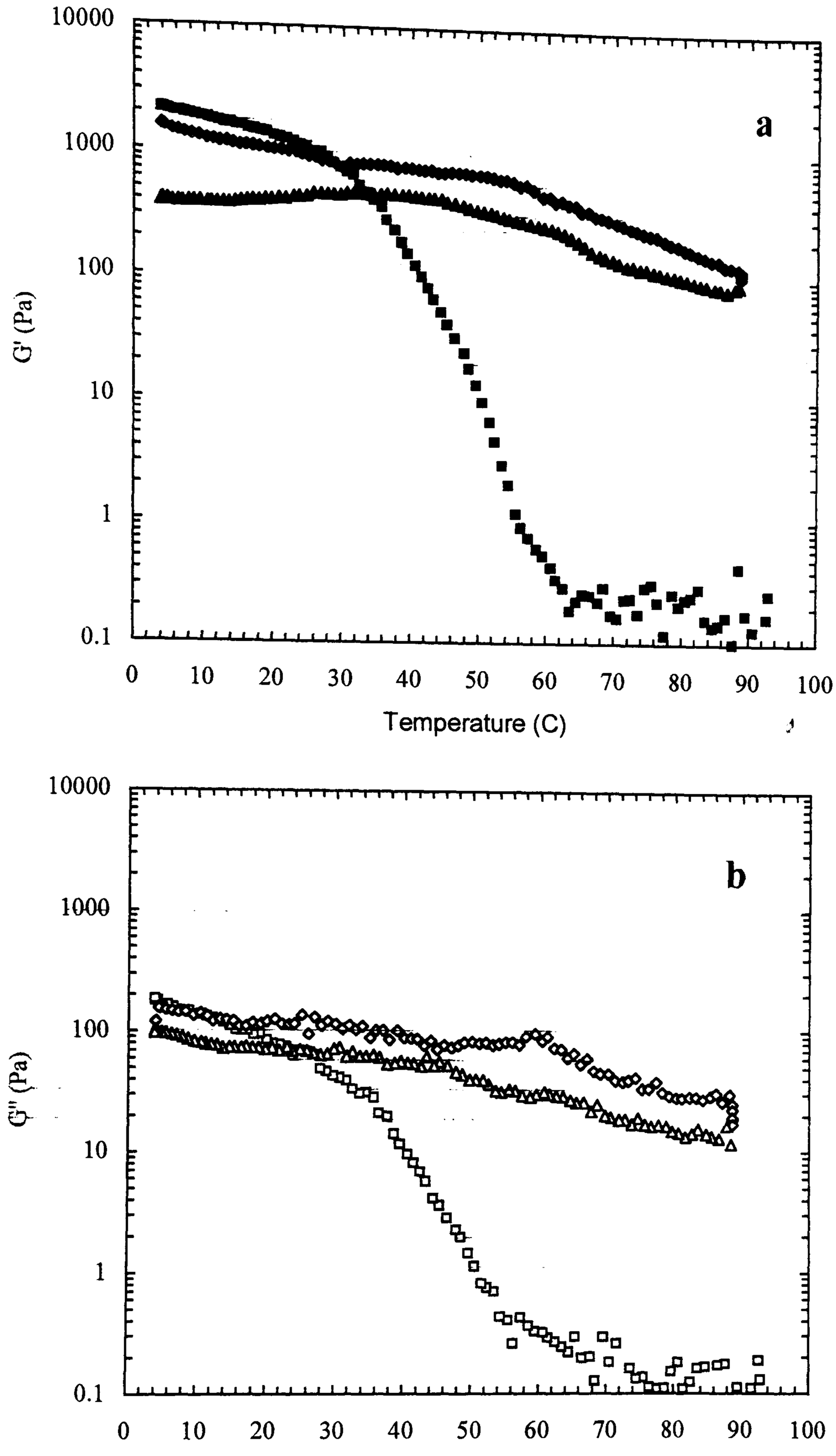

Figure 5.4. Changes in G' (filled symbols) and G" (open symbols), measured at 1 rad s^{-1} and 0.5 % strain, for 1.0 wt % high methoxy pectin (DE 70; pH 3.0) on initial cooling (squares), heating (diamonds) and re-cooling (triangles) at 1.0 °C/min in the presence of 65 wt % xylitol.

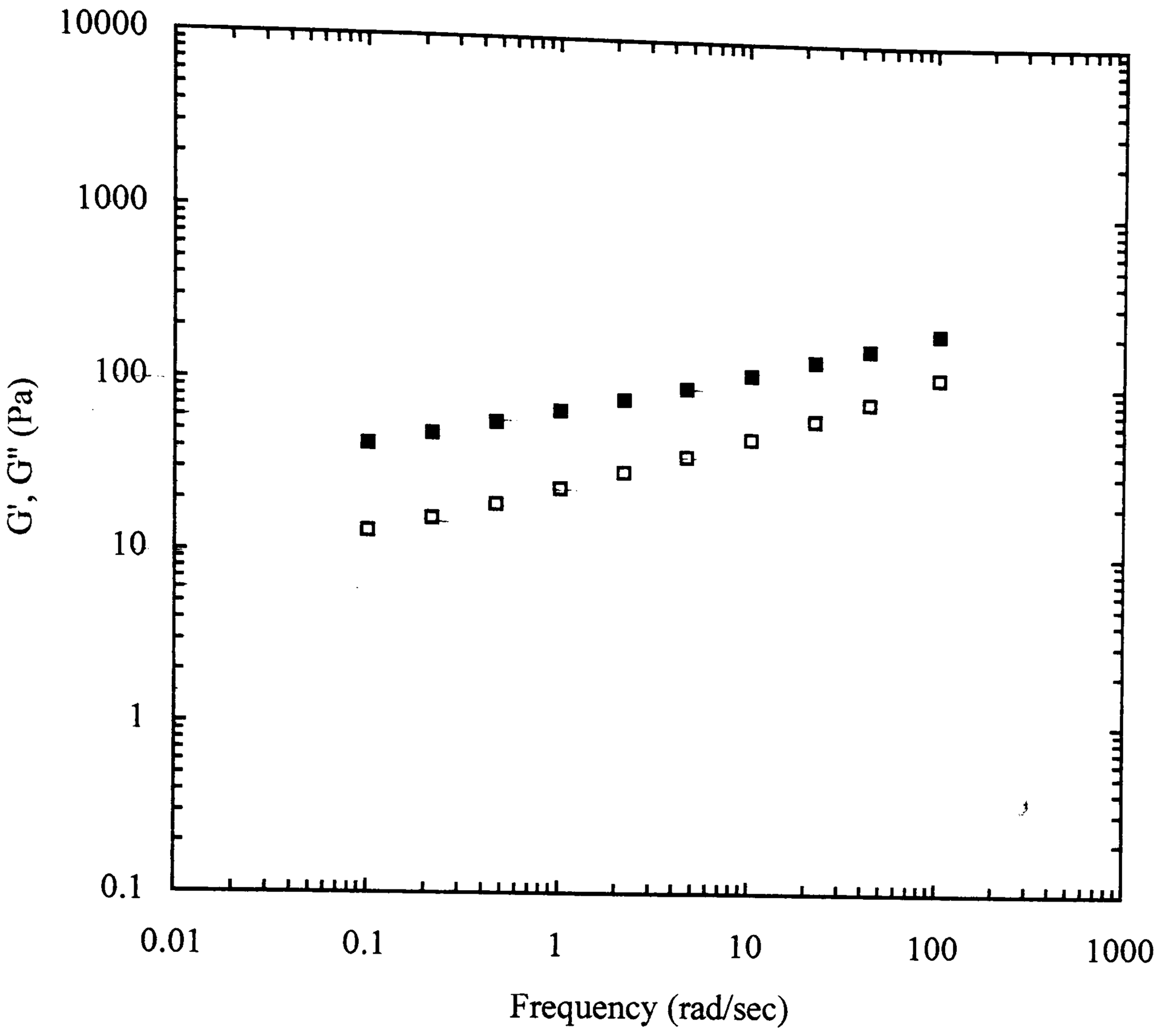

Figure 5.5. Mechanical spectrum showing the frequency-dependence of G' (■) and G" (□) for 1.0 wt % high methoxy pectin (DE 70; pH 3.0) at 5 °C after initial cooling from 90°C in the presence of 50 wt % xylitol.

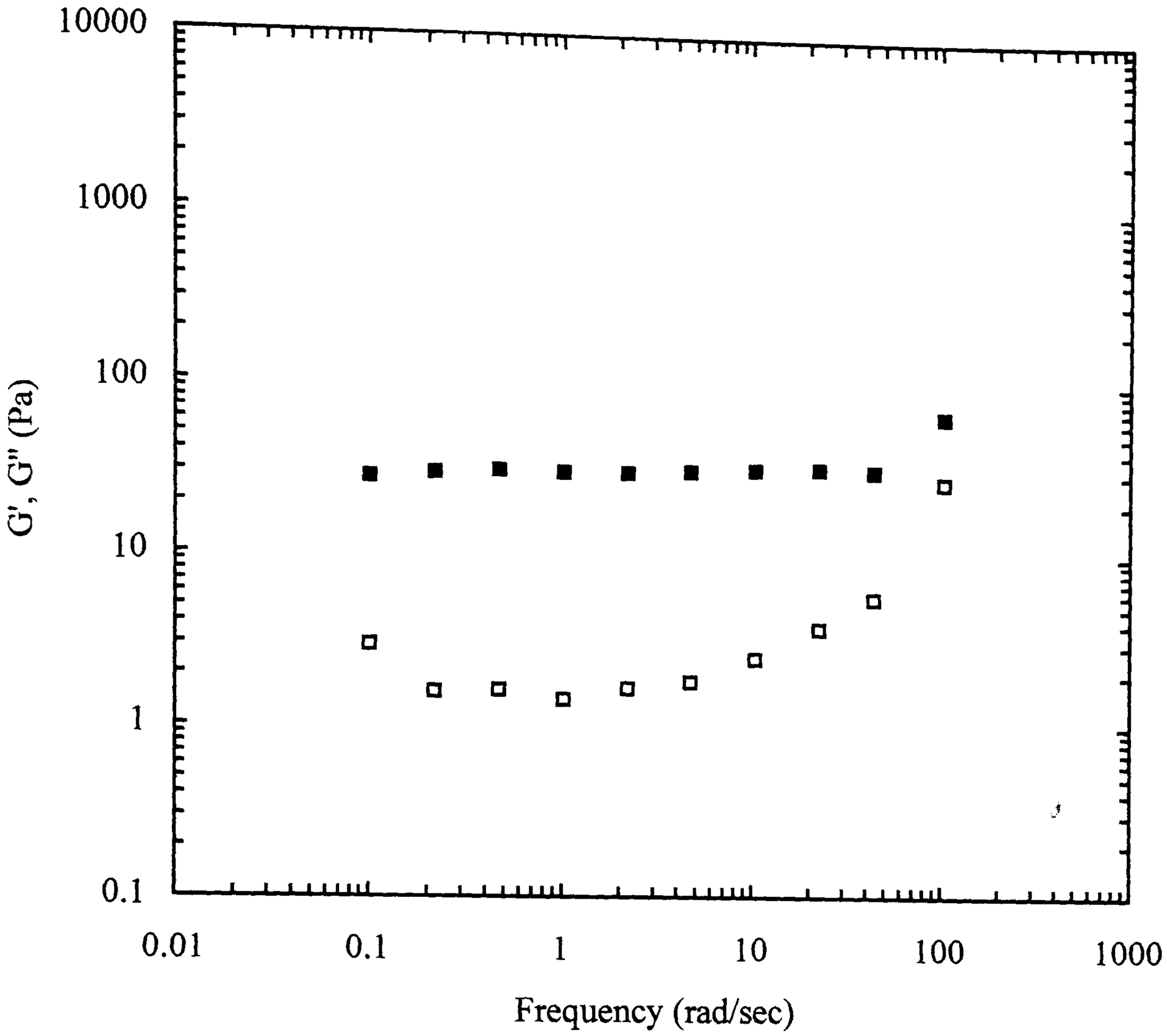

Figure 5.6. Mechanical spectrum showing the frequency-dependence of G' (■) and G" (□) for 1.0 wt % high methoxy pectin (DE 70; pH 3.0) at 90°C after heating from 5 °C in the presence of 50 wt % xylitol.

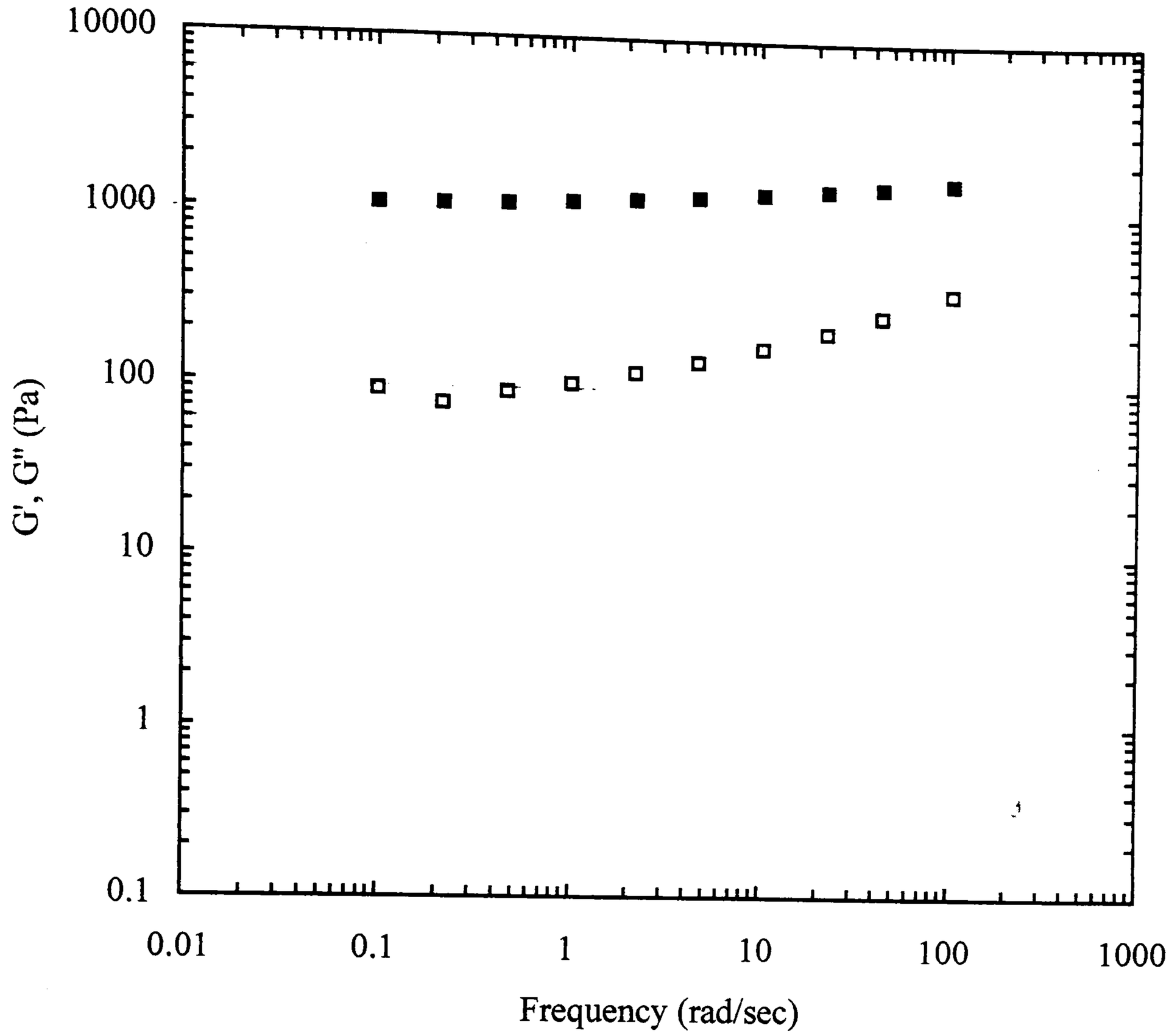

Figure 5.7. Mechanical spectrum showing the frequency-dependence of G' (■) and G" (□) for 1.0 wt % high methoxy pectin (DE 70; pH 3.0) at 5 °C after initial cooling to 5 °C, heating to 90°C and re-cooling to 5 °C in the presence of 50 wt % xylitol.

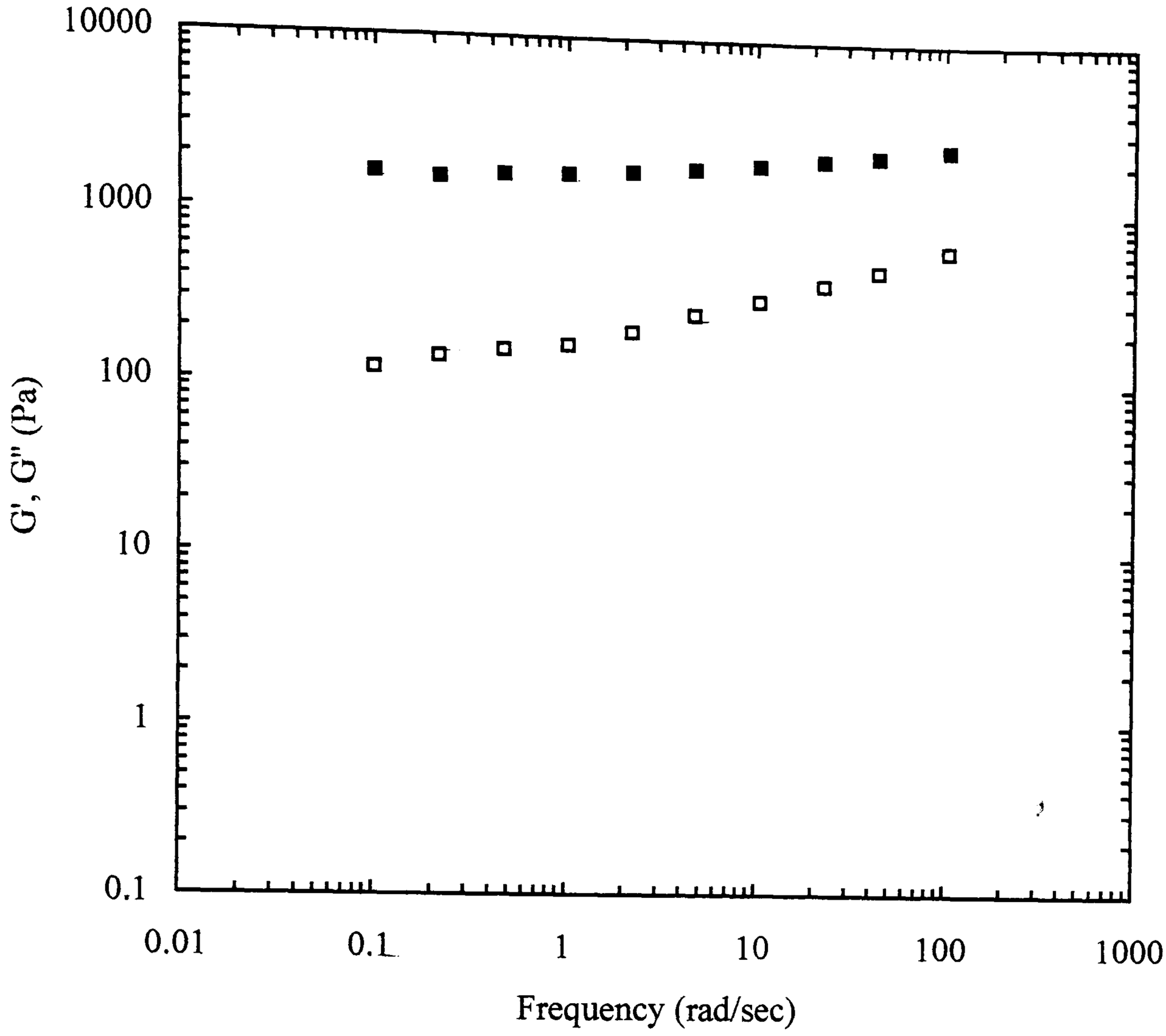

Figure 5.8. Mechanical spectrum showing the frequency-dependence of G' (■) and G" (□) for 1.0 wt % high methoxy pectin (DE 70; pH 3.0) at 5 °C after initial cooling from 90°C in the presence of 65 wt % xylitol.

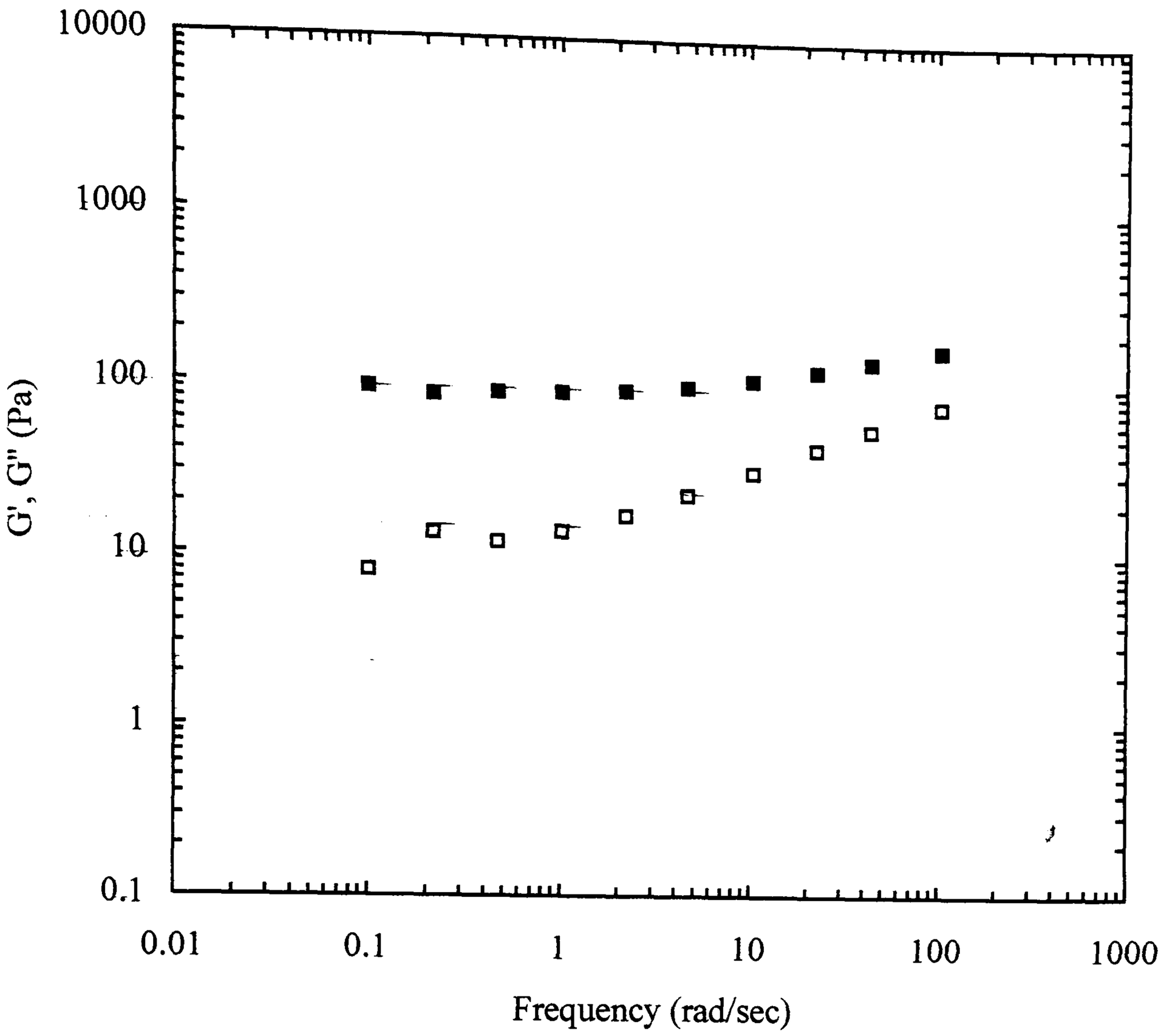

Figure 5. 9. Mechanical spectrum showing the frequency-dependence of G' (■) and G" (□) for 1.0 wt % high methoxy pectin (DE 70; pH 3.0) at 90°C after heating from 5 °C in the presence of 65 wt % xylitol.

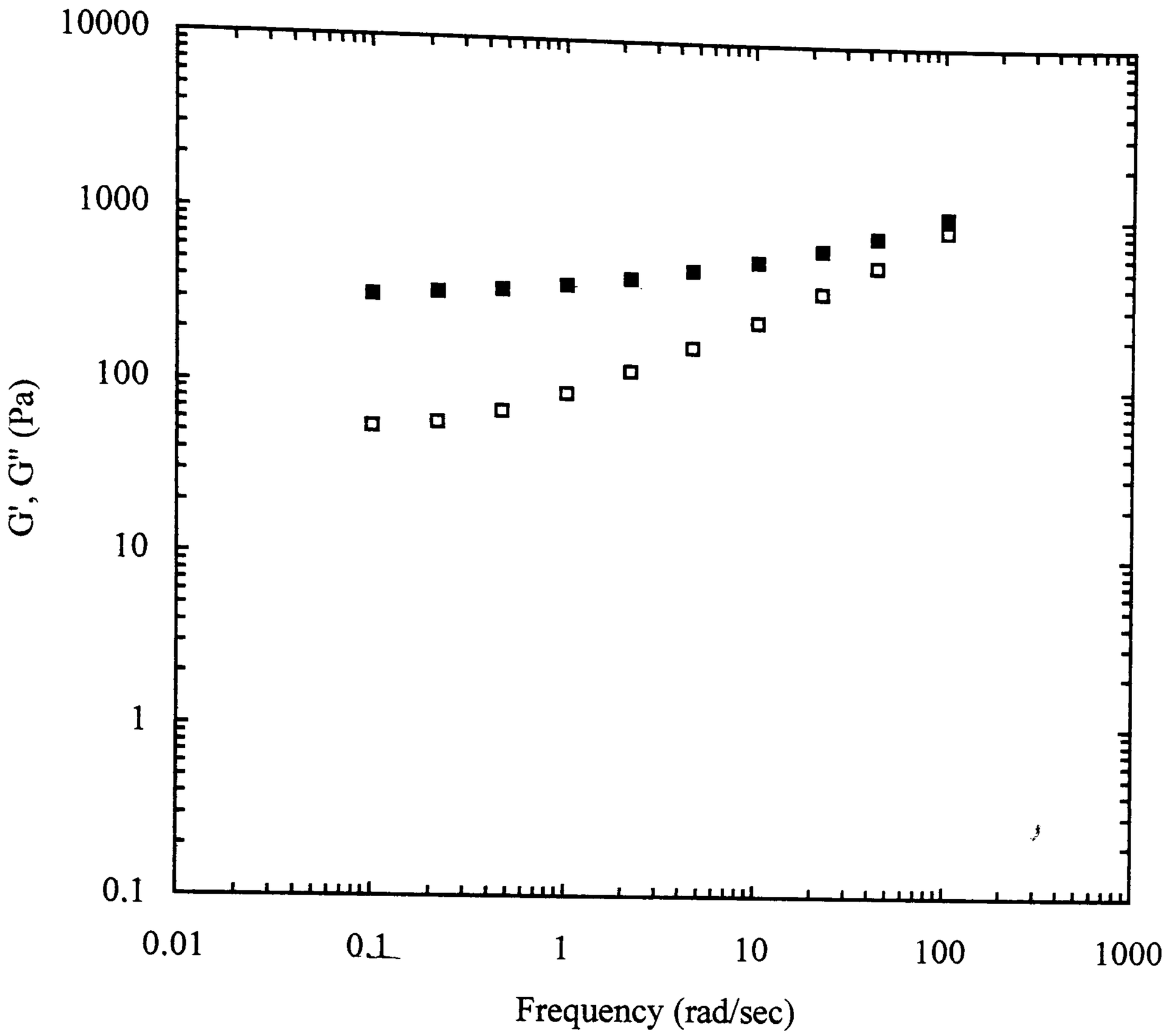

Figure 5.10. Mechanical spectrum showing the frequency-dependence of G' (■) and G" (□) for 1.0 wt % high methoxy pectin (DE 70; pH 3.0) at 5 °C after initial cooling to 5 °C, heating to 90°C and re-cooling to 5 °C in the presence of 65 wt % xylitol.

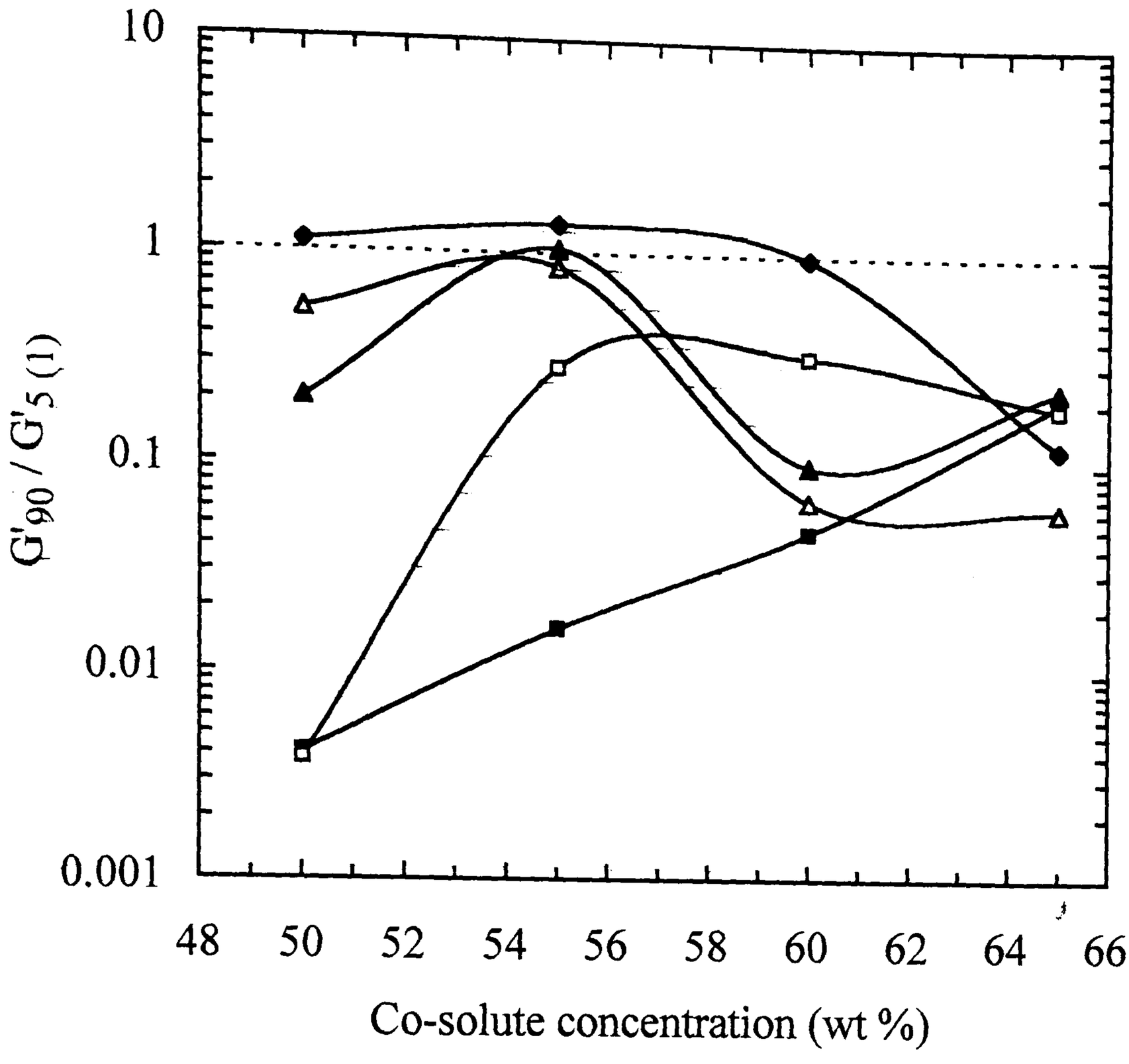

Figure 5.11. Values of G' (1 rad s^{-1}; 0.5 % strain) at 90°C after heating from 5°C, divided by the initial values at 5°C, for 1.0 wt % high methoxy pectin (DE 70; pH 3.0) in mixtures with xylitol (Δ), sorbitol (▲), glucose (□), fructose (■) or sucrose (♦).

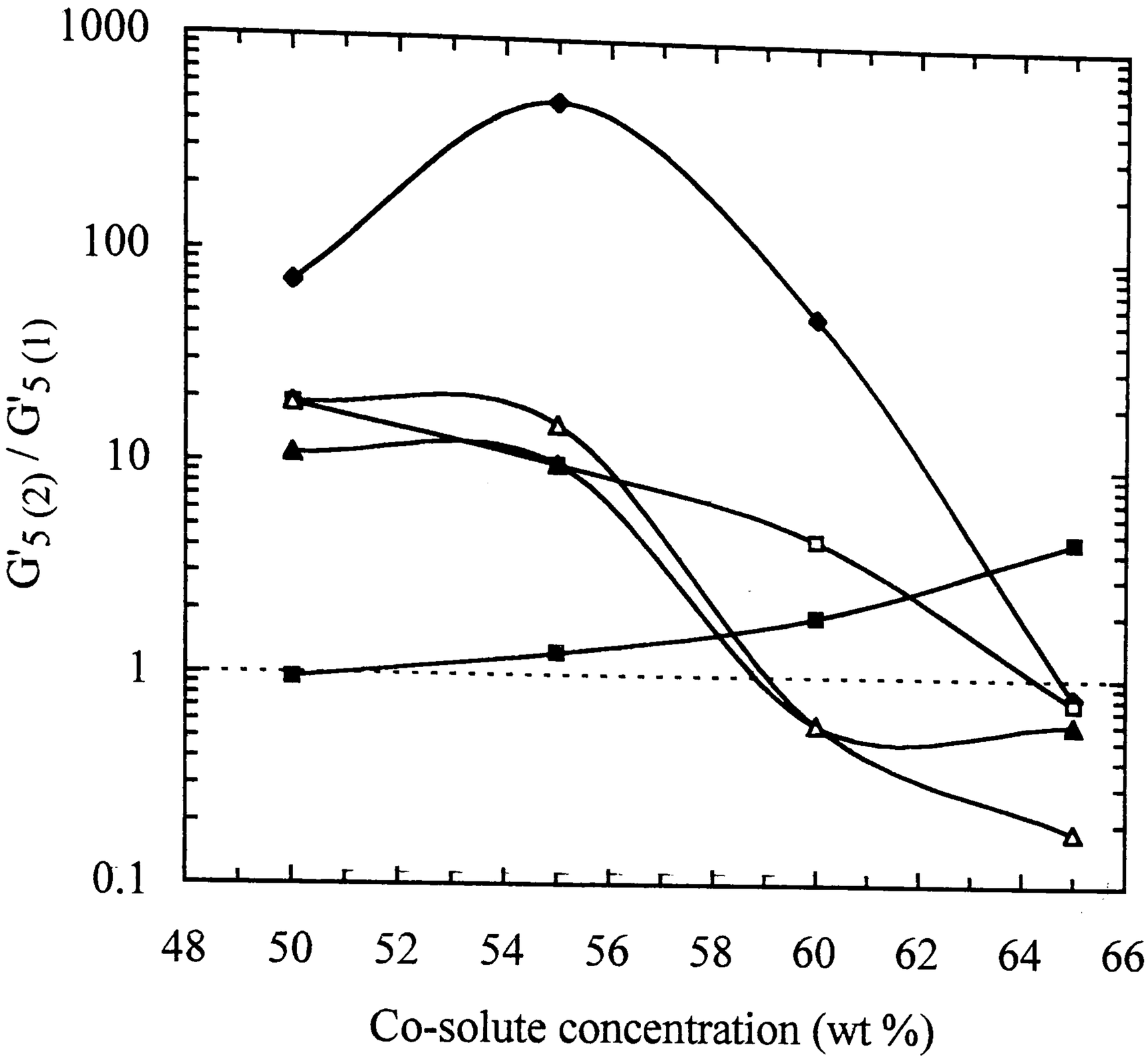

Figure 5.12. Values of G' (1 rad s^{-1}; 0.5 % strain) at 5°C after heating to 90°C and re-cooling, divided by the initial values at 5°C, for 1.0 wt % high methoxy pectin (DE 70; pH 3.0) in mixtures with xylitol (Δ), sorbitol (▲), glucose (□), fructose (■) or sucrose (♦).

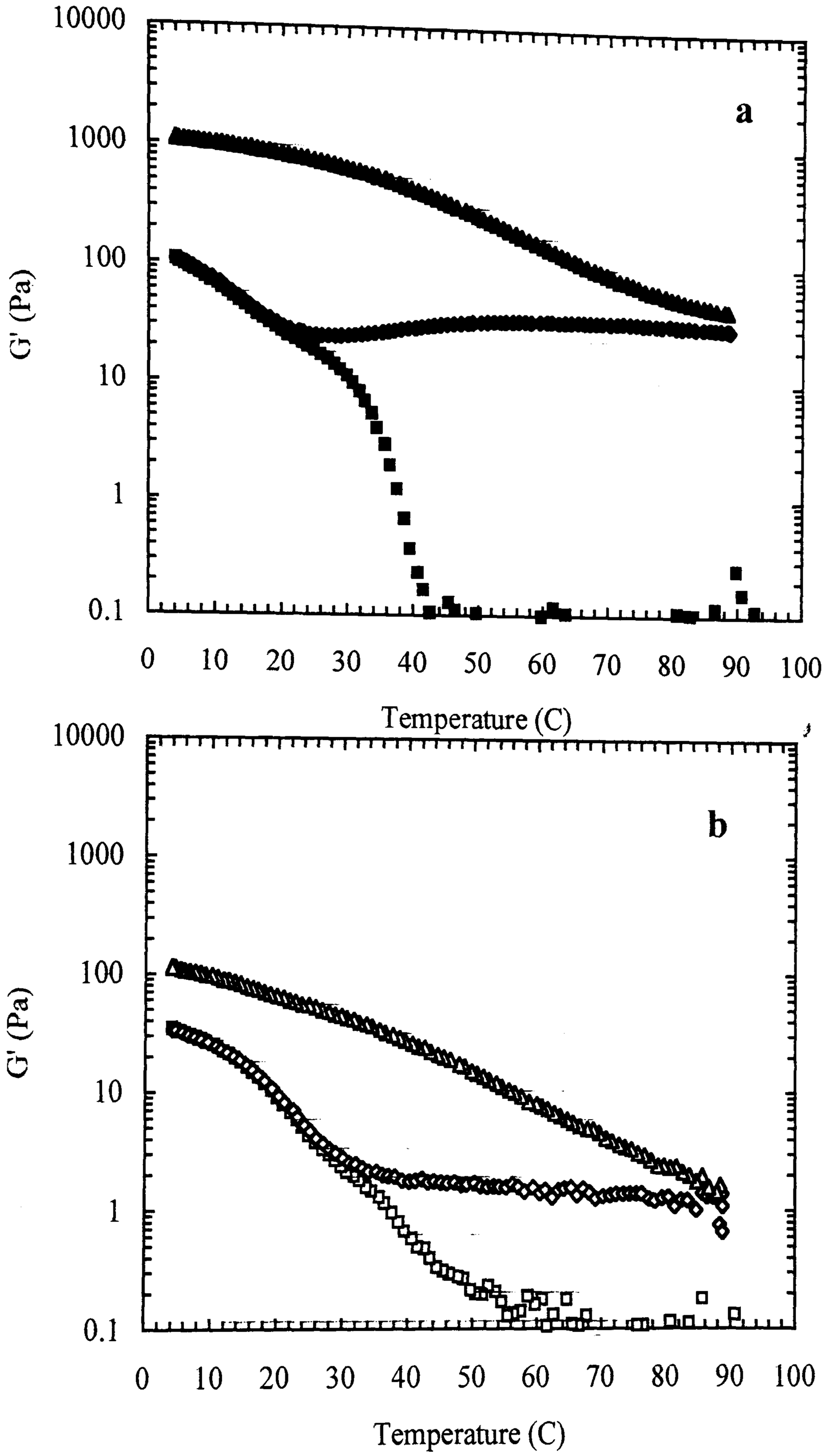

Figure 5. 13. Changes in G' (filled symbols) and G" (open symbols), measured at 1 rad s^{-1} and 0.5 % strain, for 1.0 wt % high methoxy pectin (DE 70; pH 3.0) on initial cooling (squares), heating (diamonds) and re-cooling (triangles) at 1.0 °C/min in the presence of 55 wt % glucose.

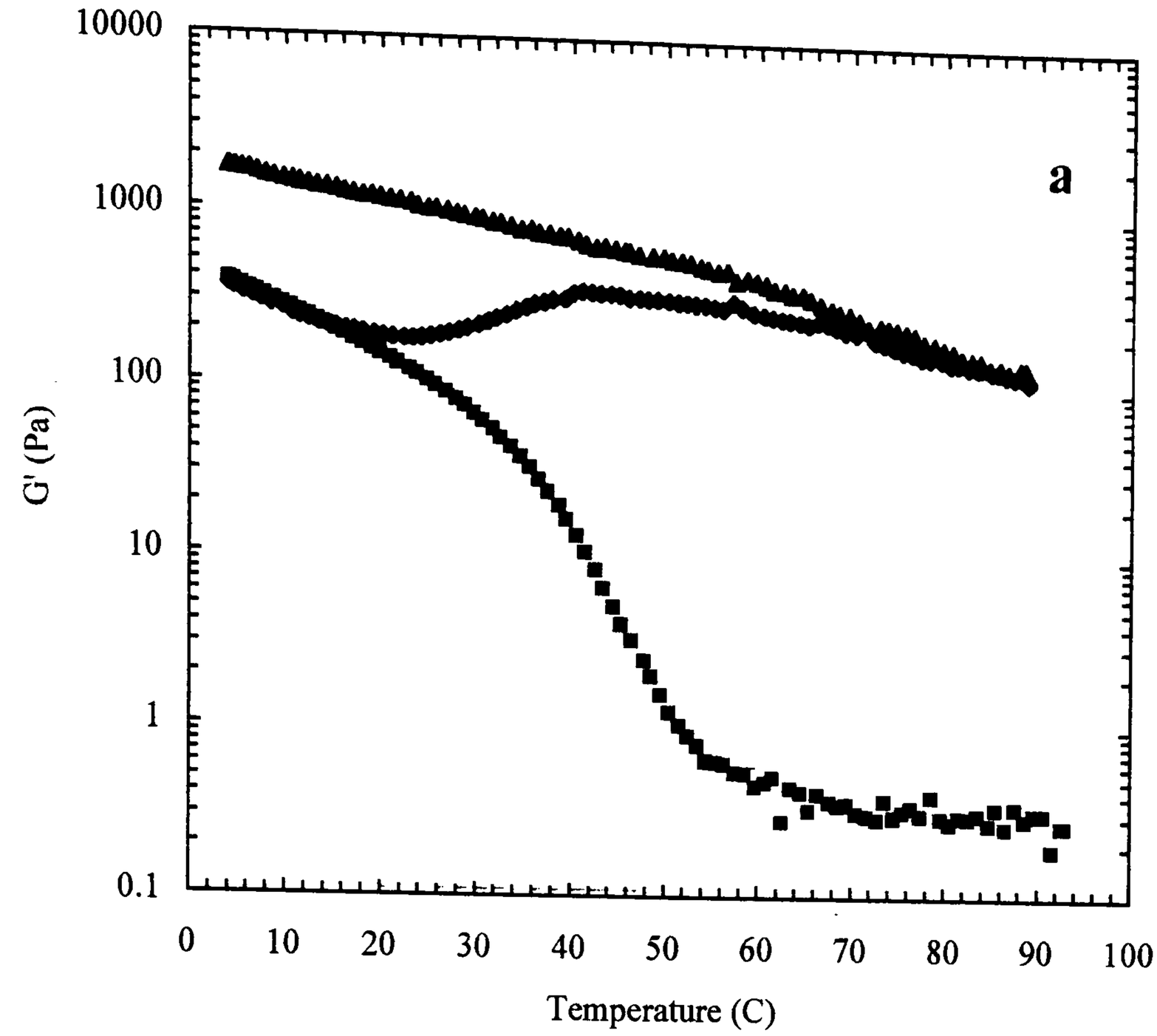

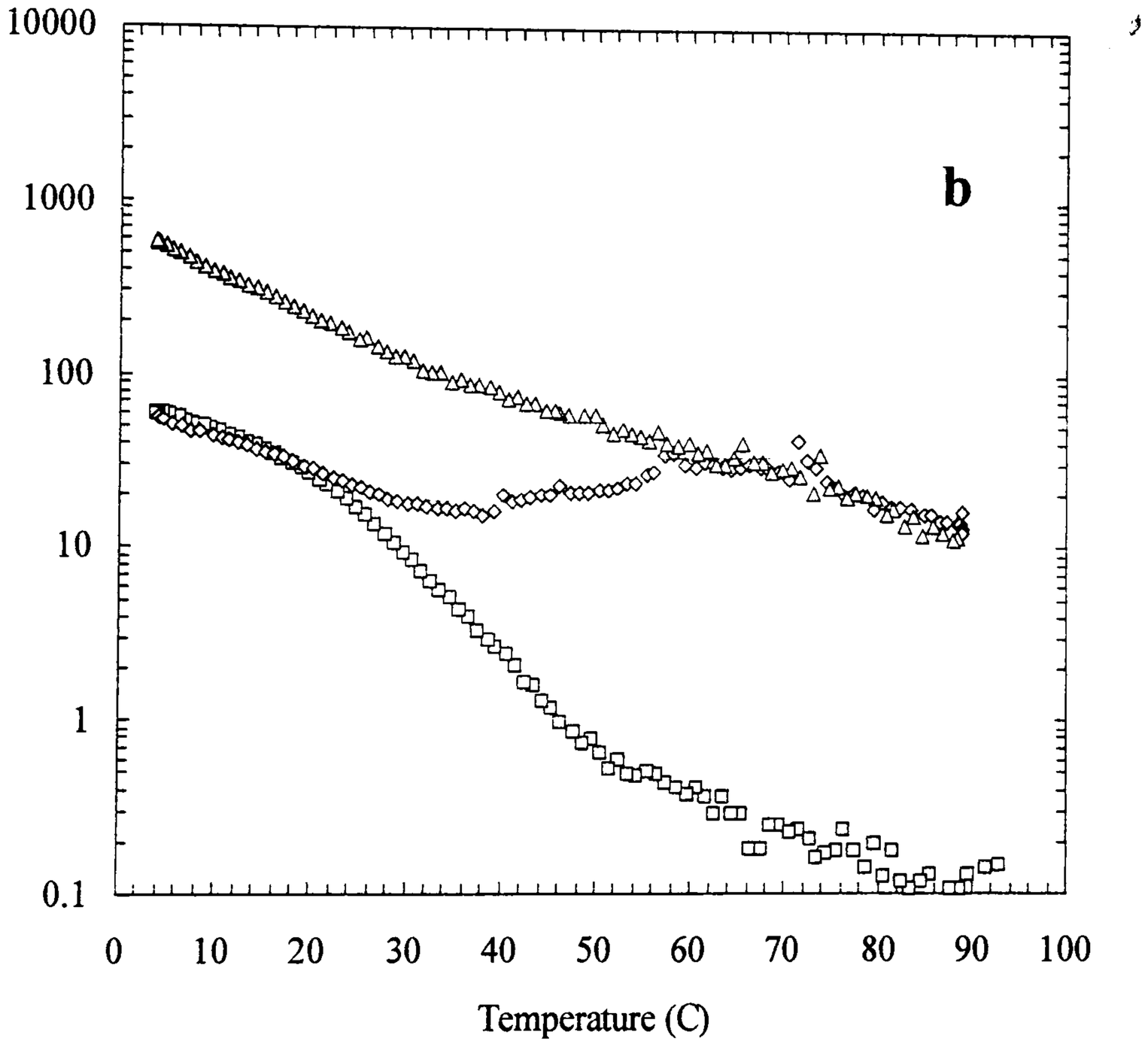

Figure 5.14. Changes in G' (filled symbols) and G" (open symbols), measured at 1 rad s^{-1} and 0.5 % strain, for 1.0 wt % high methoxy pectin (DE 70; pH 3.0) on initial cooling (squares), heating (diamonds) and re-cooling (triangles) at 1.0 °C/min in the presence of 60 wt % glucose.

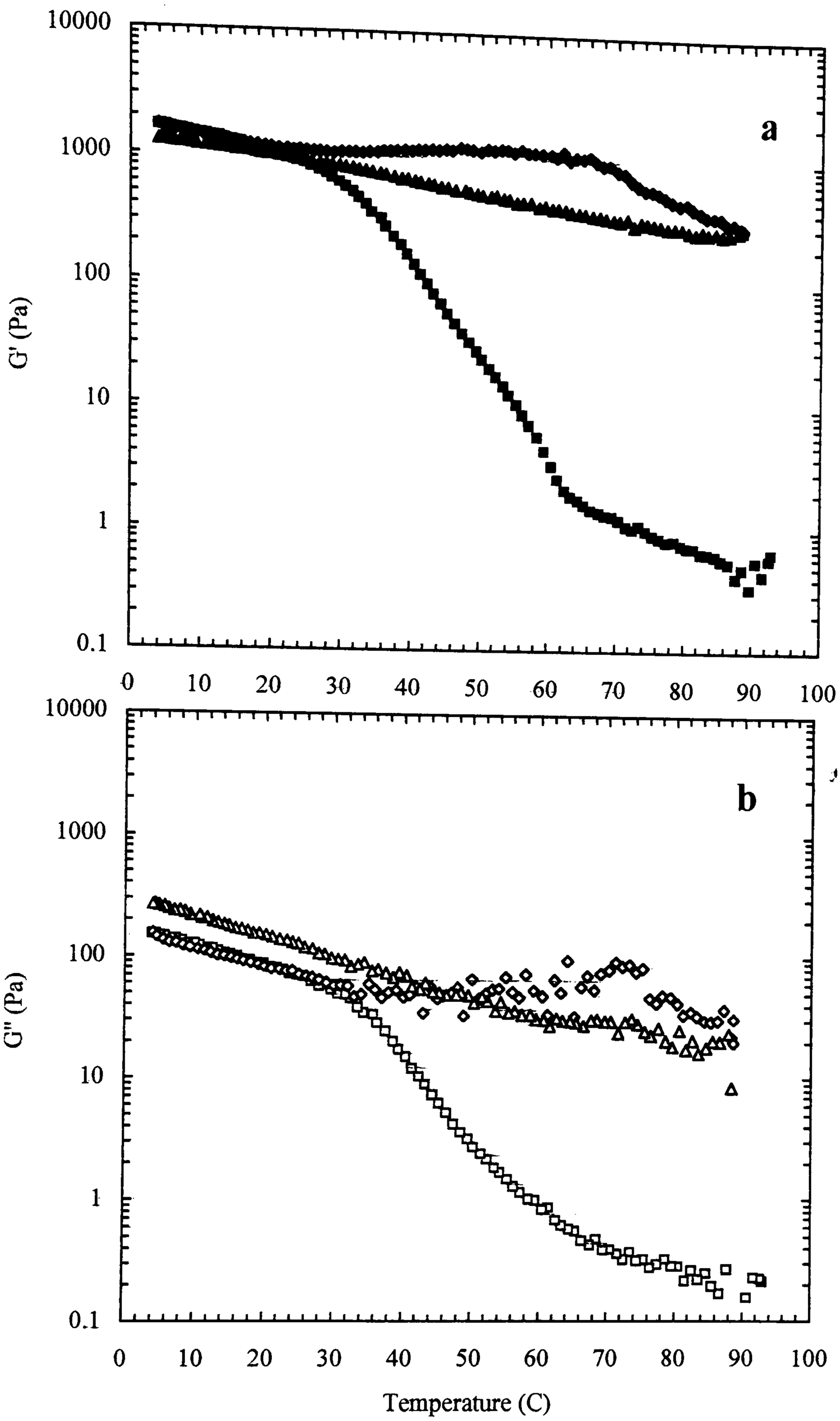

Figure 5. 15. Changes in G' (filled symbols) and G" (open symbols), measured at 1 rad s^{-1} and 0.5 % strain, for 1.0 wt % high methoxy pectin (DE 70; pH 3.0) on initial cooling (squares), heating (diamonds) and re-cooling (triangles) at 1.0 °C/min in the presence of 65 wt % glucose.

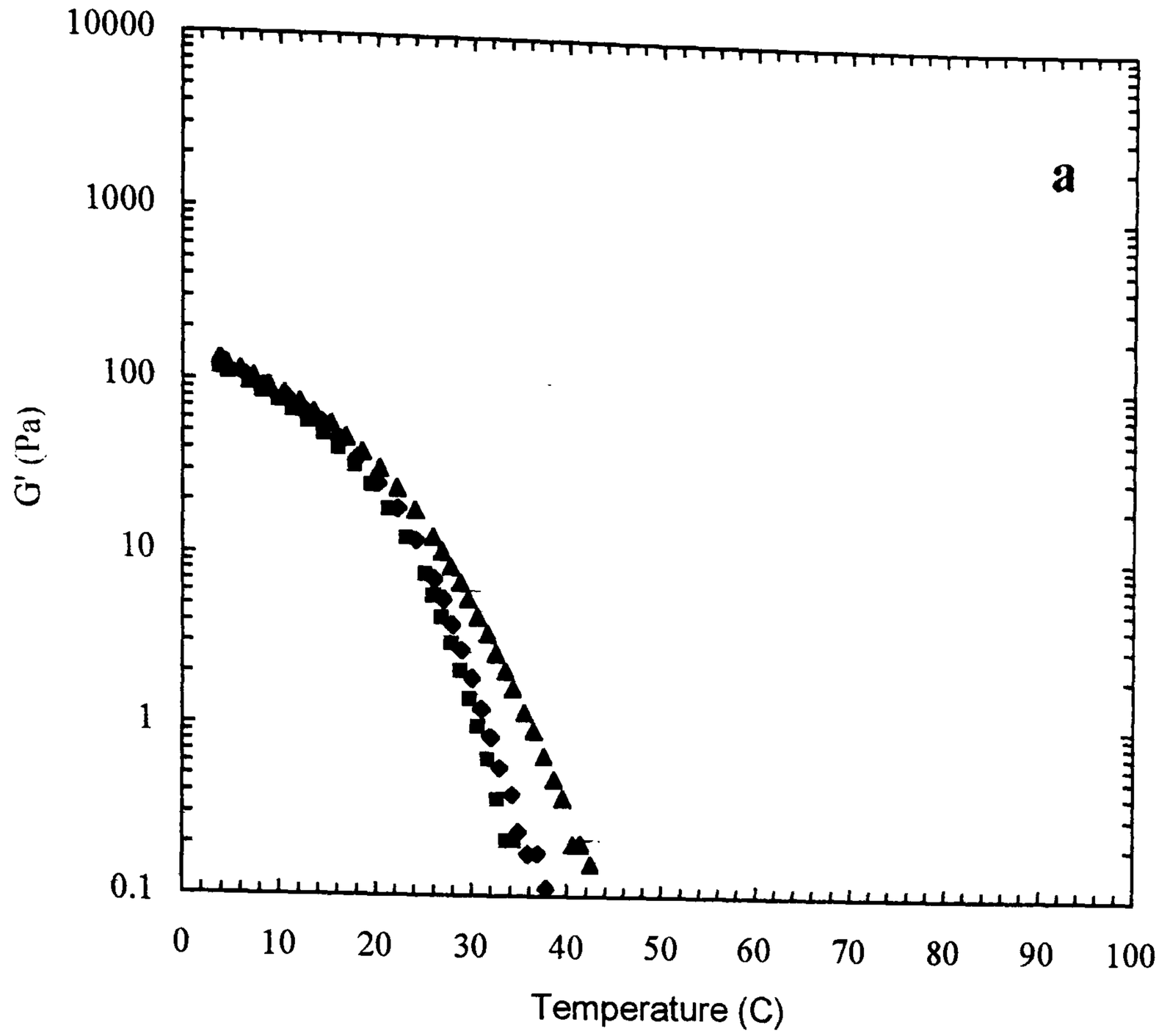

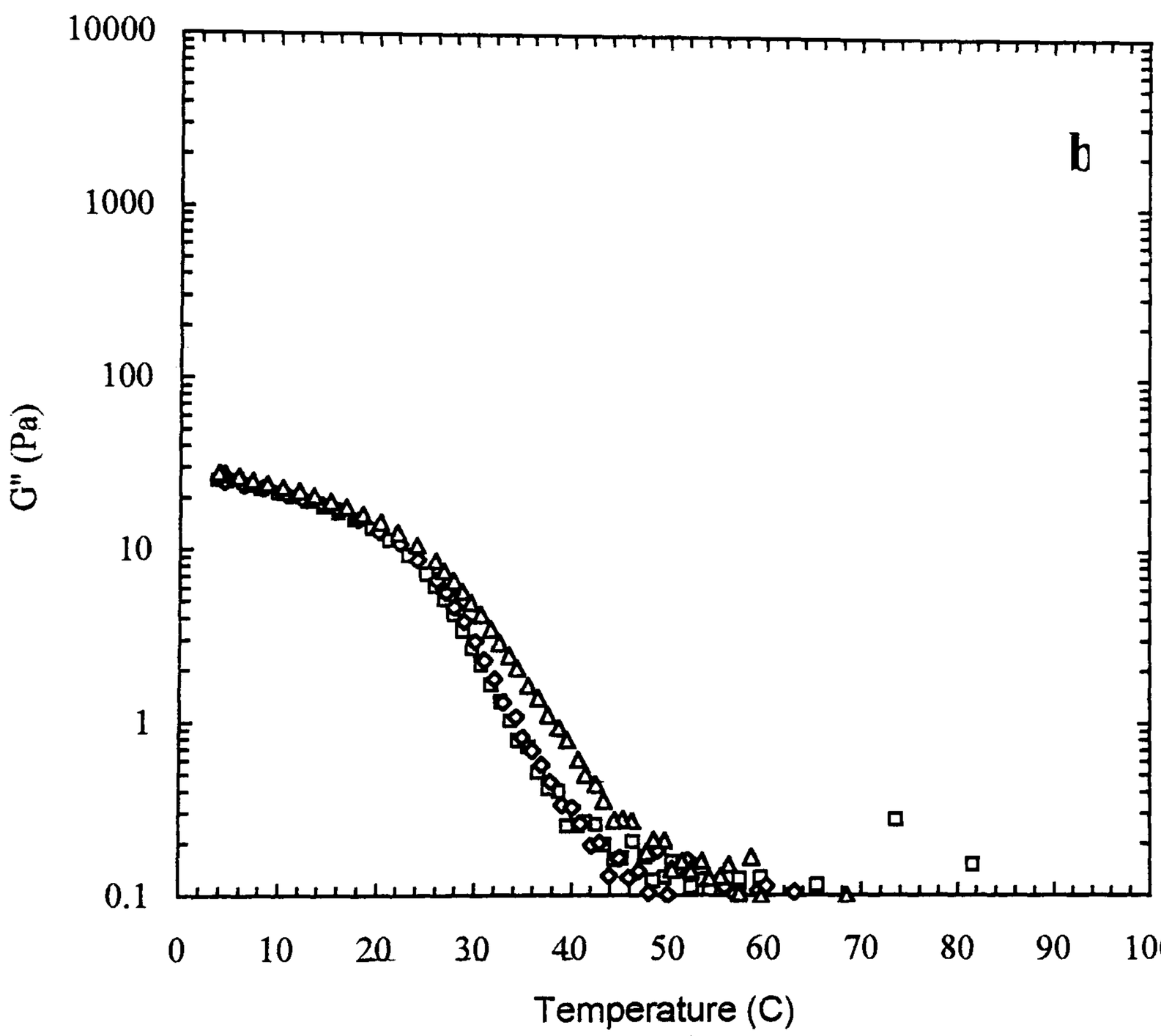

Figure 5.16. Changes in G' (filled symbols) and G" (open symbols), measured at 1 rad s^{-1} and 0.5 % strain, for 1.0 wt % high methoxy pectin (DE 70; pH 3.0) on initial cooling (squares), heating (diamonds) and re-cooling (triangles) at 1.0 °C/min in the presence of 60 wt % glycerol.

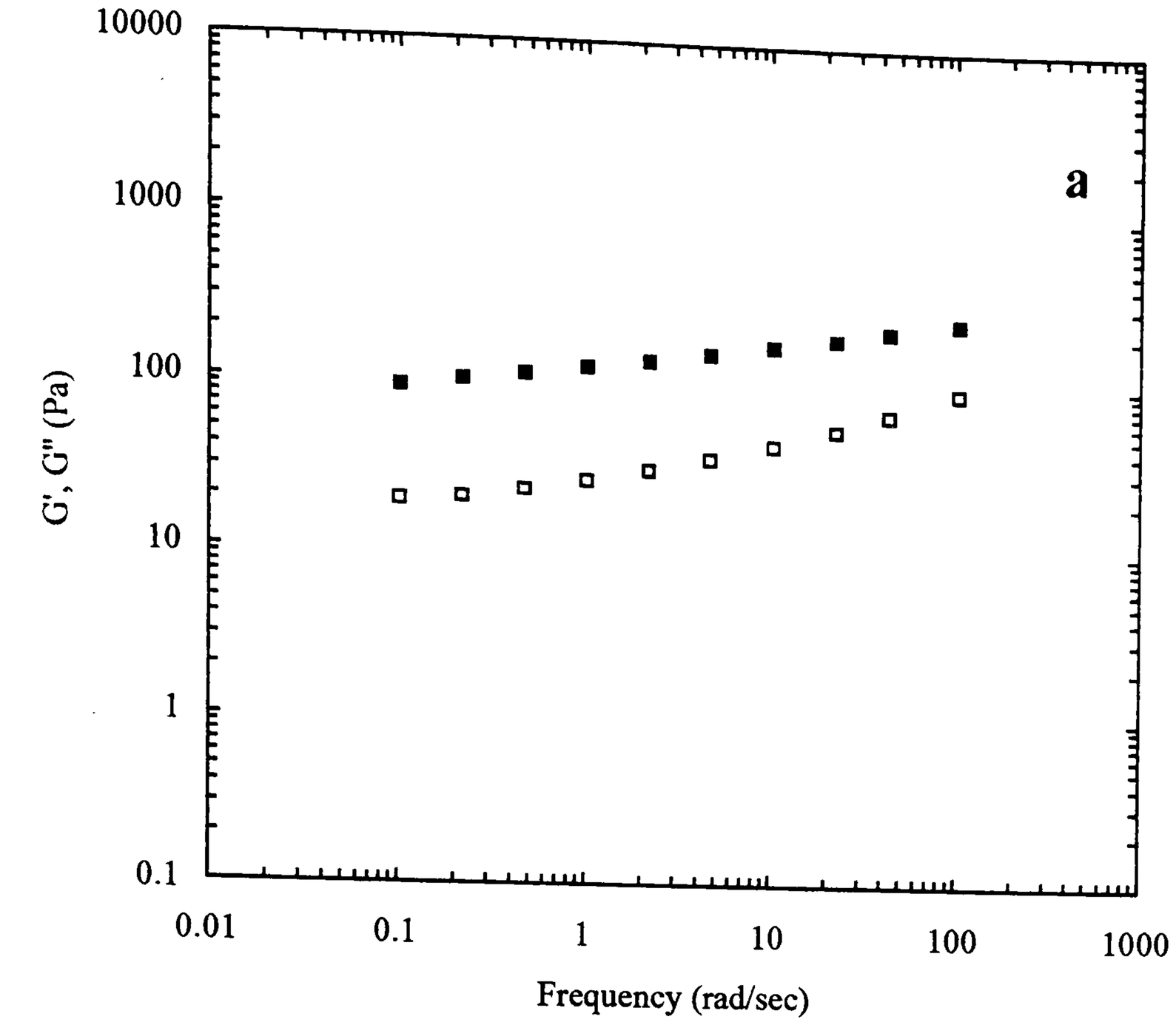

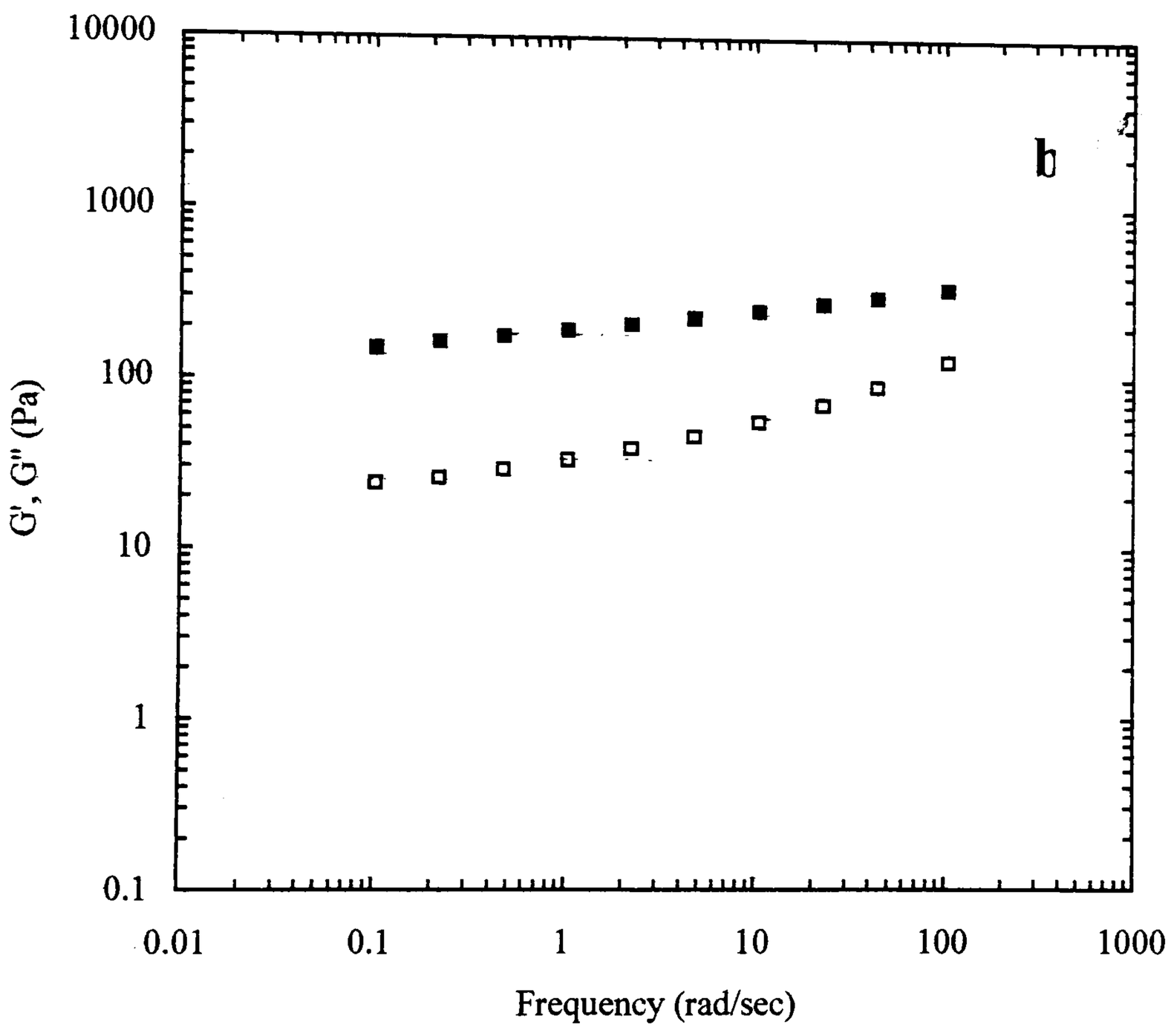

Figure 5.17. Mechanical spectra (0.5 % strain) showing the frequency-dependence of G' (■) and G" (□) at 5 °C (a) before and (b) after heating to 90°C for 1.0 wt % high methoxy pectin (DE 70; pH 3.0) in the presence of 60 wt % glycerol.

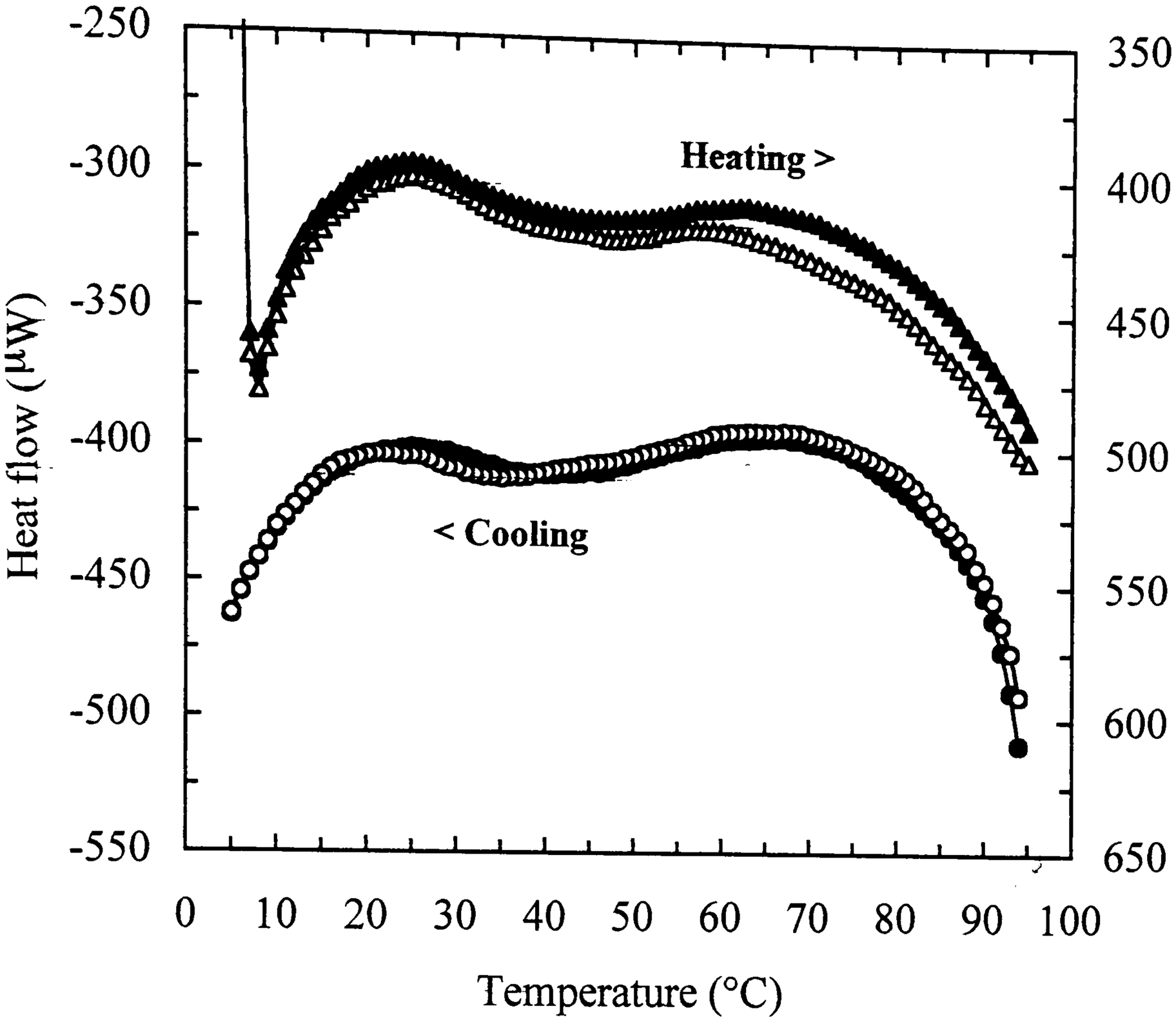

Figure 5.18. DSC traces recorded during heating (triangles) and cooling (circles) in the first (open symbols) and second (filled symbols) of two consecutive cycles at a scan rate of 0.5 °C/min for 1.0 wt % high methoxy pectin (DE 70; pH 3.0) in the presence of 55 wt % xylitol. For ease of comparison, the heat-flow values for the heating scans (right-hand axis) run from top to bottom.

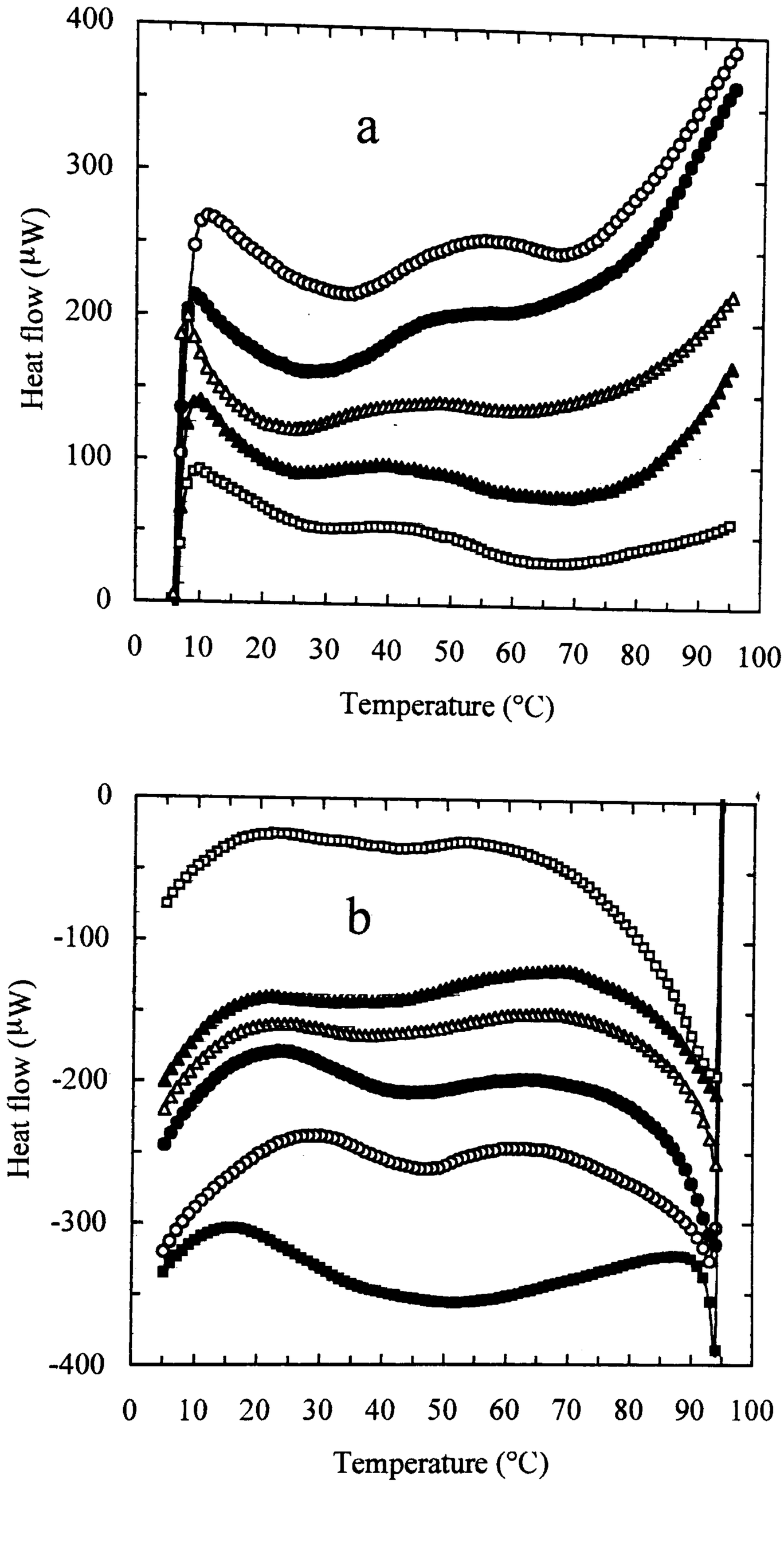

Figure 5.19. Averaged DSC curves from first and second cycles of (a) heating and (b) cooling at 0.5 °C/min for 1.0 wt % high methoxy pectin (DE 70; pH 3.0) with ethan-1,2-diol (O), glycerol (●), xylitol (Δ), sorbitol (▲), glucose (□) or fructose (■) at a fixed concentration of 55 wt %.

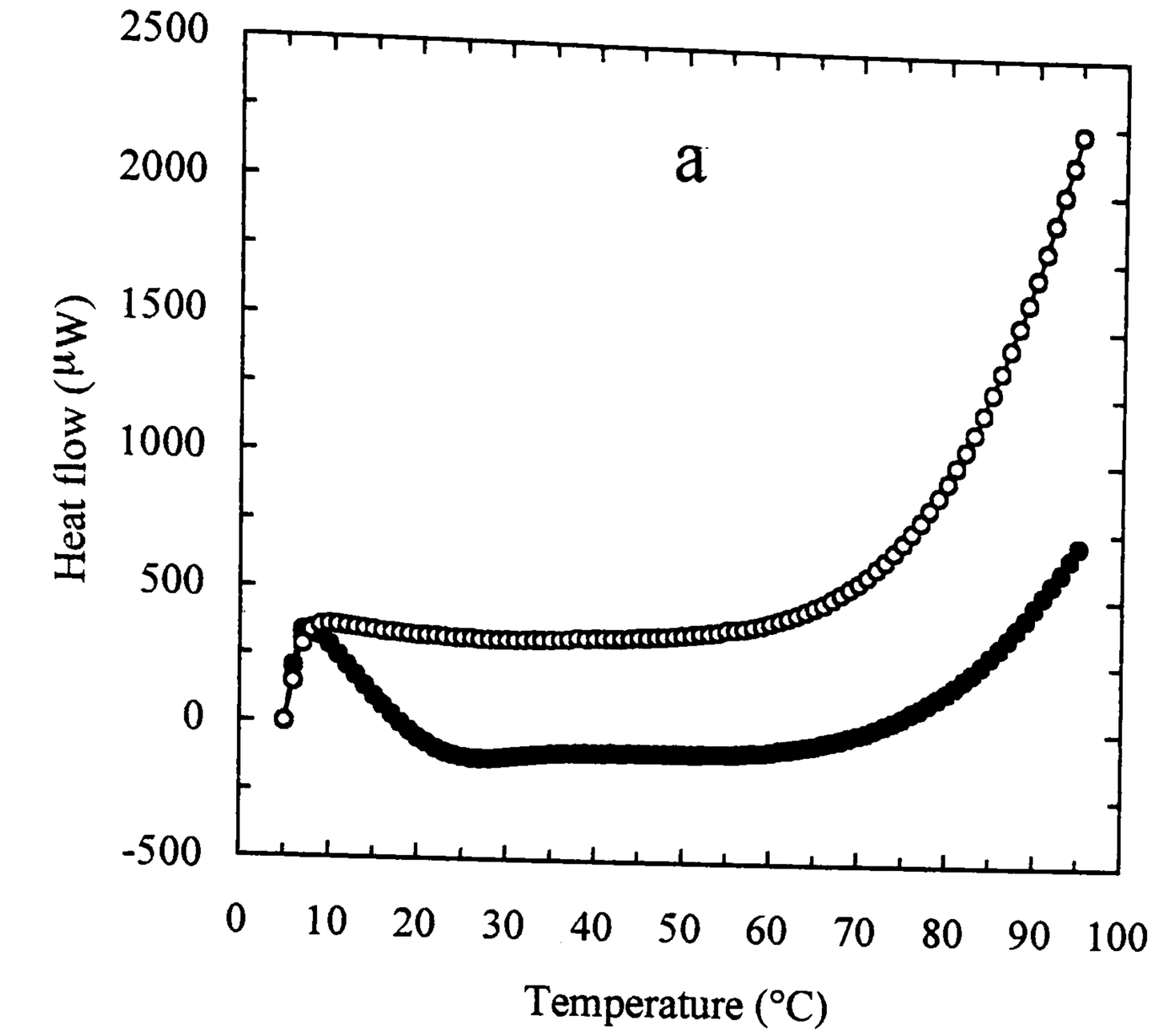

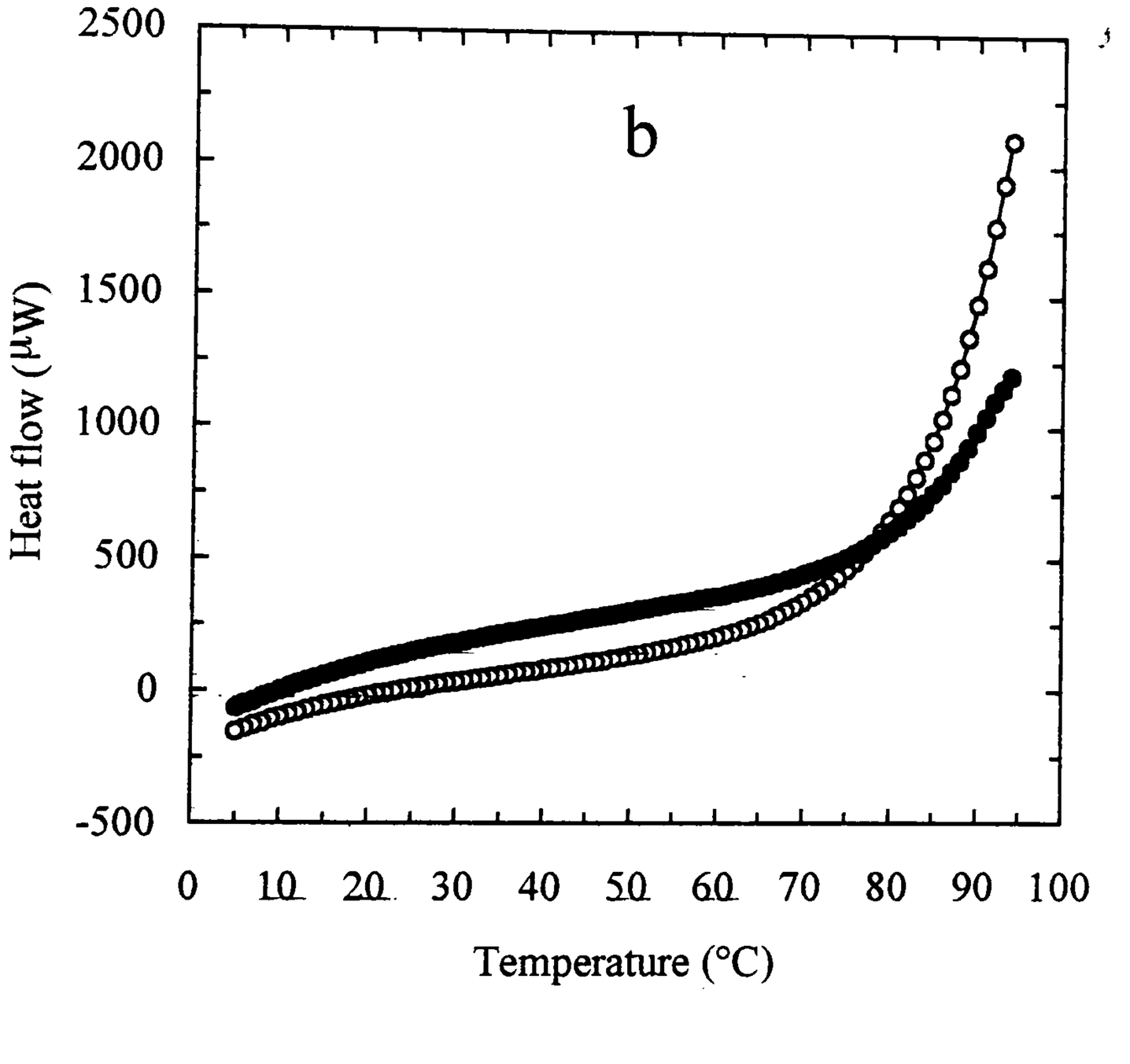

Figure 5.20. DSC traces recorded at 0.5 °C/min for 1.0 wt % high methoxy pectin (DE 70; pH 3.0) in the presence of 55 wt % sucrose during (a) heating and (b) cooling in the first (O) and second (●) of two consecutive cycles.

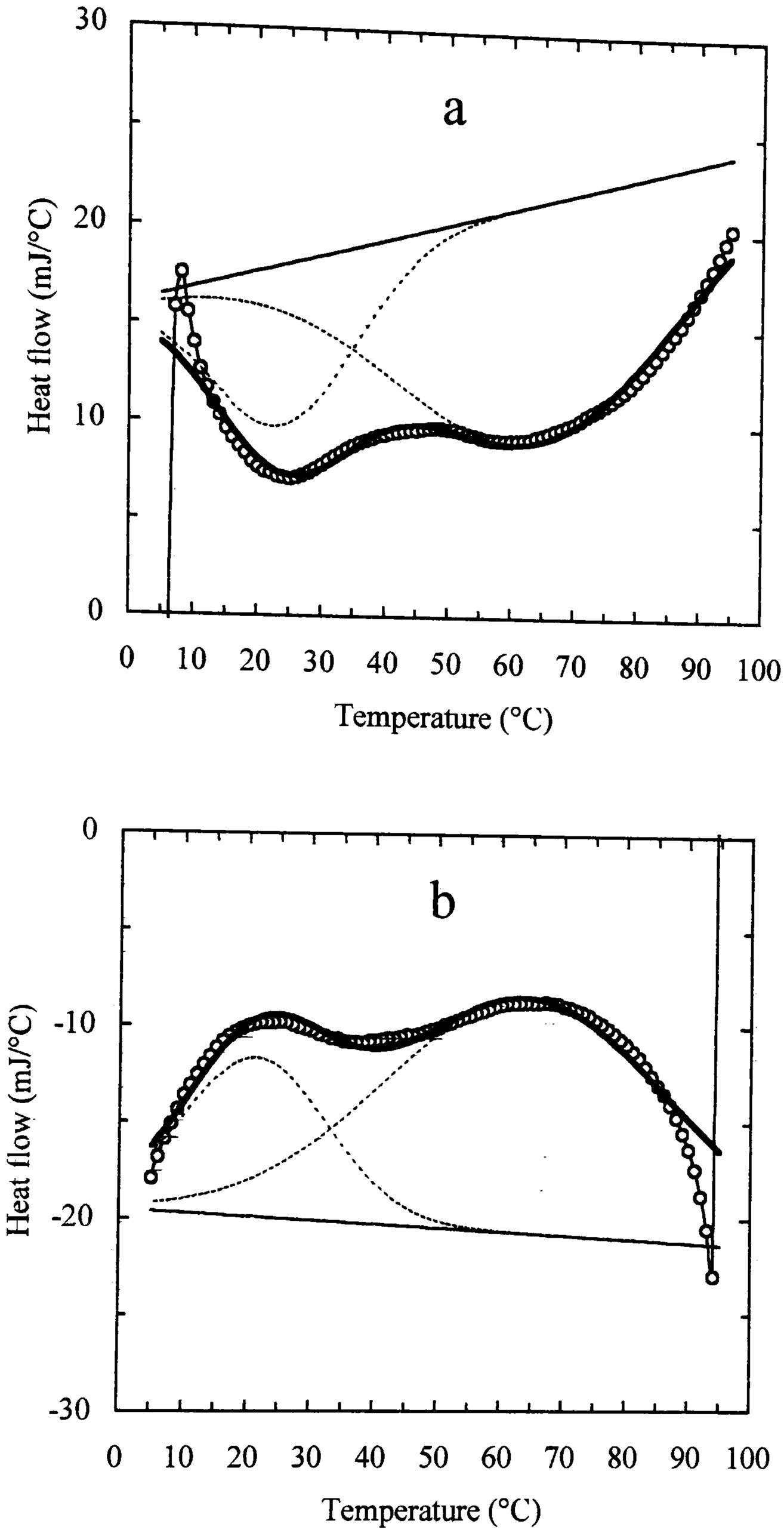

Figure 5.21. DSC traces (O) from Figure 19 for 1.0 wt % high methoxy pectin (DE 70; pH 3.0) on (a) heating and (b) cooling in the presence of 55 wt % xylitol, fitted to two Gaussian bands (- - -) by the procedure described in the text. The bold and fainter solid lines show, respectively, the total spectrum and baseline from the curve-fitting analysis.

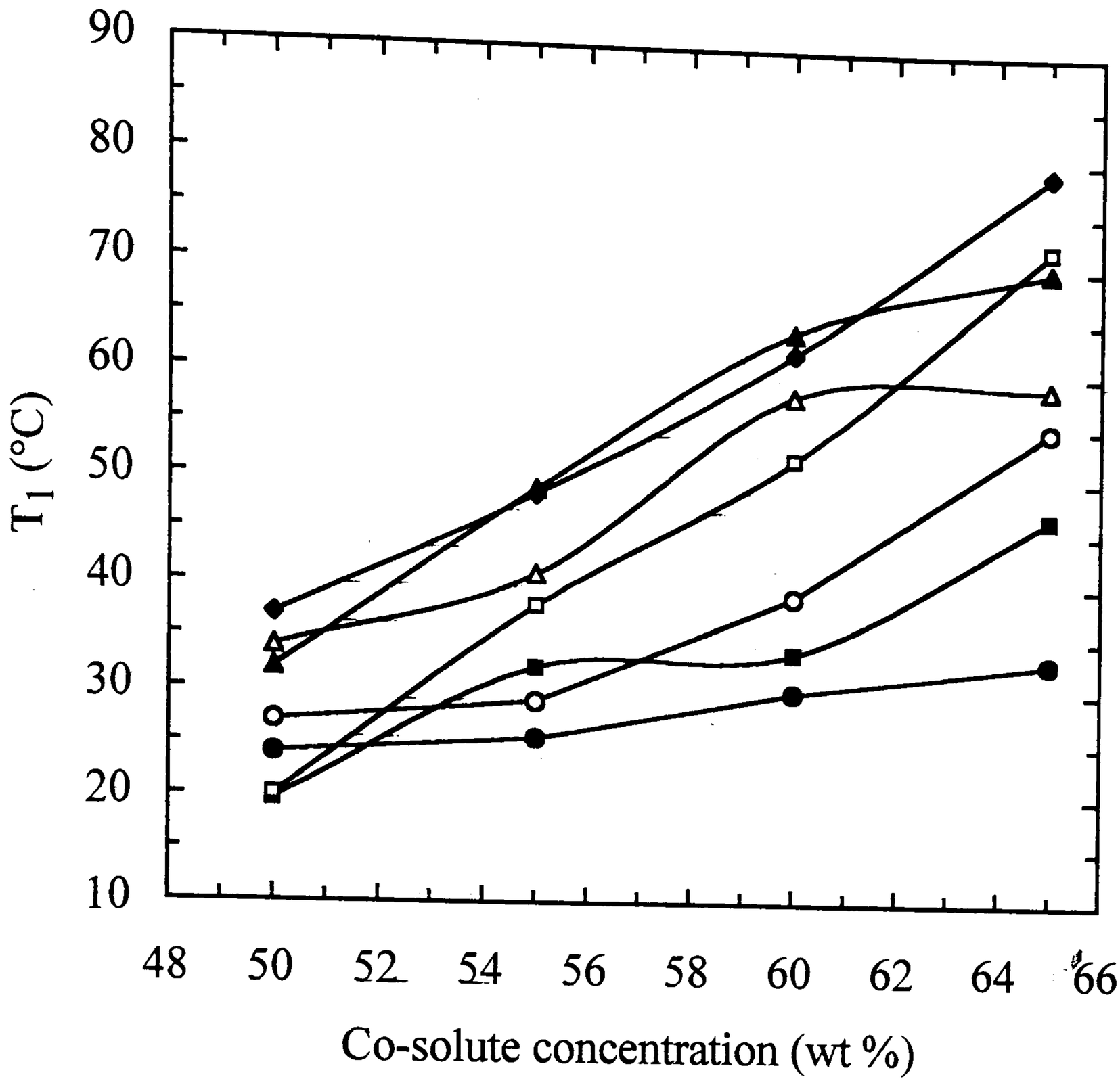

Figure 5.22. Effect of cosolute concentration on the temperature (T_1) at which G' (1 rad s^{-}; 0.5 % strain) reached a value of 1.0 Pa s during initial cooling, for mixtures of 1.0 wt% high methoxy pectin (DE 70; pH 3.0) with ethan-1,2-diol (O), glycerol (●), xylitol (Δ), sorbitol (▲), glucose (□), fructose (■) or sucrose (♦).

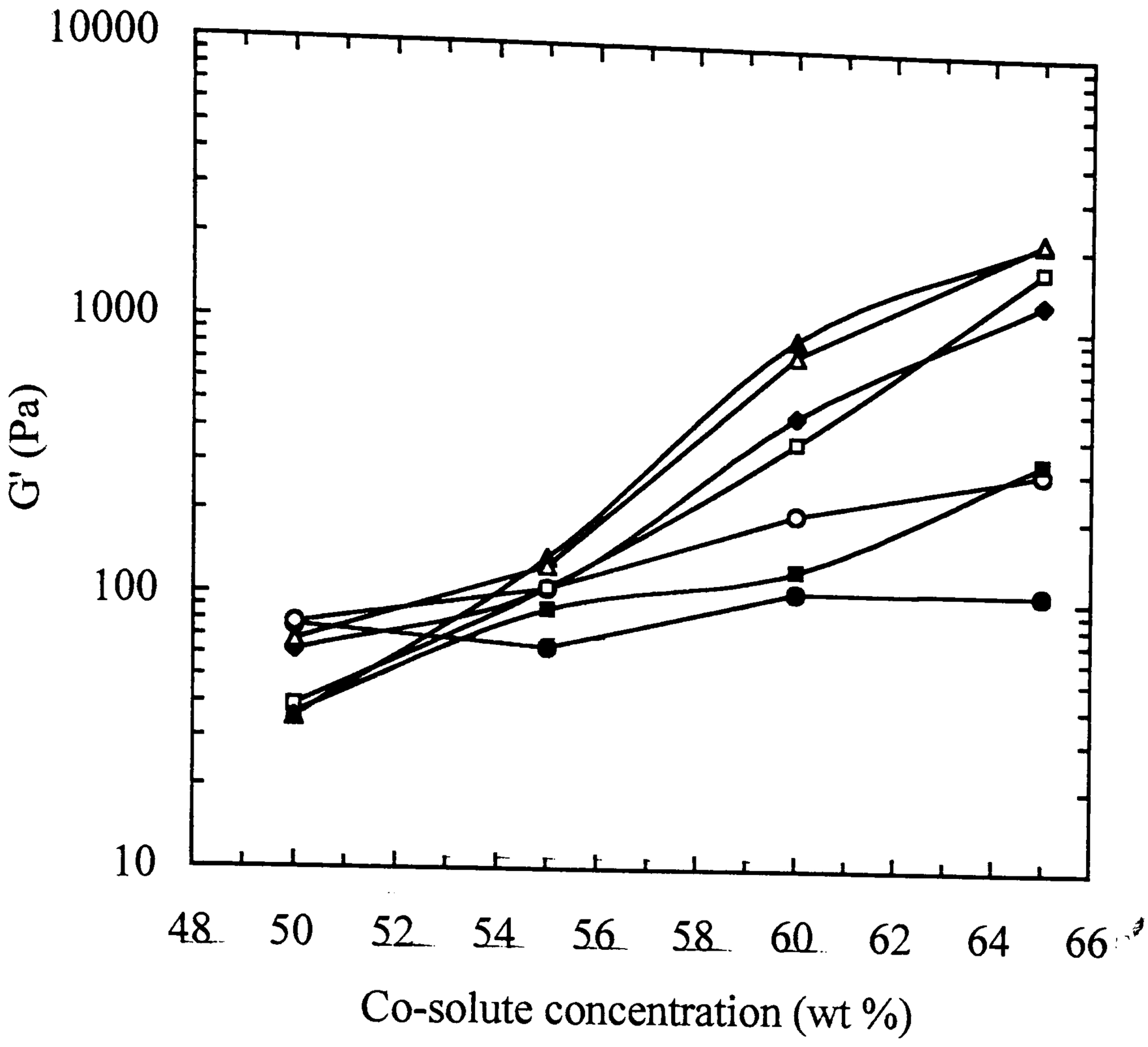

Figure 5.23. Effect of cosolute concentration on the values G' (1 rad s^{-1}; 0.5 % strain) recorded at 5°C after initial cooling, for mixtures of 1.0 wt % high methoxy pectin (DE 70; pH 3.0) with ethan-1,2-diol (O), glycerol (●), xylitol (Δ), sorbitol (▲), glucose (□), fructose (■) or sucrose (♦).

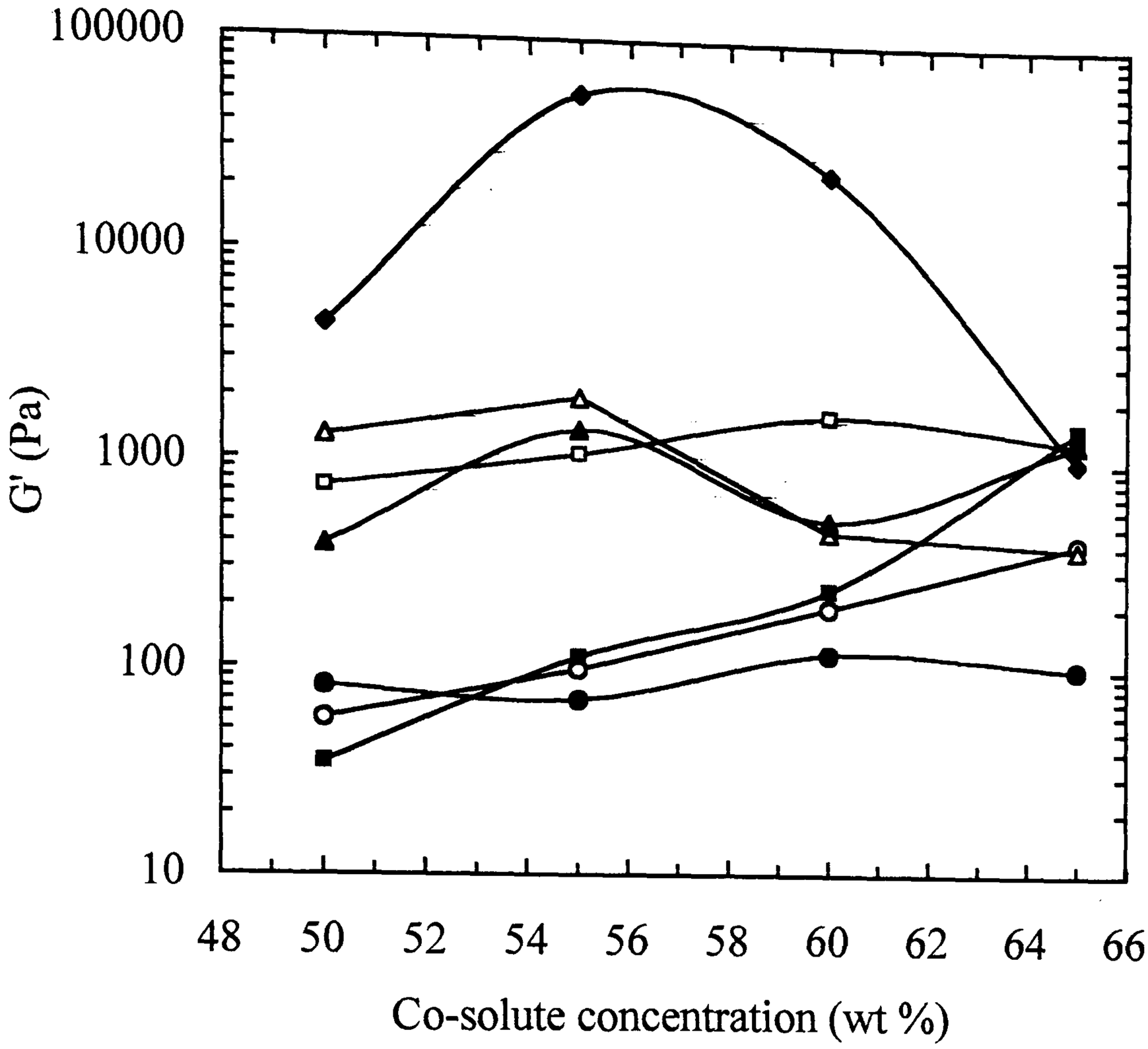

Figure 5. 24. Effect of cosolute concentration on the values G' (1 rad s^{-1}; 0.5 % strain) recorded at 5°C after heating to 90°C and re-cooling, for mixtures of 1.0 wt % high methoxy pectin (DE 70; pH 3.0) with ethan-1,2-diol (O), glycerol (●), xylitol (Δ), sorbitol (▲), glucose (□), fructose (■) or sucrose (♦).

By: Tsoga, A., Richardson, R. K. and Morris, E. R.

For submission to: Food Hydrocolloids

CHAPTER 6

ROLE OF COSOLUTES IN GELATION OF HIGH-METHOXY PECTIN. PART 2. ANOMALOUS BEHAVIOUR OF FRUCTOSE: CALORIMETRIC EVIDENCE OF SITE-BINDING

6.1. ABSTRACT

Gels of high-methoxy pectin (DE 70; 1.0 wt %; pH 3.0) in the presence of fructose at concentrations of 50, 55, 60 and 65 wt % showed an intense endotherm followed immediately by an intense exotherm on heating. These transitions occurred over approximately the same temperature-range as initial gelation on cooling (characterised by low-amplitude oscillatory measurements of G' and G") and increased in magnitude with increasing concentration of fructose. The displacement of both transitions, and particularly the exotherm, to progressively higher temperature as the rate of heating was increased was much greater than anticipated from simple thermal lag, indicating that the underlying structural changes are slow. The proposed interpretation is that fructose is capable of site-binding to pectin in both the ordered (3-fold helix) and disordered state; the endotherm is attributed to helix melting and displacement of fructose; the subsequent exotherm is attributed to re-attachment of fructose to disordered chains, and the slow kinetics of this process to the conformational mobility of disordered pectin. On cooling over the same temperature range, a single exotherm was observed; the absence of detectable splitting is attributed to rapid re-attachment of fructose to conformationally-rigid helices. The magnitude of this endotherm ($\Delta H \approx 20$ J/g) is close to the value found for cosolutes that show no evidence of site-binding, and to the net change in enthalpy for the endothermic and exothermic processes observed on heating, suggesting that the values of ΔH for

displacement and re-attachment of fructose as essentially equal and opposite, with the net change coming from formation or melting of 3-fold helices. A smaller thermal process at higher temperature (endothermic on heating and exothermic on cooling) is attributed to hydrophobic association, which was also seen as an increase in G' and G" on heating in two consecutive cycles of temperature change.

6. 2. INTRODUCTION

The work reported here, and in the preceding paper (Tsoga, Richardson & Morris, 2001), arose from an investigation of the high methoxy pectin–sucrose gel system in mixtures with oxidised starch (Evageliou, Richardson & Morris, 2000a) or potato maltodextrin (Evageliou, Richardson & Morris, 2000b). During the course of these studies, there was concern that the strength of the pectin–sucrose networks might be affected by hydrolysis of sucrose at the high temperatures used to prepare the samples and to induce melting of the starch or maltodextrin networks. A brief comparison was therefore made of the strength of pectin gels prepared with sucrose and with 50/50 mixtures of glucose and fructose. The results seemed sufficiently interesting to warrant a fuller investigation, which was reported separately (Evageliou, Richardson & Morris, 2000c).

Glucose and fructose, either separately or in combination at fixed ratios, were used at concentrations equal to those that would result from complete hydrolysis of sucrose. Since hydrolysis of 1 mole (342 g) of sucrose yields 1 mole (180 g) of glucose plus 1 mole (180 g) of fructose (i.e. a total of 360 g of monosaccharide), these "sucrose equivalent" concentrations are ~ 5 % higher than the starting concentration of sucrose. When comparison was made in this way, effectively on the basis of molar concentrations of monosaccharide residues rather than the simple weight concentrations used in the preceding paper (Tsoga et al., 2001), it was found that relative effectiveness in promoting gelation of

high methoxy pectin under acidic conditions (pH 3.0) followed the order: glucose > sucrose > fructose.

Interpretation of this sequence (Evageliou et al., 2000c) was based on two previous publications. The first, which is summarised in greater detail in the preceding paper (Tsoga et al., 2001), was by Nilsson, Piculell and Malmsten (1990), who presented compelling evidence that the polymer–polymer interactions necessary for gel formation can be inhibited by associative interactions between polymer and cosolute. The second was by Plashchina et al. (1986), who showed evidence that methanol forms a stoichiometric complex with pectin by hydrogen bonding to the lone-pair electrons of the carbonyl moiety at C(6), and attributed the stability of the complex to the strong acidity (i.e. polarity of the hydroxyl group) of methanol in comparison with other aliphatic alcohol. In an extension of this concept it was suggested by Evageliou et al. (2000c) that, since primary hydroxyl groups are more polar than secondary, the order of effectiveness of glucose, sucrose and fructose in promoting gelation of high methoxy pectin might be related to their content of primary hydroxyl groups (1 per residue in glucose, 1.5 in sucrose and 2 in fructose), with fructose therefore giving the strongest polymer–cosolute interactions and hence (Nilsson et al., 1990) the lowest gel strengths.

The experiments reported in the preceding paper (Tsoga et al., 2001) were designed to test this proposal, by comparison of the same sugars with a range of polyols each of which, like fructose, has two primary hydroxyl groups per molecule, and might therefore be expected to cause similar inhibition of network formation in mixtures with high methoxy pectin. The results demonstrated clearly that the initial postulate was wrong, since sorbitol [$CH_2OH{\cdot}(CHOH)_4{\cdot}CH_2OH$] and xylitol [$CH_2OH{\cdot}(CHOH)_3{\cdot}CH_2OH$)] were found to be roughly comparable to glucose in their ability to induce pectin gelation (Tsoga et al., 2001). Nonetheless, fructose did appear to be anomalous in its behaviour in comparison with the other solid cosolutes studied, giving gelation temperatures and moduli similar to those

obtained with cosolutes of much lower molecular weight and melting point: glycerol [$CH_2OH{\cdot}CHOH{\cdot}CH_2OH$] and ethan-1,2-diol [$CH_2OH{\cdot}CH_2OH$].

In the present work, we have made a more detailed study of the gelation of high methoxy pectin in mixtures with these liquid cosolutes or with fructose, with the conclusion that the apparent similarity is superficial, and that the inhibitory effect of fructose, in comparison with other solid cosolutes, on network formation arises in a different way.

6.3. MATERIALS AND METHODS

All materials were identical to those used in the investigation reported in the preceding paper (Tsoga et al., 2001): high methoxy pectin (DE 70) from Hercules and AnalaR grade ethan-1,2-diol, glycerol, fructose, citric acid and trisodium citrate from BDH. Samples were again prepared at 95°C, with acidification from ~ pH 4 to pH 3.0 as the final step, using a fixed pectin concentration of 1.0 wt %.

The procedure used for differential scanning calorimetry (DSC) was also identical: two consecutive cycles of heating and cooling between 5 and 95°C. The only modification to the protocol used by Tsoga et al. (2001) for oscillatory rheology was that, after initial loading at ~ 95°C and cooling to 5°C, the sample was subjected to two cycles of heating and cooling between 5 and 95°C, rather than one, and the recording of mechanical spectra at the end of each heating or cooling process was omitted, to shorten the duration of the experiments and minimise the risk of artefacts from loss of solvent (despite the coating of silicone oil around the periphery of the sample). Measurements were again made at 1 rad s^{-1} and 0.5 % strain, using a fixed heating and cooling rate of 1°C/min.

Optical rotation was measured at 365 nm on a Perkin-Elmer 241 polarimeter, using a jacketed cell of pathlength 1 cm. Temperature was controlled by a Haake circulating water bath, adjusted manually, and measured using a thermocouple in the neck of the cell, but out

of the light path. Samples were loaded at ~ 95°C immediately after acidification, and subjected to two cycles of cooling and heating between 90°C and 5°C at ~ 1°C/min. Values of optical rotation at each temperature were recorded after the readings had stabilised.

6.4. RESULTS

6.4.1. Rheology

Figure 6.1 shows the changes in storage modulus (G'; Figure 6.1a) and loss modulus (G"; Figure 6.1b) observed for high methoxy pectin (DE 70; 1.0 wt %; pH 3.0) with 55 wt % glycerol during initial cooling from 95 to 5°C and in two subsequent cycles of heating and cooling between 5°C and 90°C. The reduction in moduli during the first heating process is virtually superimposable on the increase observed on initial cooling, but in subsequent cycles there is a systematic shift to higher values of temperature at the onset of gelation on cooling and completion of melting on heating. A broadly similar pattern was observed using lower and higher concentrations of glycerol (50 and 65 wt %) and with ethan-1,2-diol as cosolute (at concentrations of 50, 55 and 60 wt %). In all cases, there was no survival of detectable network structure ($G' > 0.1$ Pa) at temperatures above 80°C, and no increase in modulus during heating.

The response to thermal cycling with fructose as cosolute was completely different. Figure 2 shows the changes in moduli observed for 1.0 wt % pectin in the presence of 55 wt % fructose. The reduction in moduli at the start of the first heating process is again superimposable on the increase seen during initial cooling, but is then followed by a sharp increase, as observed for sucrose (Evageliou et al., 2000) and other solid cosolutes (Tsoga et al., 2001), and the values remain higher on re-cooling. The same pattern is repeated in the second cycle of heating and cooling, but with a further shift to higher moduli. As discussed previously (Evageliou et al., 2000; Tsoga et al., 2001) the increases in moduli can be attributed to hydrophobic association of methyl ester groups on heating.

6.4.2. Optical rotation

Figure 6.3 shows the changes in optical rotation observed during thermal cycling of 1.0 wt % high methoxy pectin (pH 3.0) in the presence of glycerol at concentrations of 55 wt % (Figure 6.3a) and 65 wt % (Figure 6.3b). The results obtained using 50 wt % glycerol were closely similar to those at 55 wt %, but offset to slightly lower temperature (by ~ 3°C). All traces show a sigmoidal increase in optical rotation over the temperature range of the increases in moduli observed (Figure 6.1) on initial cooling; this can be attributed (Gilsenan, Richardson & Morris, 2000; Evageliou et al., 2000) to formation of 3-fold helices which associate to give a crosslinked network. With 50 or 55 wt % glycerol as cosolute (Figure 6.3a) the transition is fully reversible, with no systematic or significant differences between the values of optical rotation recorded in the first and second thermal cycles or between those observed on cooling and on heating. At 65 wt % glycerol (Figure 6.3b), the cooling and heating values in the first temperature cycle are again virtually identical, but there is a systematic difference in optical rotation between the first and second cycles, which may reflect the influence of hydrophobic associations formed during the first heating step on the extent of conformational ordering (formation of 3-fold helices) on subsequent cooling. The difference, however, is only slightly beyond experimental error (~10 mdeg, in comparison with fluctuations of ± 2 mdeg in the individual values of optical rotation at each temperature), and should therefore be interpreted with caution.

Similar experiments were carried out with fructose as cosolute, but any changes in optical rotation arising from conformational ordering/disordering of pectin were swamped by the temperature-dependent changes in the optical rotation of fructose at the high concentrations required to promote gelation of high methoxy pectin. Earlier studies with ethan-1,2-diol as cosolute (Jones, 1992) gave similar results to those obtained (Figure 6.3) using glycerol, and were not therefore repeated in the present investigation.

At temperatures above the range corresponding to formation and melting of 3-fold helices, the optical rotation plots in Figure 6.3 are featureless and essentially linear, with no

indication of conformational changes during hydrophobic association. As reported in the preceding paper (Tsoga et al., 2001), however, both processes are accompanied by large thermal transitions in DSC, which are discussed further in the following Section.

6.4.3. Differential scanning calorimetry (DSC)

Figure 6.4 shows DSC traces for 1.0 wt % high methoxy pectin on heating (Figure 6.4a) and cooling (Figure 6.4b) at 0.5°C/min in the presence of ethan-1,2-diol at concentrations of 50, 55 and 60 wt %. As found previously (Tsoga et al., 2001), there were no significant differences between the values obtained in the first and second cycles of heating and cooling, and the curves shown are averages from both cycles. The corresponding averaged curves for 1.0 wt % high methoxy pectin in the presence of glycerol at concentrations of 50, 55 and 65 wt % are presented in Figure 6.5. In all cases, two thermal processes can be seen, one over the temperature range of formation and melting of 3-fold helices, and the second at the higher temperatures anticipated for hydrophobic association.

Since the transitions are broad, it is difficult to determine their mid-point temperatures by simple inspection of the DSC traces. Instead, the curves were fitted to two Gaussian bands by the procedure described in the preceding paper (Tsoga et al., 2001) and the temperature (T_o) at the maximum of each band was taken as the mid-point temperature (T_m) of the corresponding transition. The standard of fit obtained is illustrated in Figure 6.6 for 1.0 wt % high methoxy pectin in the presence of 65 wt % glycerol.

The T_m values obtained from the cooling scans (Figures 6.4b and 6.5b) for the transition at low temperature (attributed to formation of 3-fold helices) are shown in Figure 6.7, where they are compared with the temperature (T_1) at which G' (1 rad s^{-1}; 0.5 % strain) for the same samples reached a value of 1 Pa s during initial cooling. For both cosolutes, there is a progressive increase in T_m as the cosolute concentration is increased, with a similar slope for both, but the temperatures are ~3°C higher for ethan-1,2-diol than for glycerol. The

values of T_1, characterising the temperature at the onset of gelation, are systematically higher than the corresponding values of T_m, and the divergence increases as the concentration of cosolute is raised. This demonstrates that the helix fraction required for formation of a continuous network is less than 50 % (the value at T_m) even for the lowest cosolute concentration studied (50 wt %), and decreases further at higher concentrations. The values of T_1, like those of T_m, are higher with ethan-1,2-diol as cosolute than with glycerol, showing consistency between the findings from oscillatory rheology and DSC.

In contrast to the results presented in Figure 6.7 for the lower-temperature transition, the T_m values obtained from the curve-fitting procedure for the transition at higher temperature showed no significant or systematic variation with concentration of cosolute. As would be expected from the effect of "thermal lag", discussed in the preceding paper (Tsoga et al., 2001), the values of T_m obtained from the heating traces (Figures 6.4a and 6.5a) were slightly higher than the corresponding values (Figure 6.7) from the cooling curves (Figures 6.4b and 6.5b), but the variation with cosolute concentration was closely similar.

Figure 6.8 shows the DSC cooling curves obtained, at a scan rate of 0.5°C/min, for 1.0 wt % high methoxy pectin in the presence of fructose at concentrations of 50, 55, 60 and 65 wt %. For direct comparison, the trace recorded with 55 wt % fructose as cosolute is reproduced in Figure 6.9, together with those obtained using the same concentration of ethan-1,2-diol (Figure 6.4b) or glycerol (Figure 6.5b). The low-temperature transition, corresponding to formation of 3-fold helices, occurs at lower temperature with fructose than with the liquid cosolutes, and the other transition is displaced to higher temperature. Indeed, this transition, with fructose as cosolute, appears to extend above the temperature-range of the measurements (i.e. to above 95°C), with the peak being distorted in shape by the "start-up kick" of the calorimeter at the beginning of the cooling process. This effect becomes more pronounced (Figure 6.8) as the concentration of fructose is increased.

The major difference between fructose and the other cosolutes studied, both in this investigation and in the work reported in the preceding paper (Tsoga et al., 2001), however,

is in the DSC scans recorded on heating. Figure 6.10 shows the heating curves obtained, at a scan rate of 0.5°C/min, for 1.0 wt % high methoxy pectin in the presence of fructose at concentrations of 50, 55, 60 and 65 wt %. Instead of the comparatively broad endotherm seen for the other cosolutes over the temperature range of initial gelation on cooling (Figures 6.1 and 6.2) and the associated sigmoidal change in optical rotation (Figure 6.3), the samples incorporating fructose show a sharper and much more intense endotherm, immediately followed by a sharp exotherm.

To illustrate the intensity of this endotherm–exotherm doublet, Figure 6.11 shows the heating trace for 1.0 wt % pectin with 60 wt % fructose, in direct comparison with the cooling trace (Figure 6.8) for the same sample. The endotherm and exotherm in the heating trace are both about an order of magnitude larger than the single exotherm observed over the same temperature range on cooling. Figure 6.11 also demonstrates that the transition at higher temperature, attributed to hydrophobic interactions, is centred at roughly the same temperature, and has approximately the same intensity, on heating and on cooling.

The endotherm at the start of the heating curves (Figure 6.10), although much larger than expected from the results obtained with other cosolutes, is consistent with a normal melting process, where heat is absorbed in dissociation of intermolecular and/or intramolecular bonds. An exothermic process during heating, however, is unusual, and suggests that melting of an existing structure (as an endothermic process) allows a new structure to be formed, with consequent release of heat (as occurs normally during structure formation on cooling). Resolution of the endothermic and exothermic events as detectable separate transitions implies that the restructuring process must be slow, occurring on a timescale comparable to the rate of temperature-change in the DSC experiment, otherwise the heat released by formation of new bonds would simply reduce the apparent intensity of the endothermic process by offsetting the heat absorbed in breaking existing bonds.

This interpretation was tested by exploring the effect of scan rate on the DSC traces obtained for 1.0 wt % pectin in the presence of a fixed concentration of fructose (55 wt %). The scan rates used were 0.3, 0.5, 0.8 and 1.0°C/min. The results are shown in Figure 12.

In the cooling direction (Figure 6.12b), the higher-temperature exotherm becomes progressively more obscured and distorted by the start-up kick of the calorimeter as the rate of cooling is increased. At the lowest scan rate used (0.3°C/min), however, the peak is symmetrical and well-defined, confirming that the thermal process occurring for mixtures of pectin with fructose is qualitatively similar to those observed (Tsoga et al., 2001) with other cosolutes However, as indicated in Figure 6.9, it is smaller than the corresponding process with the liquid cosolutes (ethan-1,2-diol and glycerol) and occurs at higher temperature. The lower-temperature exotherm in Figure 6.12b is less affected by scan rate, showing only a slight decrease in temperature (T_{max}) at the peak maximum as the rate of cooling is increased.

The effect of scan rate is much more pronounced in the DSC traces recorded on heating (Figure 6.12a). As the rate of heating is increased (from 0.3 to 1.0°C/min), the exotherm becomes progressively more evident, and the subsequent endotherm is displaced to progressively higher temperature. At the highest scan rate used (1.0°C/min) it is virtually undetectable, suggesting that much of the transition would occur at temperatures above the upper limit of the present experiments (95°C). The initial endotherm, immediately after the start-up kick on commencement of heating, and the subsequent exotherm, also shift to progressively higher temperatures as the scan rate is increased.

The magnitude of these shifts is quantified in Figure 6.13a, which shows the scan-rate dependence of T_{max}, the temperature at the maximum values of exothermic or endothermic heat flow, for the initial endotherm and subsequent exotherm on heating (Figure 6.12a) and for the associated (lower-temperature) exotherm on cooling (Figure 6.12b). The T_{max} values for the two processes observed on heating both show a steep, linear decrease with decreasing scan rate. The slope is slightly lower for the initial endotherm than for the

subsequent exotherm, so that the separation between the two processes increases with increasing scan rate. For the exothermic transition on cooling, the values of T_{max} again vary linearly with scan rate, but increasing rather than decreasing as the scan rate is reduced.

To illustrate the magnitude of the rate-dependent changes in Figure 6.13a, Figure 6.13b shows corresponding plots from a previous investigation, using the same calorimeter, of deacylated gellan ("gellan gum") in the tetramethylammonium (Me_4N^+) salt form at a polymer concentration of 1.0 wt % in water and in 0.25 M Me_4NCl (Robinson, Manning & Morris, 1991). Me_4N^+ gellan was chosen to provide a typical example of the DSC behaviour of a system that undergoes a simple, thermally-reversible conformational transition (coil–double helix), with no complications from any other processes.

The T_{max} values for the exothermic transition accompanying double-helix formation on cooling (Robinson et al., 1991) increase linearly with decreasing scan rate (Figure 6.13b). The corresponding values for the endotherm arising from melting of double helices on heating decrease linearly with decreasing scan rate. As discussed in the preceding paper (Tsoga et al., 2001), these changes in apparent transition temperatures arise from finite rates of heat transfer between the inner surface of the DSC pan and the interior of the sample ("thermal lag"). The plots of T_{max} versus scan rate for Me_4N^+ gellan on heating or cooling in water (Figure 6.13b) extrapolate to a common intercept at zero scan rate, which defines the true mid-point temperature of the reversible coil–helix transition. The corresponding plots at higher salt concentration (0.25 M Me_4NCl) are displaced to higher temperatures, but their slopes are virtually identical to those observed for gellan in water, demonstrating that the effects of thermal lag remain the same over different ranges of temperature. The slope is greater on cooling than on heating, indicating that transfer of heat out of the sample on cooling occurs more slowly than transfer into the sample during heating.

The slope observed (Figure 6.13a) for high methoxy pectin (1.0 wt %; pH 3.0) on cooling in the presence of 55 wt % fructose is similar to the slope of the cooling plots shown in

Figure 6.13b for Me_4N^+ gellan, suggesting that it arises from simple thermal lag. The slopes for the initial endotherm and subsequent exotherm on heating, however, are much steeper than those of the heating plots in Figure 6.13b, which is consistent with slow thermal processes occurring at rates comparable to the rate of temperature increase in the DSC experiments. The T_{max} values for the endothermic and exothermic processes on heating extrapolate (Figure 6.13a) to intercepts of, respectively, 8.7°C and 23.2°C at zero scan rate. The corresponding intercept for the low-temperature exotherm observed on cooling falls almost exactly mid-way between these, at 16.1°C. This suggests that the cooling exotherm is a composite, arising from rapid reversal of the two processes (endothermic and exothermic) observed on heating.

To test this proposal, the initial endotherm and subsequent exotherm in the trace obtained for 1.0 wt % pectin with 55 wt % pectin on heating at 0.5°C/min (the scan rate used in most of the DSC studies reported above) were fitted to two Gaussian bands by the procedure described in the preceding paper (Tsoga et al., 2001). To avoid further increase in the already large number of adjustable parameters, no attempt was made to fit the second endotherm at higher temperature. The same procedure was used to fit the two exotherms observed on cooling of the same sample.

As shown in Figure 6.14, a good fit to both curves was obtained. The Gaussian bands fitted to the heating trace (Figure 6.14a) are both broader than the apparent observed transitions, because of substantial overlap between them. The fitted baseline seems reasonable, running into the observed trace at around the onset of the high-temperature endotherm. The value of ΔH for the endothermic Gaussian band in the fitted spectrum is 85.6 J/g; ΔH for the exothermic band is -65.8 J/g, giving an overall value of ΔH = 19.8 J/g for the two transitions. The corresponding value of ΔH for the Gaussian band fitted to the lower-temperature exotherm in the cooling trace (Figure 6.14b) is -19.7 J/g. In view of the number of parameters used to generate each fit (eight), this standard of agreement must be regarded as fortuitous. It does, however, seem reasonable to conclude that the results are at least

consistent with the proposal that the exotherm observed on cooling results from reversal of the separate endothermic and exothermic processes seen on heating.

6.5. DISCUSSION AND CONCLUSIONS

On the basis of the evidence presented in the preceding paper (Tsoga et al., 2001) it was suggested that hydrophobic association on heating of high-methoxy pectin gels formed with ethan-1,2-diol or glycerol as cosolute is a "cyclisation" process, occurring between methyl ester substituents on the same chain, or within small clusters of chains which were still linked together by residual 3-fold helix structure when the onset temperature for hydrophobic association was reached. The progressive development of detectable network structure at high temperature during the additional thermal cycles performed in the present work (Figure 6.1) indicates some limited crosslinking from hydrophobic interactions between individual clusters, but the central picture of small, isolated bundles of chains shielded from contacts with other clusters by a surrounding condensed layer of cosolute molecules remains unchanged.

It seems reasonable to expect that the opportunities for hydrophobic contacts within such clusters would be greater than in an extended network. This may explain the observation (Tsoga et al., 2001) that the high-temperature DSC transition for pectin in the presence of ethan-1,2-diol or glycerol is larger than with the solid cosolutes studied, which, because of their stronger tendency to self-association (shown by their higher melting points), are suggested to form fewer associative contacts with the polymer, and therefore cause less inhibition of crosslinking. The optical rotation results presented in Figure 6.3 show no indication of conformational change over the temperature range of hydrophobic association, suggesting that the hydrophobic junctions are amorphous.

Although giving similar setting temperatures and moduli on initial cooling (Tsoga et al., 2001), fructose differs from the liquid cosolutes (ethan-1,2-diol and glycerol) in its effect

on pectin gelation in the following ways: increase in moduli during heating (Figure 6.2); smaller DSC transition over the temperature-range of hydrophobic association (Figure 6.9); displacement of this transition to higher temperature (Figure 6.9); intense endothermic and exothermic transitions on heating over the temperature range for melting of 3-fold helices, rather than the single, much smaller, endotherm seen with other cosolutes. The last of these is the most important, and offers an explanation of the other differences.

As discussed in Section 6.4.3, an exothermic process on heating, immediately after an endothermic process, indicates melting of one structure and its replacement by another. Resolution of the endotherm and exotherm as separate observable transitions indicates that the underlying structural changes are slow. This conclusion is reinforced by the pronounced scan-rate dependence shown in Figure 6.13a. Since no such effects are observed for the other cosolutes studied (Tsoga et al., 2001), we suggest that fructose is capable of binding specifically to high-methoxy pectin, both in its disordered conformation and in the 3-fold helical form. The initial endotherm on heating would then correspond to melting of 3-fold helices complexed with fructose, with the intensity of the transition reflecting the heat required to dissociate pectin–fructose bonds, in addition to that required for dissociation of the helix structure itself. The subsequent exotherm can be attributed to the heat released on binding of fructose to the disordered pectin chains liberated by dissociation of the initial complex.

The curve-fitting analysis shown in Figure 6.14a indicates that the net change in enthalpy is around 20 J/g. Similar analysis of both heating and cooling traces for pectin in the presence of xylitol or other solid cosolutes (Tsoga et al., 2001) gave ΔH values of around 24 J/g for formation and melting of 3-fold helices. The similarity of these values suggests that the heat required to displace fructose from the surface of the helices is essentially the same as the heat released on re-binding to the disordered chains, with the overall change in enthalpy coming predominantly from helix melting.

Although the calorimetric studies reported here do not, of course, give any indication of the nature of the pectin–fructose complex, an attractive possibility is suggested by inspection of physical models. Comparison of space-filling (CPK) models for the poly-D-galacturonate regions of pectin and for fructose in its more stable (β-D-furanosyl) ring form shows that the distance between the primary hydroxyl groups at C(1) and C(6) of fructose matches closely the separation between the C(6) carboxyl groups on alternate galacturonate residues of pectin. Unstrained hydrogen bonds can be readily inserted between these hydroxyl and carboxyl groups, and a third hydrogen bond then falls naturally into place between the (secondary) hydroxyl group at C(3) of the intervening galacturonate residue and the ring oxygen of fructose. A photograph of a molecular model incorporating these three hydrogen bonds in shown in Figure 6.15.

If the first site-bound fructose molecule is denoted as spanning residues 1 to 3 of the polygalacturonate chain, further molecules of fructose can be attached across residues 2 to 4, 5 to 7, 6 to 8, and so on, with no mutual interference between them. Methyl ester substituents on any, or all, of the pectin carboxyl groups present no steric barrier to binding. The molecular model shown in Figure 6.15 was constructed with the polygalacturonate chain in the 2-fold conformation that is believed to be adopted preferentially by pectin at neutral pH (Ravanat & Rinaudo, 1980; Cesàro, Ciana, Delben, Manzini & Paoletti, 1982) and under acidic conditions at high temperature (Gilsenan, Richardson & Morris, 2000). Similar binding, however, is also possible with the chain in the ordered, 3-fold conformation that is adopted on acidification at ambient temperature (Ravanat & Rinaudo, 1982; Cesàro et al., 1982) or on cooling at acidic pH (Gilsenan et al., 2000).

Physical (or computer) model building cannot, of course, prove that the structures generated exist in reality. Nonetheless, specific site-binding of fructose to pectin by a bonding scheme along the general lines proposed above seems consistent with the experimental findings.

As discussed previously, the increase in apparent intensity of the exothermic process observed on heating (Figure 6.12a), and its progressive separation from the initial endotherm (Figure 6.13a) as the heating rate is increased, indicates that re-attachment of fructose to the disordered pectin chains released by melting of 3-fold helices (also complexed with fructose) is a slow process. This can be explained by constant fluctuation of chain conformation, with attachment of fructose occurring only when the participating sequence of the pectin chain has the correct geometry to provide the required binding site. The corresponding process in the cooling direction is attachment of fructose to conformationally-rigid 3-fold helices, which would be expected to occur much more rapidly. Thus displacement of fructose from disordered chains would be accompanied by rapid re-attachment to helices, with the changes in enthalpy from displacement, helix formation, and re-attachment appearing together as a single thermal process, as observed (Figure 6.12b).

The central requirement for gelation on cooling, however, is not simply the formation of ordered helices, but their association to give a crosslinked network. Inhibition of helix–helix association by helix–cosolute interactions would be expected to be much greater for site-binding than for non-specific condensation of cosolute molecules around the helices, which would explain why the gels formed by pectin in the presence of fructose are much weaker than those obtained with the other solid cosolutes studied (Tsoga et al., 2001). If, however, the sequence of events on cooling proposed above is correct, then helix formation, helix–helix association and helix–fructose association would be occurring together, allowing helices formed in close proximity to one another to associate before becoming coated with site-bound fructose, thus giving some network structure, albeit weak.

Site-binding of fructose would be expected to cause similar inhibition of hydrophobic association of pectin chains on heating; this would explain why the accompanying thermal transition is smaller and centred at higher temperature with fructose as cosolute than with ethan-1,2-diol or glycerol (Figure 6.9) or with the other solid cosolutes studied by Tsoga et

al. (2001). It is evident from the increases in moduli observed during heating of high-methoxy pectin gels prepared with fructose as cosolute, however, that same limited intermolecular hydrophobic association does occur. This suggests that the complex formed between fructose and disordered pectin is comparatively labile, and presumably becomes more so as the temperature is increased, thus allowing hydrophobic bonds to be formed between short sequences of pectin that are transiently devoid of fructose. Once formed, short hydrophobic contacts of this type might act as nuclei for longer junctions when other neighbouring galacturonate residues also lose their attached fructose.

The central distinction from the interpretation proposed at the beginning of this Section for ethan-1,2-diol and glycerol is that fructose, rather than allowing extensive hydrophobic association to occur within localised clusters while inhibiting association between clusters by condensing around them, appears to limit the overall extent of hydrophobic association by coating the surface of individual chains (or of aggregated 3-fold helices), but does not introduce any preferential drive to localised association (cyclisation) at the expense of network crosslinking..

As described in Section 6.2, the experiments reported here and in the preceding paper (Tsoga et al., 2001) were designed to test the proposal that the strong inhibitory effect of fructose on gelation of high-methoxy pectin is due to the presence within the fructose molecule of two primary hydroxyl groups each capable of forming comparatively strong, but transient, hydrogen bonds with carboxyl groups of pectin and thus promoting condensation of cosolute around the polymer chains. The absence of any comparable inhibitory effect with sorbitol or xylitol as cosolute (Tsoga et al., 2001) demonstrates that the content of primary hydroxyl groups is not, in itself, an important determinant of the strength of pectin–cosolute interactions. However, if the model illustrated in Figure 6.15 is broadly correct, then the two primary hydroxyl groups in fructose do have a key role in inhibition of gelation, by participating in site-binding of fructose molecules to the pectin chains, rather than by promoting non-specific condensation.

Sorbitol and xylitol also have two primary hydroxyl groups per molecule, but at either end of a flexible chain rather than attached to a sugar ring. The likely reason why they do not appear to form a complex with pectin is that the enthalpic advantage of site-binding is not sufficient to compensate for the large reduction in entropy that would arise from loss of conformational mobility. Since fructose has a comparatively rigid ring structure, the reduction in entropy on binding will be much smaller, allowing site binding to occur. For the smaller polyols (ethan-1,2-diol and glycerol) the distance between the primary hydroxyl groups is insufficient to allow them both to bond simultaneously to carboxyl groups of pectin.

In summary, we conclude, largely on the basis of the massive, rate-dependent endothermic and exothermic transitions observed on heating (Figure 6.12a), that fructose forms a specific complex with pectin, analogous to the pectin–methanol complex proposed by Plaschina et al. (1986), and that this diminishes, but does not abolish the pectin–pectin associations required for gel formation.

REFERENCES

Cesàro, A., Ciana, A., Delben, F., Manzini, G. & Paoletti, S. (1982). Physicochemical properties of pectic acid. I. Thermodynamic evidence of a pH-induced conformational transition in aqueous solution. *Biopolymers*, **21,** 431-449.

Evageliou, V., Richardson, R. K. & Morris, E. R. (2000a). Effect of oxidised starch on high methoxy pectin–sucrose gels formed by rapid quenching. *Carbohydrate Polymers*, **42**, 219-232.

Evageliou, V., Richardson, R. K. & Morris, E. R. (2000b). Co-gelation of high methoxy pectin with oxidised starch or potato maltodextrin. *Carbohydrate Polymers*, **42**, 233-243.

Evageliou, V., Richardson, R. K. & Morris, E. R. (2000c). Effect of pH, sugar type and thermal annealing on high-methoxy pectin gels. *Carbohydrate Polymers*, **42**, 245-259.

Gilsenan, P. M., Richardson, R. K. & Morris, E. R. (2000). Thermally-reversible acid-induced gelation of low-methoxy pectin. *Carbohydrate Polymers*, **41**, 339-349.

Jones, A. K. (1992). Hydrophobicity in polysaccharide gelation. Ph. D Thesis. Cranfield University.

Nilsson, S., Piculell, L. & Malmsten, M. (1990). Nature of macromolecular denaturation by urea and other cosolutes: experiments on agarose interpreted within a lattice model for adsorption from a mixed solvent. *Journal of Physical Chemistry*, **94**, 5149-5154.

Plashchina, I.G., Semenova, M.G., Slovokhotov, Yu.L., Struchkov, Yu.T., Braudo, E.E., Tolstoguzov, V.B. & Ignatov, G.I. (1986). Studies of the interaction of methanol with pectin in aqueous solution. *Carbohydrate Polymers*, **6**, 1-13.

Ravanat, G. & Rinaudo, M. (1980). Investigation on oligo- and polygalacturonic acid by potentiometry and circular dichroism. *Biopolymers*, **19**, 2209-2222.

Robinson, G., Manning, C.E. & Morris, E.R. (1991). Conformation and physical properties of the bacterial polysaccharides gellan, welan and rhamsan. In E. Dickinson, *Food Polymers, Gels and Colloids,* RSC Special Publication No. 82. Royal Society of Chemistry: Cambridge, UK. pp. 22-33.

Tsoga, A., Richardson, R. K. & Morris, E. R. (2001). Role of cosolutes in gelation of high-methoxy pectin. Part 1. Comparison of sugars and polyols. *Food Hydrocolloids*, submitted (accompanying typescript).

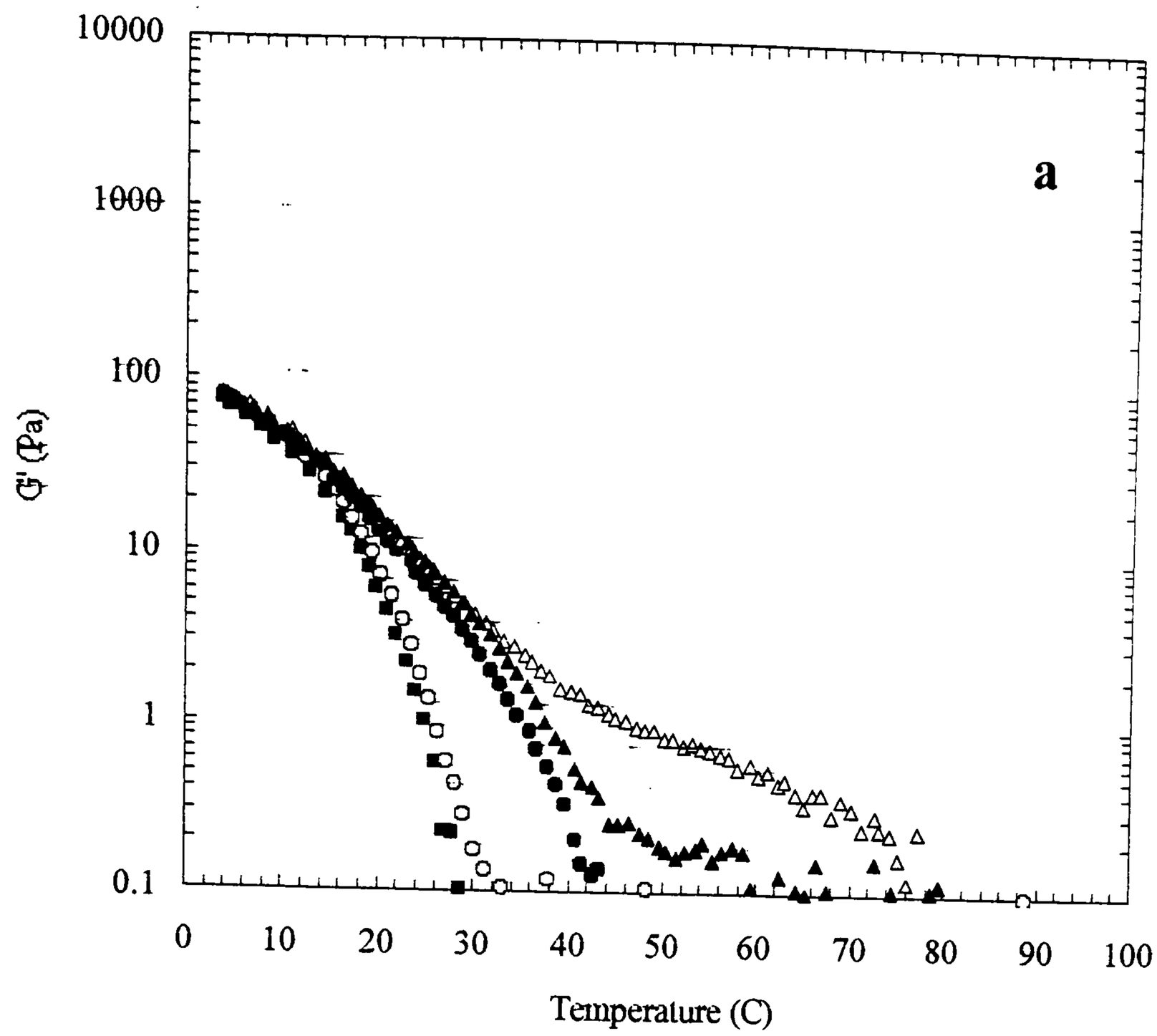

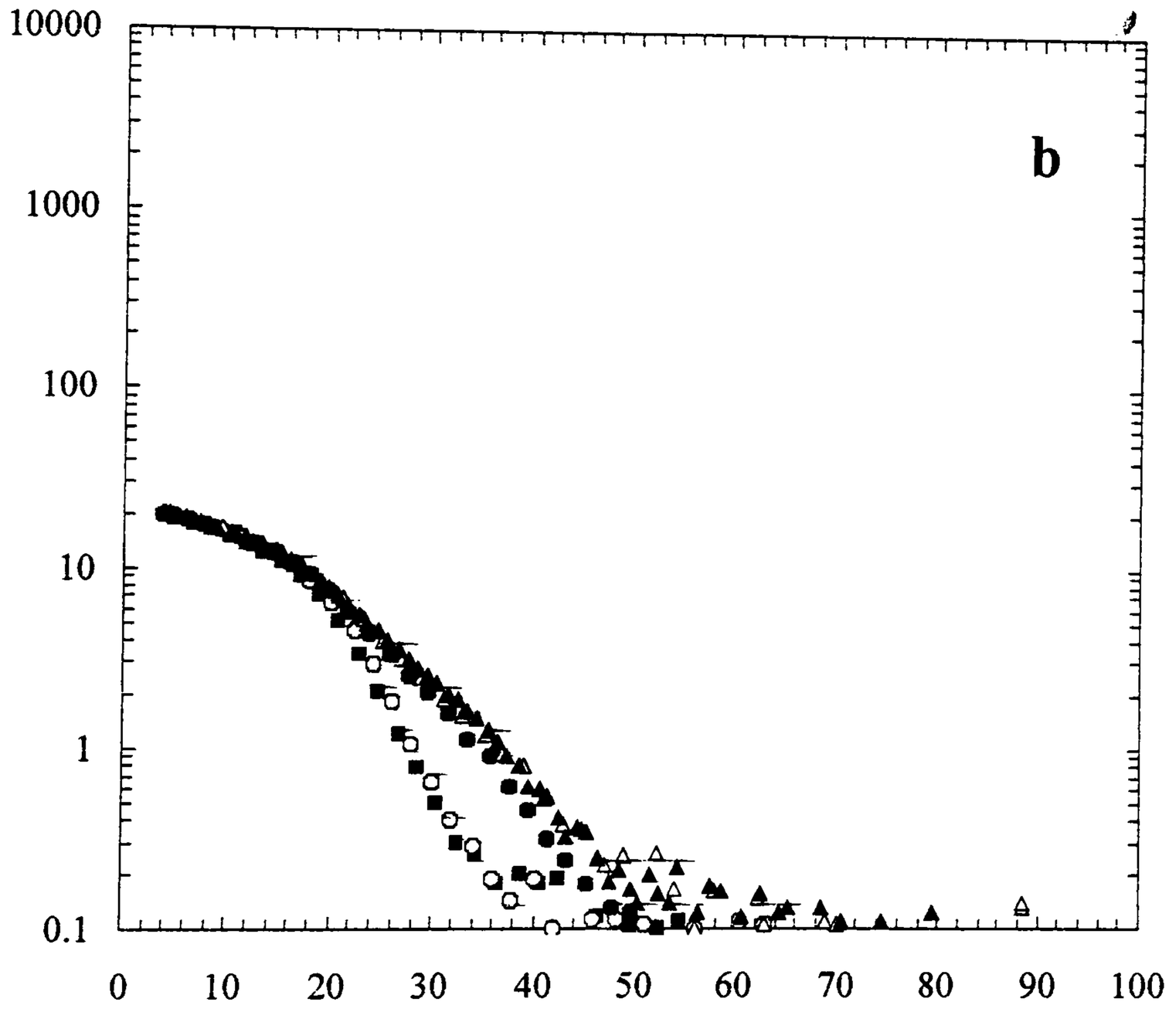

Figure 6.1. Changes in (a) G' and (b) G", measured at 1 rad s^{-1} and 0.5 % strain, for 1.0 wt % high methoxy pectin (DE 70; pH 3.0) in the presence of 55 wt % glycerol on initial cooling (■), and in the first (circles) and second (triangles) of two subsequent cycles of heating (open symbols) and cooling (filled symbols) between 5°C and 90°C at 1.0 °C/min.

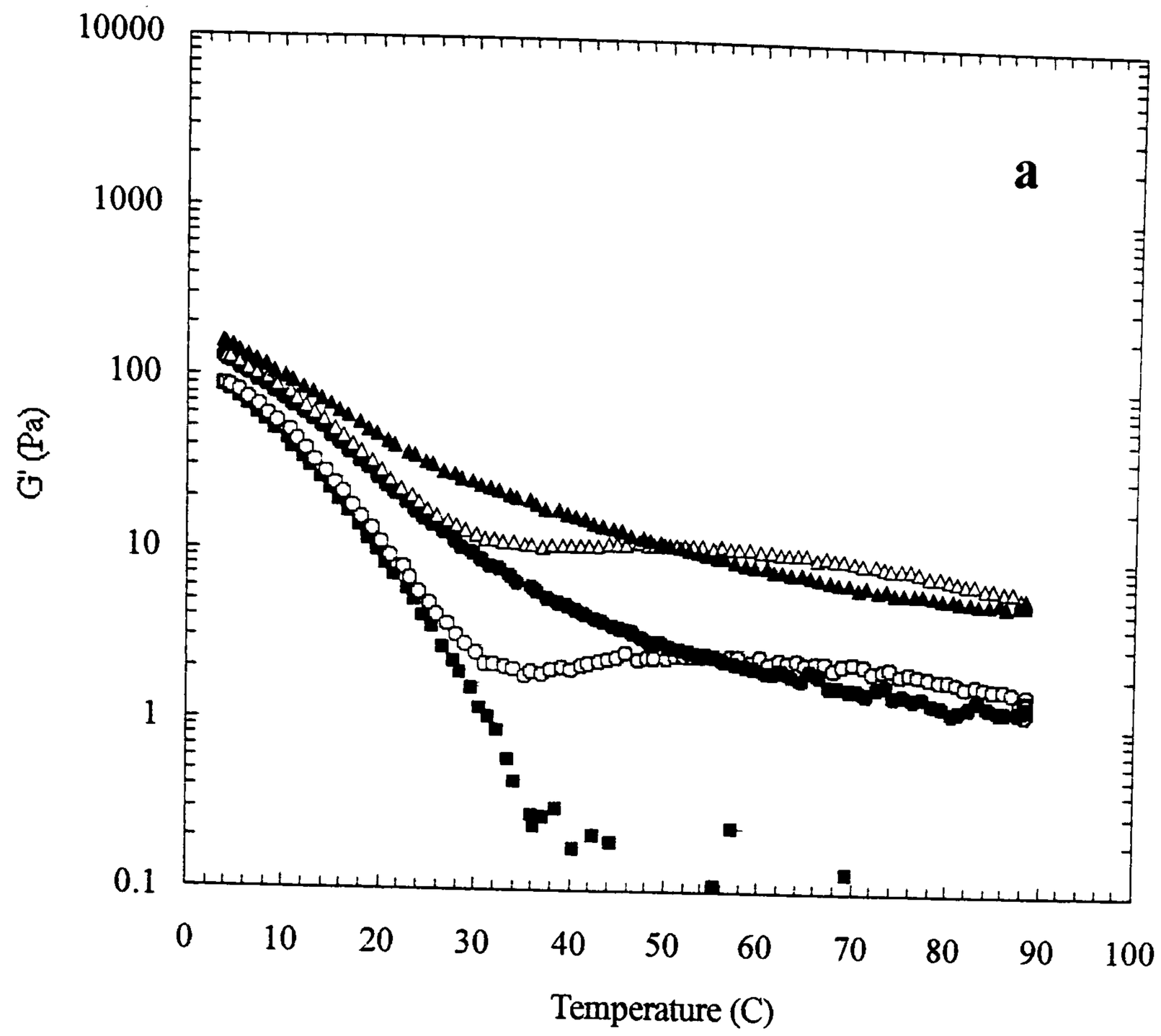

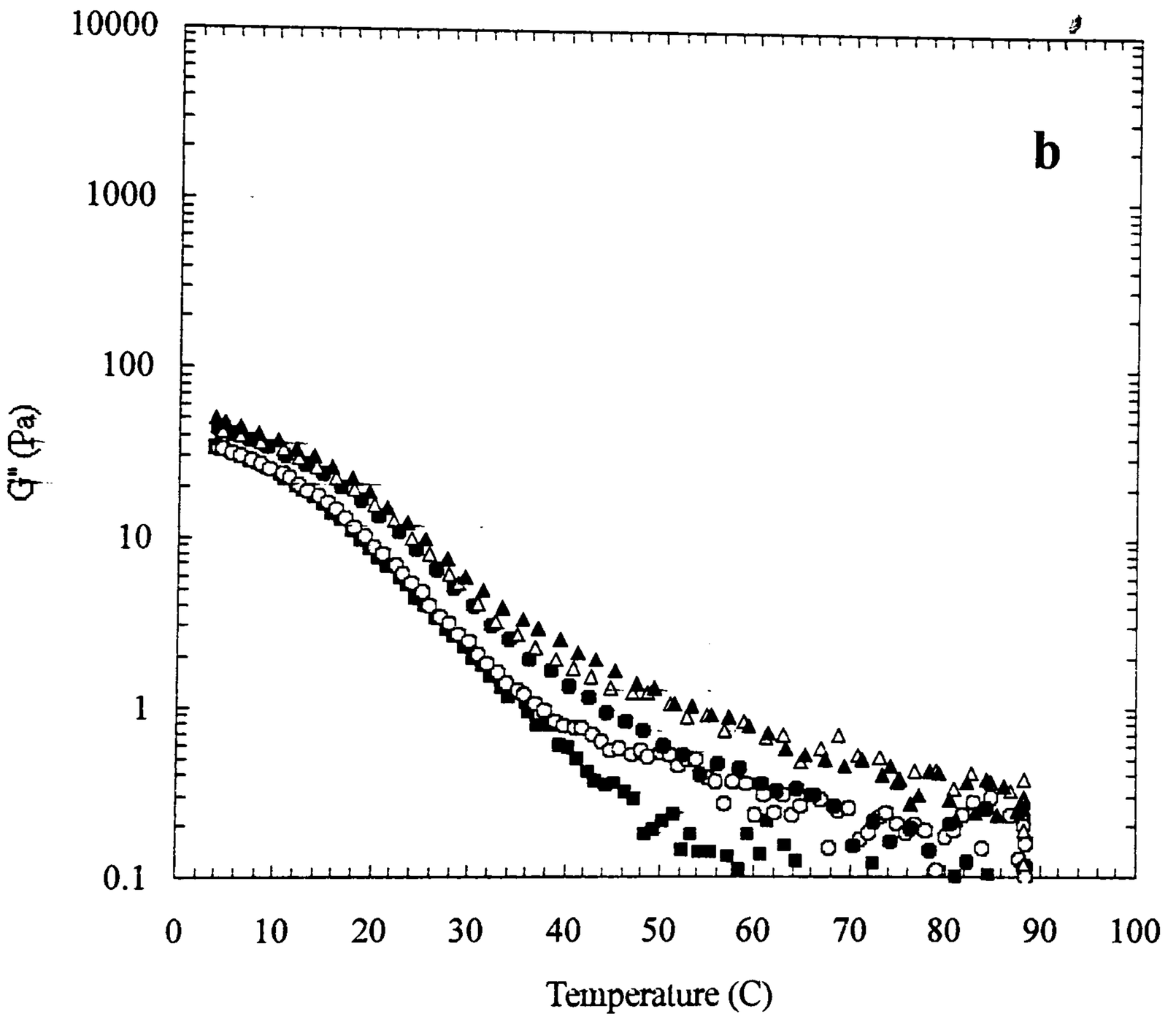

Figure 6.2. Changes in (a) G' and (b) G" , measured at 1 rad s^{-1} and 0.5 % strain, for 1.0 wt % high methoxy pectin (DE 70; pH 3.0) in the presence of 55 wt % fructose on initial cooling (■), and in the first (circles) and second (triangles) of two subsequent cycles of heating (open symbols) and cooling (filled symbols) between 5°C and 90°C at 1.0 °C/min.

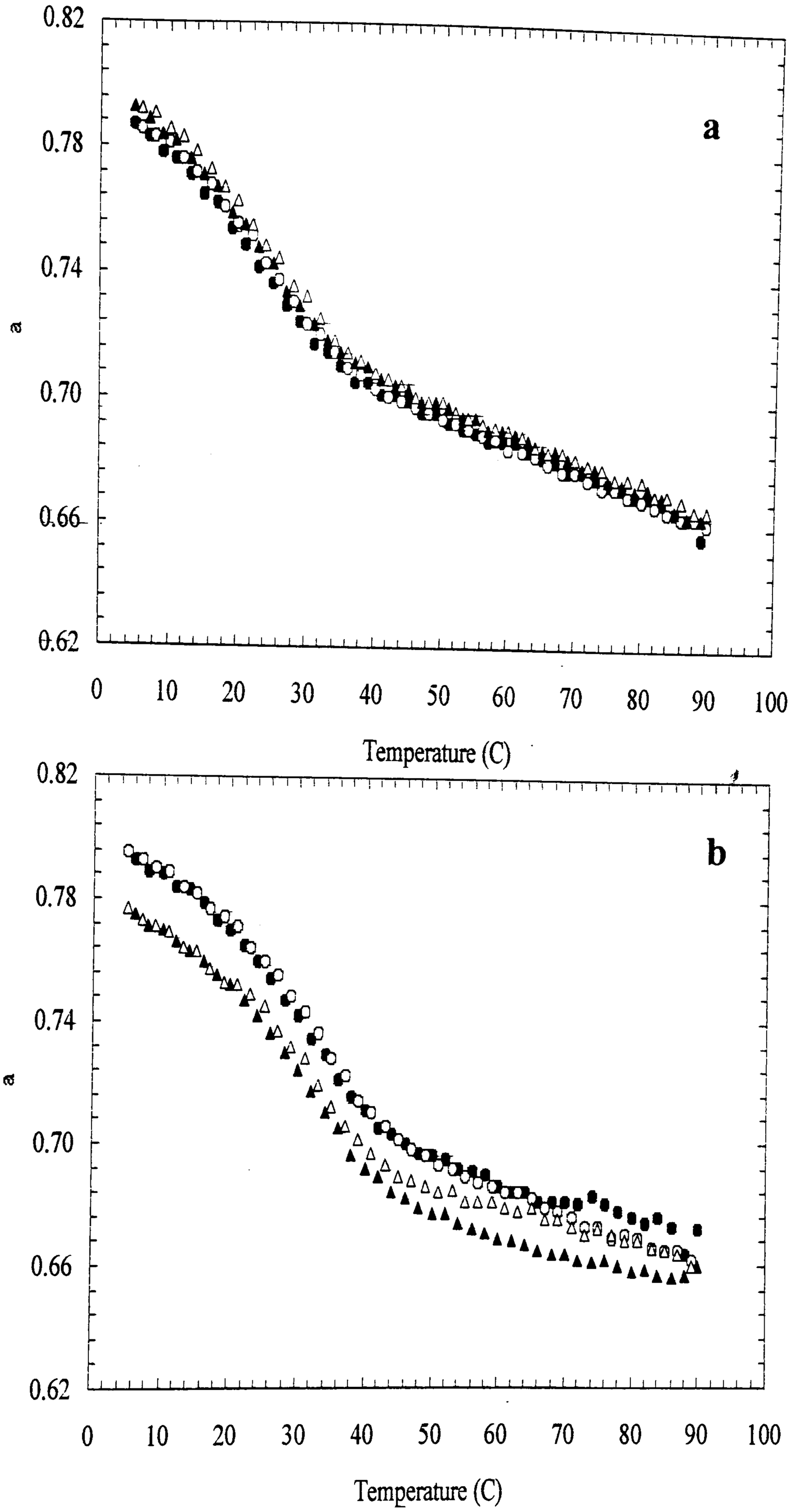

Figure 6.3. Changes in optical rotation (365 nm; 1 cm pathlength) for 1.0 wt % high methoxy pectin (DE 70; pH 3.0) in the presence of glycerol at concentrations of (a) 55 wt % and (b) 65 wt % in the first (circles) and second (triangles) of two subsequent cycles of cooling (filled symbols) and heating (open symbols) between 90°C and 5°C at ~ 1.0 °C/min.

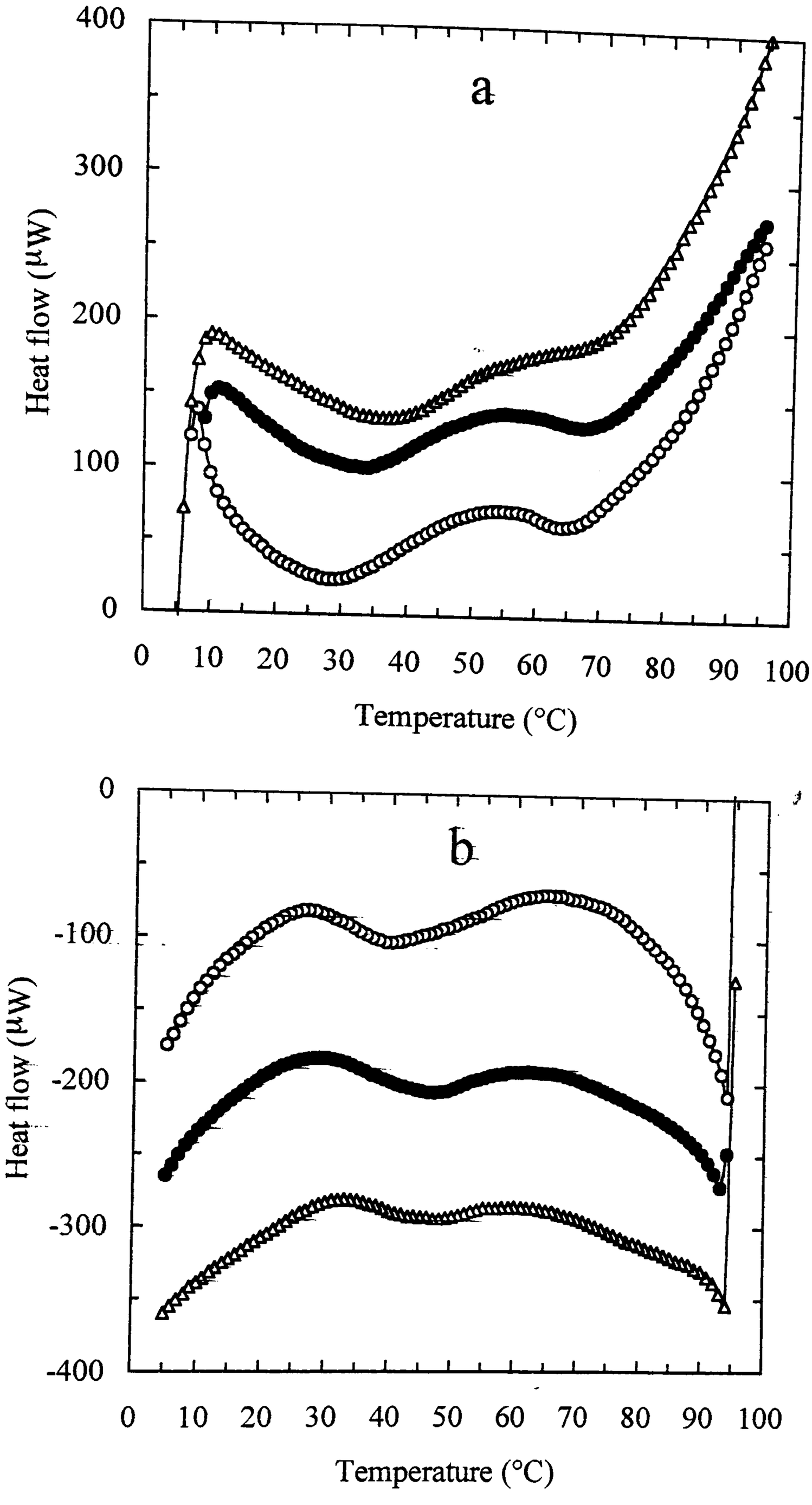

Figure 6.4. Averaged DSC curves from first and second cycles of (a) heating and (b) cooling at 0.5 °C/min for 1.0 wt % high methoxy pectin (DE 70; pH 3.0) in the presence of ethan-1,2-diol at concentrations of 50 wt % (O), 55 wt % (●) or 60 wt % (Δ). For clarity of presentation, the individual traces have been shifted vertically by arbitrary amounts.

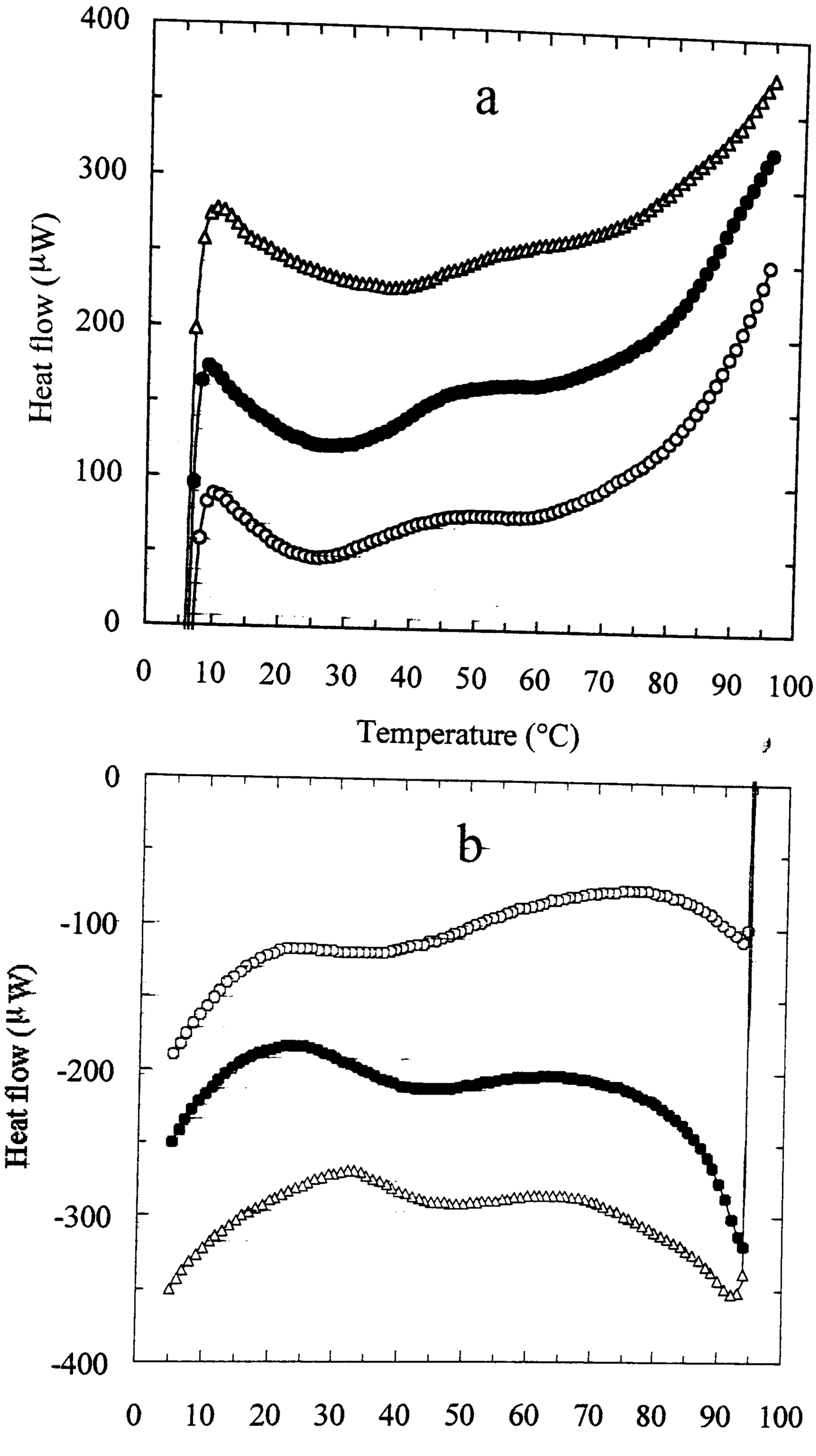

Figure 6.5. Averaged DSC curves from first and second cycles of (a) heating and (b) cooling at 0.5 °C/min for 1.0 wt % high methoxy pectin (DE 70; pH 3.0) in the presence of glycerol at concentrations of 50 wt % (O), 55 wt % (●) or 65 wt % (Δ). For clarity of presentation, the individual traces have been shifted vertically by arbitrary amounts.

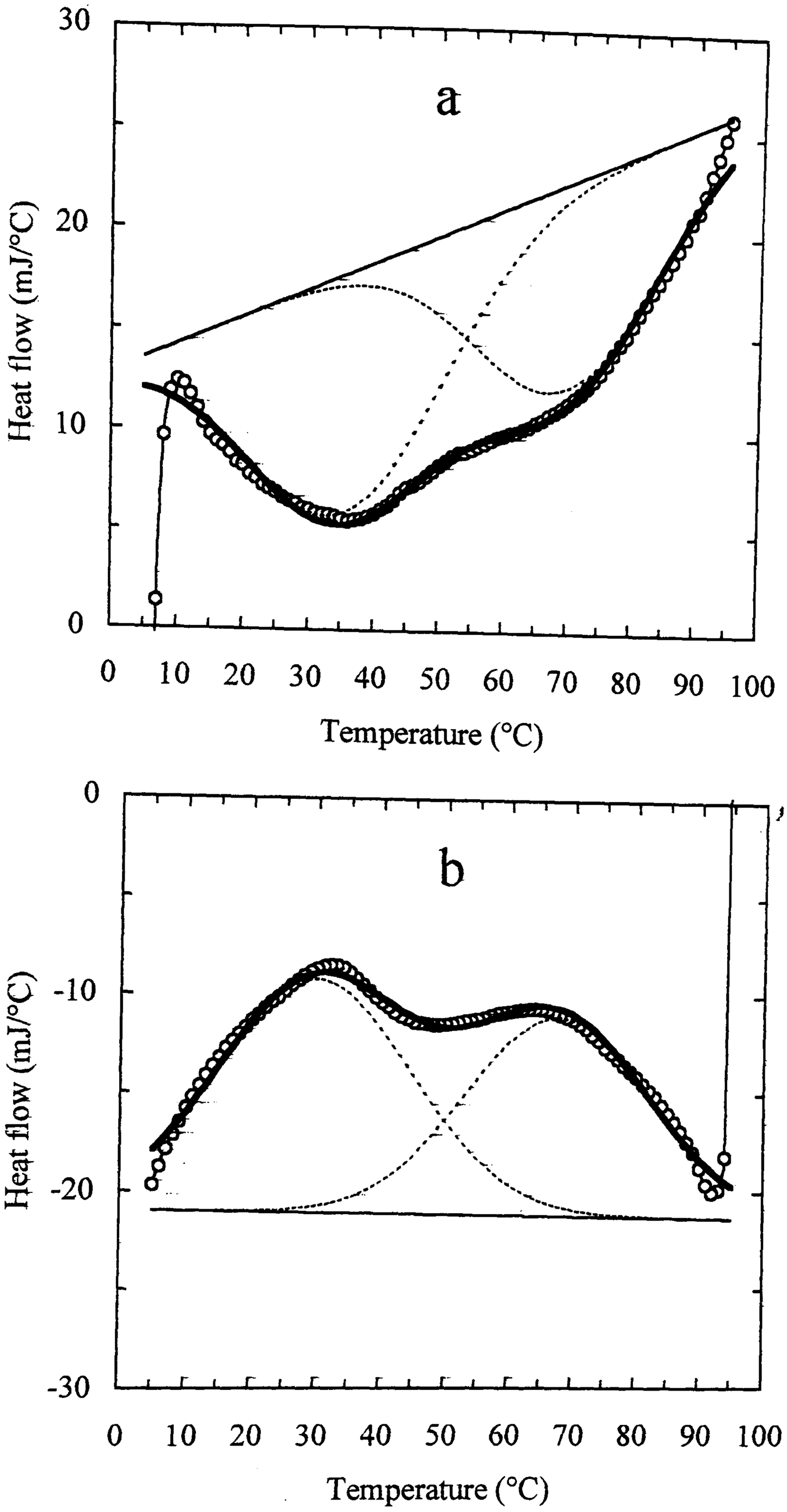

Figure 6.6. DSC traces (O) for 1.0 wt % high methoxy pectin (DE 70; pH 3.0) on (a) heating and (b) cooling in the presence of 65 wt % glycerol, fitted to two Gaussian bands (- - -) by the procedure described by Tsoga et al. (2001). The bold and fainter solid lines show, respectively, the total spectrum and baseline from the curve-fitting analysis.

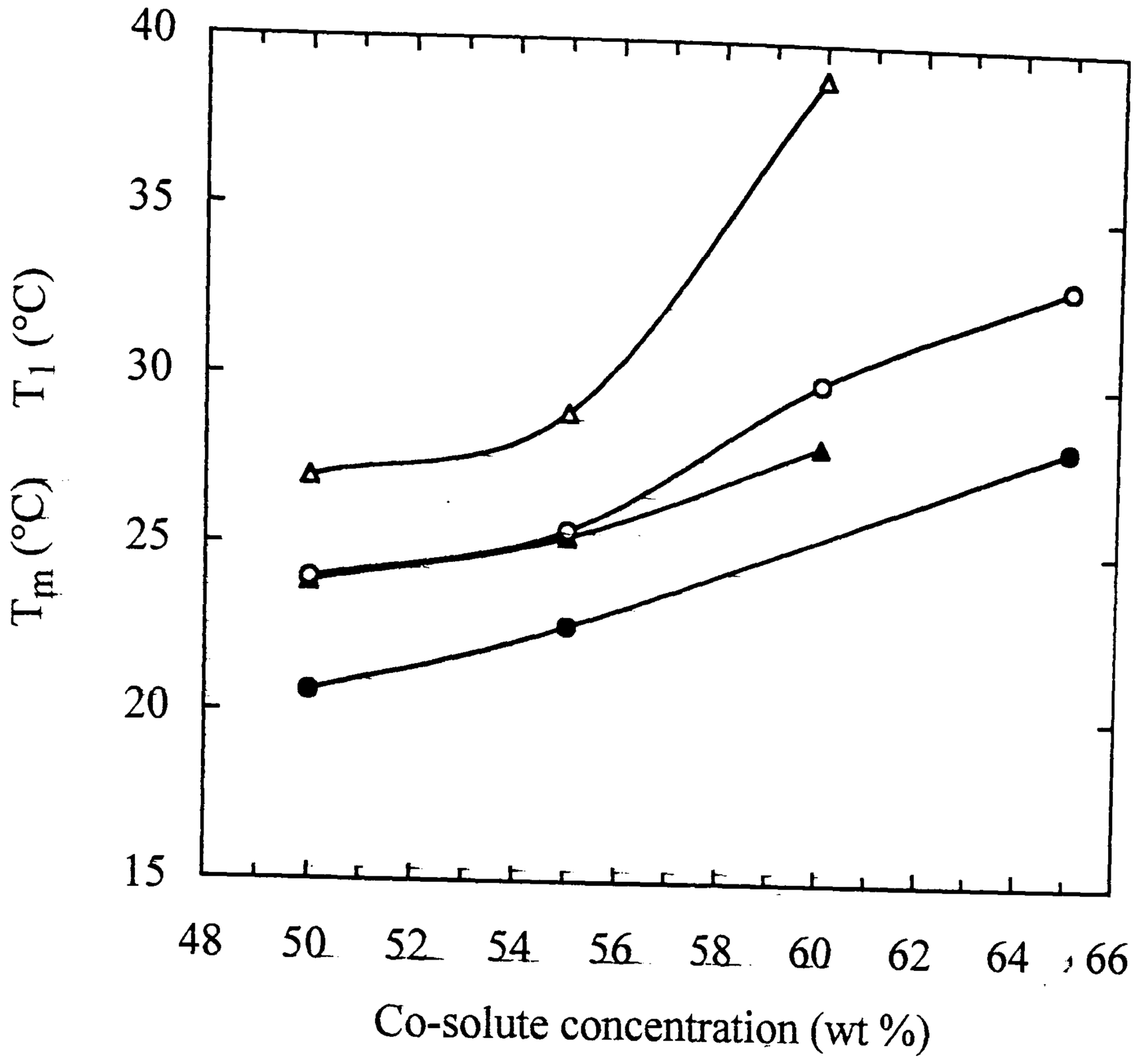

Figure 6.7. Effect of cosolute concentration on the temperature (T_1) at which G' (1 rad s^{-1}; 0.5 % strain) reached a value of 1.0 Pa s during initial cooling (open symbols), and on transition midpoint temperature (T_m) for helix formation (filled symbols), for mixtures of 1.0 wt % high methoxy pectin (DE 70; pH 3.0) with ethan-1,2-diol (triangles) or glycerol (circles).

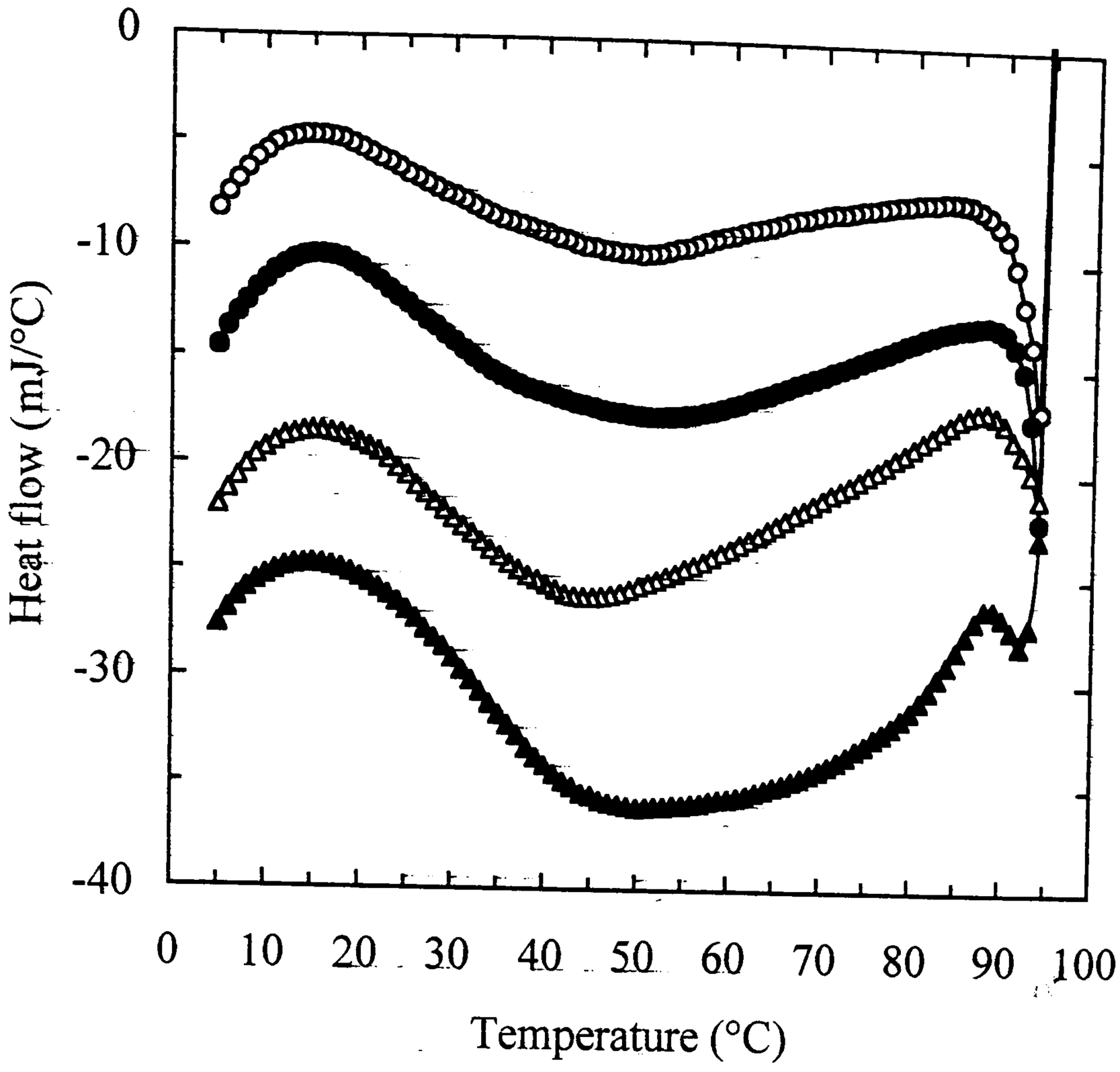

Figure 6.8. DSC traces recorded during cooling at a scan rate of 0.5 °C/min for 1.0 wt % high methoxy pectin (DE 70; pH 3.0) in the presence of fructose at concentrations of 50 wt % (O), 55 wt % (●), 60 wt % (Δ) and 65 wt % (▲).

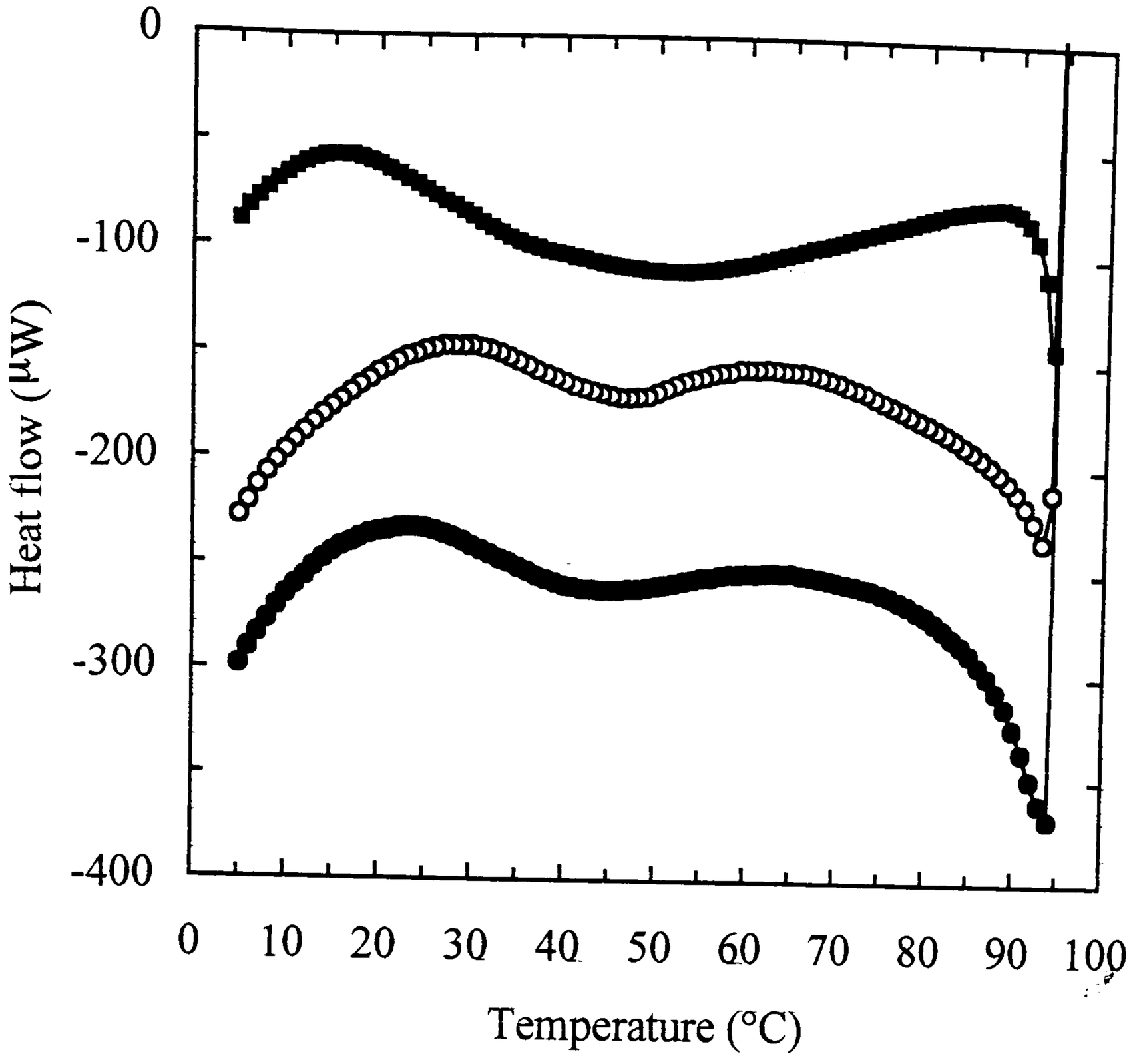

Figure 6.9. DSC traces recorded during cooling at a scan rate of 0.5 °C/min for 1.0 wt % high methoxy pectin (DE 70; pH 3.0) in the presence of 55 wt % fructose (■), glycerol (●), or ethan-1,2-diol (O).

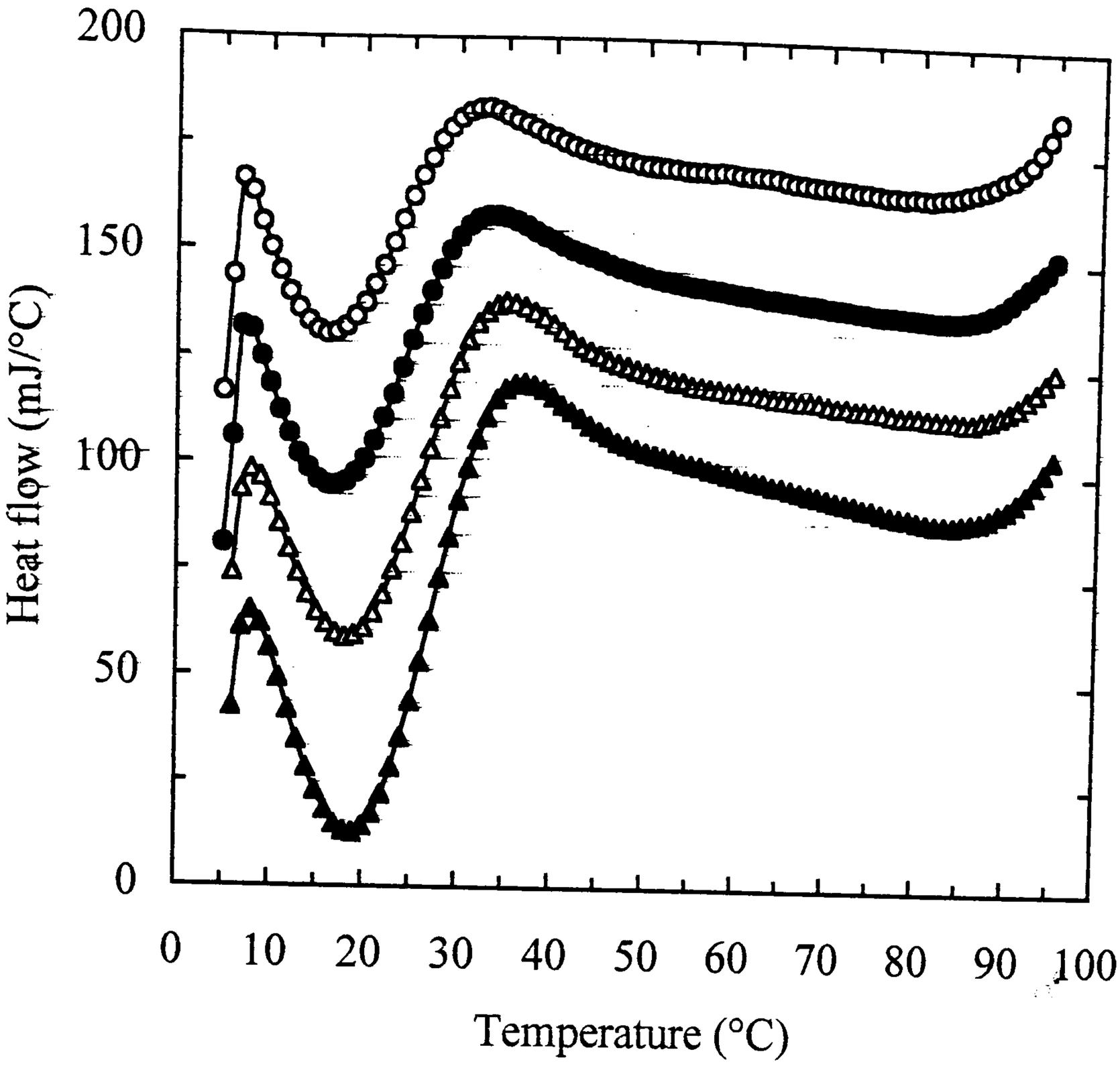

Figure 6.10. DSC traces recorded during heating at a scan rate of 0.5 °C/min for 1.0 wt % high methoxy pectin (DE 70; pH 3.0) in the presence of fructose at concentrations of 50 wt % (O), 55 wt % (●), 60 wt % (Δ) and 65 wt % (▲).

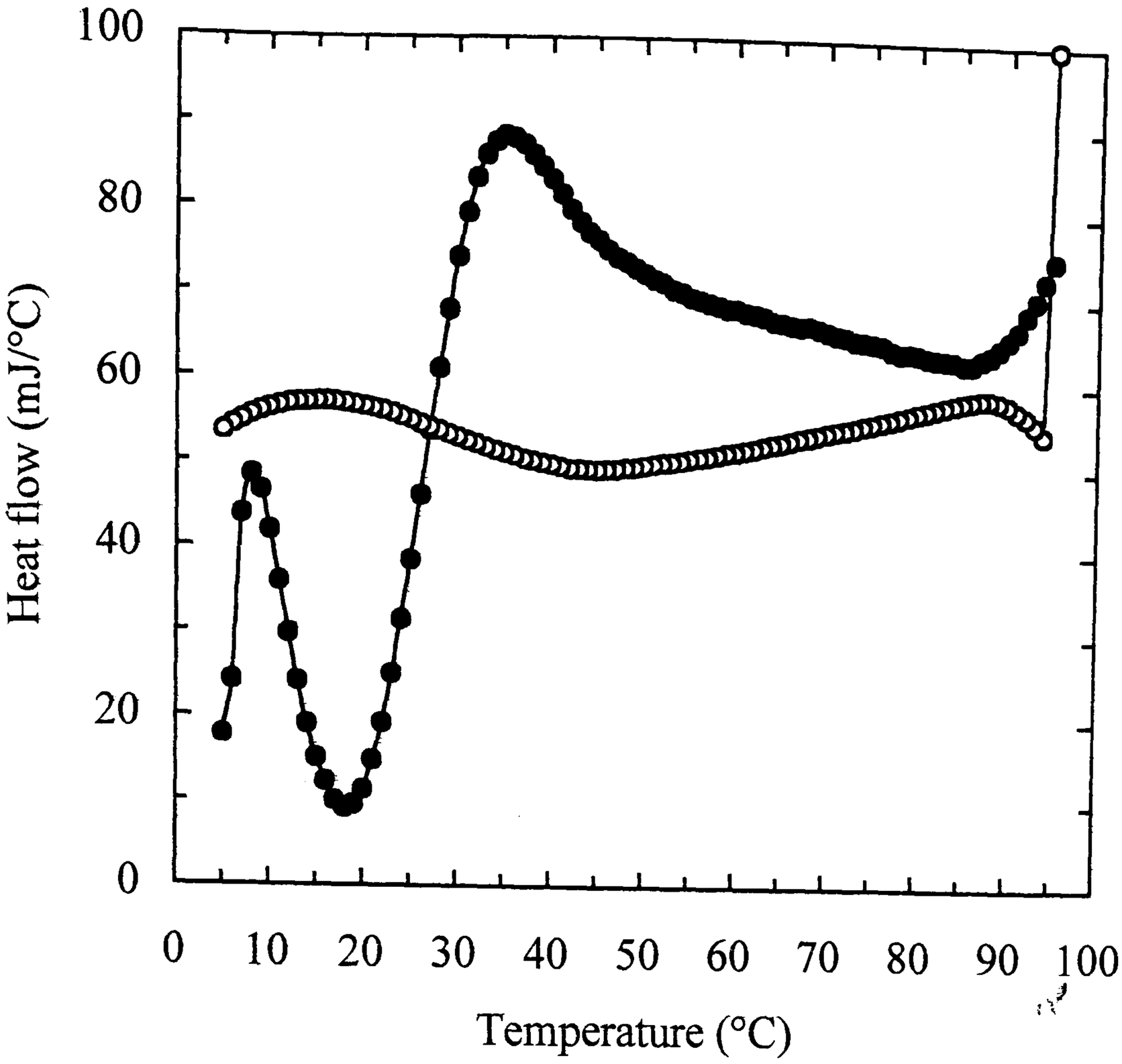

Figure 6.11. DSC traces for 1.0 wt % high methoxy pectin (DE 70; pH 3.0) in the presence of 60 wt % fructose on cooling (O) and heating (●) at a scan rate of 0.5 °C/min.

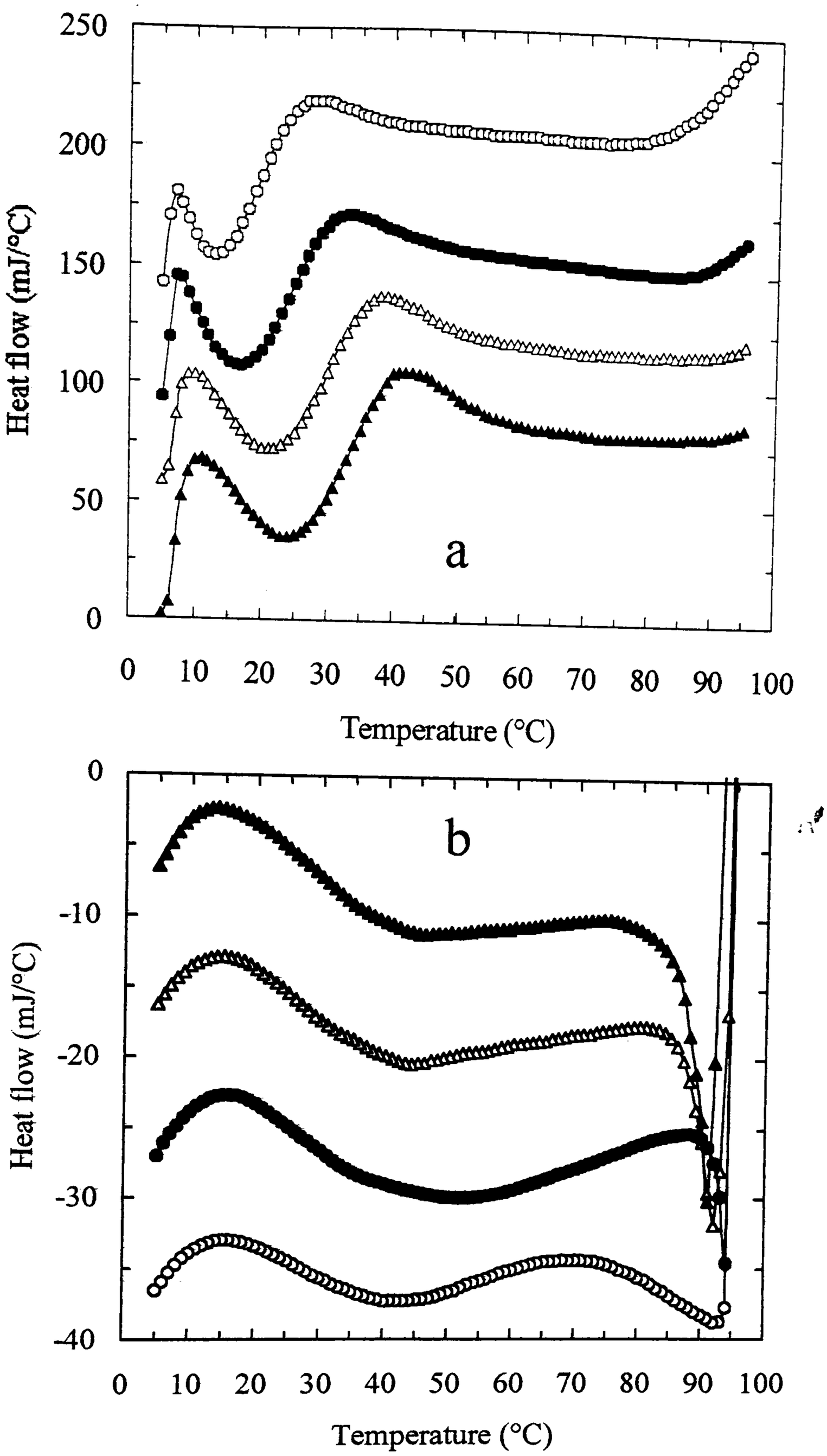

Figure 6.12. DSC traces for 1.0 wt % high methoxy pectin (DE 70; pH 3.0) in the presence of 55 wt % fructose, recorded during (a) heating and (b) cooling at scan rates (°C/min) of 0.3 (O), 0.5 (●), 0.8 (Δ) and 1.0 (▲).

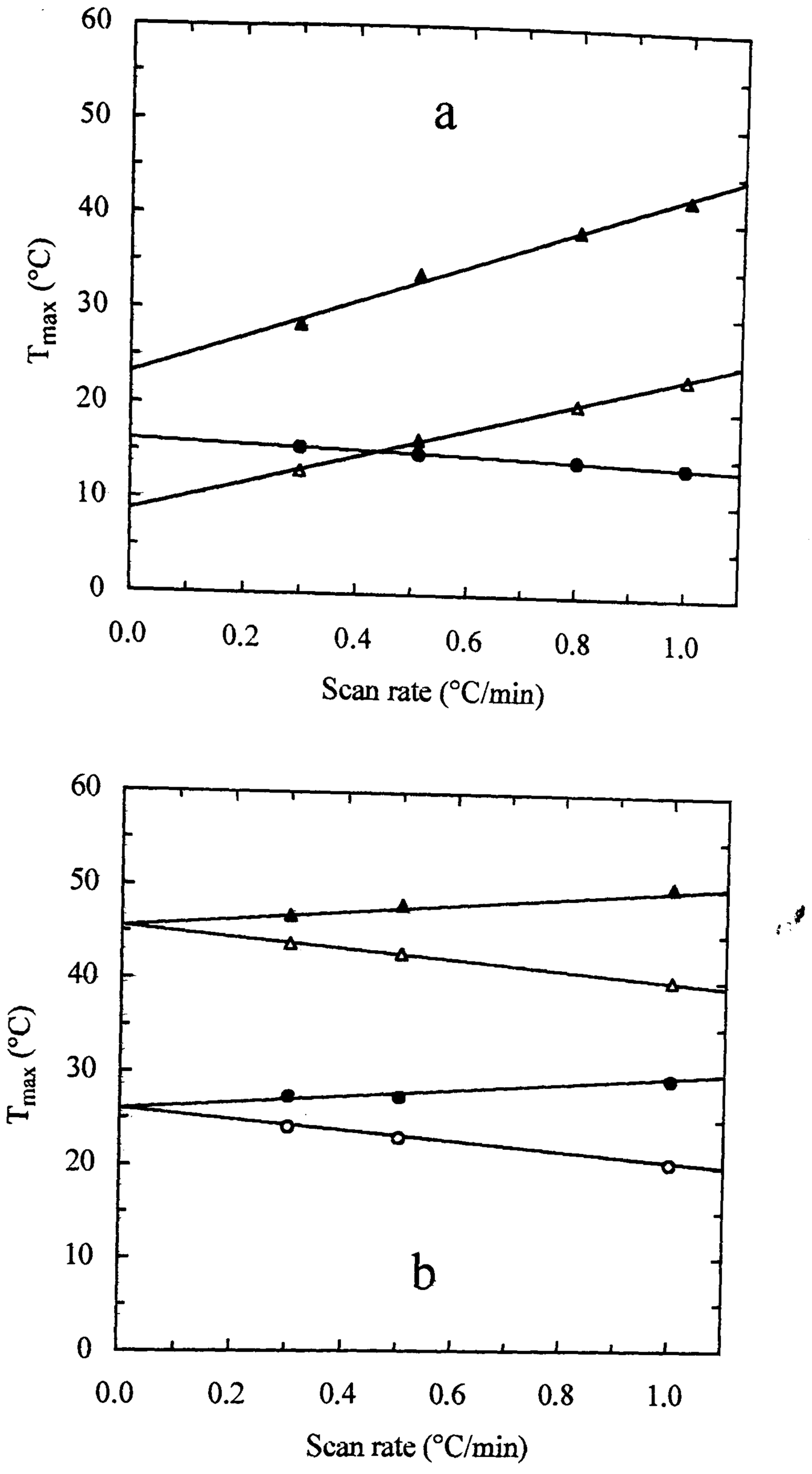

Figure 6.13. Scan-rate dependence of the temperature (T_{max}) at maximum exothermic or endothermic heat flow for (a) the initial endotherm (Δ) and subsequent exotherm (▲) observed on heating of 1.0 wt % high methoxy pectin (DE 70; pH 3.0) in the presence of 55 wt % fructose and the single exotherm (●) observed on cooling of the same sample, in comparison with (b) the heating endotherm (filled symbols) and cooling exotherm (open symbols) observed by Robinson et al. (1991) for 1.0 wt % Me_4N^+ gellan in water (circles) and in 0.25 M Me_4NCl (triangles).

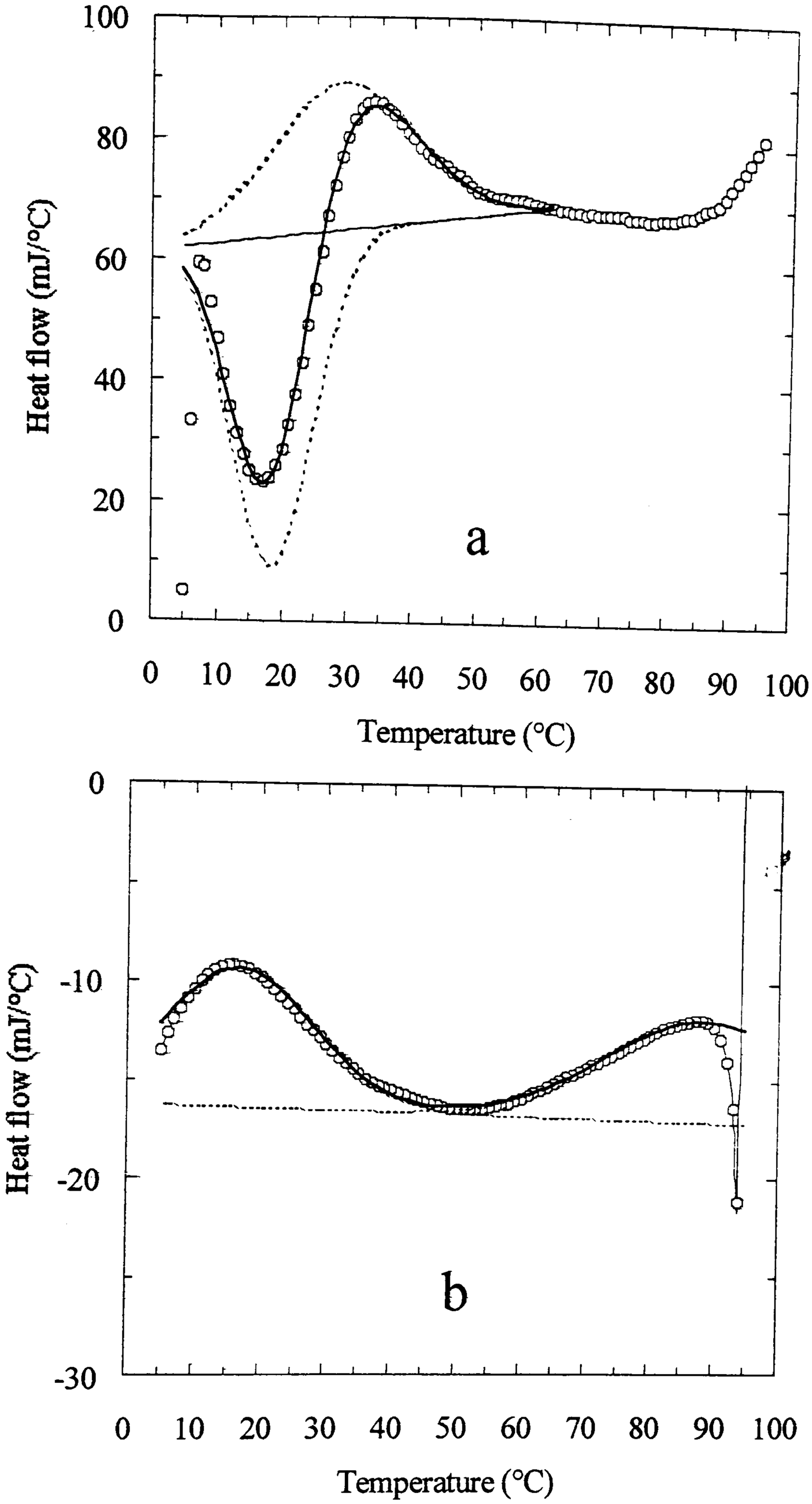

Figure 6.14. DSC traces (O) for 1.0 wt % high methoxy pectin (DE 70; pH 3.0) in the presence of 55 wt % fructose on (a) heating and (b) cooling at a scan rate of 0.5 °C/min, fitted to two Gaussian bands (- - -) by the procedure described by Tsoga et al. (2001). The bold and fainter solid lines show, respectively, the total spectrum and baseline from the curve-fitting analysis.

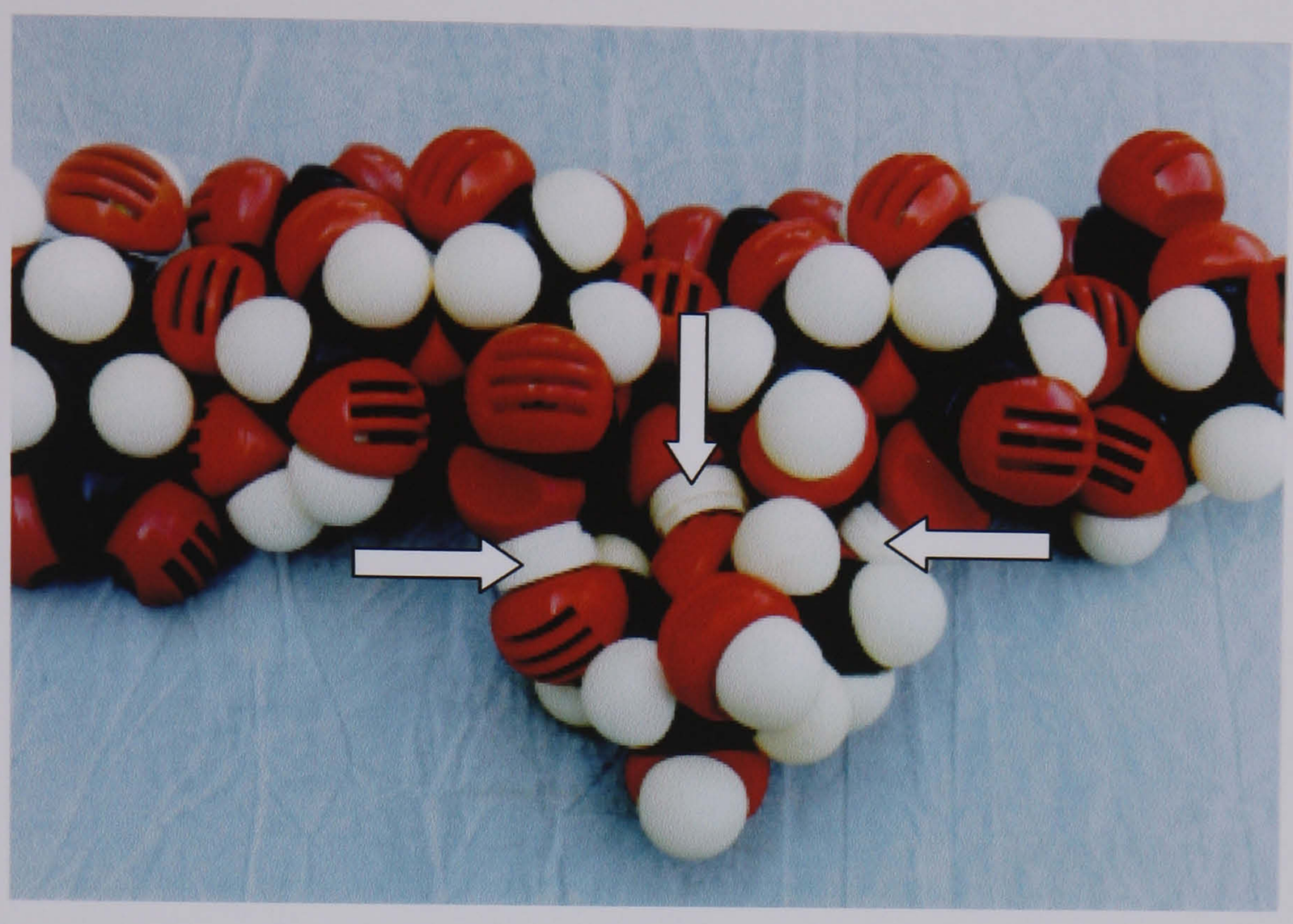

Figure 6.15. Space-filling (CPK) molecular model showing tentative proposal for site-binding of fructose to polygalacturonate sequences of pectin. The hydrogen bonds discussed in the text are indicated by arrows.